

Fe-Catalyzed Oxidative Cleavage of Unsaturated Fatty Acids

Fe-Gekatalyseerde Oxidatieve Splitsing van Onverzadigde Vetzuren

(met een samenvatting in het Nederlands)

PROEFSCHRIFT

ter verkrijging van de graad van doctor
aan de Universiteit Utrecht

op gezag van rector magnificus, prof. dr. G. J. van der Zwaan,
ingevolge het besluit van het college voor promoties
in het openbaar te verdedigen
op maandag 16 december 2013 des ochtends te 10.30 uur

door

Peter Spannring

geboren op 29 oktober 1985 te Graz, Oostenrijk

Promotoren: Prof. dr. R. J. M. Klein Gebbink
Prof. dr. ir. B. M. Weckhuysen
Co-promotor: Dr. P. C. A. Bruijninx

Utrecht University and the financial support through the 'Focus and Massa' program are acknowledged.

Fe-Catalyzed Oxidative Cleavage of Unsaturated Fatty Acids

Spannring, Peter

Title: Fe-Catalyzed Oxidative Cleavage of Unsaturated Fatty Acids

Utrecht, Utrecht University, Faculty of Science

Ph. D. thesis Utrecht University – with ref. – with summary in Dutch

ISBN: 978-94-6108-558-0

The work described in this thesis was carried out at the groups of Organic Chemistry & Catalysis and Inorganic Chemistry & Catalysis, Debye Institute for Nanomaterials Science, Faculty of Science, Utrecht University, the Netherlands.

Cover Design: Peter Spannring

Table of contents

Preface	1
<i>Introduction</i>	
Chapter 1 Transition metal-catalyzed oxidative double bond cleavage of simple and bio-derived alkenes and unsaturated fatty acids	9
<i>Metal-free oxidative cleavage of terpenes and unsaturated fatty acids</i>	
Chapter 2 A metal-free, one-pot method for the oxidative cleavage of internal aliphatic alkenes into carboxylic acids	75
<i>Iron-catalyzed oxidative cleavage of terpenes and unsaturated fatty acids</i>	
Chapter 3 Fe-catalyzed one-pot cleavage of unsaturated fatty acids into aldehydes with hydrogen peroxide and sodium periodate	93
Chapter 4 Regioselective cleavage of electron-rich double bonds in dienes with [Fe(OTf) ₂ (mix-BPBP)] and a combination of H ₂ O ₂ and NaIO ₄	107
Chapter 5 Fe(6-Me-PyTACN)-catalyzed, one-pot oxidative cleavage of methyl oleate and oleic acid into carboxylic acids with H ₂ O ₂ and NaIO ₄	123
<i>Design of non-heme iron catalysts for alkene oxidations</i>	
Chapter 6 Synthesis, characterization and catalytic properties of non-heme [Fe(OTf) ₂ (bapbpy)] and [Fe(OTf) ₂ (<i>o,p</i> -di-Me-bapbpy)]	141
Addendum	179
Summary	185
Samenvatting	191
Graphical Abstract	197
List of publications	199
Dankwoord	201
Curriculum Vitae	205

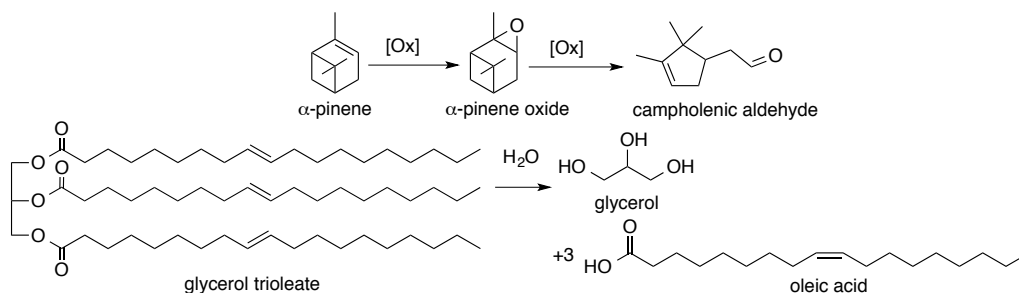
Preface

Nature annually generates about 170 billion metric tons of biomass, of which only 3-4% is currently used for food purposes, for the production of fuels or for chemicals manufacturing.^[1] As far as renewable chemicals production is concerned, the oleochemical industry serves as a longstanding example of a biobased industry, one that over the last century has developed in parallel with the petrochemical industry.^[2] Around 14% of vegetable and animal raw materials worldwide are used for the production of chemicals, with soybean, palm, rapeseed and sunflower oil being the most important feedstocks used. The use of fats and oils for the production of chemicals can be considered as part of a larger effort, i.e. the use of biomass as a sustainable resource for the production of renewable platform chemicals, as it is the only abundantly available carbon-containing feedstock with low oxygen content.^[3] Notably, the development of such biobased routes should not only be aimed at the replacement of existing synthesis routes of chemicals derived from petroleum (producing so-called 'drop-in', molecularly identical products), but should rather also make use of the many functional groups present in the various biomass components (and lacking in petroleum) to allow new compounds with improved properties and novel applications to be produced. Indeed, the various degrees of oxygenation of the components of biomass offer different synthetic opportunities for their valorization.^[4]

Polysaccharide-derived platform molecules, for instance, have a relatively high oxygen content and conversion of these substrates to platform molecules or end products often involves a reduction in oxygen content, such as in the dehydration of monosaccharides.^[1] Terpenes and vegetable oils, on the other hand, have a relatively high carbon content and conversion routes of these substrates therefore often involve reactions to increase the oxygen-content for the production of chemicals. The compound classes of the terpenes and vegetable oils furthermore have in common that they both are natural sources of alkenes, a functional group that offers many possibilities for further derivatization. For example, the oxidation of the C=C double bonds in terpenes yields terpenoids (e.g. α -pinene oxide, Scheme 1 top), which are used in fragrances,^[5] as food additives or as building blocks for the formation of alcohols, ethers or carbonyls (Scheme 1 top, oxidation of α -pinene oxide to campholenic aldehyde).^[1]

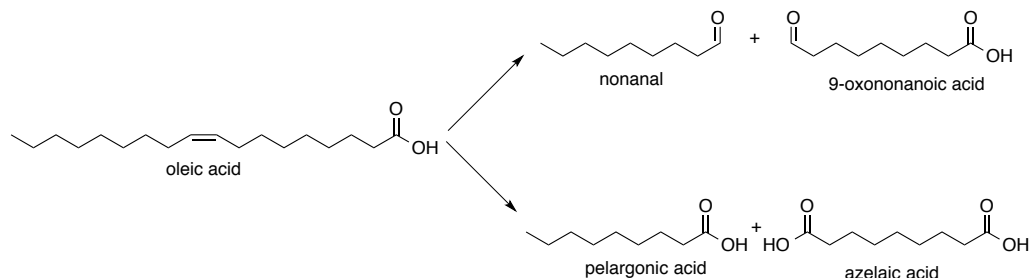
The double bond in vegetable oils and their constituent fatty acids, which are derived from hydrolysis of unsaturated triglycerides (e. g. glycerol trioleate to oleic acid, Scheme 1 bottom), can also be oxidized in numerous ways.^[2, 6-9] Epoxidation of the unsaturated moieties,^[9] for instance, yields products that can be used in the polymerization industry.^[1] Other examples involve radical oxidations at the allylic position, Wacker-type oxidations to keto fatty acids and dihydroxylation reactions.^[9] One particularly attractive conversion

of the olefin in fatty acids is its oxidative cleavage, as it gives access to a number of valuable products.



Scheme 1. Examples of common chemical processes with vegetable oils and fats and terpenes.

The oxidative cleavage of an alkene is the transformation of a C=C double bond to give either two aldehydes, or, upon over-oxidation, two carboxylic acids as products. The aldehydes or carboxylic acids obtained after oxidative cleavage of unsaturated fatty acids can be valuable products for the chemical industry.^[1, 7, 8] The industrial oxidative cleavage processes of these substrates are limited, however, to the ozonolytic cleavage of oleic acid into nonanal and 9-oxononanoic acid^[10] and the over-oxidation of these products to give pelargonic and azelaic acid (Scheme 2).^[1] Oxidative cleavage of fatty acids thus yields both a monofunctional and an α,ω -bifunctionalized product. The saturated monofunctionalized molecules can be used as chemical building blocks. For example, the production of nonanal, which is used as precursor for the synthesis of alcohols, as a perfume or in flavors, provides an alternative to the petrochemical production route, which involves the Rh-catalyzed hydroformylation of 1-octene. Pelargonic acid is a surfactant and finds application as emulsifier in the paint industry, or as plasticizer additive in the product of materials, e. g. PVC. The difunctionalized moieties are especially useful for polymerization purposes, e.g. for the production of polyesters or polyamides such as Nylon. Azelaic acid can also be used as stabilizer or as treatment against acne, as it kills bacteria that infect skin pores.



Scheme 2. Oxidative cleavage of oleic acid into aldehydes (top) and into carboxylic acids (bottom).

The limited commercial application of the ozonolysis process is clearly related to the challenges associated with the use of ozone, which is particularly hazardous because of its explosion risks and needs to be prepared in-situ prior to usage.^[1] Catalytic alternatives are desired to eventually replace this oxidative cleavage method and to make full use of the potential of this versatile conversion reaction for the production of renewable building blocks for the chemical industry. Much work has been done in this respect in academia on the development of second- and third-row transition metal catalysts based on Ru,^[11, 12] Os^[13, 14] and W^[15-18] for this reaction. However, the cost, toxicity and low natural abundance of these metals hamper the industrial applicability of these methods.

Methods using catalysts based on first-row transition metals would provide attractive alternatives to substitute such second- and third-row metals. For this, lessons can be taken from Nature, as enzymes that incorporate metals such as iron, copper and manganese in their active sites mediate a multitude of biological oxidative transformations.^[19, 20] The family of iron-containing enzymes capable of oxidative transformations is particularly large and versatile. The non-heme iron enzyme carotenoid oxygenase even provides an example of oxidative cleavage of one of the double bonds of β -carotene to yield retinal, using O₂ as the oxidant.^[21-23] The active site of this enzyme features a mononuclear iron center in an all-N ligand environment and can serve as a source of inspiration for the development of synthetic iron-based catalysts for oxidative cleavage reactions. Indeed, this example shows that synthetic Fe-based complexes could be designed to catalyze oxidative cleavage reactions as well. In principle, Fe is a metal of low cost, no toxicity and high natural abundance, and would thus be an attractive alternative to the Ru, Os or W-based catalysts. While many synthetic Fe-based catalysts have been developed over the years for a wide variety of oxidative transformations, their potential for oxidative cleavage reactions has hardly been explored, with the few known examples being limited to the oxidative cleavage of activated substrates, such as styrenes.^[24] The development of Fe-based catalysts for the oxidative cleavage of aliphatic alkenes such as those found in unsaturated fatty acids and terpenes is still a challenge, which if met successfully can have considerable potential in chemical industry. In general, the design and the study of non-heme Fe-based complexes for oxidation purposes remain research goals of many synthetic chemists,^[24, 25] and such new complexes could eventually also be applied in oxidative alkene cleavage reactions.^[25, 26]

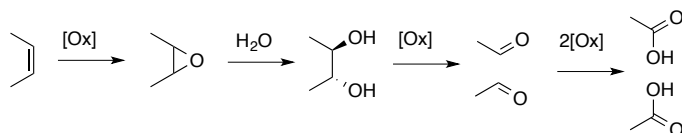
Aim and scope of this thesis

The aims of the work described in this thesis were to i) develop environmentally benign methods for the oxidative cleavage of unsaturated fatty acids into either aldehydes or carboxylic acids; ii) apply first-row transition-metal systems for this purpose, preferably

using Fe as a metal together with the 'green' oxidant H₂O₂ and iii) design and investigate new non-heme Fe-based systems for olefin oxidation reactions.

Chapter 1 gives a comprehensive review on transition-metal catalyzed oxidative cleavage methods reported over the last thirty years. It has been subdivided into reports concerning i) simple alkenes and ii) unsaturated fatty acids. The review shows that, while many examples are available of methods using second- and third-row transition metals, first-row transition metal systems have primarily been used for the oxidative cleavage of styrene derivatives. No examples have been reported of the oxidative cleavage of unsaturated fatty acids with first row transition metal complexes.

Building on the existing oxidative cleavage systems described in Chapter 1, the main strategy for oxidative cleavage in the subsequent chapters aims at a sequence of reactions consisting of alkene epoxidation, followed by hydrolysis into *trans*-diols, and over-oxidation into either aldehydes or carboxylic acids (Scheme 3).



Scheme 3. Main strategy for the alkene cleavage into aldehydes or carboxylic acids.

Chapter 2 introduces a metal-free method for the oxidative cleavage of unsaturated fatty acids into their corresponding carboxylic acids. The combination of oxone and periodate is shown to be capable of cleaving a series of alkenes and unsaturated fatty acids in a clean and highly selective manner. The method involves a straightforward experimental procedure and allows for the facile isolation of the product, making it a convenient and readily applicable synthetic protocol for the lab-scale synthesis of carboxylic acids from alkenes.

In **Chapter 3** an Fe-based system is presented capable of the catalytic oxidative cleavage of internal alkenes and unsaturated fatty acids to the corresponding aldehydes with hydrogen peroxide and sodium periodate without any over-oxidation of the products to the carboxylic acids. Compared to the metal-free method described in Chapter 2, oxone is replaced by a combination of an Fe-catalyst and hydrogen peroxide, generating significantly less waste and allowing the system to operate at milder reaction conditions and lower temperatures.

Chapter 4 explores the substrate scope as well as the chemo- and regioselectivity of the system developed in Chapter 3. The system is shown to be capable of regioselective oxidative cleavage of the electron-rich double bond to aldehydes in substrates containing

multiple double bonds. This is illustrated by the selective oxidative cleavage of some polyunsaturated terpenes.

Chapter 5 reports the Fe-based oxidative cleavage of unsaturated fatty acids and esters to carboxylic acids with hydrogen peroxide and sodium periodate. The Fe-catalyst is capable to oxidize the aldehyde intermediates to the carboxylic acids with sodium periodate, a reaction that did not occur in the previous two chapters. Likewise, a methodology is provided that is complementary to the systems reported in chapters 3 and 4.

Finally, **Chapter 6** presents a study of new Fe-based complexes of the non-heme babbpy ligand family including structural, spectroscopic, electrochemical and spin-crossover features of two Fe(II) complexes. The reaction with peroxides of these complexes is studied by computational means and through mechanistic studies at low temperatures is studied by spectroscopic and mass-spectrometric means. The investigation is completed with a reactivity study on catalytic alkene epoxidations with hydrogen peroxide.

References

- [1] A. Corma, S. Iborra, A. Velty *Chem. Rev.* **2007**, *107*, 2411.
- [2] K. Hill *Pure Appl. Chem.* **2000**, *72*, 1255.
- [3] J. O. Metzger, A. Hüttermann *Naturwissenschaften* **2009**, *96*, 279.
- [4] J. Zakzeski, P. C. A. Bruijninx, A. L. Jongerius, B. M. Weckhuysen *Chem. Rev.* **2010**, *110*, 3552.
- [5] A. Calogirou, B. R. Larsen, D. Kotzias *Atmos. Environ.* **1999**, *33*, 1423.
- [6] H. Baumann, M. Bühler, H. Fochem, F. Hirsinger, H. Zobelein, J. Falbe *Angew. Chem. Int. Ed.* **1988**, *27*, 41.
- [7] U. Biermann, U. Bornscheuer, M. A. R. Meier, J. O. Metzger, H. J. Schäfer *Angew. Chem. Int. Ed.* **2011**, *50*, 3854.
- [8] U. Biermann, W. Friedt, S. Lang, W. Lühs, G. Machmüller, J. O. Metzger, M. Rüschen, Klaas, H. J. Schäfer, M. P. Schneider *Angew. Chem. Int. Ed.* **2000**, *39*, 2206.
- [9] A. Köckritz, A. Martin *Eur. J. Lipid Sci. Technol.* **2008**, *110*, 812.
- [10] Ozonolysis on industrial scale is performed by Novasep.
- [11] H. J. Carlsen, T. Katsuki, V. S. Martin, K. B. Sharpless *J. Org. Chem.* **1981**, *46*, 3936.
- [12] R. Noyori, M. Aoki, K. Sato *Chem. Commun.* **2003**, 1977.
- [13] B. R. Travis, R. S. Narayan, B. Borhan *J. Am. Chem. Soc.* **2002**, *124*, 3824.
- [14] D. C. Whitehead, B. R. Travis, B. Borhan *Tetrahedron Lett.* **2006**, *47*, 3797.
- [15] A. Haimov, H. Cohen, R. Neumann *J. Am. Chem. Soc.* **2004**, *126*, 11762.
- [16] V. Kogan, M. M. Quintal, R. Neumann *Org. Lett.* **2005**, *7*, 5039.
- [17] E. Antonelli, R. D'Aloisio, M. Gambaro, T. Fiorani, C. Venturello *J. Org. Chem.* **1998**, *63*, 7190.

- [18] C. Venturello, M. Ricci *J. Org. Chem.* **1983**, *48*, 3831.
- [19] M. Costas, K. Chen, L. Que Jr. *Coord. Chem. Rev.* **2000**, *200-202*, 517.
- [20] L. Que Jr., R. Y. N. Ho *Chem. Rev.* **1996**, *96*, 2607.
- [21] N. H. Fidge, F. R. Smith, D. S. Goodman *Biochem. J.* **1969**, *114*, 689.
- [22] D. P. Kloer, S. Ruch, S. Al-Babili, P. Beyer, G. E. Schulz *Science* **2005**, *308*, 267.
- [23] M. G. Leuenberger, C. Engeloch-Jarret, W. D. Woggon *Angew. Chem. Int. Ed.* **2001**, *40*, 2613.
- [24] A. R. McDonald, L. Que Jr. *Coord. Chem. Rev.* **2013**, *257*, 414.
- [25] M. Costas, M. P. Mehn, M. P. Jensen, L. Que Jr. *Chem. Rev.* **2004**, *104*, 939.
- [26] J. Bautz, P. Comba, C. Lopez de Laorden, M. Menzel, G. Rajaraman *Angew. Chem. Int. Ed.* **2007**, *46*, 8067.

Introduction

Chapter 1

Transition metal-catalyzed oxidative double bond cleavage of simple and bio-derived alkenes and unsaturated fatty acids

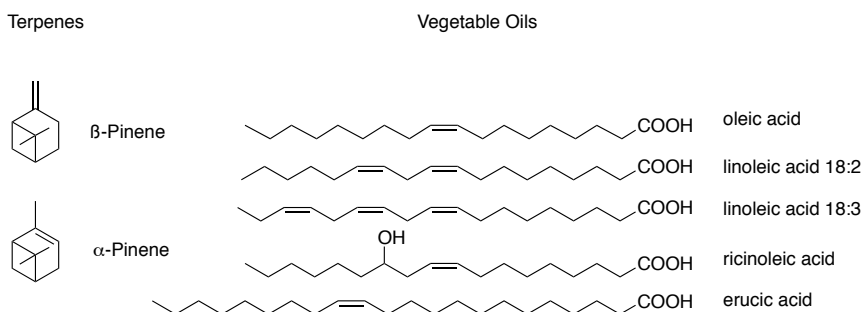
Abstract

The oxidative cleavage reaction of the C=C double bond in unsaturated fatty acids into aldehydes or into carboxylic acids is a process that is currently being performed on industrial scale by ozonolysis. Alternatively, catalytic methods for this conversion that are not based on this hazardous oxidant are highly desired. The use of transition metal catalysts would allow the application of milder reaction conditions and more benign oxidants. This review covers the various transition metal-based catalysts that have been reported for the oxidative cleavage of alkenes in general and the cleavage of unsaturated fatty acids in particular. Catalytic systems based on second- and third-row metals such as Ru, Os, and W have been widely studied and are well-known to catalyze the cleavage of various alkenes and unsaturated fatty acids. Apart from the use of simple metal salts, metal oxides or peroxides, also coordination metallic complexes were made to decrease the toxicity of some systems and to induce chemo- and regioselective olefin cleavage. Also, heterogeneous systems have been developed that focus on catalyst reuse. The use of these second- and third-row metal catalysts comes with significant disadvantages, however, as these metals are either expensive, toxic or not very abundant. First-row transition metal catalysts would be preferred from this point of view, but the examples of such catalysts for oxidative olefin cleavage are scarcer. The applications of these Fe- or Mn-based systems are furthermore limited to activated alkenes, e.g. styrene derivatives. The many possibilities that are offered by careful ligand design together with the recent advances in the field of first-row transition metal oxidative (cleavage) systems should ultimately allow for such systems to substitute ozone or second- and third-row cleavage systems of unsaturated fatty acids.

Review based on: Peter Spanning, Pieter C. A. Bruijninx, Bert M. Weckhuysen and Robertus J. M. Klein Gebbink, manuscript in preparation

1.1 Introduction

Biomass, an abundant and renewable feedstock, is one of the most promising sustainable alternatives to fossil resources. Apart from being used in the food industry or in the production of fuels and energy, large industrial potential lies in the production of valuable chemicals from this renewable resource.^[1, 2] Considering the relatively high carbon content, the oxidation of terpenes and unsaturated vegetable oils or animal fats (forming unsaturated fatty acids upon hydrolysis, see Preface) is especially interesting, as these constitute a natural resource of alkenes to which functionalities can be added. Nevertheless, the number of industrial processes that are known to use these sources of renewables is rather limited, despite the possibilities that the C=C double bond oxidation allows. Terpenes can be oxidized into α -terpenoids (see Preface),^[3] which can be used as fragrance materials, acrylates or other derivatives,^[4] or are reactive intermediates to form alcohols, ethers or carbonyl compounds.^[5] Perhaps more interesting are oxidation reactions on the double bond of unsaturated fatty acids. Epoxidation reactions enable the production of polymer building blocks, for example. Radical-type oxidations on the allylic position, Wacker-type oxidations to form ketones, or dihydroxylations generally form products that are surface active compounds, soaps and find applications in coatings or in the production of PVC.^[1, 2, 4, 6-9] Of particular interest for this review are oxidative cleavage reactions of C=C bonds. Common biomass-derived substrates for this reaction are terpenes and unsaturated fatty acids such as those listed in Scheme 1.1.

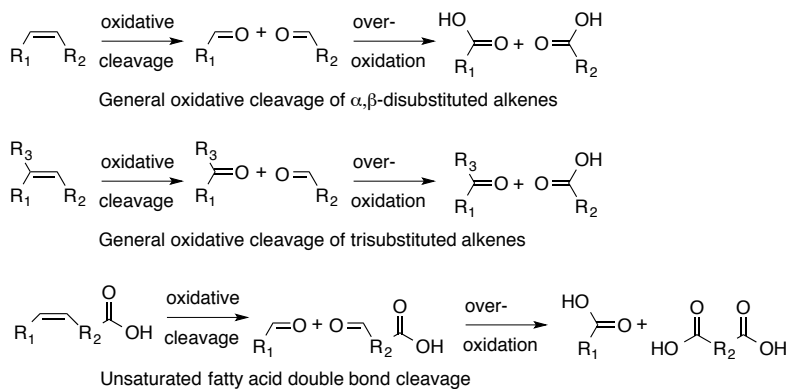


Scheme 1.1. Common naturally occurring or nature-derived terpenes and unsaturated fatty acids.

The oxidative cleavage of a carbon-carbon double bond entails scission of the double bond with incorporation of oxygen in the two fragments (Scheme 1.2). The initial oxidation products of α,β -disubstituted alkenes, i.e. those generally found in unsaturated fatty acids, are aldehydes, but over-oxidation results in carboxylic acids. Trisubstituted internal alkenes yield both an aldehyde and ketone product, of which the latter is generally not over-oxidized to carboxylic acids. In this way, oxidative cleavage adds functionality to the

Chapter 1

substrate, providing access to intermediates susceptible for sequential reactions or directly to valuable products.

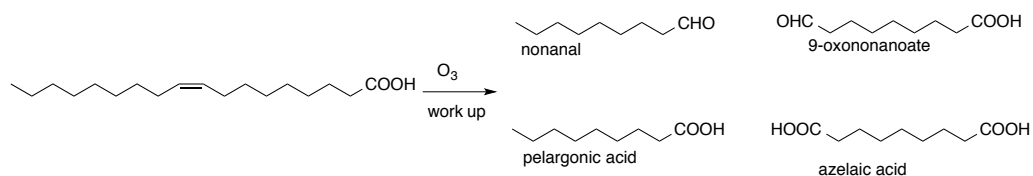


Scheme 1.2. The oxidative double bond cleavage of alkenes and unsaturated fatty acids to various valuable aldehyde, ketone and carboxylic acid products.

Oxidants are the suppliers of oxygen during oxidative (cleavage) reactions; commonly one equivalent (equiv.) of an oxygen atom is added to the substrate per molecule of oxidant. Oxidants such as sodium periodate, peroxymonosulfate (active species in $2\text{KHSO}_5 \cdot \text{KHSO}_4 \cdot \text{K}_2\text{SO}_4$, oxone), peracetic acid and tert-butyl hydroperoxide (TBHP) are often used in oxidation reactions. These are relatively strong oxidants, as they are often capable of oxidizing substrates without the aid of a transition metal. However, they generate waste. Oxidants such as H_2O_2 and O_2 leave no waste behind, yet the use of these oxidants almost always requires a transition metal in order to oxidize the substrate.

The oxidant considered to be most suitable for oxidative cleavage reactions, in theory, is ozone. Ozonolysis of olefins is the process of transforming alkenes into aldehydes or carboxylic acids without the use of a metal.^[10] Nevertheless, ozone is dangerous because of its instability and needs to be formed in-situ as its storage is unwanted. Additionally, high-technology equipment is needed, which additionally increases the costs.^[11] Despite these disadvantages, ozone is used commercially for the oxidative cleavage of oleic acid (Scheme 1.3).^[1]

Ozonolysis of oleic acid yields a number of valuable products: the formation of nonanal can be considered as an alternative to hydroformylation of 1-octene. 9-Oxononanoate and nonanal are popular chemical building blocks for sequential reactions, e.g. the formation of alcohols. Nonanoic acid, or pelargonic acid, is a surfactant, while azelaic acid is used medically against treatment of acne, and can be used in the formation of nylons.^[1, 2, 6, 8, 9] In order to find alternatives for ozone, it is important that the selectivity towards the cleavage products is high. Common side reactions such as epoxidations, dihydroxylations or allylic oxidations should be prevented, and this still remains a challenge.



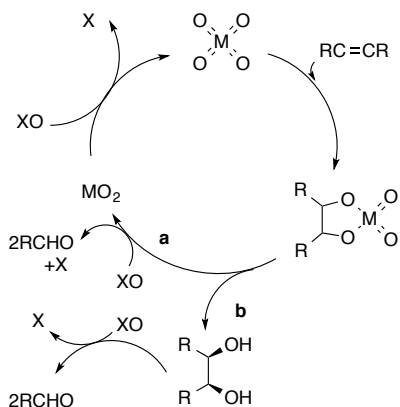
Scheme 1.3. Ozonolysis of oleic acid into valuable saturated aldehydes and acids.

Several stoichiometric oxidants are known to very selectively transform alkenes into aldehydes or carboxylic acids. *m*-Chloroperbenzoic acid (mcpba), for example, can directly cleave 1,1-diarylethylene derivatives to the ketone with 1.5 oxidizing equivalents in reactions performed at $-78\text{ }^{\circ}\text{C}$ in CH_2Cl_2 .^[12] Also, PhIO/HBF_4 (1.1 equiv. each) induces alkene scission into the aldehydes selectively.^[13]

A typical example of a transition metal-containing stoichiometric oxidant is potassium permanganate, KMnO_4 , which allows olefins to be transformed selectively into aldehydes^[14] or acids.^[15-17] A drawback is that organic substrates are often poorly soluble because of the aqueous environment, which is necessary to dissolve the permanganate ion. This drawback can be addressed by the use of a quarternary ammonium salt as phase transfer agent at elevated temperatures.^[18, 19] Crown ethers can also be used for such purposes and work at ambient temperatures.^[20] Also, polyethylene glycol^[21] and triethylbenzylammonium chloride^[16] have been used as additives. The reason why permanganate cannot be used in catalytic amounts is the precipitation of MnO_2 after oxidation of the substrate. MnO_2 is relatively stable and very difficult to reoxidize towards MnO_4^- . Other transition metal-containing stoichiometric oxidants are chromic oxides.^[22] CrO_2Cl_2 , for instance, transforms styrene into benzaldehyde and phenylacetaldehyde.^[23] However, such chromium salts are known to be very toxic and their use is therefore rather undesirable.

RuO_4 is an interesting metal oxide for two reasons. On the one hand, it can be used as a selective stoichiometric oxidant for the transformation of alkenes into aldehydes.^[24, 25] On the other hand, it can be used in catalytic amounts when RuCl_3 is treated with a secondary oxidant. The solubility of RuO_2 is the key to making this species catalytic. RuO_2 , unlike MnO_2 , can be dissolved in solvents like CCl_4 or MeCN and reoxidized towards RuO_4 by sodium periodate^[26] or sodium hypochlorite.^[27] RuO_4 is highly selective towards cleavage products because the reaction mechanism does not involve epoxidation or dihydroxylation intermediates (Scheme 1.4, Mechanism Aa). After coordination of the alkene, a 3+2 pericyclic reaction forms a metal-dioxyethane moiety, also called a metal-diester. A sufficient lifetime of the diester is crucial, as its rearrangement yields the desired aldehydes, while hydrolysis causes the formation of diols. The formation of carboxylic acids needs at least 4 equiv. of secondary oxidant.^[28]

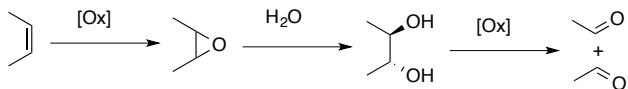
Chapter 1



Scheme 1.4. General catalytic cycle for the oxidative cleavage of alkenes involving reactions of metal (M) tetroxides (Mechanism A) with oxidants (OX). A metal-diester species is shown here as key intermediate.^[29]

The use of Os as a catalyst in oxidative alkene cleavage reactions was discovered even before the use of its Ru-counterpart.^[30] Osmium is more toxic than ruthenium, yet has the advantage that usually lower catalyst loadings are needed. Interestingly, OsO₄ tends to form *cis*-diols after formation of the metal diester (Scheme 1.4, Mechanism Ab) rather than aldehydes when used in stoichiometric amount. It can be used as a catalytic reagent in the oxidative cleavage reactions when NaIO₄ is added as a secondary oxidant. As with RuCl₃, sodium periodate can form the tetroxide from an Os-precursor, yet in this case the periodate has the additional role of oxidizing *cis*-diols towards aldehydes. Because the latter process generally proceeds smoothly, OsO₄ and NaIO₄ can be used as catalyst and secondary oxidant for the selective transformation of alkenes into aldehydes.

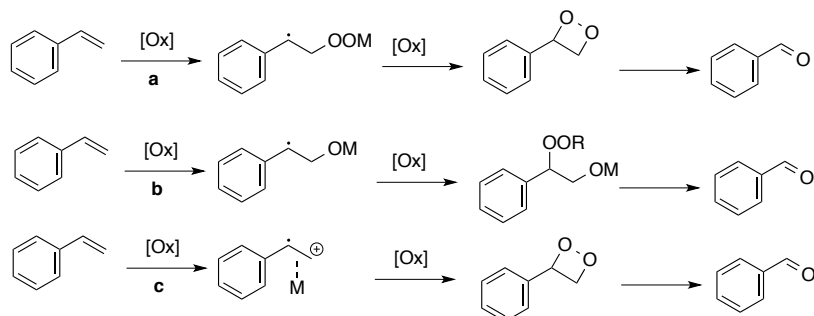
Nevertheless, ruthenium and osmium are expensive metals, with osmium in addition being very toxic. Cheaper and less toxic metals as well as alternatives to hypochlorite or CCl₄ are therefore desirable. Alternatives to Ru and Os-based systems, e. g. W-based systems, often apply a mechanism involving epoxidation, followed by hydrolysis to *trans*-diols and further oxidation to the aldehyde or carboxylic acids stage (Mechanism B, Scheme 1.5).



Scheme 1.5. General mechanism for oxidative cleavage reactions involving epoxide formation, hydrolysis and cleavage of the diol to the aldehyde (Mechanism B). [Ox] = oxidant.

Radical pathways have also been proposed, primarily for styrene derivatives (Mechanism C, Scheme 1.6). A benzyl radical is often suggested to be formed after metal-oxides or metal-peroxides attack at the β -position with respect to the phenyl group. From metal-peroxides, a four-membered dioxethane moiety is formed that rearranges to the

aldehyde (e. g. Co, Mechanism Ca). Alternatively, with the metal-oxide another peroxide binds prior to rearrangement to the aldehyde (e. g. Fe or Mn, Mechanism Cb). Finally, the styrene derivative can be oxidized to a radical cation, which is bound to the metal (e. g. Cu, Cr Mechanism Cc), followed by the formation of the four-membered dioxyethane, which rearranges to the aldehyde.



Scheme 1.6. Oxidative cleavage of styrene derivatives following a radical pathway (Mechanism C).

The catalytic oxidative cleavage of alkenes in general and in particular unsaturated fatty acids has been sparsely reviewed to our knowledge.^[4, 6, 9] It felt timely to elaborate on the most recent developments in this field. Also, there has been much effort focused lately on the development of greener alternatives to the conventional agents used for oxidative cleavage. Our objective is to describe and discuss the current state of the art in transition metal-catalyzed oxidative double bond cleavage of alkenes and of unsaturated fatty acids. This review aims to cover all reports on homogeneous and heterogeneous catalytic systems of oxidative double bond cleavage of the period 1980-2013. Some textbook examples developed before this period have been addressed already in the introduction. In addition to the examples of cleavage of simple alkenes (section 1.2), such as styrene derivatives, cyclic olefins and non-fatty linear olefins, specific emphasis is placed on the use of renewable terpene substrates. Moreover, section 1.3 deals exclusively with oxidative cleavage reactions of unsaturated fatty acids. The sections are further subdivided into transition metal-catalyzed oxidative cleavage reactions of second- and third-row (sections 1.2.1 and 1.3.1), or first-row metals (section 1.2.2). Finally, the sections are subdivided into reports based on metal salts, metal-oxides or metal-peroxides (sections 1.2.1.1 and 1.3.1.1), metal complexes (sections 1.2.1.2 and 1.3.1.2) and heterogeneous catalysts (sections 1.2.2.3 and 1.3.1.3).

Chapter 1

1.2 Cleavage of non-fatty alkenes

1.2.1 Second and third-row transition metals

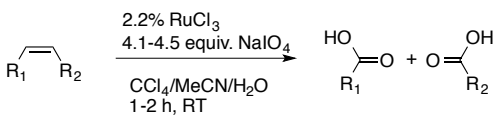
Second and third-row transition metal systems can be used as simple metal salts that are oxidized to their metal-oxo species, which are capable of performing oxidative cleavage. These metals can also be used as coordination complexes, with the ligand often being added for selectivity issues or to detoxify some metals. Also, heterogeneous systems have been developed, aiming for reuse of the catalyst. Literature on those three types of catalysts is covered in this section.

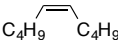
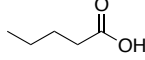
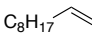
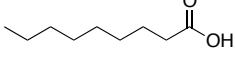
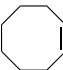
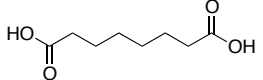
1.2.1.1 Metal salts and metal-oxo or peroxo catalysts

1.2.1.1.1 Ruthenium

Sharpless and co-workers have reported on the use of RuCl_3 in combination with NaIO_4 for oxidative cleavage of alkenes with $\text{CCl}_4/\text{MeCN}/\text{H}_2\text{O}$ mixtures as solvent.^[26] The Sharpless system has been widely explored^[31] and further developed by other groups (see 1.3.1.1.1). In this biphasic mixture the active species RuO_4 is generated, and after the oxidation of the substrate, the formed RuO_2 is reoxidized to RuO_4 . This reoxidation of RuO_2 is possible because of its high solubility in the solvent mixture, as it would otherwise precipitate in organic solvents^[24] and thus halt the catalytic cycle. Electron-rich olefins such as *cis*-5-decene (entry 1), 1-decene (entry 2) and *cis*-cyclooctene (entry 3) are converted into carboxylic acids with high isolated yields (75-89%), as shown by Carlsen *et al.* (Table 1.1).^[26] Ambient conditions and 2 h of reaction time are sufficient to reach complete substrate conversion. Only a slight excess of oxidant and 2.2 mol% catalyst are required. MeCN is crucial for the catalytic reaction: it is suggested that its ligating ability can prevent product inhibition. The strongly oxidizing conditions seem to rule out the use of organic ligands, such as phosphines, sulfides, amines or isonitriles, which can be oxidized themselves. Acetonitrile, on the other hand, can be regarded as a monodentate ligand resistant to the strongly oxidizing conditions of this system. A downside of the system is the use of toxic CCl_4 as cosolvent, as only MeCN shows no activity for cleavage.

Table 1.1. Oxidative cleavage of olefins with RuCl₃ and NaIO₄ in CCl₄/MeCN/H₂O^a by Carlsen *et al.*^[26]



Entry	Substrate	Product	Yield (%)
1 ^b	 1a	 1b	88
2	 2a	 2b	89
3	 3a	 3b	75 ^c

^a Reaction conditions: 2.2 mol% RuCl₃, 4.1 equiv. NaIO₄, CCl₄/MeCN/H₂O, 1-2 h reaction at ambient temperature, yield represented as isolated yield; ^b Both *cis*- and *trans*-alkenes; ^c Isolated as methyl esters, 4.5 equiv. NaIO₄.

The Sharpless system has been extensively studied and continuously improved. A modified system was applied to cleave electron-poor cyclic enolic olefins (C=C bond on the β-position) towards aldehydes, as reported by Torii *et al.*^[32] The protocol involves reaction in CCl₄/H₂O with 2.4 mol% RuO₂·2H₂O and 2.1 – 6 equiv. NaIO₄ with aldehyde yields between 35-97%. Likewise, it was shown that functional groups adjacent to the alkene remain untouched and that no over-oxidation to the acids occurs even at high oxidant loading. Longer reaction times are required nonetheless (10-50 h) compared to RuCl₃/NaIO₄ systems (Table 1.1).

Other alterations involved changing the oxidant to molecular oxygen instead of sodium periodate, using acetaldehyde and small amounts of pyromellitic acid in acetone for the conversion of simple olefins into carboxylic acids (Table 1.2), as shown by Kaneda *et al.*^[33] In this case, the oxidant peracetic acid is generated in-situ by reaction of acetaldehyde with O₂. Although a catalyst loading as low as 0.7 mol% can be used in this system, large amounts of acetaldehyde (23 equiv.) have to be present to activate molecular oxygen. The addition of pyromellitic acid (0.16 mol%) accelerates the autooxidation of acetaldehyde to give the peracetic acid, which in turn oxidizes RuO₂ to RuO₄. Slightly elevated temperatures (40 °C) are required with this system. Regarding the substrate scope of this system, styrene derivatives, the terminal alkenes 1-octene and 3-methyleneheptane show good conversions into the corresponding ketones or carboxylic acids (entries 4-5, 7), only the internal alkene *trans*-2-octene gives mediocre conversion to hexanoic acid (entry 6). Also, methyl methacrylate and the naturally occurring terpene isophorone were also cleaved successfully in high isolated yield without affecting the other functional groups (entries 8-9).

Chapter 1

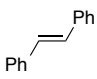
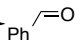
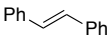
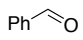
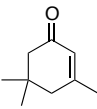
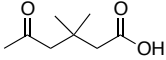
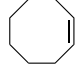
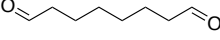
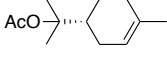
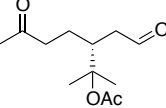
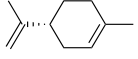
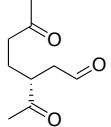
Table 1.2. Oxidative cleavage of olefins to carboxylic acids with RuO₂ and O₂^a by Kaneda *et al.*^[33]

Entry	Substrate	Product	Yield (%)
4			76
5			75
6			38
7			88
8			85
9			91

^a Reaction conditions: 0.7 mol% RuO₂, 23 equiv. CH₃CHO, 0.16 mol% pyromellitic acid, 40 °C, acetone, 3 h, yields represented as isolated yields.

RuCl₃ can also be used for the selective formation of aldehydes instead of carboxylic acids from styrene derivatives and electron-rich olefins, as shown by Yang *et al.*^[34] Using 3.5 mol% RuCl₃, 1.5 equiv. oxone and 4.7 equiv. NaHCO₃ in a mixture of MeCN and water, styrene derivatives are cleaved towards aldehydes (Table 1.3, entries 10-11). Oxone tends to over-oxidize the dialdehydes towards the carboxylic acids with cyclic alkenes, as under similar conditions, isophorone converts to the carboxylic acid with 2 equiv. of oxone (entry 12). Therefore, different conditions have to be applied on cycloalkenes in order to stop the oxidation at the aldehydes, being 3.5-5.2 mol% RuCl₃, 1.5 equiv. NaIO₄ and a biphasic mixture of 1,2-dichloroethane and water. This way, the electron-rich alkene *cis*-cyclooctene is transformed into palmetaldehyde at 70% isolated yield, which is an interesting industrial building block (entry 13). Another interesting substrate, the naturally occurring (*R*)- α -terpinyl acetate, smoothly converts into the keto aldehyde **12b** in 52% isolated yield (entry 14). The reaction with the terpene (+)-limonene shows that both double bonds within the molecule are oxidized when using 4 equiv. of NaIO₄, this results in diol and ketone side products being observed, nevertheless. Furthermore, only 38% isolated yields are observed of the diketone **13b** from limonene (entry 15). Both methods stand out in short reaction times (0.5-0.7 h).

Table 1.3. Oxidative cleavage of styrene derivatives and cyclic olefins to aldehydes with Ru and oxone/NaIO₄^a by Yang *et al.*^[34]

Entry	Substrate	Product	Yield (%)
10			73
11			85
12 ^b			94
13			70
14 ^c			52
15 ^{c,d}			38 ^e

^a Reaction conditions: 3.5 mol% RuCl₃, i) styrene derivatives: 1.5 equiv. oxone, 4.7 equiv. NaHCO₃, MeCN/H₂O (3:2 v/v), 0.5 h at ambient temperatures, ii) cycloalkenes: 1.5 equiv. NaIO₄, 1,2-dichloroethane:H₂O (1:1 v/v), 0.7 h at ambient temperature, yields represented as isolated yield; ^b 2 equiv. oxone used; ^c 5.2 mol% RuCl₃ used; ^d 70% substrate conversion ^e Diols and keto alcohols observed as byproducts, 4 equiv. NaIO₄ used.

For complex substrates containing several functional groups, stoichiometric amounts of RuO₄ are often required. Piccialli *et al.* applied stoichiometric amounts of RuCl₃ and NaIO₄ in acetone/water on several substituted steroidal alkenes, since catalytic amounts did not work (Table 1.4).^[35] Only tetra-substituted steroidal alkenes (entries 18-19) can be cleaved with this system. 3 β -Acetoxy-6-methylpregn-5-en-20-one (**14a**) can be quantitatively converted into its dialdehyde **14b** (entry 16), leaving the ester functionalities untouched. On the other hand, tetrasubstituted alkene 5 α -Cholest-8(14)-ene-3 β ,7 α -diol acetate (**15a**) renders only 44% yield of **15b**, with additional allylic oxidation byproducts observed (entry 17). Moreover, a series of related trisubstituted steroidal alkenes could not be cleaved with stoichiometric amounts of RuO₄, as diols or ketones are formed. Kinetic studies indicated that also in these reactions a Ru(VI)-cyclic diester moiety is involved as an intermediate (mechanism Aa, Scheme 1.4). Piccialli *et al.* later managed to isolate the Ru(VI)-diester moiety in the reaction with pinene.^[36] Workup

Chapter 1

in CCl_4 rendered the dialdehyde from the Ru(IV)-diester, whereas workup in acetone-water gave the α -keto-acid, which indicates the solvent dependence of this system.

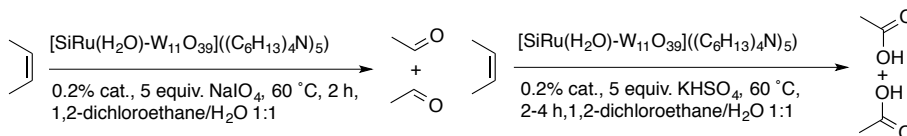
Table 1.4. Oxidative cleavage of tetrasubstituted steroidal alkenes with stoichiometric amounts of RuO_4^a by Piccilli *et al.*^[35]

Entry	Substrate	Time (min)	Product	Yield (%)
16		20		100
17 ^b		10		44 ^b

^a Reaction conditions: 1.38 equiv. $\text{RuO}_2 \cdot \text{H}_2\text{O}$, 8.69 equiv. NaIO_4 in acetone/ H_2O 1:1 (v/v), 10-20 minutes at ambient temperatures, yields represented as isolated yields; ^b Allylic byproducts formed, carbon atom marked with (*) transformed to ketone.

Ruthenium-polyoxometallates (POMs)^[37] can also be employed in oxidative alkene cleavage, as shown by Neumann and co-workers. $[\text{SiRu}(\text{H}_2\text{O})\text{-W}_{11}\text{O}_{39}][(\text{C}_6\text{H}_{13})_4\text{N}]_5$ (0.2 mol%) was found to be active in the transformation of alkenes into aldehydes with the use of NaIO_4 , or for the cleavage into carboxylic acids with KHSO_5 (Table 1.5).^[38] The quarternary tetrahexylammonium cation was essential for sufficient solubility of the catalyst in organic solvent, as the simple potassium cations make the POMs too hydrophobic. 98% benzaldehyde is formed in reactions with styrene and NaIO_4 . Likewise, 95% benzoic acid is formed with KHSO_5 as oxidant. Other oxidants such as iodobenzene or TBHP are less successful with this catalyst, in the sense that styrene oxide and phenylacetaldehyde are formed. Also, cyclohexene can be oxidatively cleaved into 67% isolated yield of adipic acid with KHSO_5 (entry 21). On the other hand, only 31% GC yield is obtained in reactions with NaIO_4 (entry 20). Furthermore, 1-octene only converts into heptanoic acid in 30% yield with KHSO_5 (entry 22), and reactions with NaIO_4 yield hardly any conversion (not shown). Especially the low catalyst loadings are remarkable with this system. Most other POMs reported for the oxidative cleavage of olefins are tungsten-based (see 1.2.1.1.2).

Table 1.5. Oxidative cleavage of alkenes into aldehydes and carboxylic acids with Ru-POM with NaIO₄ or KHSO₅^a by Neumann *et al.*^[37]



Entry	Substrate	Oxidant	Product	Yield (%)
18		10a NaIO ₄		10b 98
19		10a KHSO ₅		4b 95
20		16a NaIO ₄		16b 31
21		16a KHSO ₅		17b 67 ^b
22 ^c		5a KHSO ₅		5b 30

^a Reaction conditions: 0.2 mol% [SiRu(H₂O)-W₁₁O₃₉]((C₆H₁₃)₄N)₅, 5 equiv. oxidant, 60 °C, 2 h, 1,2-dichloroethane/H₂O 1:1 (v/v), yields are based on GC yields; ^b Isolated yield; ^c 4 h reaction.

More Ru-salts and Ru-oxides have been reported than coordination complexes (section 1.2.1.2.1), as, for example, under the applied conditions of the Sharpless system, ligands attached to the metal center often detach, as shown by Shoair and co-workers.^[26, 39] In cleavage of alkenes to carboxylic acids with *cis*-[RuCl₂(bipy)₂·H₂O] (bipy = 2,2'-bipyridine) with IO(OH)₅ as the oxidant under biphasic conditions (CCl₄-MeCN-H₂O) at ambient temperatures, RuO₄ appeared to be the active species.^[39] The yields obtained with this system are comparable to the method using RuCl₃·nH₂O and IO(OH)₅.^[40] Addition of the bipy ligand does, on the other hand, enable a tenfold lower catalyst loading of 0.5 mol%. Interestingly, the yields are generally higher than for the [RuCl₂(PPh₃)₃]/PhIO system reported by Muller *et al.*^[41]

1.2.1.1.2 Tungsten

One of the advantages of tungsten-based systems is that they can be used in combination with H₂O₂ in alkene oxidations. The metal oxide of tungsten that is capable of performing oxidative cleavage is tungstic acid, H₂WO₄, as shown by Oguchi *et al.*^[42] The cleavage of cyclohexene to adipic acid can be performed by 4 equiv. hydrogen peroxide and 5 mol% of tungstic acid in refluxing *t*-BuOH for 24 h. This way, 62% of adipic acid can be formed next to 18% diols. For example, tungstophoric acid, H₃PW₁₂O₄₀, generates 50% adipic acid and 22% diols, under similar conditions at a pH of 4-5.^[43] The system has a strong pH dependence: at neutral pH, tungstic acid gives lower adipic acid yields than H₃PW₁₂O₄₀. At pH between 2-3, the adipic acid yields are poorer with tungstic acid than at neutral pH.

Chapter 1

W-based POM systems commonly use phase-transfer agents for good solubility, yet the latter can also influence the selectivity of oxidative cleavage to a great extent. $\text{H}_3\text{PW}_{12}\text{O}_{40}$ can be refluxed in excess H_2O_2 and cetyl-pyridinium chloride to form $([\text{PW}_4\text{O}_{24}](\text{C}_5\text{H}_5\text{N}-\text{C}_{16}\text{H}_{33})_3)_3$, which is the peroxy form of tungstophoric acid (PCWP).^[44] For oxidative cleavage of alkenes, 2 mol% of PCWP in combination with 4 equiv. of H_2O_2 in refluxing *t*-BuOH enables the conversion of aliphatic and cyclic alkenes into carboxylic acids (Table 1.6), as shown by Ishii *et al.*^[43] This way, cycloalkenes and *trans*-2-octene can be cleaved in high yield. On the other hand, only mediocre conversion is obtained with 1-octene (entry 25). The observation of internal alkenes being cleaved more easily compared to terminal alkenes is in contrast to the observations of Kaneda^[33] for their $\text{RuO}_2/\text{O}_2/\text{CH}_3\text{CHO}$ system (Table 1.2). Mechanism B applies here (see Scheme 1.5). Although stoichiometric amounts of H_2O_2 are used in this system, the catalyst synthesis requires large excess of the oxidant. This oxidation system operates in a biphasic medium, where the PCWP complex is formed in the aqueous phase and transferred to the organic phase by the phase transfer agent, where the epoxidation takes place. A similar system using these POMs was also patented.^[45]

Table 1.6. Oxidative cleavage of terminal and internal linear olefins, and cyclic alkenes with PCWP and H_2O_2 ^a by Ishii *et al.*^[43] The arrows depict weak interactions.

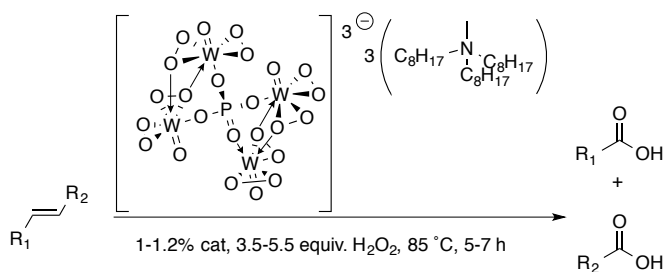
Entry	Substrate	Product	Yield (%)
23		16a $\text{HOOC}-\text{CH}_2-\text{CH}_2-\text{CH}_2-\text{COOH}$ 17b	70 ^b
24		17a $\text{CH}_3-\text{C}(=\text{O})-\text{CH}_2-\text{CH}_2-\text{CH}_2-\text{COOH}$ 18b	90
25		5a $\text{CH}_3(\text{CH}_2)_6-\text{COOH}$ 5b	45
26		6a $\text{CH}_3(\text{CH}_2)_5-\text{COOH}$ 6b	72

^a Reaction conditions: 2 mol% $([\text{PW}_4\text{O}_{24}](\text{C}_5\text{H}_5\text{N}-\text{C}_{16}\text{H}_{33})_3)_3$, 4 equiv. H_2O_2 , *t*-BuOH, reflux, 24 h, the yields are determined by GC-MS analysis; ^b Analyzed as methyl esters.

Methyltrioctylammonium can also be used as the counter-ion to peroxy phosphotungstate, replacing the cetylpyridinium cation. This catalyst can be applied in the

oxidative cleavage of a wide variety of unsaturated fatty acids (see section 1.3.1.1.3) and a series of alkenes with only 3.5-5.5 equiv. of hydrogen peroxide, as shown by Antonelli and co-workers.^[46] No solvent was required. The carboxylic acids can be isolated in good yields (77-85%, Table 1.7) with a series of internal and terminal aliphatic alkenes, styrene and cyclic alkenes. While cyclohexene is nicely converted to adipic acid (entry 28), *cis*-cyclooctene only yields 24% of suberic acid (entry 30). Also, 1,7-octadiene converts in good yield to adipic acid (entry 34).

Table 1.7. Oxidative cleavage of W-based POM of internal aliphatic alkenes towards carboxylic acids^a by Antonelli *et al.*^[46]



Entry	Substrate	Product	Yield (%)
27 ^b			87
28			87
29 ^c			85
30			24
31 ^b			80
32			80
33			77
34			60

^a Reaction conditions: 1-1.2 mol% [(PW₄O₂₄)](Me(C₈H₁₇)₃N)₃, 3.5-5.5 equiv. H₂O₂, 85 °C, 5-7 h, yields represented as isolated yields; ^b 5.5 equiv. H₂O₂; ^c 3.5 equiv. H₂O₂.

The sodium salt of tungstic acid (Na₂WO₄) is also a suitable catalyst for oxidative cleavage. This is a much more convenient source than its acidic or peroxy form and can be applied at lower catalyst loadings than systems with H₂WO₄ for the cleavage of alkenes into carboxylic acids, as shown by Noyori *et al.*^[47] The cleavage of cyclic olefins can be

Chapter 1

performed under aqueous biphasic conditions with 1 mol% of catalyst in very high isolated yields. No organic solvent is needed in the system. The quarternary ammonium salt methyl-trioctyl ammonium hydrogen sulfate is employed as the phase transfer agent at relatively high temperatures (75-90 °C, Table 1.8). Only a slight excess of H₂O₂ (4.4 equiv. compared to 4.0 in theory) is needed. The cyclopentene and the relatively more electron-poor tetrahydrophthalic anhydride and tetrahydrophthalic acid are selectively cleaved (entries 35-37). On the other hand, the reaction with phenanthrene (entry 38) results only in a 41% isolated yield. The authors also report that the reaction with *cis*-cyclooctene renders predominantly cyclooctene oxide, since the epoxide is resistant to acid-catalyzed hydrolysis under these conditions.

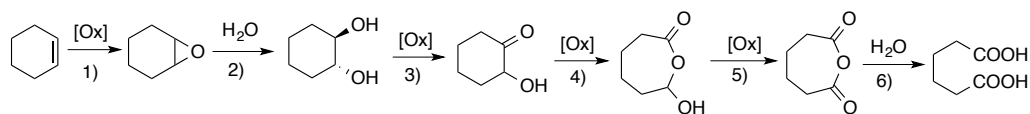
Table 1.8. Oxidative cleavage of cycloalkenes by the Na₂WO₄/H₂O₂/QHSO₄ system^a developed by Noyori *et al.*^[47]

Entry	Substrate	Product	Yield (%)
35	21a	HOOC-CH ₂ -CH ₂ -CH ₂ -COOH 21b	90
36	22a	22b	91
37	23a	23b	96
38	24a	24b	41

^a Reaction conditions: 1 mol% Na₂WO₄, [HSO₄](MeN(C₁₈H₃₇)₃), 4.4 equiv. H₂O₂ 75-90 °C, 8 h, yield represented as isolated yields.

A six-step reaction mechanism has been proposed (Scheme 1.7) for this system comprising: 1) olefin oxidation to the epoxide, 2) ring-opening of the epoxide by water to form the *trans*-diol, 3) diol oxidation to an α -keto alcohol, 4) Baeyer-Villiger oxidation to give the 2-hydroxy-6-hexanolide, 5) further oxidation to the anhydride, and finally 6) hydrolysis to yield adipic acid. Several of these steps are facilitated by the acidic conditions (hydrogensulfate present). It is noteworthy that no aldehyde intermediate is thought to be involved prior to formation of the carboxylic acid, unlike in many other cases. This system was presented as a green alternative to the industrial process that currently transforms benzene to a mixture of cyclohexanol and cyclohexanone, which is

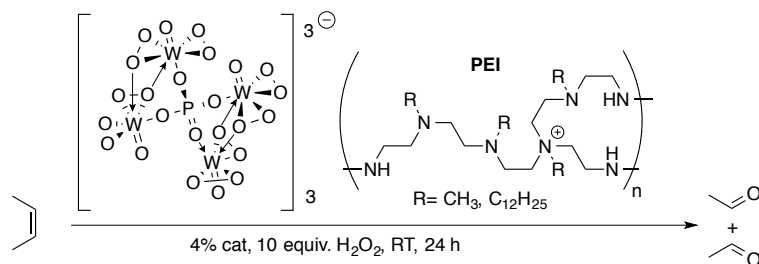
further cleaved using concentrated nitric acid to adipic acid, producing stoichiometric amounts of the greenhouse gas N₂O.



Scheme 1.7. Mechanism W-based of POM oxidative cleavage of cycloalkenes to carboxylic acids by Noyori *et al.*^[47]

Most of the examples involving tungsten and hydrogen peroxide form carboxylic acids from alkenes. The use of alkylated polyethyleneimine (PEI) in conjunction with PCWP (addition of an excess H₂O₂ to H₃PO₄ and Na₂WO₄ in this case), on the other hand, can selectively cleave styrene into 96% benzaldehyde (Table 1.9), as shown by Haimov *et al.*^[48] This method requires 4 mol% of catalyst loading, 10 equiv. of hydrogen peroxide, 70 °C temperature and 24 h of reaction time. On the other hand, cyclic alkenes are not cleaved, however, but only oxidized towards the epoxide (entry 40).

Table 1.9. Oxidative cleavage of W-based POM of styrene derivatives and cyclic alkenes into aldehydes^a by Haimov *et al.*^[48]



Entry	Substrate	Product	Yield (%)
39	Ph-CH=CH ₂ (10a)	Ph-CHO (10b)	96 ^b
40	Cyclohexene (3a)	Cyclohexene oxide (25b)	99

^a Reaction conditions: 4 mol% catalyst, 10 equiv. H₂O₂, 24 h at ambient temperatures, yields are GC yields; ^b 3% styrene oxide observed.

Overall, the nature of the phase-transfer agent has a profound influence on the solubility and the selectivity of W-based oxidative cleavage systems. Other developments with this systems involve the use of microwave irradiation. This enables the reaction with tungstic acid and hydrogen peroxide to be performed in less time and at lower catalyst concentration, as shown by Freitag *et al.*^[49] Adipic acid can be obtained in 68% isolated yield from cyclohexene with 1 mol% of tungstic acid and 1 mol% of trioctylammonium hydrogen sulfate after 90 minutes at 400 W. On the contrary, the conventional method

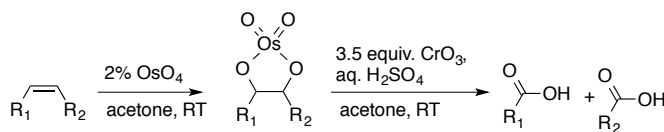
Chapter 1

using heating (75 °C-90 °C) takes more than 9 h to generate 83% yield. In this way, time consumption and energy usage can be brought down for the oxidation of cyclohexene to the diacids. Styrene can also be transformed into benzoic acid with 77% yield with 2 mol% catalyst within 45 minutes.

1.2.1.1.3 Osmium

OsO₄ is generally used less for oxidative cleavage, but more as a dihydroxylation reagent,^[50] since it is a weaker oxidant than its Ru analogue. The vicinal diols resulting from an olefin *cis*-dihydroxylation reaction can nonetheless in turn be cleaved in sequential reactions (mechanism Ab, Scheme 1.4).^[9] The use of osmium in this sense has become quite popular since low catalyst loadings can be used, as illustrated in the examples listed below.

OsO₄ can be used in only 2 mol% catalyst loading with stoichiometric amounts of chromium(VI) oxide in aqueous sulfuric acid (Jones' agent) in acetone for cleavage of alkenes to carboxylic acids, as reported by Henry *et al* (Scheme 1.8).^[51] Mechanism Ab applies here (Scheme 1.4). The acidic conditions facilitate the oxidative cleavage of the diols. Nevertheless, the large amount of chromium used is not beneficial in this method.



Scheme 1.8. Reaction sequence of oxidative olefin cleavage using OsO₄ and Jones' reagent as reported by Henry *et al*.^[51]

OsO₄ can also be applied as sole transition metal in the oxidative cleavage on a variety of alkenes, as shown by Travis *et al*,^[52] when oxone is the secondary oxidant. OsO₄ (1 mol%) with 4 equiv. of oxone yields carboxylic acids from almost any alkene in very high yields (Table 1.10). These reactions are done within 3 h at ambient temperature in dimethylformamide (DMF). Styrene, internal and terminal aliphatic alkenes and *trans*-dimethylstilbene can be converted into their corresponding acids in high isolated yield (entries 41-45). The terpene (-)-isopulegol provides a mediocre yield of its ketone, whereas the phenyl-protected analogue can be converted into the ketone with 80% isolated yield (entries 46-47). Finally, (+)-pulegone converts in 67% isolated yield into 3-methyl-adipic acid via the α -diketone as intermediate prior to ring-opening of the cyclohexane moiety (entry 48). No reaction occurs with diols, meaning that no dihydroxylation occurs in this Os-system, unlike most methods involving this metal. It was therefore proposed that olefin cleavage proceeded directly, as in the case of ozonolysis (mechanism Aa, Scheme 1.4).

Table 1.10. Oxidative cleavage of a variety of olefins towards carboxylic acids and ketones with OsO₄ and oxone^a by Travis *et al.*^[52]

Entry	Substrate		Product		Yield (%)
41		10a		4b	94
42		16a		17b	94 ^b
43		2a		2b	93
44		25a		5b	93
45		26a		26b	85
46		27a		27b	44
47		28a		28b	80
48		29a		29b	67

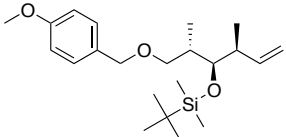
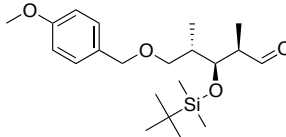
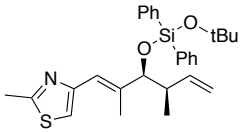
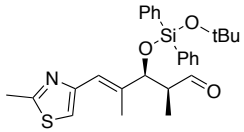
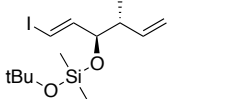
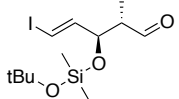
^a Reaction conditions: 1 mol% OsO₄, 4 equiv. oxone, DMF, 3 h at ambient temperatures, yield represented as isolated yields; ^b Determined by GC.

The use of OsO₄ (5 mol%) with NaIO₄ (2.2 equiv.) for 2 h at ambient temperature in ether:H₂O 1:1 (v/v) has already known for a long time as the Lemieux-Johnson oxidation of alkenes into aldehydes,^[30] yet recently it has been shown that the complexity of the alkene structure can be increased without the system losing its selectivity, making it a useful methodology for, e.g., drug syntheses. Such multi-functionalized substrates require the use of a mild and selective oxidant in order to leave other functionalities untouched (Table 1.11). The combination of osmium and sodium periodate is more selective for the transformation of an alkene to an aldehyde than ozonolysis, as the latter also reacts with other functional groups present in the complex substrates. Although toxic and expensive, osmium-based systems are thus still used when the substrate is very sensitive to side reactions, and when absolute purity of the product is of importance. Unlike the Piccialli-system,^[35] for which Ru is required in stoichiometric amounts for the very functionalized and complex steroidal alkenes, Os can be used with certain complex olefins in catalytic amounts: For the synthesis of (+)-dicodermolide, for instance, the protected alkene **30a**

Chapter 1

smoothly converts to the aldehyde **30b** (entry 49), as shown by Francavilla *et al.*^[53] Taylor *et al.*^[54] reported the conversion of another protected alkene **31a** to the aldehyde **31b** in the synthesis of epothilone analogues (entry 50), and Wang *et al.*^[55] transformed **32a** into **32b** (entry 51), during the synthesis of the central fragment of oxazolomycin.

Table 1.11. Oxidative cleavage of alkenes with OsO₄ and NaIO₄ in multi-step syntheses.^[53-55]

Entry	Substrate	Product	Yield (%) ^a
49			71
50			65
51			60

^a Isolated yields of the aldehyde^[53-55] after the Lemieux-Johnson^[30] oxidation: OsO₄ (5 mol%), NaIO₄ (2.2 equiv.), ether/H₂O 1:1 (v/v), ambient temperature for 2 h.

Regarding other complex functionalized alkenes, the addition of a base such as 2,6-lutidine (2,6-dimethylpyridine) to the OsO₄/NaIO₄ system can increase the selectivity towards aldehydes and tolerates various functionalities, as shown by Yu *et al.*^[56] The reactions of **33a** and **34a** with OsO₄ (2 mol%), 4 equiv. of NaIO₄ in dioxane:H₂O 3:1 (v/v) renders primarily α -hydroxy ketones when no base is added (entries 52-53, Table 1.12). Buffering the pH around 7 reduces the formation of the α -hydroxy ketones to almost zero, but the rate of the cleavage reaction is very slow under these conditions (not shown). On the other hand, the addition of pyridine increases the rate, yet epimerization occurs as a side reaction. Whereas 2,6-di-*t*-butylpyridine has no effect, 2,6-dimethylpyridine both increases the rate and inhibits epimerization. This way, substrate **34a** can be converted quantitatively into its aldehyde **34b** (entry 54), whereas the other substrates generated good isolated yields. In all cases, the yield of the aldehyde product increases compared to when the base was absent. Moreover, the substrates' various functional groups remain unaltered. Additionally, the base additive can be used to prevent decomposition of acid-labile groups. Furthermore, it is one of the few systems where ozonolysis yields unsatisfactory results, because of the presence of *p*-methoxybenzyl and trisbenzylsilyl protective groups that can be affected by O₃.

Table 1.12. Oxidative cleavage of highly-functionalized olefins towards aldehydes with OsO₄, NaIO₄ and 2,6-lutidine as base^a by Yu *et al.*^[56]

Entry	Substrate	Product	Time (h)	Yield (%)	Yield (%) ^b
52			1	44 ^c	83
53			20	34 ^c	99
54			3	42 ^c	71
55			24	28 ^c	77

^a Reaction conditions: 2 mol% OsO₄, 4 equiv. NaIO₄, 2 equiv. 2,6-lutidine, dioxane/H₂O 3:1 (v/v), 1-24 h at ambient temperatures, yields represented as isolated yields; Bn = benzyl, PMB = *p*-methoxybenzyl, TBS = *t*-butyldimethylsilyl, TES = triethylsilyl; ^b 2,6-lutidine added; ^c α -hydroxy ketones observed.

Other systems only briefly covered here involve literature to decrease the toxicity of osmium systems, by application of much easier-to-handle precursors such as OsCl₃, K₂OsO₄·2H₂O or polymer-bound OsO₄ instead of the toxic OsO₄ for the oxidative alkene cleavage of styrene derivatives into their carboxylic acids, as shown by Whitehead *et al.*^[57] The conditions involve 1 mol% of catalyst with 4 equiv. of oxone in DMF at ambient temperature. The downside is that longer reaction times are required (24 h) than with OsO₄. Also, another system comprises catalyst reuse studies of the OsO₄/NaIO₄ homogeneous system, by trapping the catalyst in an aqueous layer, as reported by Kim *et al.*^[58] The conditions are 1 mol% OsO₄ with NaIO₄ (0.5 equiv.) and NaClO₂ (2 equiv.) in MeCN/H₂O 1:1 (v/v) at ambient temperature for 14 h. Then, isopropyl alcohol (1.5 equiv.) and KOH can be added and stirred for additional 8 h to dissolve the catalyst in the aqueous phase and recover it by extraction. Likewise, styrene is cleaved to benzaldehyde with negligible activity loss in five consecutive runs.

1.2.1.1.4 Indium

InCl₃ is a relatively cheap and non-toxic reagent, and can be used for reactions of a variety of olefins with 4 equiv. TBHP in water for the formation of carboxylic acids, as shown by Ranu *et al.* (Table 1.13)^[59] The conditions involve 90 °C and 9 h reaction time. The

Chapter 1

advantage of this homogeneous system is that InCl_3 can be reused six times without loss of catalytic efficiency, by simple extraction of the catalyst into the aqueous phase upon addition of ethyl acetate. Styrene, 1-octene and trisubstituted substrate 1-methylcyclohexene are cleaved to the acids in high yield. *Cis*-cyclooctene converts nicely into suberic acid, which was found to crystallize in high isolated yields from the reaction mixture under the applied conditions. Moreover, the system is compatible with sensitive moieties such as amides and methyl- or tert-butyl carboxylic esters in **37a** and **38a** (entries 60-61). The influence of the oxidant is shown by the fact that yields of the carboxylic acid do not exceed 25% upon changing TBPH to H_2O_2 . The reaction is thought to proceed via mechanism B (Scheme 1.5).

Table 1.13. Oxidative cleavage of a variety of alkenes towards carboxylic acids with InCl_3 and TBHP in water at elevated temperatures^a by Ranu *et al.*^[59]

Entry	Substrate	Product	Yield (%)
56			88
57			81
58			94
59			84
60			78
61			68

^a Reaction conditions: 20 mol% InCl_3 , 4 equiv. TBHP, H_2O , 9 h, 90 °C, yields represent isolated yields.

1.2.1.1.5 Palladium

Palladium is one of the few metals that can be used in conjunction with molecular oxygen as oxidant for oxidative cleavages of alkenes. $\text{Pd}(\text{OAc})_2$ can be used in 2 mol% with O_2 to convert various alkenes into aldehydes, as shown by Wang and co-workers.^[60] No organic solvent is used in this system, only water. On the other hand, high temperatures, high oxygen pressure (8 atm) and 20 mol% of a strong acid additive paratoluenesulfonic acid (PTSA) are needed for satisfying yields. Concerning the metal precursors, $\text{Pd}(\text{OAc})_2$ outperforms PdCl_2 and Pd_2dba_3 as the Pd source. This system efficiently cleaves styrene

into 88% benzaldehyde (Table 1.14), *cis*-stilbene and acrylates (entries 64-65) show mediocre aldehyde formation. This method can also convert terminal aliphatic olefins into their aldehydes, as shown with 1-octene (entry 67, 74% isolated yield). Tetra-substituted olefins like tetraphenylethylene (entry 66) can also be cleaved, albeit in low yields. Mechanism Ab (Scheme 1.4) is proposed for this system, involving *cis*-diols as intermediates that can be obtained in either basic or acidic media.

Table 1.14. Oxidative cleavage of a variety of alkenes with a Pd(OAc)₂, O₂ and a Brønsted acid in water at elevated temperatures^a by Wang *et al.*^[60]

Entry	Substrate		Product		Yield (%)
62		10a		10b	88
63		11a		10b	53
64		39a		39b	67
65		40a		40b	69
66		41a		41b	23
67		5a		42b	74

^a Reaction conditions: 2 mol% Pd(OAc)₂, O₂ (8 atm), 20 mol% paratoluenesulfonic acid (PTSA), 24 h, 100 °C, yield represent isolated yields.

1.2.1.2 Metal complexes

So far, with few exceptions only the use of metal salts has been addressed. A powerful tool in organometallic/coordination chemistry is applying ligands for electronic and steric modulation. However, care should be taken as the ligand backbone can decompose or get oxidized itself under the applied reaction conditions.

1.2.1.2.1 Ruthenium

Coordination of 2,9-dimethyl-1,10-phenanthroline (dmp) to Ru generates a species mild enough to be used in conjunction with hydrogen peroxide for oxidative cleavages of alkenes into aldehydes, as shown by Kogan *et al.*^[61] Such examples are rare as high-valent metal compounds with high redox potentials often dismutate H₂O₂. As little as 1 mol% of [*cis*-Ru(II)(dmp)₂(H₂O)₂](PF₆)₂ can be used with 10 equiv. of hydrogen peroxide at 50 °C for 6 h in MeCN in order to convert terminal olefins into aldehydes. As opposed to metal salts that form RuO₄ (section 1.2.1.1.1), the active species [*cis*-Ru(VI)(O)₂(dmp)₂](PF₆)₂ is

Chapter 1

formed in-situ by the oxidant. Amongst the chosen substrates depicted in Table 1.15, entries 69 and 70 show the significant preference for terminal alkenes compared to internal, secondary alkenes. With 4-vinylcyclohexene (entry 71), and limonene (entry 72), only the exocyclic double bonds are cleaved, thus allowing regioselectivity in diene cleavage. However, the yields remain low. This regioselectivity allows for substrates containing both internal and terminal double bonds to react only at terminal sites, even with excess of oxidant, whereas the 'naked' RuO₄ species cleave all double bonds present. It has been proposed that [cis-Ru(II)(dmp)₂(H₂O)₂]²⁺ has a hindered active site as, where terminal alkenes can approach better than internal ones.^[62]

Table 1.15. Oxidative cleavage of predominantly terminal alkenes in MeCN towards aldehydes using a Ru(II)-dmp complex and H₂O₂^a by Kogan *et al.*^[61]

1% [cis-Ru(II)(dmp)₂(H₂O)₂](PF₆)₂
10 equiv. H₂O₂, 50 °C, 6 h, MeCN

Entry	Substrate	Product	Yield (%)
68			92
69			80
70			18
71			21 ^b
72			11 ^c

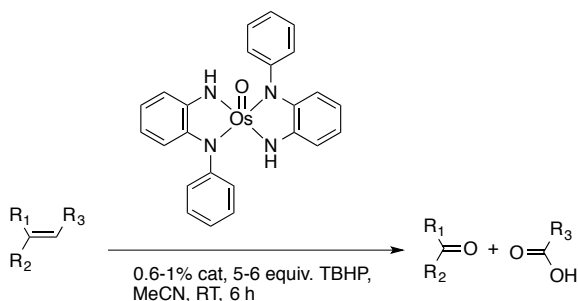
^a Reaction conditions: 1 mol% [cis-Ru(dmp)₂(H₂O)₂](PF₆)₂, 10 equiv. H₂O₂, MeCN, 50 °C, 6 h, yields are GC yields; ^b 97% selectivity, enols and enones observed; ^c 95% selectivity, enols and enones observed.

1.2.1.2.2 Osmium

[OsO(N-aryl-1,2-arylenediamine)₂] is a discrete metal coordination complex of Os that is much less toxic than OsO₄, since Os(VI) is used instead of Os(VIII), and the system can be used with TBHP instead of oxone to convert olefins into carboxylic acids, as shown by Samanta *et al.*^[63] The ligand is formed in-situ on the Os center by *ortho*-C-N fusion of arylamines to give rise to [OsO(N-aryl-1,2-arylenediamine)₂] under inert atmosphere. The complex is pentacoordinated with a distorted square pyramidal geometry. The system with 0.6-1.0 mol% catalyst loading and 5-6 equiv. TBHP in MeCN is able to convert styrene, cyclohexene and 1-octene to the corresponding carboxylic acids (Table 1.16). Also, phenanthrene (entry 76) and the naturally occurring chalcone derivative **44a** (entry 77) can be converted conveniently. Experiments under similar conditions with OsO₄ yield

a mixture of products, showing that indeed the coordination complex is the active species and that it can outperform the simple metal-oxo species.

Table 1.16. Oxidative cleavage of various olefins with an Os-complex and TBHP^a by Samanta *et al.*^[63]



Entry	Substrate	Catalyst	Product	Time (h)	Yield (%)
73		10a		8	80
74		16a		6	86
75		5a		7	80
76		24a		10	65
77		44a		8	82

^a Reaction conditions: 0.6-1.0 mol% [OsO(N-aryl-1,2-arylenediamine)₂], 5-6 equiv. TBHP, MeCN, 6 h at ambient temperatures, yields represent isolated yields.

1.2.1.2.3 Rhenium

Rhenium is another example of a metal that is able to perform oxidation reactions with hydrogen peroxide, for it has little affinity to disproportionate the oxidant. Methyltrioxorhenium (MTO) is a commercially available coordination complex that is used for the oxidation of olefins^[64, 65] with H₂O₂, where the oxidation of the alkene can be tuned to stop at the aldehyde level at elevated temperatures, as reported by Herrmann and co-workers,^[66] unlike the examples of tungsten that predominantly yield carboxylic acids. The use of the catalyst can be restricted to 1 mol%, and even an excess of H₂O₂ (6 equiv.) can be used to still obtain aldehydes after 7 h at 60 °C, with MgSO₄ present (Table 1.17). Nevertheless, diols are still formed as side-products with this protocol. Formally, the hydrogen peroxide forms TBHP from *t*-BuOH. The catalytically active species is

Chapter 1

bis(peroxo)rhenium and is labile to hydrolysis, therefore MgSO_4 is added. *t*-BuOH as the solvent generates lower amounts of aldehydes than methyltertbutylether (MTBE) (entries 78-81). Also, the fatty terminal alkene 1-octadecene can be converted using the MTO system into 54% heptadecanal (entry 82). Again, the removal of water seems to be important: without drying agent (MgSO_4), diols are formed selectively in *t*-BuOH at 70% substrate conversion (entry 81). However, in organic solvents that are immiscible with water, e.g. MTBE, only a slight drop in the aldehyde yield occurs when omitting MgSO_4 (entry 80). Mechanism B is proposed (Scheme 1.5), two competing routes yield either the hydrolyzed diol adduct or the aldehyde. The diol does hardly transform into the aldehyde under these conditions. With additional catalyst and oxidant, the selectivity can be shifted towards the aldehydes.

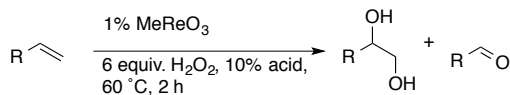
Table 1.17. Oxidative cleavage of aliphatic terminal alkenes with MeReO_3 and H_2O_2 in organic solvents into a mixture of aldehydes and diols^a by Hermann *et al.*^[66]

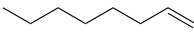
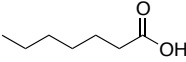
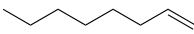
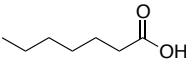
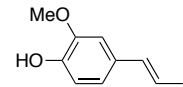
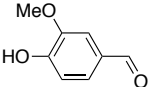
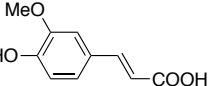
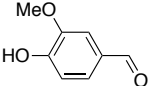
Entry	Substrate	Product	Solvent ^b	Yield (%)
78		42b	MTBE	65
79		42b	<i>t</i> -BuOH	35
80		42b	MTBE ^c	58
81		42b	<i>t</i> -BuOH ^c	0 ^d
82	$\text{C}_{16}\text{H}_{33}$	$\text{C}_{16}\text{H}_{33}$ 47b	MTBE	54

^a Reaction conditions: 1 mol% MeReO_3 , 6 equiv. H_2O_2 , solvent, 60 °C, 7 h, yields determined by GC-MS, diols formed as byproducts; ^b MgSO_4 used as drying agent; ^c No drying agent; ^d 70% substrate conversion.

This system can also be tuned to obtain carboxylic acids instead. Reactions of terminal fatty olefins with a Brønsted acid in a solvent-free system form carboxylic acids. The conditions involve 6 equiv. of hydrogen peroxide and 1-octene as substrate, 2 h reaction time, 1 mol% of catalyst and 10 mol% of Brønsted acid at 60 °C. Again, diols are observed as side products (Table 1.18). HBF_4 generates slightly more carboxylic acid than HClO_4 . Styrene derivatives *trans*-isoeugenol and *trans*-ferulic acid quantitatively convert to the aldehydes under similar conditions (entries 85-86), and thus differ in reactivity from the terminal aliphatic alkenes.

Table 1.18. Oxidative cleavage of aliphatic terminal alkenes into a mixture of carboxylic acids and diols in a solvent-free system using a Brønsted acid with MeReO₃ and H₂O₂^a by Herrmann *et al.*^[66]



Entry	Substrate		Product		Yield (%)
83 ^b		5a		5b	73 ^d
84 ^c		5a		5b	68 ^d
85		46a		48b	99
86		47a		49b	99

^a Reaction conditions: 1 mol% MeReO₃, 6 equiv. H₂O₂, 10 mol% acid, 60 °C, 2 h, yields determined by GC-MS; ^b HBF₄ added; ^c HClO₄ added; ^d Diols observed.

1.2.1.2.4 Gold

[Au(I)Cl(neocuproine)] (neocuproine = 2,9-dimethyl-1,10-phenanthroline) enables the formation of aldehydes from styrene derivatives with TBHP in aqueous solution, as shown by Xing and co-workers.^[67] 2.5 equiv. of oxidant with 5 mol% catalyst are needed to cleave styrene derivatives at 90 °C. Interestingly, the reaction can be performed in either toluene or water, showing similar activity. The electronic nature of the substrate has a large influence on the outcome with this system. 1,1-diphenyl ethylene can be readily converted to its ketone within 3 h, whereas the more electron-rich α -methyl styrene shows a lower conversion to the ketone after 36 h (entries 87-88, Table 1.19). *Trans*- β -methyl styrene, on the other hand, converts in higher yield to benzaldehyde than styrene does (entries 89-90). 2-(1-phenylvinyl)thiophene **51a** can also be cleaved with this system, albeit at somewhat lower yields (entry 91). No over-oxidation to acids is found. The proposed mechanism does not proceed via epoxidation with this system. Free radicals are thought to be involved, as addition of the radical-inhibitor TEMPO inhibits the reaction. This corresponds to a mechanism of type C (Scheme 1.5), yet no further mechanistic details were specified. Interestingly, similar reactivity has not been documented for simple Au-salts.

Chapter 1

Table 1.19. Oxidative cleavage of styrene derivatives into their carbonyl compounds with a gold catalyst and TBHP^a by Xing *et al.*^[67]

Entry	Substrate	Product	Time (h)	Yield (%)
87			3	93
88			36	39
89			36	56
90			36	66
91			24	53

^a Reaction conditions: 5 mol% [AuCl(neocuproine)], 2.5 equiv. TBHP, H₂O, 90 °C, isolated yields.

1.2.1.3 Heterogeneous catalysts

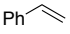
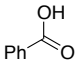
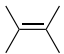
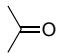
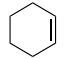
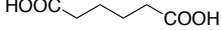
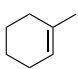
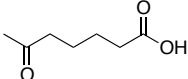
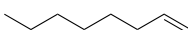
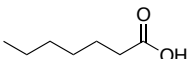
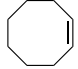
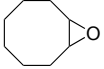
Various solids have been used to anchor the active catalyst to form a heterogeneous, supported catalyst, or as additives to aid a homogeneous systems in cleaving double bonds. Especially reusability, important for cost issues and environmental reasons, has been the driving force for the development of such heterogeneous catalysts in oxidative alkene cleavage reactions.

1.2.1.3.1 Mo and W polyoxometallates

Mo and W POMs can be immobilized on oxide supports for oxidative cleavage of various alkenes with hydrogen peroxide, as shown by Brooks *et al.*^[68] 12-molybdophosphoric (PMA), 12-phosphotungstophoric (PWA) or 6-molybdo-6-tungstophosphoric acid (PMWA) can be deposited onto magnesium, aluminium or zinc oxide and subsequently calcined in order to make an active catalyst. In the preparation of the catalysts, the POMs are either deposited onto preformed oxides of Mg or Al, or the catalyst is co-precipitated during the formation of the hydroxide. Calcination temperatures of either 150 °C or 500 °C are used. These heterogeneous catalysts are able to cleave styrene derivatives, and aliphatic alkenes to carboxylic acids, using the poorly nucleophilic solvent 2-methyl-2-propanol at 60 °C with 3-4 equiv. H₂O₂ (Table 1.20). Tetramethylethylene, 1-octene, cyclohexene, 1-methyl-cyclohexene or styrene all give excellent isolated yields of the acid using the co-precipitation method for PMA, PWA and PMWA (entries 92-96). *Cis-*

cyclooctene, on the other hand, can only be converted into its epoxide in 30% yield, with 50% substrate conversion (entry 97), using the PMWA catalyst deposited on preformed Al oxides. Interestingly, Mo is inactive as metal salt in homogeneous oxidative alkene cleavage reactions,^[43] yet is able to convert cyclohexene (PMA) in 90% into adipic acid when used as a heterogeneous catalyst (entry 94). Mechanism B applies here (Scheme 1.5). Finally, the catalysts are reusable, but generally lose their activity after the fourth consecutive cycle.

Table 1.20. Oxidative cleavage of various alkenes using POM with hydrogen peroxide on oxide supports^a by Brooks *et al.*^[68]

Ent.	Substrate	Product	Time (h)	POM ^b	Yield (%)
92		10a 	4b 24	PWA:Al:500/4	90
93		52a 	52b 8	PMWA:Mg:150/0.5	91
94		16a 	17b 24	PMA:Al:150/0.5	90
95		17a 	18b 24	PWA:Al:150/0.5	96
96		5a 	5b 4	PMWA:Mg:150/0.5	100
97 ^c		3a 	25b 10	PMWA:Al:150/0.5	30

^a Reaction conditions: 50 wt% catalyst, co-precipitation during formation of the hydroxide, 3-4 equiv. H₂O₂, 60 °C, 2-methylpropan-2-ol, yields represent isolated yields; ^b Nature of the POM: oxide support : calcination temperature (°C)/ calcination time (h); ^c Deposited onto preformed oxides.

1.2.1.3.2 Ruthenium

Ru nanoparticles supported on hydroxyapatite (nano-RuHAP) can be used as a recyclable solid catalyst for oxidative cleavage of styrene derivatives and cyclic alkenes into aldehydes with sodium periodate, as shown by Ho *et al.*^[69] 4 mol% catalyst loading and 2 equiv. of NaIO₄ are sufficient to transform a variety of alkenes into their aldehydes in 1,2-dichloroethane (Table 1.21). This heterogeneous system is very active at ambient temperatures, as opposed to Mo and W systems. *Trans*-stilbene converts nicely to the corresponding aldehydes, yet styrene forms mediocre amounts of benzaldehyde and 1-dodecene only forms 10% aldehyde at 12% conversion (entries 98-99, 101). Also,

Chapter 1

cyclohexene produces 51% isolated yield of adipaldehyde (entry 100), showing that this is one of the few examples able to isolate this valuable dialdehyde. Another drawback of the system is that tri- or tetra-substituted alkenes prove to convert poorly (not shown). Yet, when oxone was used instead of periodate, good yields of the carboxylic acids can be obtained, as the terpenoids isophorone and (+)-pulegone can be nicely converted to their corresponding carboxylic acids with 2.5 equiv. of oxone in MeCN:H₂O 3:2 (entries 102-103). Catalyst recycling studies show 20-30% weight loss after each run. This weight loss is attributed to slow dissolution of the HAP support in the acidic reaction medium.

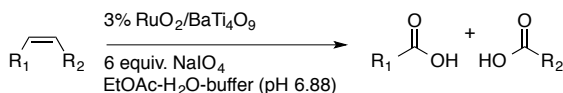
Table 1.21. Oxidative cleavage of various olefins towards aldehydes with Ru nanoparticles on hydroxyapatite and periodate^a by Ho *et al.*^[69]

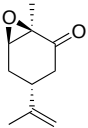
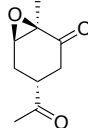
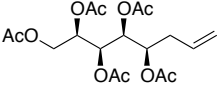
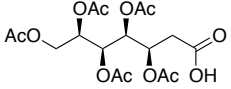
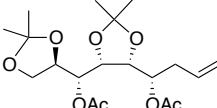
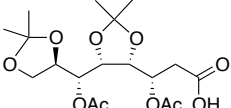
Entry	Substrate	Product	Time (h)	Yield (%)
98			2	91
99			2	66
100			3	51 ^b
101			12	10 ^c
102 ^d			7	85 ^b
103 ^d			3	84 ^b

^a Reaction conditions: 4 mol% nano-RuHAP, 2 equiv. NaIO₄, 1,2-dichloroethane, 2-12 h at ambient temperature, yields are GC yields; ^b Isolated yield; ^c 12% substrate conversion; ^d Reaction conditions: 2.5 equiv. oxone, 7.7 equiv. NaHCO₃, MeCN:H₂O 3:2 (v/v).

Ruthenium also exists as a composite material RuO₂/BaTi₄O₉, which can catalytically convert a series of naturally occurring, functionalized alkenes into carboxylic acids under ambient conditions using NaIO₄ in ethyl acetate and water at neutral pH, as shown by Okumoto *et al.*^[70] The system uses 3 mol% of catalyst loading, yet needs an excess of oxidant with 6 equiv. of NaIO₄ (Table 1.22). The excess of periodate shows that the functionalities remain untouched, nevertheless. Both ketones and carboxylic acids can be isolated after the reaction. The neutral pH is essential given the presence of acid-labile epoxide **54a**. The sugar derivatives **55a** and **56a** also undergo smooth oxidation (entries 105-106). These substrates also show that this system is active with terminal alkenes, unlike the report by Ho *et al.*^[69] Catalyst reuse experiments can be conducted by removing the product by decantation and adding more oxidant and substrate: about 25% activity loss is observed.

Table 1.22. Oxidative cleavage of terpenoids and sugar derivatives with RuO₂/BaTi₄O₉ with periodate and a neutral pH buffer^a by Okumoto *et al.*^[70]



Entry	Substrate	Product	Time (h)	Yield (%)
104			21	84
105			4	76
106			11	98

^a Reaction conditions: 3 mol% RuO₂/BaTi₄O₉, 6 equiv. NaIO₄, EtOAc/H₂O at ambient temperatures, yields represent isolated yields.

A different approach to the synthesis of a heterogeneous Ru catalyst is by deposition on charcoal (Ru/C). This way, only 1 mol% of catalyst loading and 1.1 equiv. of NaIO₄ are able to convert a series of alkenes into aldehydes, as shown by Kumar *et al.*^[71] The reactions are conducted in an ice-bath in MeCN:OAcEt:H₂O 1:1:1 (v/v). Styrene renders benzaldehyde in high yields within 4 h (Table 1.23, entry 107). The reactions of cyclohexene and *cis*-cyclooctene shows that a drop in conversion is observed in the reaction of cyclic alkenes towards dialdehydes after 7.5-8 h (entries 108-109), and that illustrates that the larger cyclic olefin is cleaved in higher yields. Unlike nano-RuHAP (Table 1.21),^[69] this system shows relatively high activity towards terminal alkenes, since undecanal shows 61% yield of decanal (entry 110). Also, the double bond in the terpenoid (+)-pulegone can be cleaved into 3-methyl-adipic acid (entry 111). The catalyst is recyclable with negligible loss of activity in five consecutive runs; it is recovered by centrifugation, washing with water and oven-drying overnight.

Chapter 1

Table 1.23. Oxidative cleavage of various olefins to form aldehydes using Ru on charcoal as a catalyst with limiting amounts of NaIO₄^a by Kumar *et al.*^[71]

Entry	Substrate	Product	Time (h)	Yield (%)
107			3.5	81
108			7.5	42
109			8	65
110			8	61
111			8	67 ^b

^a Reaction conditions: 1 mol% Ru on charcoal (Ru/C), 1.1 equiv. NaIO₄, MeCN:EtOAc:H₂O 1:1:1 (v/v), 0 °C, yields represent isolated yields; ^b Retention of optical rotation.

1.2.1.3.3 Osmium

OsO₄ can be microencapsulated (Os EnCat) in a polyuria matrix with an in situ polymerization approach, as documented by Ley *et al.*^[72] In general, 2 mol% of the microencapsulated-Os catalyst with 3 equiv. NaIO₄ works excellently for cleavage of internal, terminal aliphatic and aryl alkenes into aldehydes (Table 1.24). The aliphatic alkene 1-octene can be converted quantitatively to the aldehyde (entry 114). Styrene also converts well to benzaldehyde, yet *cis*-β-methyl styrene shows slightly lower yields (entries 112-113). The Os EnCat microcapsules can be recovered by simple filtration and reused five times without loss of activity.

Table 1.24. Oxidative cleavage of styrene derivatives, linear alkenes and internal alkenes to carbonyls with microencapsulated Os with periodate^a by Ley *et al.*^[72]

Entry	Substrate	Product	Yield (%)	GC yield (%)
112			92	-
113			79	-
114			66	100

^a Reaction conditions: 2 mol% Os EnCat, 3 equiv. NaIO₄, THF:H₂O 2:1 (v/v), 1-8 h at ambient temperatures, yields are represented as isolated yields or GC yields.

1.2.2 First-row transition metals

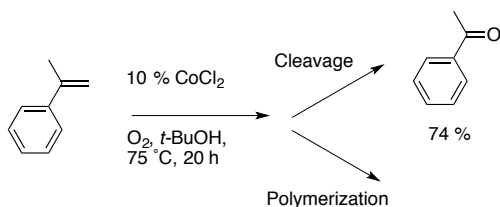
First-row transition metal complexes generally have a lower oxidizing potential than second- and third-row complexes, often involve a different mechanism, but usually are cheaper and more environmentally friendly. The examples listed in this section often concern coordination metal complexes rather than the simple metal salts. In addition, several examples of heterogeneous systems are given.

1.2.2.1 Metal Salts

1.2.2.1.1 Cobalt

The cobalt salt Co(II)oxime is capable of cleaving activated styrene derivatives, such as dihydroxystilbenes with molecular oxygen as the oxidant into aldehydes at room temperature, as shown by Simandi *et al.*^[73] Such systems generate diols as byproducts, nonetheless.

Cobalt dichloride and molecular oxygen are sufficient to cleave α -methyl styrene selectively towards the ketone at 70 °C using *t*-BuOH as the solvent, as shown by Lin *et al.*^[74] 67% of acetophenone is obtained at 91% conversion after 20 h; polymerization is observed as a minor side-reaction (Scheme 1.9). The selectivity towards cleavage products strongly depends on the nature of the substrate, the catalyst and the solvent used. For activated substrates containing electron-donating groups, polymerization becomes the major reaction pathway. Styrene cleavage is significantly less effective than α -methyl styrene or 4-methyl styrene cleavage; linear terminal and cyclic olefins show no activity (not shown). Concerning the cobalt catalysts, CoBr₂ shows slightly lower conversions than CoCl₂, Co(acac)₃ gave mediocre yields, whereas Co(OAc)₂·xH₂O and CoF₂ yield hardly any product. Mechanism Ca is thought to apply with this system (Scheme 1.6). In competing reactions, the benzyl radical species can act as an initiator in polymerization reactions. This intermediate then collapses to yield a 4-membered dioxyethane moiety that decomposes to acetophenone and acetaldehyde. The short reaction times with O₂ as oxidant with this protocol are appealing.



Scheme 1.9. Oxidative cleavage of CoCl₂ with O₂ of α -methyl styrene into acetophenone, with polymerization as a route to byproducts, by Lin *et al.*^[74]

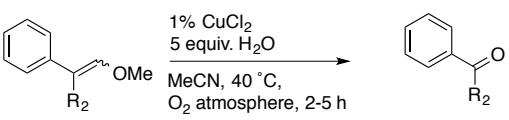
Chapter 1

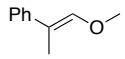
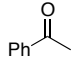
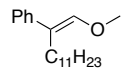
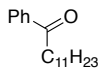
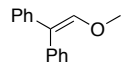
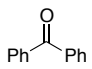
1.2.2.1.2 Copper

Copper can also catalyze C=C bond fission as a metal salt, using O₂ as oxidant, as shown for enamines by Kaneda *et al.*,^[75] demonstrating that tri- and tetra-substituted substrates without β-vinyl hydrogen atoms exclusively yield aldehydes and ketones with 5 mol% CuCl₂. A similar system catalyzes the cleavage of styrene derivatives, as reported by Koyama *et al.*^[76]

Additionally, Tokunaga *et al.* showed that a series of phenyl enol ethers be cleaved under similar conditions.^[77] With 1 mol% CuCl₂, 5 equiv. H₂O under O₂ atmosphere in MeCN, 1-methoxy-2-phenylpropene, 1-methoxy-2-phenyltridecene and 1-methoxy-2,2-diphenylethene convert well into the corresponding ketones within 5 h (Table 1.25, entries 115-117). CuCl₂ works best, but Cu(OTf)₂, CuBr₂, PdCl₂(PhCN)₂ and [RuCl₂(*p*-cymene)]₂ catalyze the reaction as well. Interestingly, the copper chloride catalyst is superior to the Ru and Pd chloride complexes. Protic solvents are supposed to accelerate the reaction, therefore traces of water are used in the reaction. A mechanism of type Cc is proposed for this reaction (Scheme 1.6).

Table 1.25. Oxidative cleavage of enol ethers with CuCl₂ and O₂ to ketones^a by Tokunaga *et al.*^[77]



Entry	Substrate	Product	Time (h)	Yield (%)
115			1	86
116			5	88 ^b
117			3	92 ^b

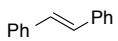
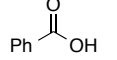
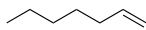
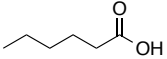
^a Reaction conditions: 1 mol% CuCl₂, 5 equiv. H₂O, MeCN, O₂ atmosphere, 2-5 h at ambient temperatures, yields are GC yields; ^b Isolated yield.

1.2.2.1.3 Iron

The only iron salt known to be active in oxidative alkene cleavage in the absence of a ligand is FeCl₃·6(H₂O). 5 mol% of this salt in combination with 6 equiv. TBPH in water at 80 °C for 10 h enables the conversion of *trans*-stilbene towards their carboxylic acids (Table 1.26, entry 118), as shown by Shaikh *et al.*^[78] Additionally, 1-heptene can be transformed into valeric acid in 44% isolated yield after 14 h (entry 119). The system uses water as the only solvent, 4 equiv. NaOH and acidic workup in the end. When anhydrous FeCl₃ was used, reactions were performed at 50 °C or when K₂CO₃ was used instead of NaOH, lower product yields were obtained. Moreover, the addition of the radical inhibitor

TEMPO showed no activity. In this protocol, the products do not need to be purified by chromatographic workup, but can be filtered off easily at the end of the reaction. If hydrogen peroxide is used instead of TBHP, it does not produce any significant amounts of product.

Table 1.26. Oxidative cleavage of *trans*-stilbene and 1-heptene by FeCl₃ and TBHP^a by Shaikh *et al.*^[78]

Entry	Substrate	Product	Yield (%)
118	 11a	 4b	98
119	 62a	 60b	44 ^b

^a Reaction conditions: 5 mol% FeCl₃·6H₂O, 6 equiv. TBHP, 4 equiv. NaOH, H₂O, 80 °C, 10 h, yields represent isolated yields; ^b 14 h reaction.

1.2.2.2 Metal complexes

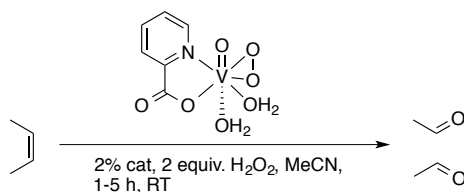
Most examples of homogeneously-catalyzed double bond scission with first-row transition metals involve the use of discrete metal coordination complexes. Some report in-situ prepared complexes. Often the ligands are chelating polydentate ligands such as porphyrine or salen.

1.2.2.2.1 Vanadium

[VO(O₂)(Pic)₂·2H₂O] (Pic = pyridine-2-carboxylate) is a suitable metal coordination complex for cleaving alkenes into aldehydes with H₂O₂ in MeCN, as reported by Mimoun *et al.*^[79] The active catalyst consists of an octahedral V(V)-center (Table 1.27), containing weakly coordinated water molecules and the oxo/peroxo moieties in a *cis*-position. With 2 mol% catalyst loading, 2 equiv. H₂O₂ in MeCN, styrene derivatives, *cis*-2-butene and 2-methyl-2-pentene are cleaved in mediocre yields to the aldehydes (entries 120-121, 123), with *cis*- and *trans*-epoxides being detected as byproducts. *Trans*-2-butene only shows low amount of aldehydes (entry 122), and reactions with cyclohexene generate no cleavage products at all (not shown). The catalyst outperformed [VO(O₂)(Pic)₂]-H⁺·H₂O, [VO(O₂)(Pic)₂]-H⁺·HMPT (HMPT = hexamethylphosphoric triamide) [VO₂(Pic)]₂·H₂O and [VO₂(Pic)(HMPT)]. Mechanism B is proposed here (Scheme 1.5). After the epoxidation of the alkene, the active catalyst can form the dimer [VO₂(Pic)]₂·H₂O that might catalyze the reverse reactions or deactivate the system.

Chapter 1

Table 1.27. Oxidative cleavage of various olefins with a V-oxo-peroxo pyridyl-carbaldehyde catalyst and H₂O₂^a by Mimoun *et al.*^[79]



Entry	Substrate	Product	Yield (%)
120			45 ^b
121			20 ^c
122			3 ^d
123			15 ^e

^a Reaction conditions: 2 mol% [V(O)(O₂)(pic)(H₂O)₂], 2 equiv. H₂O₂, MeCN, 0.25-2 h at ambient temperatures, GLC yields; ^b 40% acetaldehyde, 6% epoxide; ^c 19% *cis*-epoxide, 8% *trans*-epoxide after 0.25 h; ^d 12% *trans*-epoxide, 2% *cis*-epoxide after 2 h; ^e 23% acetaldehyde, 10% epoxide after 1.5 h.

Alternatively, [V(O)(O₂)(OAc)₂(H₂O)₂] can be prepared in-situ prepared to cleave styrene derivatives to the aldehydes at high yields, as shown by Choudary *et al.*^[80] Vanadyl acetate is reacted in acetic acid with continuous addition of H₂O₂ until the active species is formed (indicated by a persistent red color). The reactions are run with 10 mol% V(O)(OAc)₂ with H₂O₂ in acetic acid at 70 °C for 12 h (Table 1.28). This way, the reaction with *trans*-stilbene gives mediocre yield of the corresponding aldehyde (entry 125), whereas styrene, 4-methoxy styrene and 4-bromo styrene show nearly quantitative isolated yields of the cleavage product (entries 124, 126-127). The acidic ligands are thought to play a dual role: one is to prevent the formation of the dimer (as observed in Table 1.27); the other is to enhance the reactivity towards aldehydes as more basic ligands are proposed prevent the cleavage of the epoxides towards the aldehydes to larger extent. Also, no degradation of the catalyst is observed.

Table 1.28. Oxidative cleavage of styrene derivatives to aldehydes with an in-situ prepared V-oxo-peroxo catalyst and stoichiometric amounts of H₂O₂^a by Choudary *et al.*^[80]

Entry	Substrate	Product	Yield (%)
124		10a →	10b 95
125		11a →	10b 46
126		67a →	62b 98
127		68a →	63b 91

^a Reaction conditions: 10 mol% VO(OAc)₂, H₂O₂, acetic acid, 70 °C, 12 h, isolated yields.

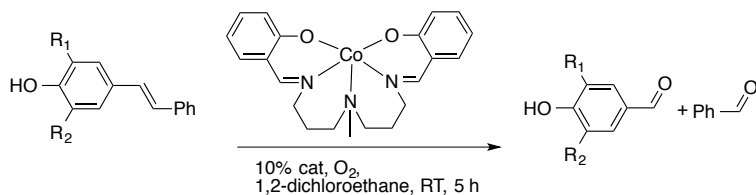
1.2.2.2.2 Cobalt

Cobalt can be bound to pentadentate N,N,N,O,O Schiff bases to form bis(salicylideneiminato-3-propyl)methylaminocobalt(II) [Co(SMDPT)]^[81] in order to cleave the styrene derivative *trans*-isoeugenol (**46a**) to vanillin (**48b**, 71% yield) with 18 mol% catalyst loading and molecular oxygen in toluene at 60 °C, as reported by Drago *et al.*^[82]

Ganeshpure and Satish^[83] reported the use of 10 mol% [Co(SMDPT)] at ambient temperatures, catalyzing the oxidative cleavage of *trans*-4-stilbenols to its aldehydes with O₂ as oxidant in 1,2-dichloroethane (Table 1.29). The isolated aldehyde yields are high (96%, entry 128), only the *trans*-*m,m'*-di-*t*-Bu-stilbenol (entry 129) shows the formation of a radically coupled dimer in 18% yield as byproduct. The radical mechanism of type Ca is invoked to proceed via a phenoxide radical intermediate (Scheme 1.6). Thus, the OH-group on the substrate can facilitate the radical-induced oxidative cleavage. No polymerization side products are observed here, unlike other Co-based systems (Scheme 1.9).

Chapter 1

Table 1.29. Oxidative cleavage of stilbenol derivatives with [Co(SMDPT)] and O₂^a by Ganeshpure and Satish.^[83]



Entry	Substrate		Product		Yield (%)
128		69a		64b	96 ^b
129		70a		65b	80 ^c

^a Reaction conditions: 10 mol% [Co(SMDPT)], O₂, 1,2-dichloroethane, 5 h, isolated yield; ^b 92% benzaldehyde; ^c 78% benzaldehyde, 18% dimer byproducts observed.

1.2.2.2.3 Iron

The iron salen complex [Fe(salen)Cl] (salen = *N,N'*-ethylenebis(salicylideneaminato)) catalyzes the cleavage of the C=C bond of various styrene derivatives in acetonitrile, under ambient conditions (FeCl₃·6H₂O is inactive at this temperature, Table 1.26) and with 10 equiv. H₂O₂ as oxidant, as demonstrated by Pitchumani *et al.*^[84] Aldehydes are formed, yet the yields and TON's remain low with this homogeneous system (0-68%, method A, Table 1.30). In order to increase the activity, a heterogeneous system was developed (method B, Table 1.30), based on a clay material (K10-montmorillonite). The clay interlayer localizes the substrate and the active iron-oxo complex in close proximity, whereas such high local concentrations are difficult to achieve in solution. Styrene and 1,1-diphenyl-ethylene significantly benefit from immobilization of the catalyst on the clay support (entries 130-131). Also, the chalcones dibenzylidene-cyclohexanone **71a** and dimethoxy-dibenzylideneacetone **72a** contain two double bonds each and can be converted in 85-87% yield towards their corresponding aldehydes (entries 132-133). Furthermore, for 1,1-diphenyl-ethylene, the clay anchored catalyst can be reused with 86% aldehyde yield in the second cycle as compared to 98% in the first (entry 131). The radical mechanism Cb is proposed here (Scheme 1.6). As reactions are done in air, molecular oxygen can also take part in the catalytic cycle. Further evidence for the radical reaction is that the reaction can be inhibited to a great extent upon addition of sodium azide. The azide ion can interact with hydrogen peroxide to generate the azidyl radical with Fe, as is known from the heme group of the enzyme catalase.^[85]

Table 1.30. Oxidative cleavage of styrene derivatives into their corresponding aldehydes using [Fe(salen)Cl] and H₂O₂ in MeCN with and without clay support by Pitchumani *et al.*^[84]

Entry	Substrate	Product	Yield A (%) ^a	Yield B (%) ^b
130		10a → Ph-CHO (10b)	14	30
131		48a → Ph-CO-Ph (50b)	68	98 ^c
132		71a → Ph-CHO (10b)	-	87
133		72a → 4-MeO-C6H4-CHO (63b)	38	85

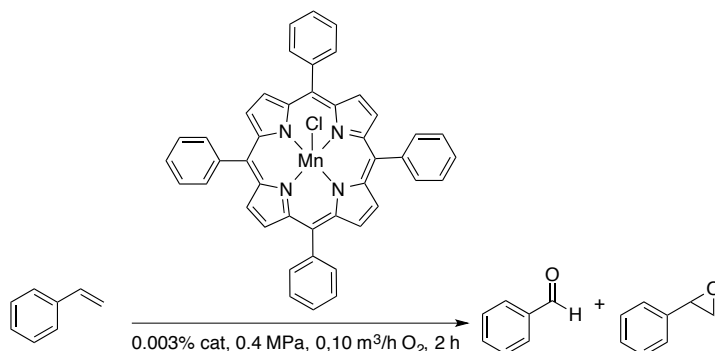
^a Method A: 0.05 g alkene, 0.028 mmol [Fe(salen)Cl] (6-16 mol%), 10 equiv. H₂O₂, MeCN, 24 h at ambient temperature; ^b Method B: 0.05 g olefin, 0.084 mmol [Fe(salen)Cl] (18-48 mol%), 10 equiv. H₂O₂, MeCN, 24 h at ambient temperature, 200 wt% K10- montmorillonite (clay) with respect to [Fe(salen)Cl]; ^c 86% yield if the catalyst was reused.

1.2.2.2.4 Manganese

Manganese tetraphenyl-porphyrines oxidize styrene to benzaldehyde and styrene oxide under pressurized air, using only a trace amount of catalyst and no organic solvent, as shown by Li *et al.*^[86] The [Mn(*meso*-tetraphenylporphyrine)Cl] (MnTPPCl) catalyst can be used with a catalyst loading of 0.003 mol% to form benzaldehyde from styrene at 0.4 MPa with a 0.1 m³/h airflow in 2 h (Table 1.31). However, the reaction yields styrene oxide (**64b**) as the major product, in addition to the minor byproducts benzoic acid and acetophenone. Alterations in airflow, temperature and pressure influence the reaction to a great extent. An increase in pressure increases the selectivity for the aldehyde and a higher airflow both increases the conversion and the selectivity. On the other hand, the temperature was found to be optimal at 110 °C in terms of selectivity, yet the conversion was only 20% (entry 134). Raising the temperature to 120 °C improved the conversion, but resulted in a dramatic drop in selectivity (entry 135). No reaction occurs at lower temperatures. The formation of benzaldehyde also proceeds non-catalytically to some extent, since the aldehyde is also formed in a blank reaction without catalyst (not shown).

Chapter 1

Table 1.31. Oxidative cleavage styrene towards benzaldehyde involving MnTPPCL without solvent at high temperatures with O₂^a by Li *et al.*^[86]



Entry	Substrate	Product	Product	Selectivity (%)	Product	Selectivity (%)
134 ^b	Ph-CH=CH ₂	Ph-CHO (10b)	Ph-CHO (10b)	82	Ph-CH(O)CH ₂ (64b)	13
135 ^c	Ph-CH=CH ₂	Ph-CHO (10b)	Ph-CHO (10b)	48	Ph-CH(O)CH ₂ (64b)	41

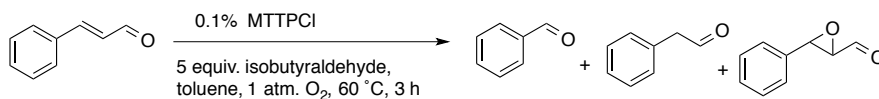
^a Reaction conditions: 0.003 mol% MnTPPCL, 0.4 mPa, 0.10 m³/h O₂, 2 h at ambient temperatures, GC yield; ^b T = 110 °C, 20% conversion; ^c T = 120 °C, 93% conversion.

Similarly, styrene can also be transformed into 59% benzaldehyde and 41% of styrene oxide (**64b**) at lower temperatures, with 0.001 mol% loading of MnTPPCL in combination with benzotrifluoride as solvent, 3 equiv. isobutyraldehyde and O₂ at 80 °C for 5 h, as shown by Zhou *et al.*^[87] FeTPPCL (59% benzaldehyde), RuTPPCL (57%) or CoTPP (86%) are also suitable catalysts for this reaction.

MnTPPCL complexes also catalyze the transformation of the naturally occurring cinnamyl aldehyde to benzaldehyde with O₂ in toluene at atmospheric pressure and 60 °C in 3 h, as shown by Chen and co-workers.^[88] Besides MnTPPCL, also other metals can be employed like Ru, Co, Mn and Fe for the oxidative cleavage of cinnamaldehyde (Table 1.32). The reported conditions invoke the solvent toluene at 60 °C and atmospheric oxygen pressure. On the contrary, this system uses a higher catalyst loading with 0.1 mol% and 5 equiv. of a sacrificial aldehyde in the form of isobutyraldehyde. The manganese catalyst yields the best selectivity for benzaldehyde (71%, entry 139) from all metals, with the epoxide and phenylacetaldehyde as common byproducts. The FeTPPCL also yields 36% selectivity (entry 140). As previously shown by Li *et al.*^[86], the styrene derivative can also be converted without a catalyst (entry 136), but again in only very low yields with 4% and 6% conversion. Toluene shows a higher selectivity towards cleavage products than MeCN, cyclohexane or benzotrifluoride. The addition of isobutyraldehyde is necessary for the reaction to occur: it is proposed that isobutyraldehyde activates the catalyst via a radical mechanism Cb (Scheme 1.6) before the latter is able to oxidatively cleave the substrates. Indeed, the selectivity and yield increase linearly with the initial amount of

isobutyraldehyde. The peracid facilitates the formation of a high-valent Mn(IV)=O intermediate, which is assumed to perform the oxidative cleavage on cinnamaldehyde. Owing to variable valence, manganese porphyrine thus provides an appropriate reduction potential to facilitate formation of a high-valent metal-oxo ligand.^[89]

Table 1.32. Oxidative cleavage of cinnamaldehyde to benzaldehyde using various metals with a TTP porphyrine ligand and O₂^a by Chen *et al.*^[88]



Entry	Metal	Substrate	Conversion (%)	Product	Yield (%)
136	-	Ph-CH=CH-CHO 73a	6	Ph-CHO 10b	4
137	Ru	Ph-CH=CH-CHO 73a	88	Ph-CHO 10b	54
138	Co	Ph-CH=CH-CHO 73a	97	Ph-CHO 10b	49
139	Mn	Ph-CH=CH-CHO 73a	99	Ph-CHO 10b	71
140	Fe	Ph-CH=CH-CHO 73a	66	Ph-CHO 10b	36

^a Reaction conditions: 0.1 mol% MTTPCI, M = Ru, Co, Mn or Fe, O₂, 5 equiv. isobutyraldehyde, toluene, 60 °C, 3 h, yields represent isolated yields.

In an alternative system, the addition of sodium periodate and an axial ligand in the form of imidazole enables MnTPPCI to catalyze the oxidative cleavage of also cyclic alkenes and styrene, in MeCN/H₂O, as reported by Liu *et al.*^[90] The conditions involve 0.13-1 mol% [Mn(TPP-PEO)Cl] (PEO = poly(ethylene glycol)), 0.5 – 1 equiv. imidazole and 3-4 equiv. NaIO₄ in MeCN/H₂O at ambient temperatures (Table 1.33). Quantitative aldehyde yields are obtained from styrene at 80 °C (small amount of acetophenone byproduct) and with cyclopentene at ambient temperature (entries 141-142). The terpene α -pinene is cleaved to give 44% isolated yield of the corresponding aldehyde (143). With the terpene limonene, a high isolated yield can be obtained of the dialdehyde cleavage product stemming from endocyclic cleavage, showing that this system has high a regioselectivity towards internal alkenes (see Chapter 4). Additionally, the complexes are recyclable due to the amphiphilic PEO chains on the porphyrine, making the catalyst soluble in water with only minimal loss of activity. In this way, the organic fraction and the catalyst can be easily separated by simple extraction. Any deactivation of the catalyst upon reuse is attributed to the accumulation of salt in the aqueous phase upon repeated extraction of the organics. No leaching of the catalyst or formation of byproducts such as epoxides is reported.

Chapter 1

Table 1.33. Oxidative cleavage of a variety of substrates in aqueous acetonitrile using a recyclable [Mn(TPP-PEO)Cl] catalyst with periodate and an imidazole axial ligand^a by Liu *et al.*^[90]

R^1
 R^2 R^3 $\xrightarrow[\text{RT-80 } ^\circ\text{C, MeCN:H}_2\text{O 2:1, 24 h}]{\text{0.3-1\% cat, 3-4 equiv. NaIO}_4, \text{0.5-1 equiv. imidazole,}}$ R^1
 R^2 R^3

Entry	Cat. (%)	Imid. (equiv.)	NaIO ₄ (equiv.)	Substrate	Product	Yield (%)
141 ^b	0.3	1	4		10a 10b	97 ^c
142	0.13	0.5	3		21a 65b	99
143	1	1	4		74a 66b	44
144	1	1	3		43a 67b	89

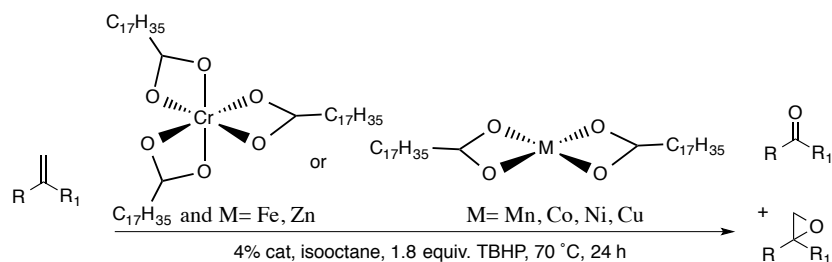
^a Reaction conditions: 0.13-1 mol% [Mn(TPP-PEO)Cl], MeCN:H₂O 2:1 (v/v), 0.5-1 equiv. imidazole, 3-4 equiv. NaIO₄, 24 h at ambient temperatures, yields are isolated yields; ^b T = 80 °C, ^c Acetophenone and styrene oxide visible at ambient temperature.

1.2.2.2.5 Chromium

Chromium(III)-stearate is a metalloamphiphile that performs the oxidative cleavage of terminal olefins to aldehydes, as shown by Jarupinthusophon *et al.*^[91] The hydrophobic ligands were used to alter the procedure for CrO₃-assisted double bond cleavage in combination with Jones' agent,^[22, 23] making it less toxic. Additionally, this system is one of the few that works in apolar solvent. The applied reaction conditions include the use of 1.8 equiv. TBHP as oxidant, isooctane as the solvent and a reaction temperature of 70 °C. The catalyst loading for this system is 4 mol%. Up to 85% of acetophenone can be obtained from α -methyl styrene with 91% substrate conversion, forming epoxides as minor byproduct (entry 145, Table 1.34). Similarly, other first-row metals can be utilized such as Mn(II), Fe(III), Co(II), Ni(II), Cu(II), Zn(III) (entries 146-151), albeit with lower

acetophenone yields. Mn(II), Fe(II) and Cu(II) give less epoxide byproduct (about 2-4%) than Co(II), Ni(II) and Zn(II) (10-18%). The system can be applied on some other alkenes: reactions with styrene selectively yields 72% benzaldehyde with 28% of the substrate recovered after 24 h. The oxidation of methyl methacrylate shows 55% yield of its ketone, with 14% substrate recovery. On the other hand, the terpene camphene and 1-dodecene do not show any activity at all with this system (all not shown). High valent Cr(V) species are invoked as intermediates of the type in mechanism Cc (Scheme 1.6).

Table 1.34. Oxidative cleavage of α -methyl styrene to acetophenone with different metal stearates and TBHP^a by Jarupinthusophon *et al.*^[91]



Entry	Metal	Substrate	Conversion (%)	Product	Yield (%)	
145	Cr(III)		49a	91	26b	85 ^b
146	Mn(II)		49a	60	26b	57 ^b
147	Fe(III)		49a	63	26b	59 ^b
148	Co(II)		49a	91	26b	71 ^c
149	Ni(II)		49a	81	26b	66 ^d
150	Cu(II)		49a	69	26b	63 ^b
151	Zn(III)		49a	54	26b	42 ^e

^a Reaction conditions: 4 mol% catalyst, isooctane, 1.8 equiv. TBHP, 70 °C, 24 h, GC yields; ^b Trace amounts of 2-methyl-2-phenyloxirane observed; ^c 18% epoxide observed; ^d 15% of epoxide observed; ^e 10% of epoxide observed.

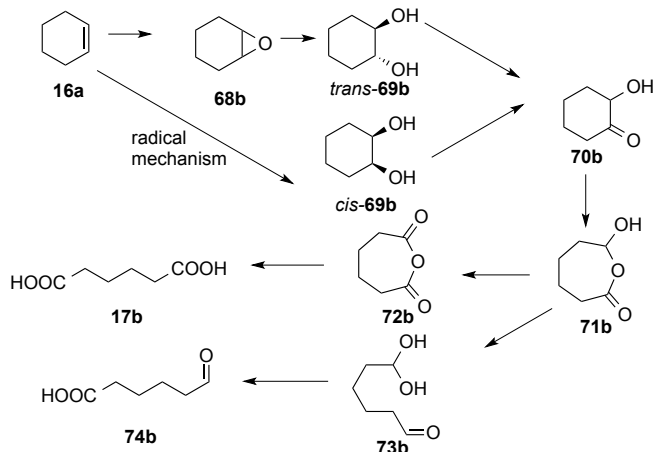
Chapter 1

1.2.2.3 Heterogeneous catalysts

The reported examples of heterogeneous first-row transition metal systems for oxidative alkene cleavage involve either metals grafted on a solid support, or they exist as metal organic frameworks or nanoparticles as solid particles in solution.

1.2.2.3.1 Titanium

Titanium can be incorporated in the framework of aluminophosphates (Ti-AlPO) in order to convert cyclohexene into adipic acid with hydrogen peroxide, as demonstrated by Lee *et al.*^[92] The reaction is run at 80 °C in an autoclave without solvent with 3.5 equiv. H₂O₂. Mechanistic studies show that the formation of adipic acid indeed involves a competition between a concerted and a radical mechanism (Scheme 1.10). Mechanism B (Scheme 1.5) applies for the concerted mechanism to the *trans*-diol (*trans*-**69b**) stage. The radical pathway involves formation of *cis*-cyclohexandiol (*cis*-**69b**) as intermediate. Both diols eventually form 1,2-cyclohexane hydroxy ketone **70b**. The hydroxy ketone is then over-oxidized into **71b**, which can either form **73b** or the anhydride **72b**. The anhydride **72b** can eventually hydrolyze towards adipic acid (**17b**). **73b** oxidizes into 6-oxohexanoic acid **74b**, yet the latter pathway only occurs in trace amounts. No adipaldehyde is seen anywhere during the reaction. The yield of adipic acid at full conversion is 30% after 3 days, being the major component of the product mixture.



Scheme 1.10. Proposed mechanism for the oxidative cleavage of cyclohexene to carboxylic acids with Ti-AlPO by Lee *et al.*^[92]

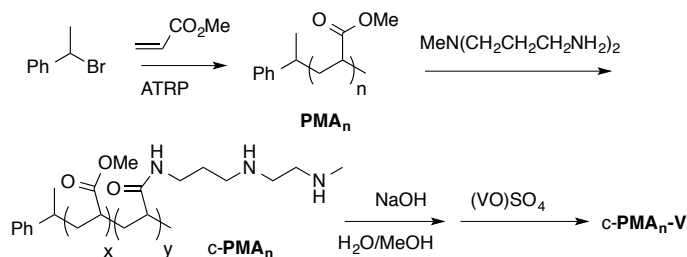
TiO₂ can also be anchored onto silica in order to form TiO₂/SiO₂ (1:1). This catalyst converts styrenes into benzaldehyde with molecular oxygen, as reported by Nie *et al.*^[93] 36% benzaldehyde can be formed at 36% conversion after 2 h with 10 atm O₂ at 100 °C and 7 mol% catalyst loading for 0.72 g styrene on 470.3 m²/g surface area of the catalyst. Longer reaction times and other conditions produce side products, such as styrene oxide,

phenylacetaldehyde or acetophenone. $\text{TiO}_2/\text{SiO}_2$ is proposed to be solely responsible for the cleavage of the diol intermediates. The formation of the diol itself is postulated to proceed via autooxidation with molecular oxygen.

Another example of a heterogeneous catalyst with titanium in order to transform styrene into benzaldehyde is the acidic titanium silicalite (TS-1) zeolite catalyst, reported by Zhuang *et al.*^[94] The reaction is performed in an autoclave in acetone with hydrogen peroxide, under oxidant-limiting conditions. However, with this system the cleavage product is only a byproduct compared to phenylacetaldehyde.

1.2.2.3.2 Vanadium

$(\text{VO})\text{SO}_4$ cross-linked onto polyacrylate (**c-PMA_n-V**) catalyzes the oxidative cleavage of a variety of alkenes into carboxylic acids with 8 equiv. TBHP in water at elevated temperature between 60 °C and 105 °C (Table 1.35), as shown by Hsiao *et al.*^[95] The catalyst is prepared by complexation of vanadium ions with cross-linked polyacrylate (**c-PMA_n**) of various chain lengths (Scheme 1.11). All cross-linked PMA vanadium complexes outperform analogues of the simple ester 'parent' complexes, (**PMA_n**, prepared by atom transfer radical polymerization of (1-bromoethyl)benzene with methacrylate) but no significant differences are observed for the different chain lengths of the polymer. The importance of the cross-linking is postulated to stem from the metal ions being fixed in a rigid matrix.



Scheme 1.11. Synthesis of **c-PMA_n-V**. ATRP = atom transfer radical polymerization.

The catalysts can be filtered off after each catalytic run, washed with ethanol, dried and reused for five runs without significant loss of activity. No metal leaching is said to occur. Unlike vanadium-based coordination complexes (see 1.2.2.2.1), indeed this system cleaves cyclohexene to adipic acid and styrene to benzoic acid (entries 154-155). On the other hand, no reaction was observed with 1-octene (entry 156). Mechanism B applies here (Scheme 1.5).

Chapter 1

Table 1.35. Oxidative cleavage of various olefins with polyacrylate-supported V complexes and TBHP in water^a by Hsiao *et al.*^[95]

Entry	Substrate	Product	Time (h)	Yield (%)
154		16a HOOC-CH ₂ -CH ₂ -CH ₂ -COOH 17b	32 ^b	67
155		10a 4b	14 ^c	84
156		5a -	16 ^d	0

^a Reaction conditions: 1 mmol substrate, 30 mg c-PMA_n-V (27-38 wt%), 8 equiv. TBHP, H₂O, 80-105 °C, yields based on NMR integration with internal standard; ^b 105 °C; ^c 100 °C; ^d 80 °C.

1.2.2.3.3 Chromium

Cr(NO₃)₃·9H₂O with 1 equiv. of terephthalic acid and 1 equiv. of HF in H₂O forms the metal-organic framework MIL-101 after heating in an autoclave at 220 °C for 8 h. MIL-101 with an excess of H₂O₂ (10 equiv.) catalyzes the cleavage of cyclic and terminal alkenes into carboxylic acids in MeCN, after which the catalyst can be recovered by filtration, as shown by Saedi *et al.*^[96] The conditions involve 1.32 mol% catalyst loading to obtain the carboxylic acids in 8 h in refluxing MeCN (Table 1.36). Indeed, this heterogeneous system cleaves cyclohexene and 1-octene to the carboxylic acids in good yields (entries 157-158). Also, indene can be quantitatively cleaved within 3 h (entry 159). At the end of the reaction, the catalyst can be filtered off, washed with additional MeCN and is reusable. However, partial Cr leaching occurs and the carboxylic acid yield drops in reactions with indene from 100% to 81% in three runs. The products are isolated after chromatography over a short silica column.

Table 1.36. Oxidative cleavage of aliphatic alkenes into carboxylic acids with Cr-based metal-organic framework MIL-101 and H₂O₂^a by Saedi *et al.*^[96]

Entry	Substrate	Product	Yield (%)
157		16a HOOC-CH ₂ -CH ₂ -CH ₂ -CH ₂ -COOH 17b	90
158		5a HOOC-CH ₂ -CH ₂ -CH ₂ -CH ₂ -CH ₂ -CH ₂ -COOH 5b	90
159 ^b		75a 75b	100

^a Reaction conditions: 1.32 mol% MIL-101, 10 equiv. H₂O₂, MeCN, 8 h, reflux, GC yields; ^b 3 h.

1.2.2.3.4 Iron

Fe₂O₃ nano-particles selectively cleave styrene derivatives to the aldehydes at an elevated temperature of 75 °C, 2 equiv. of H₂O₂ and 1 mol% catalyst loading (Table 1.37), as shown by Shi *et al.*^[97] The substrate conversions are mediocre with 14-36%, yet very high chemoselectivity towards the aldehydes can be achieved, i.e. styrene and its Br-derivative (entries 160-161) can be converted to the corresponding aldehydes with >99% selectivity. Only *p*-methyl styrene (entry 162) shows a lower selectivity of 75%. The nanosized iron oxide is active because of the high surface area, and presence of low-coordination sites and surface vacancies. A particular advantage of this system is the simplicity of catalyst recycling. Taking advantage of their high ferromagneticity, the nano-γ-Fe₂O₃ particles can be isolated with a stirring bar. Subsequently, the catalyst can be recovered by simple decantation of the solution. After washing with acetone and drying in air, the catalytic particles are ready to be reused without any observed deactivation in five consecutive rounds. The Fe particles retain their crystal structure and particle size after each reaction.

Chapter 1

Table 1.37. Oxidative cleavage of styrene derivatives to aldehydes with nano- γ -Fe₂O₃ particles and H₂O₂^a by Shi *et al.*^[97]

Entry	Substrate	Product	Yield (%)	Selectivity (%)
160		10a	10b 19	> 99
161		67a	76b 14	> 99
162		76a	77b 36	75

^a Reaction conditions: 1 mol% nano- γ -Fe₂O₃, 2 equiv. H₂O₂, 75 °C, 5 h, yields determined by GC.

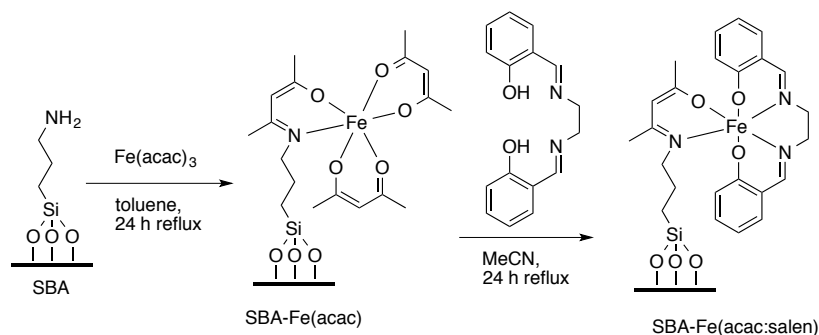
Nanosized spinel-type Mg_{0.4}Fe_{2.6}O₄ are mixed oxide catalysts that can be synthesized by co-precipitation of Fe(NO₃)₃ and Mg(NO₃)₂ with NH₄OH and NH₄HCO₃ at 50 °C for 24 h. The mixed oxide catalyzes the cleavage of styrene to benzaldehyde with 1 equiv. H₂O₂ as oxidant, as documented by Ma *et al.*^[98] High selectivity towards the benzaldehyde can be achieved in acetone at 50 °C after 36 h, under which conditions the oxidant is incorporated relatively efficiently (Table 1.38). Mg_{0.4}Fe_{2.6}O₄ shows higher activity than the pure spinel MgFe₂O₄.

Table 1.38. Oxidative cleavage by nanosized spinel-type Fe-oxide catalysts with H₂O₂^a by Ma *et al.*^[98]

Entry	Substrate	Conversion (%)	Product	Yield (%)
163		10a 45		10b 28

^a Reaction conditions: 10 mmol styrene, 100 mg Mg_{0.4}Fe_{2.6}O₄ (48 equiv.), 1 equiv. H₂O₂, acetone, 50 °C, 36 h, GC yields.

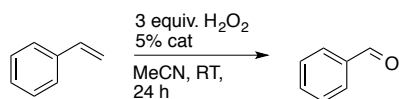
Fe(III)(salen) complexes anchored on mesoporous silica SBA-15^[99] represent an immobilized Fe coordination complex. The reaction of Fe(acac)₃ with a silica propylamine linker on SBA forms SBA-Fe(acac), and subsequent addition of the schiff base ligand (Scheme 1.12) eventually forms SBA-Fe(acac:salen), as shown by Anand *et al.*^[100]



Scheme 1.12. Schematic presentation of the immobilization of an Fe(III)salen complex on a silica support, as proposed by Anand *et al.*^[100]

The reaction conditions involve 3 equiv. of hydrogen peroxide, 5 mol% catalyst loading with MeCN as solvent and stirring at RT for 24 h (Table 1.39). The immobilized SBA-Fe(acac) already shows slightly higher conversion and selectivity towards benzaldehyde than the homogeneous catalysts (entries 164-166). Moreover, the immobilized SBA-Fe(acac:salen) shows quantitative selectivity towards benzaldehyde at 45% substrate conversion (entry 167).

Table 1.39. The oxidative cleavage of styrene towards benzaldehyde with the aid of an Fe(III)salen catalyst immobilized on silica with hydrogen peroxide^a by Anand *et al.*^[100]



Entry	Catalyst	Substrate	Product	Conversion (%)	Selectivity (%)
164	[Fe(salen)Cl]	Ph-CH=CH ₂	Ph-CHO	20	70
165	Fe(acac) ₃	Ph-CH=CH ₂	Ph-CHO	5	65
166	SBA-Fe(acac)	Ph-CH=CH ₂	Ph-CHO	22	72
167	SBA-Fe(acac:salen)	Ph-CH=CH ₂	Ph-CHO	45	> 99

^a Reaction conditions: 5 mol% cat, 3 equiv. H₂O₂, MeCN, 24 h, ambient temperatures, GC yields.

Chapter 1

1.3 Cleavage of unsaturated fatty acids

Unsaturated fatty acids differ from the styrene and cyclic olefin examples previously discussed in various ways. First, radical intermediates are not as easily formed in this case, unlike the relatively stable benzylic radicals that are often involved in the oxidation of styrene derivatives. Secondly, release of ring-strain upon oxidation cannot contribute to driving the reaction as with the cyclic olefins. Finally, the carboxylic acid functional group can cause side-reactions. Unsaturated fatty acids are therefore often more difficult to cleave than other commonly used alkenes. Notably, the oxidative cleavage systems in this chapter comprise only second- and third-row transition metal methods. Examples involving KMnO_4 induced cleavage reactions,^[9, 11, 101, 102] or two-step cleavages involving terminal unsaturated fatty acids obtained by metathesis are not discussed.^[6, 29, 103-105] First-row transition metal systems have to our knowledge not yet been reported at start of writing this chapter, and the first examples will be discussed in chapters 3 and 5.

1.3.1 Second- and third-row transition metals

1.3.1.1 Metal salts and metal-oxo or peroxo catalysts

1.3.1.1.1 Ruthenium

The Sharpless system discussed in 1.2.1.1.1 also found application in oxidative cleavage of unsaturated fatty acids. Catalytic amounts of RuCl_3 with stoichiometric amounts of NaIO_4 in $\text{CCl}_4/\text{MeCN}/\text{H}_2\text{O}$,^[26, 31] can also be used to oxidatively cleave oleic acid into nonanoic and azelaic acid, as reported by Nakano and co-workers.^[106] Optimization of the system involved the replacement of CCl_4 by ethyl acetate in the solvent system $\text{H}_2\text{O}:\text{MeCN}:\text{AcOEt}$ 3:2:2 (v/v) in order to nearly quantitatively cleave a series of unsaturated fatty acids within 2-4 h at ambient temperatures, using 2.2 mol% catalyst loading and 4.1 equiv. NaIO_4 , as reported by Zimmermann *et al.*^[107] Additionally, the addition of the emulsifier Aliquat® 336 and ultrasonification increases the reaction rate of oleic acid cleavage to yield 81% azelaic acid and 96% pelargonic acid in $\text{MeCN}:\text{H}_2\text{O}$ 1:1 (v/v) in only 45 minutes at ambient temperature (entry 168).^[108] Under these conditions, also *trans*-unsaturated fatty acids of different chain lengths can be readily cleaved with this system (entries 169-171, Table 1.40), as has been done with *trans*-5-decene (entry 173). Moreover, the terminal alkene 1-decene renders 92% of nonanoic acid in only 5 minutes (entry 172). Only the reaction with 10-undecenoic acid shows other selectivity, as diones are formed (entry 168). The products can be isolated by extraction in ethyl acetate, the monoacids can be separated from the diacids because of different solubilities in hot water. The formation of diones in other substrates than entry 168 is significantly decreased by ultrasonification and addition of emulsifiers. Mechanism Aa is proposed here (Scheme 1.4).

Table 1.40. Oxidative cleavage of unsaturated fatty acids into their corresponding carboxylic acids using RuCl_3 , NaIO_4 , ultrasonic radiation and emulsifiers^a by Zimmermann *et al.*^[108]

Entry	Substrate	Time (min)	Product	Yield (%)
168		45		96
169		15		99
170		30		80 ^b
171		40		97 ^c
172		30		82 ^d
173		5		92
174		15		89

^a Reaction conditions: 2.2 mol% RuCl_3 , 4.1 equiv. NaIO_4 , 2 mol% Aliquat 336, $\text{H}_2\text{O}:\text{MeCN}$ 1:1 (v/v), ultrasonic irradiation, yields are isolated yields; ^b 93% azelaic acid detected; ^c 80% undecanedioic acid detected; ^d 98% tridecanedioic acid detected.

Alternatively, the use of organic solvents with this system can even be omitted, when reacting oleic acid under 20 kHz ultrasonic irradiation and with Aliquat® 336 in aqueous solution for 6 h, as shown by Rup *et al.*^[109] Up to 98% of nonanoic acid can be isolated using this method. The reactivity with 1-decene is severely higher, as 76% of nonanoic acid can be isolated within 0.5 h.

1.3.1.1.2 Osmium

OsO_4 catalyzes the oxidative cleavage of methyl oleate into nonanoic acid in 93% GC yield (Table 1.41), using 1 mol% catalyst loading with 4 equiv. of oxone in DMF, which is the same system as reported by Travis *et al.* for the cleavage of a variety of alkenes (Table 1.10).^[52] Also, 80% isolated yields of the combined acids can be obtained. This system can cleave the unsaturated fatty acid ester at ambient temperature without the addition of an additive.

Chapter 1

Table 1.41. Osmium/oxone-catalyzed oxidative cleavage of methyl oleate into carboxylic acids^a by Travis *et al.*^[52]

Entry	Substrate	Product	Yield (%)
175			93 ^b

^a Reaction conditions: 1 mol% OsO₄, methyl oleate, 4 equiv. oxone, DMF, 3 h, RT, yields determined by GC; ^b 93% monomethyl azelate observed, 80% of combined acids can be isolated.

Similarly, the microencapsulated system of OsO₄ in a polyuria matrix (Table 1.24)^[72] can also cleave *cis*-7-tetradecene in 100% GC yield to heptanal, which can be regarded as a mimic to unsaturated fatty acids (Table 1.42). 55% of the combined aldehydes can also be isolated with this method. Especially the high yields of the aldehydes at ambient temperatures with this system are unmet.

Table 1.42. Os/NaIO₄-catalyzed oxidative cleavage of *cis*-7-tetradecene into heptanal^a by Ley *et al.*^[72]

Entry	Substrate	Product	Yield (%)	GC yield (%)
176			55	100

^a Reaction condition: 2 mol% OsEnCat, 3 equiv. NaIO₄, THF:H₂O 2:1 (v/v), 1-8 h reaction at ambient temperature, yields represent isolated yield.

1.3.1.1.3 Tungsten

Tungstic acid (H₂WO₄) can be used to dihydroxylate unsaturated fatty acids, yet needs Co(acac)₃ and N-hydroxyphthalimide (NHPI) in O₂ in order to over-oxidize the diols into carboxylic acids, as shown by Oakley *et al.*^[110] Clean dihydroxylation of unsaturated fatty acids can be achieved with tungstic acid and 1.2 equiv. of hydrogen peroxide in *t*-BuOH. Unlike other systems using W in the form of polyoxometallates, this system can use limited amounts of hydrogen peroxide. Mechanism B applies here (Scheme 1.5). NHPI is a radical initiator that allows autooxidation of the formed diols, with the radical formation being initiated by the reaction of the cobalt catalyst with molecular oxygen. The presence of tungstic acid is still necessary for over-oxidation of the diols.^[111-113] Reactions performed in one-pot with this system can cleave oleic acid into 15% nonanoic and 15% azelaic acid (entry 176, Table 1.43). The cleavage of methyl oleate shows similar results, with 20% nonanoic acid and 19% of monomethyl azelate (entry 177). Methyl erucate, on

the other hand, shows higher selectivity towards the desired products with 54% of nonanoic acid and 41% monomethyl brassylate (entry 178).

Table 1.43. Oxidative cleavage of unsaturated fatty acids and their methyl ester in a one-pot reaction with H_2WO_4 , H_2O_2 and $\text{Co}(\text{acac})_3$ and O_2 ^a by Oakley *et al.*^[110]

Entry	Substrate	Product	Yield (%)
177	 77a	 2b	15 ^b
178	 83a	 2b	20 ^c
179	 85a	 2b	54 ^d

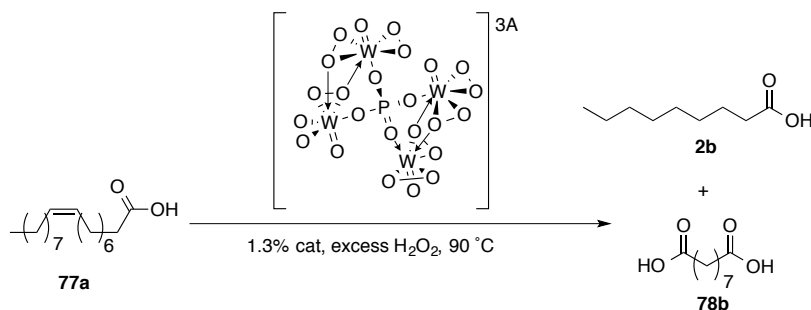
^a Reaction conditions: 1 mol% H_2WO_4 , 1.2 equiv. H_2O_2 , *t*-BuOH, 70 °C for 2 h, then 1 mol% $\text{Co}(\text{acac})_3$, 2.5 mol% NHPI, 75 °C, 3 h, O_2 bubbling, GC Yields; ^b 15% of azelaic acid observed; ^c 19% of monomethyl azelate observed; ^d 41% of monomethyl brassylate observed.

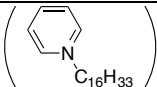
In a similar system, the diol oxidation can also be performed with $\text{Co}(\text{OAc})_2$, as shown by Santacesaria *et al.*^[112, 113] The in-situ generated catalytic species appears to be a cobalt polyoxometallate $\text{H}_6\text{CoW}_{12}\text{O}_{40}$.

Tungsten-based POMs (see 1.2.1.1.2) can also cleave unsaturated fatty acids one step with an excess of hydrogen peroxide: Turnwald *et al.*^[114] showed that the PCWP are suitable catalysts for the scission of oleic acid into azelaic and pelargonic acid in conjunction with H_2O_2 . No organic solvent is needed at vigorous stirring, and only a catalyst loading of 0.6 mol% is applied, yet an excess H_2O_2 is required. In the example of oleic acid cleavage, PCWP yields 57% azelaic acid within 5 h at 90 °C (entry 179, Table 1.44). Nevertheless, the PCWP catalyst partially breaks down after longer reaction times. Instead of the cetylpyridinium cation, Cs^+ can be used as counter-ion to circumvent catalyst loss during the reaction. The substrate converts completely and renders 28% acids (entry 181). Therefore, the PCWP catalyst appears to be more desirable than the cesium variant in terms of product formation, despite its partial decomposition.

Chapter 1

Table 1.44. Oxidative cleavage of oleic acid into pelargonic and azelaic acid with a W polyoxometallate and distinct counterions with H₂O₂^a by Turnwald *et al.*^[114]

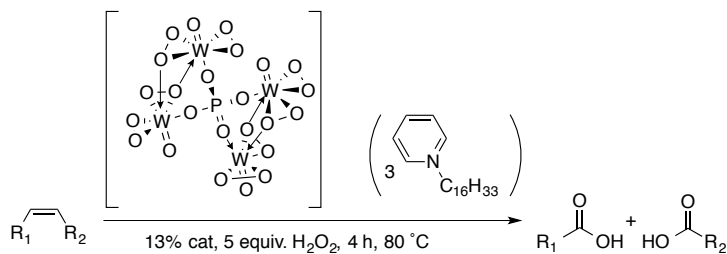


Entry	Counter-ion (A)	Time	Conversion (%)	Yield (%)	Product
180		5 h	100	57	78b^b
181	Cs ⁺	10 h	100	28	78b

^a Reaction conditions: Oleic acid, 1.3 mol% cat, excess H₂O₂, 90 °C, GC yields of pelargonic and azelaic acid. ^b After 10 h, the yield of azelaic acid was 64%, yet catalyst decomposition was observed.

The conversion and the selectivity of the PCWP mediated oleic acid cleavage can be increased when the reaction is performed at 80 °C with only 5 equiv. of H₂O₂ in 4 h, as shown by Pai *et al.*^[115] 86% of azelaic acid can be isolated from oleic acid (entry 182, Table 1.45) with 82% of nonanoic acid. Additionally, the alcohol functional group in ricinoleic acid stays intact with this system and yield 84% of both the azelaic as the mono-acid derivative **79b** (entry 183). Trace amounts of diols were still observed with both entries.

Table 1.45. Oxidative cleavage of oleic acid and its derivative into carboxylic acids with W and H₂O₂^a by Pai *et al.*^[115]



Entry	Substrate	Product	Yield (%)
182	 77a	 2b	82 ^b
183	 86a	 79b	84 ^c

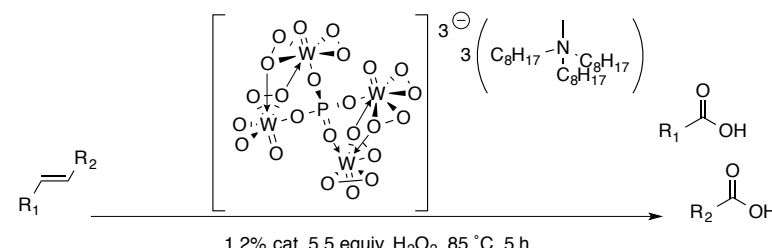
^a Reaction conditions: 13 mol% PCWP, 5 equiv. H₂O₂, 4 h, 80 °C, yields are GC yields; ^b 86% azelaic acid isolated; ^c 84% azelaic acid isolated.

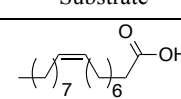
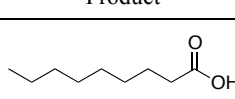
Alternatively, methyl oleate and ricinoleic acid methyl ester are converted with 1-1.2% PCWP and 5 equiv. H₂O₂ to the acids in 83-85% yield after 4 h, at an optimal reaction temperature of 85 °C, as shown by Khlebnikova *et al.*^[116] A lower catalyst loading is thus required for PCWP catalysts for the methyl esters of the unsaturated fatty acids.

Methyltrioctylammonium can also be used as the counter-ion to peroxophosphotungstate, replacing the cetyl-pyridinium cation and being applicable to oleic acid cleavage to the carboxylic acids with only 1.2 mol% catalyst loading and 5.5 equiv. of hydrogen peroxide, as shown by Antonelli and co-workers (Table 1.7).^[46] The products can be isolated in good yields after the reaction. The conditions further involve a temperature of 85 °C over 5 h reaction time. The yield of 82% nonanoic acid (Table 1.46) from reaction with oleic acid with this system is similar to the one obtained with cetyl-pyridinium as counterion (Table 1.45), yet significantly lower catalyst loadings can be applied.

Chapter 1

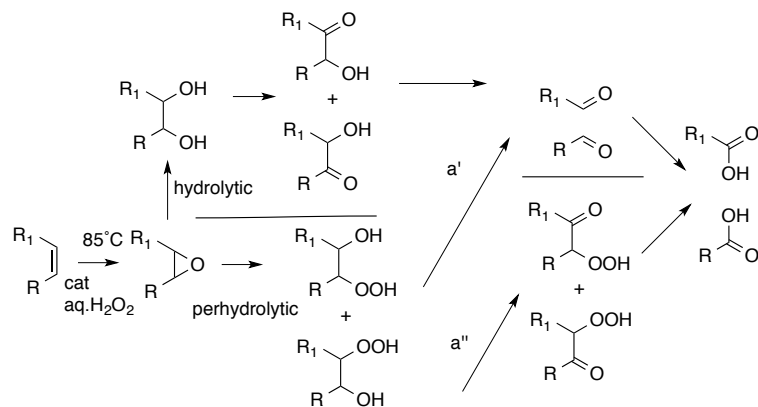
Table 1.46. Oxidative cleavage of oleic acid towards carboxylic acids by a W-based POM with a methyl-trioctyl ammonium cation^a by Antonelli *et al.*^[46]



Entry	Substrate	Product	Yield (%)
184	 77a	 2b	82 ^b

^a Reaction conditions: 1.2 mol% cat., 5.5 equiv. H₂O₂, 5 h, 80 °C, GC yield; ^b 79% azelaic acid observed.

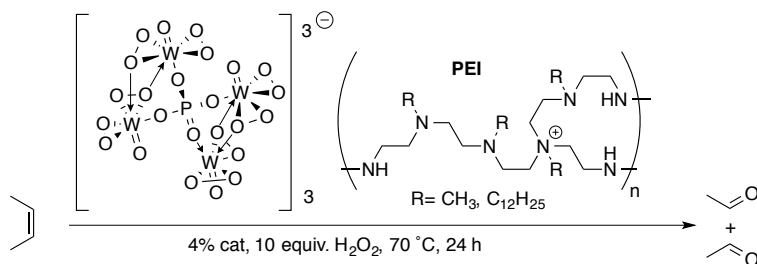
The proposed mechanism (Scheme 1.13) is similar to mechanism B, yet here hydroxy ketones are also proposed as intermediates. Moreover, a perhydrolytic pathway is proposed as well. The competition between the hydrolytic and perhydrolytic pathway is governed by the greater or lesser lipophilic character of the epoxide involved, the nature of the acid catalyst, the concentration of H₂O₂, and the relative reactivity of the two nucleophiles. The perhydrolytic pathway appears to be the major route for the present two-phase oxidation of medium- and long-chain alkenes to carboxylic acids.



Scheme 1.13. Hydrolytic vs. perhydrolytic mechanism as discussed by Antonelli *et al.*^[46]

Most of the examples involving tungsten and hydrogen peroxide form carboxylic acids from alkenes. The use of alkylated polyethyleneimine (**PEI**) with peroxophosphotungstate, on the other hand, can selectively cleave methyl oleate into 97% nonanal (Table 1.47), as shown by Haimov *et al.*^[48] This method requires 4 mol% of catalyst loading, 10 equiv. of hydrogen peroxide, 70 °C and 24 h of reaction time. When unmodified polyethyleneimine was used, no aldehydes are formed at all, which additionally shows the importance of the counter-ion with such tungsten-based POMs.

Table 1.47. Oxidative cleavage of methyl oleate towards its aldehydes with W-based POM catalyst with alkylated polyethyleneimine counter-ions and H₂O₂ by Haimov *et al.*^[48]



Entry	Substrate	Product	Yield (%)
185	83a	80b	97 ^b

^a Reaction conditions: 4 mol% cat., 10 equiv. H₂O₂, 24 h at 70 °C, yields are GC yields; ^b 100% conversion, 9-oxononanoic methyl ester observed in 97% yield.

1.3.1.2 Metal complexes

1.3.1.2.1 Ruthenium

Recent developments showed that Ru can also be reacted with an excess of H₂O₂ to cleave methyl oleate and oleic acid into the carboxylic acids when an excess of ligand is added in-situ. The protocol involves use of Ru(acac)₃ (1 mol%) and 2,6-dipicolinic acid (20 mol%) in *t*-BuOH/H₂O 1:1 (v/v) with the addition of 8 equiv. H₂O₂ over 20 h at 80 °C and 24 h total reaction time (Table 1.48), as shown by Behr *et al.*^[117] As with [*cis*-Ru(II)(dmp)₂(H₂O)₂](PF₆)₂,^[61] (see Table 1.15) the use of this complex enables the use of H₂O₂ with Ru for oxidative cleavage, albeit at high oxidant loadings due to oxidant disproportionation. Nevertheless, minor amounts of side products are observed with this protocol, and the nonanoic acid yields (**2b**) from methyl oleate (81%) and oleic acid (59%) are lower than protocols involving the Ru as metal salt. Interestingly, mechanism B (Scheme 1.5) is proposed as intermediate,^[118] unlike systems with bear Ru-salts and NaIO₄. The active species is proposed to be [Ru(2,6-dipicolinate)₂].^[118]

Chapter 1

Table 1.48. Oxidative cleavage of oleic acid and methyl oleate to carboxylic acids with a Ru catalyst with dipicolinic acid and hydrogen peroxide^a by Behr *et al.*^[117]

Entry	Substrate	Product	Conversion (%)	Yield (%)
186			100	59
187			99	81

^aReaction conditions: 1 mol% Ru(acac)₃, 20 mol% 2,6-dipicolinic acid, 8 equiv. H₂O₂, *t*-BuOH:H₂O 1:1 (v/v), 24 h at 80 °C, yields are GC yields.

1.3.1.2.2 Molybdenum

With molybdenum, the active oxo-peroxo complex [MoO(O₂)(2,6-dipicolinate)](H₂O) can be isolated^[119] and used with an excess hydrogen peroxide to transform oleic acid into pelargonic and azelaic acid, as reported by Turnwald.^[114] Both an oxo as a peroxo group are bound to the metal, and the 2,6-dipicolinate ligand is bound as dianion in a tridentate O,N,O fashion (Table 1.49). This system shows 82% GC yield of azelaic acid with quantitative conversion in an excess of hydrogen peroxide at 90 °C after 5 h. A mechanism of type B applies here (Scheme 1.5).

Table 1.49. Oxidative cleavage of oleic acid to carboxylic acids with a Mo catalyst with picolinic acid and hydrogen peroxide^a by Turnwald *et al.*^[114]

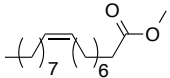
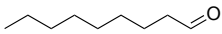
Entry	Substrate	Conversion (%)	Product	Yield (%)
188		100		82

^aReaction conditions: 1.3 mol% [MoO(O₂)(2,6-dipicolinate)](H₂O), excess H₂O₂, GC yield.

1.3.1.3 Heterogeneous catalysts

The system described by Ho *et al.*^[69] (1.2.1.3.2) involving Ru nanoparticles on hydroxyapatite can also cleave methyl oleate towards aldehydes with NaIO₄ in 1,2-dichloroethane after 12 h, albeit at low substrate conversions (Table 1.50). 13% aldehyde yield can be obtained at 16% substrate conversion with a selectivity of 84%. Compared to styrene derivatives and cyclic alkenes (1.2.1.3.2), the substrate conversion is incomplete after 12 h, whereas full conversion is obtained with other alkenes between 2-7 h. An advantage of this system is that ambient temperatures can be applied to oxidatively cleave methyl oleate to nonanal.

Table 1.50. Oxidative cleavage of methyl oleate towards aldehydes with Ru nanoparticles on hydroxyapatite and NaIO₄^a by Ho *et al.*^[69]

Entry	Substrate	Product	Conversion (%)	Yield (%)
189	 3a	 8b	16	13 ^b

^a Reaction conditions: 4 mol% nano-RuHAP, 2 equiv. NaIO₄, 12 h at ambient temperatures in 1,2-dichloroethane:H₂O 5:1 (v/v), GC yield; ^b 13% 9-oxononanoate formed.

Alternatively, silica-supported W oxide (13.3 wt% catalyst loading) is sufficient for catalytic oxidation of oleic acid in *t*-BuOH at 130 °C to azelaic and pelargonic acids with 4 equiv. of H₂O₂, as shown by Nouredini *et al.*^[120] The supported tungsten oxide yields 36% nonanoic acid at 87% conversion after 1 h (Table 1.51, entry 191), with C8 byproducts being detected. Overall, 79% of the oleic acid is converted into oxidized products. The unsupported W oxide only yields 26% nonanoic acid at 71% conversion, forms C5-C8 byproducts and converts 56% of the substrate into oxidation products (entry 190). The supported catalyst thus outperformed the unsupported catalyst in terms of activity and selectivity. Tantalum oxides and alumina-supported catalysts show lower product yields. Also longer reaction times barely increase the yields of nonanoic and azelaic acids. No recycling experiments are reported for this system.

Chapter 1

Table 1.51. Oxidative cleavage of methyl oleate by W an Ta oxide catalysts with hydrogen peroxide in *t*-BuOH^a by Nouredдини *et al.*[120]

Ent.	Catalyst	Substrate	Product	Conv. (%)	Yield (%)
190	W oxide powder			71	26 ^b
191	Silica-supported W oxide			87	36 ^c

^a Reaction conditions: 13.3 wt% W oxide powder or silica supported W oxide, 4 equiv. H₂O₂, *t*-BuOH, 1 h, 130 °C, GC yield; ^b 26% diacid observed, C5-C8 mono- and diacids visible as byproducts, 56% conversion into oxidation products; ^c 32% diacid observed, C8 mono- and diacids visible as byproducts, 79% conversion into oxidation products.

1.4 Outlook and concluding remarks

This review shows that a large number of transition metal-catalyzed oxidative cleavage reactions of alkenes are known with second- and third-row transition metal systems, in particular with Ru, W and Os. In recent years, advances have been made in order to improve systems involving metal-salts, metal-oxides or metal-peroxides with these metals, e. g. decrease of catalyst loading or use of less and more benign oxidants. Some coordination metal complexes have been reported that focus on regioselectivity and the decrease of the toxicity these systems. Also, several heterogeneous catalysts have been developed that enable catalyst reuse. Moreover, unsaturated fatty acids can nowadays be cleaved at high efficiency with these second- and third-row metals. Efforts have been made to make use of more environmentally friendly oxidants for these reactions, such as H₂O₂ and O₂, in order to address issues concerning the use of stoichiometric or other undesired oxidants. Nevertheless, the examples of unsaturated fatty acid cleavage reactions still make use of either toxic, expensive or not very abundant second- and third-row transition metals.

The advances in the use of first-row transition metals for oxidative cleavage of alkenes are also vast, albeit that most reactions focus on activated substrates, such as styrene derivatives. Some systems report cleavage reactions of terpenes, yet no oxidative cleavage reactions have been reported for unsaturated fatty acids. Most first-row systems involve abundant, non-toxic and cheap metals, such as Fe or Mn, comprise ligands that are readily synthesized or commercially available and make use of benign oxidants. Promising examples are known in nature comprising several first-row metals to be active for the

desired oxidative cleavage reactions. The examples of carotenoid oxygenases^[121-124] show that Fe can be used in oxidative double bond cleavage reactions as a catalyst and can serve as a source of inspiration for the design of biomimetic catalysts capable of cleaving unsaturated fatty acids, for instance. The possibilities to develop first-row transition metal-catalyzed oxidative cleavage systems given the analogies for non-fatty alkenes and the examples shown in nature can be considered fruitful for future research on such systems for oxidative cleavage reactions of unsaturated fatty acids. The same holds for the use of environmentally benign oxidants such as H₂O₂ or O₂ instead of ozone, hypochlorite or other oxidants.

1.5 References

- [1] H. Baumann, M. Bühler, H. Fochem, F. Hirsinger, H. Zobelein, J. Falbe *Angew. Chem. Int. Ed.* **1988**, 27, 41.
- [2] U. Biermann, U. Bornscheuer, M. A. R. Meier, J. O. Metzger, H. J. Schäfer *Angew. Chem. Int. Ed.* **2011**, 50, 3854.
- [3] A. Severino, A. Esculcas, J. Rocha, J. Vital, L. S. Lobo *Appl. Catal., A* **1996**, 142, 255.
- [4] A. Corma, S. Iborra, A. Velty *Chem. Rev.* **2007**, 107, 2411.
- [5] G. Gündüz, R. Dimitrova, S. Yilmaz, L. Dimitrov *Appl. Catal., A* **2005**, 282, 61.
- [6] U. Biermann, W. Friedt, S. Lang, W. Lühs, G. Machmüller, J. O. Metzger, M. Rüschen, H. J. Schäfer, M. P. Schneider *Angew. Chem. Int. Ed.* **2000**, 39, 2206.
- [7] M. C. Kuo, T. C. Chou *Ind. Eng. Chem. Res.* **1987**, 26, 277.
- [8] K. Hill *Pure Appl. Chem.* **2000**, 72, 1255.
- [9] A. Köckritz, A. Martin *Eur. J. Lipid Sci. Technol.* **2008**, 110, 812.
- [10] D. G. Diaper *Can. J. Chem.* **1955**, 33, 1720.
- [11] B. Zaidman, A. Kisilev, Y. Sasson, N. Garti *J. Am. Oil Chem. Soc.* **1988**, 65, 611.
- [12] F. V. Singh, H. M. S. Milagre, M. N. Eberlin, H. A. Stefani *Tetrahedron Lett.* **2009**, 50, 2312.
- [13] K. Miyamoto, N. Tada, M. Ochiai *J. Am. Chem. Soc.* **2007**, 129, 2772.
- [14] R. U. Lemieux, E. Von Rudloff *Can. J. Chem.* **1955**, 33, 1701.
- [15] K. B. Wiberg, K. A. Saegbarth *J. Am. Chem. Soc.* **1957**, 79, 2822.
- [16] T. Ogino, K. Mochizuki *Chem. Lett.* **1979**, 5, 443.
- [17] P. Viski, Z. Szevernyi, L. I. Simandi *J. Org. Chem.* **1986**, 51, 3213.
- [18] C. M. Starks *J. Am. Chem. Soc.* **1971**, 93, 195.
- [19] A. P. Krapcho, J. R. Larson, J. M. Elridge *J. Org. Chem.* **1977**, 32, 3749.
- [20] D. J. Sam, H. E. Simmons *J. Am. Chem. Soc.* **1972**, 94, 4024.
- [21] D. G. Lee, V. S. Chang *J. Org. Chem.* **1978**, 43, 1532.
- [22] L. F. Fieser, J. Szmuszkovicz *J. Am. Chem. Soc.* **1948**, 70, 3352.
- [23] F. Freeman, N. J. Yamachika *J. Am. Chem. Soc.* **1970**, 92, 3730.
- [24] L. M. Berkowitz, P. N. Rylander *J. Am. Chem. Soc.* **1958**, 75, 6682.
- [25] F. M. Dean, J. C. Knight *J. Chem. Soc.* **1962**, 4745.
- [26] H. J. Carlsen, T. Katsuki, V. S. Martin, K. B. Sharpless *J. Org. Chem.* **1981**, 46, 3936.
- [27] S. Wolfe, S. K. Hasan, J. R. Campbell *J. Chem. Soc. D* **1970**, 1420.
- [28] Y. Shalon, W. H. Elliott *Synth. Commun.* **1973**, 3, 287.

Chapter 1

- [29] S. Warwel, M. Sojka, M. Rüschen-Klaas, *Synthesis of dicarboxylic acids by transition-metal catalyzed oxidative cleavage of terminal-unsaturated fatty acids*, Springer, Berlin Heidelberg, **1993**, 79-98.
- [30] R. Pappo, D. S. Allen, R. U. Lemieux, W. S. Johnson *J. Org. Chem.* **1956**, *21*, 478.
- [31] B. E. Rossiter, T. Katsuki, K. B. Sharpless *J. Am. Chem. Soc.* **1981**, *103*, 464.
- [32] S. Torii, T. Inokuchi, K. Kondo *J. Org. Chem.* **1985**, *50*, 4980.
- [33] K. Kaneda, S. Haruna, T. Imanaka, K. Kawamoto *J. Chem. Soc., Chem. Commun.* **1990**, 1467.
- [34] D. Yang, C. Zhang *J. Org. Chem.* **2001**, *66*, 4814.
- [35] V. Piccialli, D. M. A. Smaldone, D. Sica *Tetrahedron* **1993**, *49*, 4211.
- [36] L. Albarella, F. Giordano, M. Lasalvia, V. Piccialli, D. Sica *Tetrahedron Lett.* **1995**, *36*, 5267.
- [37] R. Neumann, C. Abu-Gnim *J. Chem. Soc., Chem. Commun.* **1989**, 1324.
- [38] R. Neumann, C. Abu-Gnim *J. Am. Chem. Soc.* **1990**, *112*, 6025.
- [39] A. G. Shoaib, R. Mohamed *Synth. Commun.* **2006**, *36*, 59.
- [40] W. P. Griffith, A. G. Shoaib, M. Suriaatmaja *Synth. Commun.* **2000**, *30*, 3091.
- [41] P. Muller, J. Godoy *Helv. Chim. Acta.* **1981**, *64*, 2531.
- [42] T. Oguchi, T. Ura, Y. Ishii, M. Ogawa *Chem. Lett.* **1989**, *18*, 857.
- [43] Y. Ishii, K. Yamawaki, T. Ura, H. Yamada, T. Yoshida, M. Ogawa *J. Org. Chem.* **1988**, *53*, 3587.
- [44] C. Venturello, M. Ricci *J. Org. Chem.* **1983**, *48*, 3831.
- [45] T. Fujitani, M. Nakazawa *Chem. Abstr.* **1988**, *109*, 230298b.
- [46] E. Antonelli, R. D'Aloisio, M. Gambaro, T. Fiorani, C. Venturello *J. Org. Chem.* **1998**, *63*, 7190.
- [47] R. Noyori, M. Aoki, K. Sato *Chem. Commun.* **2003**, 1977.
- [48] A. Haimov, H. Cohen, R. Neumann *J. Am. Chem. Soc.* **2004**, *126*, 11762.
- [49] J. Freitag, M. Nuchter, B. Ondruschka *Green Chem.* **2003**, *5*, 291.
- [50] C. J. R. Bataille, T. J. Donohoe *Chem. Soc. Rev.* **2011**, *40*, 114.
- [51] J. R. Henry, S. M. Weinreb *J. Org. Chem.* **1993**, *58*, 4745.
- [52] B. R. Travis, R. S. Narayan, B. Borhan *J. Am. Chem. Soc.* **2002**, *124*, 3824.
- [53] C. Francavilla, W. Chen, F. R. Kinder Jr. *Org. Lett.* **2003**, *5*, 1233.
- [54] R. E. Taylor, Y. Chen, A. Beatty, D. C. Myles, Y. Zhou *J. Am. Chem. Soc.* **2003**, *125*, 26.
- [55] Z. Wang, M. G. Moloney *Tetrahedron Lett.* **2002**, *43*, 9629.
- [56] W. Yu, Y. Mei, Y. Kang, Z. Hua, Z. Jin *Org. Lett.* **2004**, *6*, 3217.
- [57] D. C. Whitehead, B. R. Travis, B. Borhan *Tetrahedron Lett.* **2006**, *47*, 3797.
- [58] S. Kim, J. Chung, B. M. Kim *Tetrahedron Lett.* **2011**, *52*, 1363.
- [59] B. C. Ranu, S. Bhadra, L. Adak *Tetrahedron Lett.* **2008**, *49*, 2588.
- [60] A. Wang, H. Jiang *J. Org. Chem.* **2010**, *75*, 2321.
- [61] V. Kogan, M. M. Quintal, R. Neumann *Org. Lett.* **2005**, *7*, 5039.
- [62] A. S. Goldstein, R. H. Beer, R. S. Drago *J. Am. Chem. Soc.* **1994**, *116*, 2424.
- [63] S. Samanta, L. Adak, R. Jana, G. Mostafa, H. M. Tuononen, B. C. Ranu, S. Goswami *Inorg. Chem.* **2008**, *47*, 11062.
- [64] W. A. Herrmann, R. W. Fischer, D. W. Marz *Angew. Chem.* **1991**, *103*, 1706.
- [65] W. A. Herrmann, R. W. Fischer, D. W. Marz *Angew. Chem. Int. Ed. Engl.* **1991**, *30*, 1638.
- [66] W. A. Herrmann, T. Weskamp, J. P. Zoller, R. W. Fischer *J. Mol. Catal. A: Chem.* **2000**, *153*, 49.
- [67] D. Xing, B. Guan, G. Cai, Z. Fang, L. Yang, Z. Shi *Org. Lett.* **2006**, *8*, 693.
- [68] C. D. Brooks, L. C. Huang, M. McCarron, R. A. W. Johnstone *Chem. Commun.* **1999**, 37.
- [69] C. M. Ho, W. Y. Yu, C. M. Che *Angew. Chem. Int. Ed.* **2004**, *43*, 3303.
- [70] H. Okumoto, K. Ohtsuka, S. Banjaya *Synlett.* **2007**, *20*, 3201.
- [71] V. A. Kumar, V. Prakash Reddy, R. Sridhar, B. Srinivas, K. Rama Rao *Synlett.* **2009**, *5*, 739.

- [72] S. V. Ley, C. Ramarao, A. L. Lee, N. Ostergaard, S. C. Smith, I. M. Shirley *Org. Lett.* **2003**, *5*, 185.
- [73] L. I. Simandi, T. L. Simandi *J. Mol. Catal. A: Chem.* **1997**, *117*, 299.
- [74] Y. H. Lin, I. D. Williams, P. Li *Appl. Catal. A: Gen.* **1997**, *150*, 221.
- [75] K. Kaneda, T. Itoh, N. Kii, K. Jitsukawa, S. Teranishi *J. Mol. Catal.* **1982**, *15*, 349.
- [76] T. Koyama, A. Kitani, S. Ito, K. Sasaki *Chem. Lett.* **1993**, *3*, 395.
- [77] M. Tokunaga, Y. Shirogane, H. Aoyama, Y. Obora, Y. Tsuji *J. Org. Chem.* **2005**, *690*, 5378.
- [78] T. M. Shaikh, F. Hong *Adv. Synth. Catal.* **2011**, *353*, 1491.
- [79] H. Mimoun, L. Saussine, E. Davire, M. Postel, J. Fisher, R. Weiss *J. Am. Chem. Soc.* **1983**, *105*, 3101.
- [80] B. M. Choudary, P. N. Reddy *J. Mol. Catal. A: Chem.* **1995**, *103*, L1.
- [81] R. S. Drago, J. P. Cannady, K. A. Leslie *J. Am. Chem. Soc.* **1980**, *102*, 6014.
- [82] R. S. Drago, B. B. Corden, C. W. Barnes *J. Am. Chem. Soc.* **1986**, *108*, 2453.
- [83] P. A. Ganeshpure, S. Satish *Tetrahedron Lett.* **1988**, *29*, 6629.
- [84] A. Dhakshinamoorthy, K. Pitchumani *Tetrahedron* **2006**, *62*, 9911.
- [85] B. Kalyanaraman, E. G. Janzen, R. P. Mason *J. Biol. Chem.* **1985**, *260*, 4003.
- [86] Y. F. Li, C. C. Guo, X. H. Yan, Q. Liu *J. Porphyrins Phtalocyanines* **2006**, *10*, 942.
- [87] X. Zhou, H. Ji *Chin. J. Chem.* **2012**, *30*, 2103.
- [88] H. Chen, H. Ji, X. Zhou, J. Xu, L. Wang *Catal. Commun.* **2009**, *10*, 828.
- [89] J. Haber, T. Młodnicka, J. Poltowicz *J. Mol. Catal.* **1989**, *54*, 451.
- [90] S. T. Liu, K. V. Reddy, R. Y. Lai *Tetrahedron* **2007**, *63*, 1821.
- [91] S. Jarupinthusophon, U. Thong-In, W. Chavasiri *J. Mol. Catal. A: Chem.* **2007**, *270*, 289.
- [92] S. O. Lee, R. Raja, K. D. M. Harris, J. M. Thomas, B. F. G. Johnson, G. Sankar *Angew. Chem. Int. Ed.* **2003**, *43*, 1520.
- [93] L. Nie, K. K. Xin, W. S. Li, X. P. Zhou *Catal. Commun.* **2007**, *8*, 488.
- [94] J. Zhuang, D. Ma, Z. Yan, X. Liu, X. Han, X. Bao, Y. Zhang, X. Guo, X. Wang *Appl. Catal. , A* **2004**, *258*, 1.
- [95] M. Hsiao, S. Liu *Catal. Lett.* **2010**, *139*, 61.
- [96] Z. Saedi, S. Tangestaninejad, M. Moghadam, V. Mirkhani, I. Mohammadpoor-Baltork *Catal. Commun.* **2012**, *17*, 18.
- [97] F. Shi, M. K. Tse, M. M. Pohl, A. Bruckner, S. Zhang, M. Beller *Angew. Chem. Int. Ed.* **2007**, *46*, 8866.
- [98] N. Ma, Y. Yue, W. Hua, Z. Gao *Appl. Catal. , A* **2003**, *251*, 39.
- [99] D. R. Burri, K. Choi, J. Lee, D. Han, S. Park *Catal. Commun.* **2007**, *8*, 43.
- [100] N. Anand, K. P. R. Reddy, V. Swapna, K. S. R. Rao, D. R. Burri *Micropor. Mesop. Mat.* **2011**, *143*, 132.
- [101] Lie Ken Jie, M. S. F., P. Kalluri *Lipids* **1996**, *31*, 1299.
- [102] I. Garti, E. Avni *J. Am. Oil Chem. Soc.* **1981**, *58*, 840.
- [103] S. Warwel, M. Rüschen, Klaas *Chem. Abstr.* **1996**, *125*, 136578.
- [104] S. Warwel, M. Rüschen, Klaas, *Oxidative Cleavage of Unsaturated Fatty Acids without Ozone*, **1997**, pp. 130.
- [105] S. Warwel, W. Pompetzki, E. A. Deckwirth *Fat. Sci. Technol.* **1991**, *93*, 210.
- [106] Y. Nakano, T. A. Foglia *J. Am. Oil Chem. Soc.* **1982**, *59*, 163.
- [107] F. Zimmermann, E. Meux, J. L. Mieloszynski, J. M. Lecuire, N. Oget *Tetrahedron Lett.* **2005**, *46*, 3201.

Chapter 1

- [108] S. Rup, F. Zimmermann, E. Meux, M. Schneider, M. Sindt, N. Oget *Ultrason. Sonochem.* **2009**, *16*, 266.
- [109] S. Rup, M. Sindt, N. Oget *Tetrahedron Lett.* **2010**, *51*, 3123.
- [110] M. A. Oakley, S. Woodward, K. Coupland, D. Parker, C. Temple-Heald *J. Mol. Catal. A: Chem.* **1999**, *150*, 105.
- [111] A. T. Herrmann, S. Warwel, M. Rüschen, Klaas, **1997**, German Patent 19724736.
- [112] E. Santacesaria, A. Sorrentino, F. Rainone, M. Di Serio, F. Speranza *Ind. Eng. Chem. Res.* **2000**, *39*, 2766.
- [113] E. Santacesaria, M. Ambrosio, A. Sorrentino, R. Tesser, M. Di Serio *Catal. Today* **2003**, *79-80*, 59.
- [114] S. E. Turnwald, M. A. Lorier, L. J. Wright, M. R. Mucalo *J. Mat. Sci. Lett.* **1998**, *17*, 1305.
- [115] Z. P. Pai, A. G. Tolstikov, P. V. Berdnikova, G. N. Kustova, T. B. Khlebnikova, N. V. Selivanova, A. B. Shangina, V. G. Kostrovskii *Russ. Chem. Bull, Int. Ed.* **2005**, *54*, 1847.
- [116] T. B. Khlebnikova, Z. P. Pai, L. A. Fedoseeva, Y. V. Matsat *React. Kinet. Catal. Lett.* **2009**, *98*, 17.
- [117] A. Behr, N. Tenhumberg, A. Wintzer *RSC Adv.* **2013**, *3*, 172.
- [118] A. Behr, N. Tenhumberg, A. Wintzer *Eur. J. Lipid Sci. Technol.* **2012**, *114*, 905.
- [119] S. E. Jacobson, R. Tang, F. Mares *Inorg. Chem.* **1978**, *17*, 3055.
- [120] H. Nouredini, M. Kanabur *J. Am. Oil Chem. Soc.* **1999**, *76*, 305.
- [121] J. A. Olson, O. Hayaishi *PNAS* **1965**, *54*, 1364.
- [122] A. Wyss *J. Nutr.* **2004**, *134*, 246S.
- [123] D. P. Kloer, S. Ruch, S. Al-Babili, P. Beyer, G. E. Schulz *Science* **2005**, *308*, 267.
- [124] F. G. Mutti *Bioinorganic Chemistry and Applications* **2012**, *2012*, Article ID 626909.

Metal-free oxidative cleavage of terpenes and unsaturated fatty acids

Chapter 2

A metal-free, one-pot method for the oxidative cleavage of internal aliphatic alkenes into carboxylic acids

Abstract

The oxidative cleavage of terpenes and unsaturated fatty acids into carbonyl compounds is an industrially interesting reaction. A metal-free protocol has been developed that can oxidatively cleave unsaturated fatty acids, terpenes and a variety of other alkenes into carboxylic acids in a synthetically straightforward, one-pot protocol. Near stoichiometric amounts of a combination of oxone and periodate are used in aqueous acetonitrile without additional additives, acids or emulsifiers. The solvent system and the reaction temperature have a profound influence on the reactivity of the substrates; conditions have been optimized for a broad scope of alkenes. The products can be isolated by simple extraction with an organic solvent without additional purification: the carboxylic acids are obtained in high yield (80-96%) as colorless solid or liquid products.

Based on: Peter Spannring, Pieter C. A. Bruijninx, Bert M. Weckhuysen and Robertus J. M. Klein Gebbink, *RSC Adv.* **2013**, 3, 6606

2.1 Introduction

Terpenes and unsaturated fatty acids derived from vegetable oils and animal fats constitute natural resources of olefins. These renewable olefins may function as a feedstock for the production of a number of linear and branched functionalized hydrocarbons, e.g. after oxidative cleavage of the double bond(s). A large-scale industrial application involving an unsaturated fatty acid is the oxidative cleavage of the internal double bond of oleic acid by ozonolysis.^[1-3] The products of this oxidative cleavage reaction are mono- or dicarbonyls (Scheme 2.1), i.e. aldehydes or carboxylic acids, which can be used for polymer, plasticizer and stabilizer production.^[1-3] A downside of this particular oxidative cleavage process is the use of the very hazardous oxidant ozone, which needs to be generated in-situ for safety reasons and can cause explosions.^[4]



Scheme 2.1. Oxidative cleavage of *cis*- or *trans*-alkenes into carboxylic acids.

Metal catalysts have been used for the catalytic oxidative cleavage of internal olefins. Expensive and often toxic transition-metal complexes of Ru,^[5-10] W^[11-17] or Os^[18-25] are known to catalyze the oxidative cleavage. From an economic and environmental perspective, it would be desirable to use catalysts based on cheaper, less toxic and more abundant metals, such as the first-row transition metals. However, catalyst systems based on these metals are only known to cleave activated olefin substrates, such as styrene derivatives, cyclic olefins and relatively electron-poor alkenes. Typical catalysts for these transformations consist of salen-type^[26, 27] and porphyrine-type^[28-30] ligands in combination with metals such as Fe or Mn. Permanganate is also commonly used for these reactions, albeit in stoichiometric amounts.^[31-39] Many different oxidants have been used with first-row transition metal catalysts for oxidative olefin cleavage. These include oxone, periodate and hydrogen peroxide. Yet, none of these metal-oxidant combinations brings about the activity and selectivity that is obtained with second- or third-row metal-oxidants or ozone.^[40]

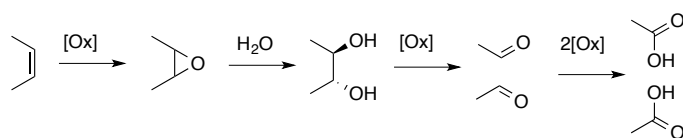
The choice of solvent system has been shown to be another factor of crucial importance in metal-catalyzed olefin cleavage reactions. Oxone (2KHSO₅·KHSO₄·K₂SO₄, 1.5 equiv.) has been used in aqueous acetonitrile (3:2, v/v) to cleave styrene derivatives and cyclic olefins to aldehydes with catalytic amounts of RuCl₃.^[8] Using trace amounts of OsO₄, oxone is known to cleave olefins in pure DMF, giving high yields of carboxylic acids above 85% for a variety of alkenes.^[22] The well-known Sharpless system uses periodate as the oxidant with RuCl₃ in different solvent mixtures, ranging from CCl₄:MeCN:H₂O (2:2:3, v/v)^[5] to EtOAc:MeCN:H₂O (2:2:3, v/v).^[41, 42] Also, 1,2-dichloroethane:H₂O (1:1, v/v),^[8] dioxane/H₂O

Chapter 2

(3:1, v/v),^[25] pure 1,2-dichloroethane,^[43] EtOAc:H₂O (3:5, v/v),^[44] EtOAc:MeCN:H₂O^[45] (1:1:1, v/v) or THF/H₂O (2:1, v/v)^[46] can be applied with this system. It should be noted that neither periodate nor oxone is known to cleave alkenes directly without a catalyst.

Enzymes can also be used for oxidative cleavage reactions,^[47] just like photochemolysis^[48] and anodic oxidation,^[49] yet the examples are scarce and have only a narrow substrate scope.

One could consider the oxidative cleavage of olefins to carboxylic acids to be the result of sequential oxidation steps, involving epoxide, diol and aldehyde intermediates (Scheme 2.2). Adaptation of systems known to catalyze epoxidation or dihydroxylation of internal olefins can therefore be of interest for the development of new catalytic systems for selective oxidative C=C bond scission.



Scheme 2.2. Oxidative cleavage mechanism.

Oxone is an attractive oxidant for alkene oxidation, as it is cheap and readily accessible. Epoxidations with oxone have been reported in water at neutral pH and without organic solvent, but the activity for electron-rich aliphatic olefins proved negligible under these conditions.^[50] Other common solvents for epoxidations with oxone are aqueous MeCN or hexafluoroisopropanol. Ketones are commonly added in such olefin oxidations with oxone,^[51, 52] to yield dioxirane intermediates, which are the active species in the epoxidation.^[53, 54] Indeed, the epoxidation activity is very low without the ketone additive.^[50] Oxone has also been reported to mediate the formation of *cis*-diols from alkenes with an Fe catalyst.^[55] The use of tetraaza-macrocyclic ligands in a MeCN:H₂O (1:1, v/v) mixture enables *cis*-diol formation for a variety of electron-deficient alkenes, such as styrene derivatives. The activity and selectivity for electron-rich internal alkenes proved to be poor, however. Alternatively, alkenes can be transformed into diols with cyclobutane malonoyl peroxide.^[56] This system omits the use of an expensive or toxic transition metal. However, it needs the active oxidative species to be made in-situ with an excess of hydrogen peroxide in the presence of an acid additive, and is primarily active for styrene derivatives. Eventually, the diol intermediates, which can be obtained by hydrolysis of the epoxide or directly formed by *cis*-dihydroxylation, can be cleaved by periodate to give the corresponding aldehydes.^[57]

Importantly, the nature of the olefin has a profound influence on the efficiency of a cleavage reaction and on the product outcome. Of the aliphatic alkenes, which are relatively electron-rich, the terminal alkenes are often more easily converted because of their lower steric demand and their higher electron deficiency compared to their internal

counterparts.^[30, 58] For styrene derivatives, a similar general trend can be observed, i.e. more electron-deficient substrates give higher yields of the cleavage product with many metal-catalyzed procedures (see Chapter 1).^[59, 60] On the other hand, some catalytic systems have been reported to display no preference for either electron-rich or electron-poor styrene substrates.^[30, 58]

In the course of an investigation aimed at the development of an oxidation catalyst based on first-row transition metals capable of oxidative olefin cleavage in renewable substrates such as unsaturated fatty acids and terpenes, significant amounts of cleavage products were observed in reactions with a combination of sacrificial oxidants only, i.e. without any metal complex. This observation was followed and a practical metal-free, one-pot method for the oxidative cleavage of olefins is presented. Here, details are provided on the overall optimization and substrate scope of this approach, which show that the combination of oxone and periodate in a MeCN:H₂O reaction mixture shows a preference for the cleavage of electron-rich internal olefins.

2.2 Results and discussion

2.2.1 Oxidative cleavage of *cis*-4-octene

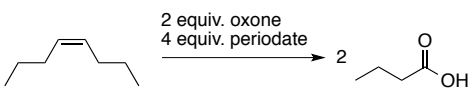
In the initial reactivity tests *cis*-4-octene was selected as substrate to mimic the electron-rich internal double bond in unsaturated fatty acids. *Cis*-4-octene is a convenient model substrate as it is generally better soluble in organic media, does not contain a functional group that may interfere with reactivity, and leads to a single product upon cleavage as a result of its symmetric structure.

The reaction between *cis*-4-octene and a combination of oxone (2 equiv., containing 4 oxidizing equiv. of peroxymonosulfate) and sodium periodate (4 equiv.) at ambient temperature shows no reaction in MeCN after 16 h (Table 2.1, entry 1) and only moderate activity in H₂O (entry 2). The introduction of an organic solvent in addition to H₂O shows the influence of solvent composition on activity and selectivity: hardly any activity is observed in DMF:H₂O (3:1, v/v) (entry 3), whereas DMF:H₂O (1:3, v/v) shows a 67% substrate conversion and 35% butyric acid yield (entry 4). When MeCN was used instead of DMF, similar results were obtained: in MeCN:H₂O (1:1, v/v) a 69% conversion and 35% yield of butyric acid were observed (entry 5). Highest substrate conversions and butyric acid yields were obtained after 16 h using a MeCN:H₂O (1:3, v/v) mixture as the reaction medium (entry 6). Under these conditions, an increase in conversion to 86% and a yield in butyric acid of 61% can be achieved after 26 h (entry 7). Notably, product analysis by means of gas chromatography of all entries showed no or hardly any other products than butyric acid. When the reaction was run for 72 h with MeCN:H₂O (1:3, v/v), full conversion was obtained with a 95% butyric acid yield (entry 8). The reaction can also be scaled up

Chapter 2

tenfold (14.4 mmol), enabling the isolation of 84% of cleavage product (see Experimental Section). Based on this solvent screening, reactions were subsequently run in MeCN:H₂O (1:3, v/v) (method A). The incomplete mass balance at intermediate reaction times shows that reaction intermediates such as, e.g., iodate esters, must be present and are not detected by GC.

Table 2.1. Solvent optimization for the conversion of *cis*-4-octene to butyric acid.^a



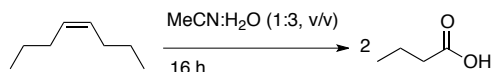
Entry	Solvent (v/v)	Time (h)	Conversion (%)	Yield (%) ^b
1 ^c	MeCN	16	0	0
2 ^c	H ₂ O	26	30	10
3	DMF:H ₂ O 3:1	16	6	2
4	DMF:H ₂ O 1:3	16	67	35
5	MeCN:H ₂ O 1:1	16	69	35
6	MeCN:H ₂ O 1:3	16	74	51
7	MeCN:H ₂ O 1:3	26	86	61
8	MeCN:H ₂ O 1:3	72	100	95

^a Reaction conditions: 2 equiv. oxone, 4 equiv. periodate, 0.135 M *cis*-4-octene in 4 mL solvent, 16 h reaction time, ambient temperature; ^b Yield determined by GC analysis, maximum yield set to 100%.

Next, the effect of the oxidant loading, the pH of the reaction medium, and the reaction temperature were investigated. It was anticipated that the initial oxidant loading of 2 equiv. oxone and 4 equiv. of periodate could be lowered without significant loss of reactivity, since 4 oxidizing equivalents should be sufficient for the full conversion of a double bond into carboxylic acids.

A decrease in periodate loading from 4 equiv. to 2 equiv. had almost no effect on the conversion (72% after 16 h; Table 2.2, entries 1-2), with the amount of butyric acid formed being almost the same (51-55%). Further decrease to 1 equiv. of periodate gave similar results, with 79% conversion and 52 product yield (entry 3). Since the cleavage of diols towards aldehydes can be achieved with 1 equiv. of periodate, over-oxidation to carboxylic acids seems to be carried out by oxone.

Table 2.2. Optimization of the oxidant loading for the conversion of *cis*-4-octene into butyric acid.^a



Entry	Oxone : NaIO ₄ (equiv.)	pH	T	Conversion (%)	Yield (%) ^b
1	2:4	1.4	RT	74	51
2	2:2	1.4	RT	72	55
3	2:1	1.4	RT	79	52
4	1:4	1.9	RT	51	29
5	0.5:4	2.0	RT	29	16
6 ^c	2:4	6.0	RT	52	34
7 ^d	2:4	7.3	RT	51	0
8 ^e	2:4	7.4	RT	39	0
9	2:4	1.4	0 °C	33	33
10	2:4	1.4	50 °C	100	82

^a Reaction conditions: 1-4 equiv. of oxidant, 0.135 M *cis*-4-octene in MeCN:H₂O (1:3, v/v), ambient temperature, 16 h, measured pH of 1.4; ^b Yield determined by GC analysis, maximum yield set to 100%; ^c 6 equiv. NaHCO₃ added; ^d 12 equiv. NaHCO₃ added; ^e 18 equiv. NaHCO₃ added.

On the other hand, lowering the amount of oxone from 2 to 1 equiv. does lead to a decrease of the conversion to 51% and of the yield of butyric acid to 29%, but does not lead to the formation of butyraldehyde (entry 4). This shows that over-oxidation proceeds readily. Further decrease of the amount of oxone to 0.5 equiv. gave a significant further decrease of these values (entry 5). The amount of periodate can therefore be decreased to 1 equiv. without any loss in conversion or selectivity at ambient temperature for the oxidative cleavage of *cis*-4-octene, whereas 2 equiv. of oxone are required to achieve high yields.

The pH of 1.4 that was recorded at the start of the reaction was not significantly changed at the end of the reaction. Increasing the pH to 6.0 by addition of NaHCO₃ (6 equiv., entry 6), led to a drop in conversion from 74% to 52%. Further increase of the pH led to even lower conversions (entries 7-8), therefore the addition of NaHCO₃ was omitted in further experiments.

Next, the reaction was performed at 0 °C, which led to a drop in the conversion from 74% to 33%, yet the selectivity to butyric acid was quantitative (entry 9). The latter shows that most likely the rate-determining step is the substrate epoxidation at this temperature,

Chapter 2

unlike reactions performed at higher temperatures. At 60 °C the substrate was fully converted and the yield in butyric acid was 82% (entry 10).

Besides oxone, *m*-chloroperbenzoic acid (mcpba) was investigated as a stoichiometric epoxidation agent. The use of mcpba enables the protocol to work under milder pH and the substrate is converted more rapidly. Additionally, small amounts of aldehyde are formed in this protocol, which are not observed with oxone. Yet, more oxidant is needed in order to arrive at reasonable amounts of cleavage product. Additionally, the epoxide remains as a byproduct in the reactions with mcpba.

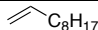
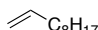
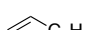
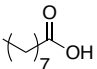
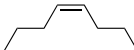
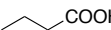
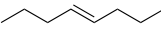
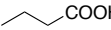
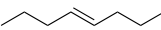
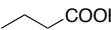
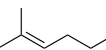
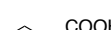
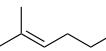
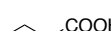
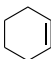
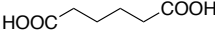


The combination of periodate and oxone was therefore preferred for further studies exploring the substrate scope of the system optimized for *cis*-4-octene, i.e. with MeCN:H₂O (1:3, v/v) as solvent and an oxidant loading of oxone:NaIO₄ 2:1.5 equiv. (method A). A slight excess of the NaIO₄ is used in the substrate scoping reactions to maximize yields. Aliphatic olefins are good mimics of unsaturated fatty acids and therefore interesting to investigate in a substrate scope. Styrenes and stilbenes are more electron-poor alkenes than aliphatic ones, yet are often used for oxidative cleavage to benzoic acid and have been included to compare the system with those previously published (Chapter 1). Furthermore, the cleavage reactions of the naturally occurring terpenes limonene (a diene) and pinene were investigated. Finally, it was investigated whether the protocol could be applied to the oxidative cleavage of unsaturated fatty acids.

2.2.2 Oxidative cleavage of aliphatic alkenes

The terminal aliphatic olefin 1-decene did hardly react under the standard conditions of method A nor at more elevated temperatures (91% substrate recovery, Table 2.3, entries 1-2). Therefore, a second method (method B) was developed that involves using a solvent composition of MeCN:H₂O (3:1, v/v) and heating to reflux first, in order to ensure dissolution of substrates not soluble under the conditions used in method A. After 16 h of reaction, the reaction mixture is then diluted with water to give again a MeCN:H₂O (1:3, v/v) mixture and is subsequently refluxed for 2 more hours, this to ensure complete dissolution and reaction of the periodate. With this method B, 47% substrate conversion of 1-decene can be achieved, yielding 42% nonanoic acid (entry 3). Method B was also applied to *cis*-4-octene, giving full substrate conversion and a high butyric acid yield after 18 h instead of the 3 days needed with method A (entry 4). *Trans*-4-octene, which showed a lower activity with method A than *cis*-4-octene (quantitative formation of butyric acid was only obtained after 5 days; entry 5), reacts also slower when method B is applied. Nonetheless, 55% conversion was observed after 18 h, with a 54% butyric acid yield (entry 6). On the other hand, with the more electron-rich trisubstituted alkene 2-methyl-2-hexene, the activity is relatively high: the substrate can be completely converted with method A in 3 days (entry 7) and with method B in 18 h (entry 8). Cyclohexene can be

completely converted with method A after 16 h, isolating adipic acid in 74% yield as a white precipitate after extraction of the reaction mixture with ether (entry 9). The oxidation of *cis*-cyclooctene, on the other hand, stops at the cyclooctene oxide stage (95% yield; entry 10). When cyclooctene oxide itself was used as substrate under the same conditions, no reaction indeed occurred at room temperature, while at 60 °C the oxide completely converted overnight into a number of different products. A similar non-selective conversion of substrate was also observed with 1-5-cyclooctadiene.

Table 2.3. Oxidative cleavage of aliphatic alkenes.^a

Entry	Substrate	Product	t (h)	Method	Conv. (%)	Yield (%) ^b
1		-	16	A	0	0 ^c
2		-	16	A ^d	0	0
3			18	B	47	42
4			18	B	100	88
5			120	A	100	> 99
6			18	B	55	54
7			72	A	100	98
8			18	B	100	99
9			16	A	100	74 ^c
10			16	A	> 99	95 ^e

^a Reaction conditions: Method A: 2 equiv. oxone, 1.5 equiv. periodate, 0.135 M olefin in MeCN:H₂O (1:3, v/v, 8 mL), ambient temperature, Method B: 0.135 M MeCN:H₂O (3:1, v/v, 8 mL), 16 h; then 2 h 0.07 M MeCN:H₂O (1:3, v/v, 16 mL); ^b Yield determined by GC, maximum yield set to 100%; ^c 91% Substrate retained by ether extraction; ^d Reflux; ^e Isolated yield.

2.2.3 Oxidative cleavage of styrenes and stilbene

Styrene and *trans*- β -methyl styrene (TBMS) gave benzoic acid selectively at significantly higher conversion with method A after 16 h compared to *cis*-4-octene (Table 2.4, entries 1-2). After 2 days of reaction, moderate isolated yields of benzoic acid can be obtained from styrene (53%) and TBMS (59%) by simple extraction with ether. *Cis*-stilbene and *trans*-stilbene, on the other hand, show hardly any reactivity with method A (entry 3, 6). Conversion of these stilbenes can still be achieved though, simply by heating to reflux under the conditions of method A, without the need to resort to method B. *Cis*-stilbene is converted for 61% into benzoic acid within 6 h (entry 6), while *cis*- and *trans*-stilbenes are

Chapter 2

converted quantitatively to benzoic acid after 16 h (entries 5, 7). Trace amounts of aldehydes and ketones were observed in these reactions. *a*-Methyl styrene also shows poor reactivity with method A, even after 5 days of reaction (entry 8), yet can be converted completely to acetophenone after 16 h with method B (entry 9). Reactions performed with method A with 4-methyl styrene showed a variety of reaction products, including ones in which the methyl group is oxidized. Also, 4-methoxy-styrene showed a non-selective conversion, with the side reactions being attributed to the formation of radical intermediates.

Table 2.4. Oxidative cleavage of styrenes and stilbenes into benzoic acid and acetophenone.^a

R = H, Me, Ph

Entry	Substrate	Time (h)	Method	Conv. (%)	Acid yield ^b	Ketone yield ^c
1		16	A	67	67	-
2		16	A	83	83	-
3 ^d		16	A	4	4	-
4 ^d		6	A ^e	61	61	-
5 ^d		16	A ^e	100	95	-
6		16	A	5	5	-
7		16	A ^e	100	95	-
8 ^f		120	A	10	-	9
9		18	B	100	-	99

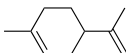
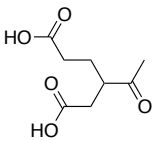
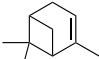
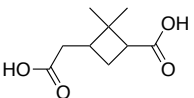
^a Reaction conditions: Method A: 4 equiv. periodate (chronology of experiments), maximum yield set to 100%; Method B; ^b Yields determined by NMR; ^c GC yield; ^d In the dark; ^e Reflux; ^f 1.5 equiv. periodate used.

2.2.4 Oxidative cleavage of terpenes

The terpene limonene contains two different types of double bonds. No regioselectivity was observed, however, in reactions with this substrate even at low oxidant loadings. The conditions chosen for this substrate, i.e. the amount of oxidant used, were therefore intended to cleave both double bonds. This resulted in the formation of γ -acetyl-adipic acid rather than the anticipated acid-diketone. Complete conversion is obtained after 72 h and up to 76% γ -acetyl-adipic acid can be isolated (Table 2.5, entry 1). The over-oxidation of one of the initially formed ketones while the other one remains untouched is remarkable.

Additionally, the terpene α -pinene can be completely converted to give the diacid pinic acid in 68% yield after 108 h. Also in this case, the intermediate acid-ketone cleavage product was only observed at shorter reaction times. The formation of pinic acid is common for pinene derivatives such as pinocarveol.^[61] Pinocarveol is the product of allylic oxidation of β -pinene, therefore isomerization of α -pinene and allylic oxidation are possible pathways in the transformation. Method B is not suitable for the terpenes as at elevated temperatures non-selective conversion of the substrates into a variety of products is observed. These side reactions are the result of intramolecular rearrangements, tautomerizations and/or allylic oxidations that are known to occur with these substrates.

Table 2.5. Oxidative cleavage of limonene and α -pinene.^a

Entry	Substrate	Time (h)	Product	Conversion (%)	Yield (%) ^b
1		72		100	76
2		108		100	68

^a Reaction conditions: Method A; ^b Isolated yield.

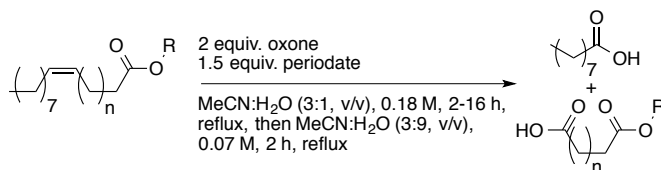
2.2.5 Oxidative cleavage of unsaturated fatty acids

The oxidation of methyl oleate (entries 1-3), oleic acid (entry 4), erucic acid methyl ester (entry 5), and elaidic acid (*trans*-isomer of oleic acid, entry 6) were investigated with the two methods (Table 2.6). These substrates all give nonanoic acid upon cleavage. With method A, no reaction occurs at all with methyl oleate either at ambient temperature or at reflux (entry 1). In MeCN:H₂O (3:1, v/v) and at reflux, methyl oleate is converted to the epoxide and diol products, but no cleavage products are observed. On the contrary, methyl oleate can be converted to nonanoic acid using method B, with 83% conversion and 70% yield obtained after 6 h. After 18 h, nonanoic acid formation is almost quantitative (entry 3). Methyl azelate was also observed by ¹H NMR in equal yields to nonanoic acid after extracting the mixture with ethyl acetate in a separate experiment. For practical reasons, only the yield of nonanoic acid is presented in Table 6, while the amount of the different difunctionalized product is assumed to be equal to this value for all substrates. The reaction with methyl oleate can be scaled up tenfold and to give a 75% isolated yield of the combined mono- and difunctionalized product (see Experimental Section). Oleic acid was found to be more reactive under the applied conditions: full and selective conversion of

Chapter 2

the substrate to form the monoacid is achieved after 6 h (entry 4). The reactivity of erucic acid methyl ester is lower compared to methyl oleate, as only 52% of nonanoic acid is obtained at 65% conversion after 18 h (entry 5). The *trans*-alkene elaidic acid can be readily converted to quantitatively give nonanoic acid after 18 h (entry 6).

Table 2.6. Oxidative cleavage of unsaturated fatty acids.^a



Entry	n	R	Time (h)	Method	Conversion (%)	Yield (%) ^b
1	6	Me	16	A	0	0
2	6	Me	6	B	83	70
3	6	Me	18	B	96	95
4	6	H	6	B	100	99
5	10	Me	18	B	65	52
6 ^c	6	H	18	B	100	99

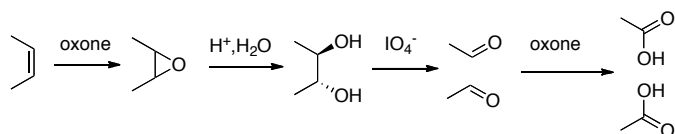
^a Reaction conditions: Method A, Method B; ^b Yield of the nonanoic acid determined by GC; ^c Elaidic acid used, containing a *trans*-double bond.

2.3 Conclusions

A synthetically straightforward, one-pot protocol for the formation of carboxylic acids from alkenes has been developed that does not require expensive or toxic transition metal reagents or catalysts. The carboxylic acid products can be isolated by simple solvent extraction and are obtained in high yield as colourless powders or oils that do not need further purification. All reagents can be added at the start and isolation of intermediate products is not required, which makes the procedure easy to carry out and broadly applicable. The protocol can be applied on a variety of alkenes. Aliphatic alkenes, including *cis*-, *trans*-, cyclic and trisubstituted alkenes, can be cleaved in high yields. Additionally, styrenes and stilbenes can be transformed into benzoic acid. Moreover, industrially interesting unsaturated fatty acids can be oxidatively cleaved into mono- and diacids and a series of terpenes can be transformed into diacids. The nature of the substrate determines which of the two optimized methods is most suited. Method A is performed at ambient conditions for 72 h using a MeCN:H₂O (1:3, v/v) solvent mixture, while method B involves heating a MeCN:H₂O (3:1, v/v) solvent mixture to reflux temperature at the start,

followed by dilution to MeCN:H₂O (3:9, v/v) after 16 h, and allowing the reaction to proceed for another 2 h.

The oxidative cleavage of alkenes by means of this protocol is believed to follow a number of sequential reaction steps (Scheme 2.3). First, oxone epoxidizes the alkene and the acidic nature of the oxidant in combination with water induces the hydrolysis of the resulting epoxide to give the diol. Subsequently, sodium periodate oxidatively cleaves the diol to the aldehydes,^[57] which are finally further oxidized to the acids by oxone. The conversion of cyclic alkenes might involve anhydride intermediates, as postulated before in the case of cyclohexene.^[62] The over-oxidation of the aldehyde is more rapid than the epoxidation of the alkene and, accordingly, aldehydes cannot be isolated with this system. A protocol that uses mcpba rather than oxone does result in the formation of aldehydes, but large amounts of epoxide remain with this oxidant combination.



Scheme 2.3. Overall proposed mechanism.

Compared to other conventional methods of oxidatively cleaving alkenes to carboxylic acids, the protocol shows a higher activity for more electron-rich double bonds. This is in contrast with the many systems using transition metal catalysts for the cleavage electron-poor alkenes.^[55] The affinity of oxone to electron-rich double bonds is crucial in this case. Unlike protocols involving permanganate^[31-39] and Ru or Os,^[8, 41, 42] the products are colourless and need no column chromatography for additional purification. Moreover, the protocol can be applied to a broad scope of alkenes, which is not the case for other metal-free alkene oxidation systems.^[50-52, 56]

This new alkene cleavage protocol may find use in the utilization of vegetable oils in industrial manufacturing and is recommended as an easy tool for synthesizing carboxylic acids out of electron-rich alkenes on a research scale. Further optimization and variation of the protocol is the topic of the next few chapters of this thesis, e.g. through the use of other oxidants, and it is aimed at obtaining aldehydes from internal aliphatic alkenes.

Chapter 2

2.4 Experimental section

2.4.1 General

Oxone (99%), sodium periodate (99%), (1R)-(+)- α -pinene (98%), cyclohexene (99%), *trans*- β -methyl styrene (97 %), *cis*-cyclooctene (95%), *trans*-stilbene (99%) and α -methyl styrene (99%) were purchased from Acros Organics. *Trans*-4-octene (90%), 1-decene (94%), styrene (99%, stabilized with 10-15 ppm *p*-*t*-butylcatechol), *cis*-stilbene (96%) and methyl oleate (99%) were purchased from Aldrich. (*S*)-(-)-Limonene (99%) and oleic acid (99%) were obtained from Fluka. *Cis*-4-octene (97%) was purchased from Alfa Aesar. 4-Methylstyrene (98%), 2-methyl-2-hexene (98%), elaidic acid (98%) and erucic acid methyl ester (90%) were purchased from ABCR. All chemicals were used as received. The reactions were conducted under ambient conditions, using distilled water, pro analysis DMF and MeCN, and technical grade ether, DCM or ethyl acetate. ^1H NMR and ^{13}C NMR measurements were recorded at 298 K using a Varian 400 MHz NMR Spectrometer, using residual solvents peaks as reference. Gas chromatography was carried out on a PerkinElmer Clarus 500 Gas Chromatograph with a Nukol TM fused silica, 15 m \times 0.53 mm \times 0.5 μm column supplied by Supelco and a PerkinElmer Autosystem XL. ESI-MS spectra were recorded using a Waters LCT Premier KE317 MT spectrometer using DCM as the solvent.

2.4.2 Method A

Alkene substrate (1.44 mmol), pentadecane (0.36 mmol; internal standard), oxone (2.88 mmol), and sodium periodate (2.16 mmol) were added to a mixture of MeCN (2 mL) and H₂O (6 mL) and vigorously stirred at ambient temperature for the duration of the experiment. Subsequently, the mixture was filtered and extracted with ether (3 \times 20 mL). The combined organic fractions were dried over MgSO₄ and filtered. The amount of carboxylic acid was determined with the Nukol column, the conversion (consumption of substrate) and formation of byproducts were determined with a polyethylene column. Reactions with the terpenes, cycloalkenes, styrene and stilbenes were done on a 14.4 mmol scale, and the isolated yield was determined after threefold extraction of the aqueous phase with ethyl acetate (terpenes) or ether (cycloalkenes, styrenes and stilbenes) and analyzed with ^1H and ^{13}C NMR. The substrate conversion was determined in a separate experiment by GC analysis on a polyethylene column, using the same work-up procedure with internal standard present at start. Reactions using α -methyl styrene were subjected to GC analysis using a polyethylene column for determination of the formation of the ketone and the substrate conversion.

The conversion of *cis*-4-octene into butyric acid was performed at a preparative scale (1.62 g, 14.4 mmol alkene) without internal standard. After extraction of the reaction mixture with ethyl acetate (4 \times 50 mL), the isolated yield of butyric was determined with ^1H and ^{13}C NMR confirmation (2.13 g, 24.2 mmol, 84%). In a similar way, the reaction of cyclohexene to form adipic acid was run on the same scale and provided 1.56 g (74%) isolated yield. Likewise, *trans*- β -methyl styrene (1.70 g, 14.4 mmol) afforded 82% benzoic acid (1.76 g, 11.81 mmol).

2.4.3 Method B

Alkene substrate (1.44 mmol), pentadecane (0.36 mmol; internal standard), oxone (2.88 mmol), and sodium periodate (2.16 mmol) were added to a mixture of MeCN (6 mL) and H₂O (2 mL) and refluxed until all of the alkene has been converted (2-26 h, depending on the substrate). Subsequently, 16 mL of H₂O was added and the reaction mixture was further refluxed for 2 h. After filtration, 10 mL of water was

added and the aqueous phase was extracted with ether (3 × 20 mL), the combined organic fractions dried with MgSO₄, filtered and subjected to GC analysis. For unsaturated fatty acids and 1-decene, the aqueous phase was extracted with ethyl acetate (4 × 20 mL). The amount of aliphatic monoacid acid was determined with the Nukol column; the conversion (consumption of substrate) and formation of byproducts were determined with a polyethylene column. α-Methyl styrene products were measured directly on the polyethylene column for determination of the formation of the ketone and substrate conversion. The conversion of methyl oleate into nonanoic acid and methyl azelate was performed at tenfold higher scale (4.27 g, 14.4 mmol alkene) without internal standard. Extraction of the reaction mixture with ethyl acetate (4 × 50 mL) gave a 1:1 mixture of nonanoic acid and methyl azelate in 75% isolated yield (3.89 g, 10.8 mmol), as determined by ¹H and ¹³C NMR.

2.5 References

- [1] H. Baumann, M. Bühler, H. Fochem, F. Hirsinger, H. Zobelein, J. Falbe *Angew. Chem. Int. Ed.* **1988**, *27*, 41.
- [2] A. Corma, S. Iborra, A. Vely *Chem. Rev.* **2007**, *107*, 2411.
- [3] U. Biermann, U. Bornscheuer, M. A. R. Meier, J. O. Metzger, H. J. Schäfer *Angew. Chem. Int. Ed.* **2011**, *50*, 3854.
- [4] B. Zaidman, A. Kisilev, Y. Sasson, N. Garti *J. Am. Oil Chem. Soc.* **1988**, *65*, 611.
- [5] H. J. Carlsen, T. Katsuki, V. S. Martin, K. B. Sharpless *J. Org. Chem.* **1981**, *46*, 3936.
- [6] S. Torii, T. Inokuchi, K. Kondo *J. Org. Chem.* **1985**, *50*, 4980.
- [7] K. Kaneda, T. Itoh, N. Kii, K. Jitsukawa, S. Teranishi *J. Mol. Catal.* **1982**, *15*, 349.
- [8] D. Yang, C. Zhang *J. Org. Chem.* **2001**, *66*, 4814.
- [9] V. Piccialli, D. M. A. Smaldone, D. Sica *Tetrahedron* **1993**, *49*, 4211.
- [10] L. Albarella, F. Giordano, M. Lasalvia, V. Piccialli, D. Sica *Tetrahedron Lett.* **1995**, *36*, 5267.
- [11] S. E. Turnwald, M. A. Lorier, L. J. Wright, M. R. Mucalo *J. Mat. Sci. Lett.* **1998**, *17*, 1305.
- [12] Z. P. Pai, A. G. Tolstikov, P. V. Berdnikova, G. N. Kustova, T. B. Khlebnikova, N. V. Selivanova, A. B. Shangina, V. G. Kostrovskii *Russ. Chem. Bull, Int. Ed.* **2005**, *54*, 1847.
- [13] E. Antonelli, R. D'Aloisio, M. Gambaro, T. Fiorani, C. Venturello *J. Org. Chem.* **1998**, *63*, 7190.
- [14] Y. Ishii, K. Yamawaki, T. Ura, H. Yamada, T. Yoshida, M. Ogawa *J. Org. Chem.* **1988**, *53*, 3587.
- [15] T. Oguchi, T. Ura, Y. Ishii, M. Ogawa *Chem. Lett.* **1989**, *18*, 857.
- [16] R. Noyori, M. Aoki, K. Sato *Chem. Commun.* **2003**, 1977.
- [17] J. Freitag, M. Nuchter, B. Ondruschka *Green Chem.* **2003**, *5*, 291.
- [18] J. R. Henry, S. M. Weinreb *J. Org. Chem.* **1993**, *58*, 4745.
- [19] C. Francavilla, W. Chen, F. R. Kinder Jr. *Org. Lett.* **2003**, *5*, 1233.
- [20] R. E. Taylor, Y. Chen, A. Beatty, D. C. Myles, Y. Zhou *J. Am. Chem. Soc.* **2003**, *125*, 26.
- [21] Z. Wang, M. G. Moloney *Tetrahedron Lett.* **2002**, *43*, 9629.
- [22] B. R. Travis, R. S. Narayan, B. Borhan *J. Am. Chem. Soc.* **2002**, *124*, 3824.
- [23] D. C. Whitehead, B. R. Travis, B. Borhan *Tetrahedron Lett.* **2006**, *47*, 3797.
- [24] S. R. Hart, D. C. Whitehead, B. R. Travis, B. Borhan *Org. Biomol. Chem.* **2011**, *9*, 4741.
- [25] W. Yu, Y. Mei, Y. Kang, Z. Hua, Z. Jin *Org. Lett.* **2004**, *6*, 3217.
- [26] A. Dhakshinamoorthy, K. Pitchumani *Tetrahedron* **2006**, *62*, 9911.
- [27] P. A. Ganeshpure, S. Satish *Tetrahedron Lett.* **1988**, *29*, 6629.
- [28] Y. F. Li, C. C. Guo, X. H. Yan, Q. Liu *J. Porphyrins Phtalocyanines* **2006**, *10*, 942.
- [29] H. Chen, H. Ji, X. Zhou, J. Xu, L. Wang *Catal. Commun.* **2009**, *10*, 828.
- [30] S. T. Liu, K. V. Reddy, R. Y. Lai *Tetrahedron* **2007**, *63*, 1821.

Chapter 2

- [31] R. U. Lemieux, E. Von Rudloff *Can. J. Chem.* **1955**, *33*, 1701.
- [32] K. B. Wiberg, K. A. Saegebarth *J. Am. Chem. Soc.* **1957**, *79*, 2822.
- [33] C. M. Starks *J. Am. Chem. Soc.* **1971**, *93*, 195.
- [34] D. J. Sam, H. E. Simmons *J. Am. Chem. Soc.* **1972**, *94*, 4024.
- [35] A. P. Krapcho, J. R. Larson, J. M. Elridge *J. Org. Chem.* **1977**, *32*, 3749.
- [36] D. G. Lee, V. S. Chang *J. Org. Chem.* **1978**, *43*, 1532.
- [37] T. Ogino, K. Mochizuki *Chem. Lett.* **1979**, *5*, 443.
- [38] P. Viski, Z. Szevernyi, L. I. Simandi *J. Org. Chem.* **1986**, *51*, 3213.
- [39] P. L. Joshi, B. G. Hazra *J. Chem. Res., Synop.* **2000**, *1*, 38.
- [40] R. Willand-Charnley, T. J. Fisher, B. M. Johnson, P. H. Dussault *Org. Lett.* **2012**, *14*, 2242.
- [41] F. Zimmermann, E. Meux, J. L. Mieloszynski, J. M. Lecuire, N. Oget *Tetrahedron Lett.* **2005**, *46*, 3201.
- [42] S. Rup, F. Zimmermann, E. Meux, M. Schneider, M. Sindt, N. Oget *Ultrason. Sonochem.* **2009**, *16*, 266.
- [43] C. M. Ho, W. Y. Yu, C. M. Che *Angew. Chem. Int. Ed.* **2004**, *43*, 3303.
- [44] H. Okumoto, K. Ohtsuka, S. Banjoya *Synlett.* **2007**, *20*, 3201.
- [45] V. A. Kumar, V. Prakash Reddy, R. Sridhar, B. Srinivas, K. Rama Rao *Synlett.* **2009**, *5*, 739.
- [46] S. V. Ley, C. Ramarao, A. L. Lee, N. Ostergaard, S. C. Smith, I. M. Shirley *Org. Lett.* **2003**, *5*, 185.
- [47] H. Mang, J. Gross, M. Lara, C. Goessler, H. E. Schoemaker, G. M. Guebitz, W. Kroutil *Tetrahedron* **2007**, *63*, 3350.
- [48] M. Tedetti, K. Kawamura, M. Narukawa, F. Joux, B. Charriere, R. Sempere *J. Photochem. Photobiol. A: Chem.* **2007**, *188*, 135.
- [49] U. S. Bäumer, H. J. Schäfer *Electroch. Acta* **2003**, 489.
- [50] W. Zhu, W. T. Ford *J. Org. Chem.* **1991**, *56*, 7022.
- [51] J. Legros, B. Crousse, J. Bourdon, D. Bonnet-Delpon, J. Bégué *Tetrahedron Lett.* **2001**, *42*, 4463.
- [52] J. Legros, B. Crousse, D. Bonnet-Delpon, J. Bégué *Tetrahedron* **2002**, *58*, 3993.
- [53] D. Yang, M. Wong, Y. Yip *J. Org. Chem.* **1995**, *60*, 3887.
- [54] D. Yang, Y. Yip, M. Tang, M. Wong, K. Cheung *J. Org. Chem.* **1998**, *63*, 9888.
- [55] T. W. S. Chow, E. L. M. Wong, Z. Guo, Y. Liu, J. S. Huang, C. M. Che *J. Am. Chem. Soc.* **2010**, *132*, 13229.
- [56] K. M. Jones, N. C. O. Tomkinson *J. Org. Chem.* **2012**, *77*, 921.
- [57] G. Dryhurst, *Periodate oxidation of diol and other functional groups. Analytical and structural applications*, **1970**.
- [58] S. Jarupinthusophon, U. Thong-In, W. Chavasiri *J. Mol. Catal. A: Chem.* **2007**, *270*, 289.
- [59] B. M. Choudary, P. N. Reddy *J. Mol. Catal. A: Chem.* **1995**, *103*, L1.
- [60] F. Shi, M. K. Tse, M. M. Pohl, A. Bruckner, S. Zhang, M. Bellert *Angew. Chem. Int. Ed.* **2007**, *46*, 8866.
- [61] F. X. Webster, J. Rivas-Enterrios, R. M. Silverstein *J. Org. Chem.* **1987**, *52*, 689.
- [62] S. O. Lee, R. Raja, K. D. M. Harris, J. M. Thomas, B. F. G. Johnson, G. Sankar *Angew. Chem. Int. Ed.* **2003**, *43*, 1520.

Iron-catalyzed oxidative cleavage of terpenes and unsaturated fatty acids

Chapter 3

Fe-catalyzed one-pot oxidative cleavage of unsaturated fatty acids into aldehydes with hydrogen peroxide and sodium periodate

Abstract

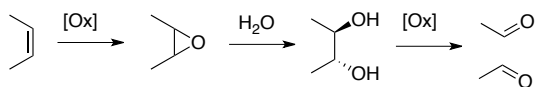
A one-pot method has been developed for the oxidative cleavage of internal alkenes into aldehydes, using 0.5 mol% of the non-heme iron complex $[\text{Fe}(\text{OTf})_2(\text{mix-BPBP})]$ (BPBP = *N,N'*-bis(2-picolyl)-2,2'-bipyrrolidine) as catalyst and 1.5 equiv. of hydrogen peroxide and 1 equiv. of sodium periodate as oxidants. A mixture of diastereomers of the optically pure BPBP-ligand (mix-BPBP) can be used, omitting the need for resolution of its optically active components. The cleavage reaction can be performed in one pot, within 20 h and under ambient conditions. Addition of water after the epoxidation, acidification and subsequent pH neutralization are crucial in order to perform the epoxidation, hydrolysis and subsequent diol cleavage in one pot. High aldehyde yields can be obtained for the cleavage of internal aliphatic double bonds with *cis*- and *trans*-configuration (86-98%) and unsaturated fatty acid (esters) (69-96%). Good aldehyde yields are obtained with reactions of trisubstituted and terminal alkenes (62-63%). The products can be easily isolated by a simple extraction step with an organic solvent. The presented protocol involves a lower catalyst loading than conventional methods based on Ru or Os. Also, hydrogen peroxide can be used as oxidant in this case, which is often disproportionated by second and third row metals. Using only mild oxidants, over-oxidation of the aldehyde to the carboxylic acid is prevented.

Based on: Peter Spannring, Vital A. Yazerski, Pieter C. A. Bruijninx, Bert M. Weckhuysen and Robertus J. M. Klein Gebbink, *Chem. Eur. J.* **2013**, *19*, 15012

3.1 Introduction

The oxidative cleavage of unsaturated fatty acids into either aldehydes or carboxylic acids is a reaction of considerable practical interest.^[1-3] This conversion is nowadays mostly performed with second- and third-row transition-metal catalysts based on Os,^[4-12] Ru,^[13-18] or W,^[19-25] on a lab scale, or with ozone in an industrial process.^[3, 26] More benign methods for these processes are clearly desired. In Chapter 2, a non-metal mediated oxidative cleavage of internal alkenes and unsaturated fatty acids into carboxylic acids with a combination of the oxidants oxone and sodium periodate was reported.^[27] This oxidative cleavage involves a cascade of reactions starting with epoxidation of an alkene with oxone, acid-catalyzed ring-opening of the epoxide to give a diol intermediate (oxone solutions are slightly acidic), periodate-mediated cleavage of the diol into aldehydes in the same pot, and finally oxidation of the aldehyde with oxone to give the carboxylic acids. The oxone/periodate combination is very useful for the preparation of fatty acid-derived carboxylic acids, but does not allow for the isolation of products at the aldehyde oxidation level.

In order to allow selective aldehyde formation in such a one-pot protocol, alternatives for oxone need to be sought for the epoxidation step, as this oxidant readily over-oxidizes the aldehydes formed to the corresponding carboxylic acids. Additionally, an alternative oxidant should preferably produce less waste than oxone. The use of periodate as the oxidizing agent of diols can be considered acceptable from a sustainability viewpoint, as this oxidant can be regenerated electrochemically.^[28, 29] Any alternative for oxone should be compatible with sodium periodate to maintain the facile, one-pot conversion approach. For these reasons, catalytic systems involving first-row transition metal systems and benign oxidants were considered to replace oxone and to arrive at a one-pot protocol to form aldehydes out of internal, electron-rich alkenes (Scheme 3.1).



Scheme 3.1. Reaction sequence for the formation of aldehydes from internal alkenes.

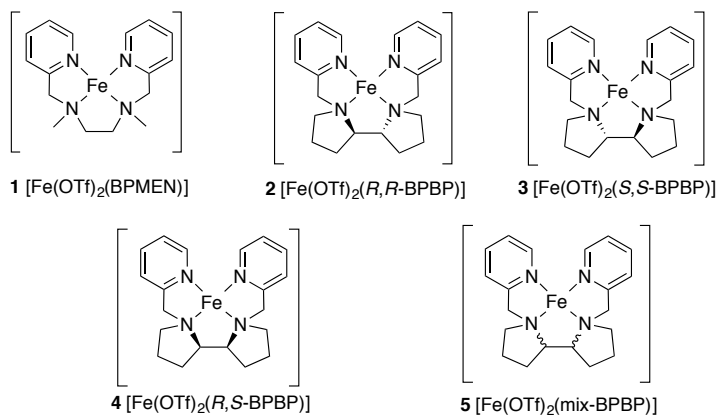
Hydrogen peroxide is widely used in epoxidation reactions and does not over-oxidize aldehydes into carboxylic acids by itself. First-row transition metal-catalyzed epoxidations with H₂O₂ typically involve non-heme Fe and Mn complexes derived from ligands such as tris(2-picolyamine) (TPA), *N,N'*-dimethyl-*N,N'*-bis(2pyridylmethyl)-1,2-diaminoethane (BPMEN),^[30] tetraalkylcyclam Me₂EBC (Me₂EBC = 4,11-dimethyl-1,4,8,11-tetraazabicyclo [6.6.2]hexadecane),^[31] bispidine ligands (dimethyl [3,7-dimethyl-9,9'-dihydroxy-2,4-di-(2-pyridyl)-3,7-diazabicyclo nonan-1,5-dicarboxylate]^[32] or *N,N'*-bis(2-picoly)-2,2'-bipyrrolidine (BPPBP).^[33-35] Alkene epoxidation reactions catalyzed by such systems are

Chapter 3

typically optimized for substrates such as *cis*-cyclooctene or styrene derivatives. When it comes to the epoxidation of internal, aliphatic alkenes, examples of such non-heme complexes are rather limited: *cis*-2-heptene can be oxidized with Fe-(Me₂EBC) complexes under oxidant-limiting conditions, yet the epoxides are only a minor product under the applied conditions, as *cis*-diols are primarily formed in pure MeCN.^[31] Ligands that mimic the active site of a group of non-heme iron oxygenases characterized by the so-called 2-His-1-carboxylate triad show similar results.^[36, 37] Under substrate-limiting conditions, significantly higher epoxide yields can be obtained: the oxidation of *cis*-2-heptene using Fe-TPA complexes affords 44% of 2,3-epoxyheptane,^[38] while Fe-BPMEN complexes give up to 77% of the epoxide.^[38] Nevertheless, high efficiencies (>90% yield) in the epoxidation of non-cyclic, internal aliphatic *cis*-alkenes with H₂O₂ are still only obtained with methods based on Re catalysts.^[12, 39-41] In addition, some V, Mo, and W-based catalysts give high epoxide yields of the *trans*-internal aliphatic alkenes^[42] and *cis*-2-heptene^[43] (90%) as substrate using H₂O₂ as the oxidant.^[43] Non-cyclic, internal aliphatic *cis*-alkenes were not investigated with these catalysts, however. Also, Mo-catalysts have been shown to give internal aliphatic epoxides in high yield, but with *t*-butyl hydroperoxide as oxidant, rather than H₂O₂.^[44]

In our search for a suitable system for the epoxidation of internal aliphatic alkenes, the recently reported catalytic performance of a Fe-BPBP catalyst stood out, given its low catalyst loading, high selectivity to the epoxide and its significant activity, also in absence of additives such as MeCOOH, which is often required for high activity with similar catalysts.^[34] In addition, Fe-BPBP-catalyzed epoxidation reactions typically result in high mass balances in pure acetonitrile, with only some minor amounts of *cis*-diol observed as byproduct.^[35] So far, the BPBP system has been applied in its enantiomerically pure form (*S,S*-BPBP) for asymmetric epoxidations,^[33] which raises the costs involved because of the need for chiral resolution. A chiral catalyst is not necessary for oxidative cleavage, however, and a cheaper, optically inert form of the Fe-BPBP catalyst can in principle be used.

Here, the results are presented on the sequential Fe/H₂O₂-catalyzed epoxidation, acid-catalyzed hydrolysis, and periodate-mediated diol cleavage for the one-pot oxidative cleavage of alkenes and unsaturated fatty acids into aldehydes. Based on the promising results previously reported, the activity and selectivity was explored of the iron complexes [Fe(OTf)₂(BPMEN)] (**1**), [Fe(OTf)₂(*R,R*-BPBP)] (**2**), [Fe(OTf)₂(*S,S*-BPBP)] (**3**), [Fe(OTf)₂(*R,S*-BPBP)] (**4**), and the complex with a mixture of BPBP stereoisomers, [Fe(OTf)₂(mix-BPBP)] (**5**) (Scheme 2). The optimization of the individual steps in the oxidative cleavage sequence is discussed as well as the substrate scope. Aldehyde cleavage products are obtained in excellent yields with a particular preference for the cleavage of electron-rich internal olefins.



Scheme 3.2. Non-heme Fe(II) complexes used in this study. The coordinating triflate species (OTf) are omitted for clarity.

3.2 Results and Discussion

The epoxidation activity toward internal alkenes was initially screened with *cis*-4-octene as substrate by adding 1.5 equiv. of H₂O₂ dropwise to a MeCN:MeCOOH (1:2 v/v) solution containing 0.5 mol% [Fe(OTf)₂(BPMEN)] (**1**). After 45 min, near complete conversion (98%) was achieved with an 89% yield of 4,5-epoxyoctane (Table 3.1, entry 1). Performing the reaction at 0 °C, improved the yield of the epoxide to 95% (entry 2). The higher epoxide yields at lower temperature can be attributed to lower disproportionation rates at such conditions, as also observed with epoxidations of *cis*-cyclooctene and **1** reported by Mas-Balleste *et al.*^[38] Identical epoxide yields were obtained whether the oxidant was added with a syringe pump or manually, which prompted us to manually add the oxidant in a dropwise fashion in all further experiments. When the loading of **1** was decreased to 0.1 mol%, the substrate conversion dropped significantly to 39% (entry 4). On the other hand, using 0.1 mol% of [Fe(OTf)₂(*R,R*-BPBP)] (**2**) quantitatively converted the substrate into 4,5-epoxyoctane within 45 min, even at ambient temperature (entry 5). Further lowering of the loading of **2** to 0.05 mol% gave 78% of the epoxide after 45 min (entry 6), resulting in a turnover number (TON) of 1560. The use of [Fe(OTf)₂(*S,S*-BPBP)] (**3**) gave almost identical results as with **2**, with full substrate conversion and 97% of epoxide yield (entry 7). On the contrary, *meso*-complex [Fe(OTf)₂(*R,S*-BPBP)] (**4**) showed no activity at all, not even at 0 °C (entry 8). Importantly, the latter complex seems rather innocent, as no side products are observed either. Therefore, a mixture of Fe-complexes [Fe(OTf)₂(mix-BPBP)] (**5**) generated from a mixture of the different diastereomers of BPBP, *i.e.* using a non-resolved mixture of BPBP ligands containing around 60% of *R,R* and *S,S* and 40% of *R,S* and *S,R* diastereoisomers, was tested. Such a mixture would represent a much cheaper source of the BPBP ligand, as the time-consuming synthetic step of ligand

Chapter 3

resolution is omitted. The use of 0.25 mol% of **5** gave quantitative *cis*-4-octene conversion to 4,5-epoxyoctane at RT after 45 min (entry 9). Lower loadings of 0.1 mol% and 0.05 mol% gave conversions of 90% and 59% of the substrate, respectively (entries 10-11). Since an excess of water is required for the subsequent epoxide hydrolysis step, the stability of the catalysts was investigated in the presence of water. The addition of only 0.25 mL water significantly decreased the conversion using 0.5 mol% **1** from 99% to 35%, and the epoxide yield from 95% to 26% (entry 12). On the other hand, 0.5 mol% of **2** quantitatively converted the substrate in the presence of up to 1 mL of water, forming 88% of the epoxide (entry 13).

Table 3.1. *Cis*-4-octene epoxidation with H₂O₂ in a MeCN/MeCOOH mixture.^a

Entry	Cat	Loading (mol%)	T (°C)	Time (min)	Conversion (%) ^b	Yield (%) ^b
1	1	0.5	25	45	98	89
2	1	0.5	0	45	99	95
3 ^c	1	0.5	0	90	100	95
4	1	0.1	0	90	39	33
5	2	0.1	25	45	100	99
6	2	0.05	25	45	78	78
7	3	0.1	25	45	100	97
8	4	0.5	0	45	0	0
9	5	0.25	25	45	100	99
10	5	0.1	25	45	90	89
11	5	0.05	25	45	59	56
12 ^d	1	0.5	0	90	35	26
13 ^e	2	0.5	0	90	100	88

^a Reaction conditions: 0.05-0.5 mol% catalyst, 0.18 M *cis*-4-octene in MeCN:MeCOOH (1:2, v/v, 3 mL), 1.5 equiv. H₂O₂ added dropwise; ^b Yield determined by GC; ^c H₂O₂ added over 1 h; ^d 0.25 mL H₂O added; ^e 1 mL H₂O added.

Subsequently, the possibility to omit acetic acid from the reaction mixture was explored, as this would facilitate product separation. Reactions were performed at low temperature

to limit oxidant disproportionation.^[35] Using 0.5 mol% of **1** in MeCN as the sole solvent component gave only 35% conversion of the substrate after 90 min at 0 °C, with 2% of *meso*-4,5-octanediol (*cis*-dihydroxylation product) and 27% of the epoxide as products (Table 3.2, entry 1). On the other hand, 0.5 mol% of either **2** or **3** gave full substrate conversion, yielding 92% epoxide and 6% diol (entry 2 for **2**). Identical results are obtained when the catalyst loading was decreased to 0.25 mol% (entry 3). Because complex **4** proved inactive in this protocol as well (entry 4), the reaction could again be performed with 0.5 mol% of **5**, giving 92% epoxide and 5% diol at full conversion (entry 6). These optimal conditions were taken for subsequent alkene epoxidations.

Table 3.2. *Cis*-4-octene epoxidation with H₂O₂ in the absence of MeCOOH.^a

Entry	Cat	Loading (mol %)	Conversion (%) ^b	Diol yield (%) ^c	Epoxide yield (%)
1	1	0.5	35	2	27
2	2	0.5	100	6	92
3	2	0.25	100	6	92
4	4	0.5	0	0	0
5	5	0.25	42	4	37
6	5	0.5	100	5	92

^a Reaction conditions: 0.25-0.5 mol% catalyst, 1.5 equiv. H₂O₂ added dropwise, 0.18 M *cis*-4-octene in MeCN (3 mL), 0 °C, 1.5 h; ^b Yields and conversions determined by GC; ^c *Meso*-4,5-octadiol.

The epoxide ring opening can be performed by a variety of strong acids in aqueous organic solvent, but isomerization, dehydration or halohydrin are common side reactions.^[45] With the one-pot sequence in mind, the ring opening of 4,5-epoxyoctane was optimized in MeCN with some added water. Reactions of the epoxide with 1 equiv. of tartaric acid with respect to the substrate in MeCN:H₂O (3:1, v/v) gave only 5% substrate conversion after 30 min at ambient temperature (Table 3.3, entry 1). Increasing the amount of acid (6 equiv.) and extending the reaction time to 90 min led to 96% substrate conversion, but with only 39% diol being formed (entry 2). Complete conversion of the epoxide was observed with 1 equiv. of paratoluenesulfonic acid (PTSA; entry 3). Using this acid also gave only 45% of the diol, while HCl converted only 50% of the epoxide and gave considerable amounts of byproducts (entry 4). Rewardingly, the use of H₂SO₄ (1 equiv. of H⁺) in MeCN:H₂O (3:1, v/v) resulted in 96% of *rac*-4,5-octanediol isolated yield after 30 min, with full substrate conversion and no detectable byproducts (entry 6).

Chapter 3

Table 3.3. Acid-catalyzed hydrolysis of 4,5-epoxyoctane into *rac*-4,5-octanediol.^a

Entry	Acid	H ⁺ (equiv.)	Time (min)	Conversion (%) ^b	Yield (%) ^b
1	tartaric	1	30	5	0
2	tartaric	6	90	96	39 ^c
3	PTSA	1	30	100	45 ^c
4	HCl	1	30	50	25 ^c
5	H ₂ SO ₄	0.1	30	28	23
6	H ₂ SO ₄	1	30	100	96 ^d

^a Reaction conditions: 0.135 M 4,5-epoxyoctane in MeCN:H₂O (3:1 v/v; 4 mL), RT; ^b Determined by GC; ^c Byproducts detected; ^d Isolated yield.

Optimization of the final step in the sequence, i.e. periodate-mediated oxidative cleavage of *rac*-4,5-octanediol into butanal, was done in MeCN:H₂O 3:1 (v/v), the same solvent system as was used for the epoxidation and hydrolysis reactions. Complete conversion was obtained with 3 equiv. of HIO₄ within 2 h, but byproducts were formed in addition to the 75% of yield of butanal (Table 3.4, entry 1). Byproduct formation could be attributed to the use of periodic acid rather than a periodate salt. Indeed, the conversion into butanal was quantitative after 30 min with 3 equiv. or even 1 equiv. of NaIO₄ (entries 2-3). Notably, oxidation of the diol did not occur in the absence of H₂O (entry 4).

Table 3.4. Oxidation of *rac*-4,5-octanediol into butanal.^a

Entry	Oxidant	Equiv.	MeCN:H ₂ O (v/v)	Conversion (%) ^b	Yield (%) ^c
1	HIO ₄	3	3:1	100	75 ^[d]
2	NaIO ₄	3	3:1	100	99
3	NaIO ₄	1	3:1	100	99
4	NaIO ₄	1	1:0	0	0

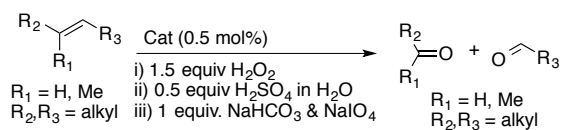
^a Reaction conditions: 0.135 M *rac*-4,5-octanediol in MeCN:H₂O (3:1, v/v; 4 ml), RT, 30 min, oxidant; ^b Determined by GC; ^c Maximum amount of butanal set to 100%; ^d Side products observed, 2 h.


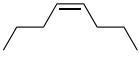
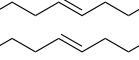
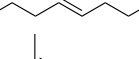
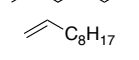


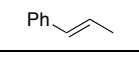
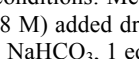
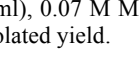
Having optimized the individual steps of alkene epoxidation, epoxide ring opening, and diol oxidation into aldehydes with our model substrate *cis*-4-octene, it was intended to combine the individual protocols for a procedure to convert *cis*-4-octene into butanal in one pot. To maximize the yield, the reaction time was increased to 2.5 h for the epoxidation reaction and to 1 h for the epoxide hydrolysis. The procedure was as follows (method A): epoxidation with 0.5 mol% of catalyst **2** or **5** at 0 °C with 1.5 equiv. of H₂O₂ in MeCN for 2.5 h, subsequent hydrolysis by addition of 0.5 equiv. of H₂SO₄ in H₂O to give a 0.135 M solution in MeCN:H₂O (3:1, v/v), which was stirred for 1 h at ambient temperature. Finally, 1 equiv. of NaHCO₃ (neutralizing the pH) and 1 equiv. of NaIO₄ were added, and the mixture stirred for an additional 0.5 h. Interestingly, the presence of all reagents did not cause side-reactions in the protocol: *cis*-4-octene was completely converted after 4 h with catalyst **2**, yielding 94% of butanal (Table 3.5, entry 1), while the use of **5** even resulted in an aldehyde yield of 98% at full substrate conversion (entry 2). The presence of the catalyst in the mixture did not cause side-reactions upon the introduction of either the acid or the base, nor did over-oxidation of the aldehyde take place when NaIO₄ was introduced.

The substrate scope of this one-pot procedure was subsequently explored with various aliphatic alkenes using catalyst **5**. Reactions with *trans*-4-octene gave 90% of conversion but only 40% of aldehyde (entry 3). As remaining traces of both epoxide and *meso*-4,5-diol suggested that the initial steps in the sequence were incomplete, reaction times were extended for the hydrolysis from 1 h to 16 h, and for the diol oxidation from 0.5 h to 1.5 h (method B). This did not result in any major improvement though, as the diol cleavage step was still found to be incomplete (95% substrate conversion with 41% of aldehydes; entry 4). Based on the observation in the metal-free one-pot protocol (Chapter 2)^[27] that transformation of diols into aldehydes works especially well once the reaction mixture is diluted with water to a MeCN:H₂O ratio of 1:3 (v/v), the same strategy was applied here (method C). Notably, 96% of *trans*-4-octene was converted into 86% of butanal with method C and only 9% of diol remained (entry 5). Method C also allowed for 70% conversion of 2-methyl-2-hexene, yielding 63% of butanal (entry 6). The terminal alkene 1-decene was also converted for 70%, generating 63% of nonanal (entry 7). Moreover, 93% of adipaldehyde was isolated from cyclohexene at complete substrate conversion with this method. The isolation of the dialdehyde was straightforward and could be conducted by simple extraction of the reaction mixture with ether and subsequent evaporation. Likewise, the reaction of the terpene α -pinene yielded the ketoaldehyde by oxidative cleavage in 60% isolated yield (entry 9). On the other hand, reactions with *trans*- β methyl-styrene gave only 60% conversion and yielded 44% benzaldehyde (entry 10). Styrenes and stilbenes generally showed poor yields and increasing the catalyst loading was not found to be beneficial (not shown).

Chapter 3

Table 3.5. One-pot oxidative cleavage of aliphatic alkenes.^a



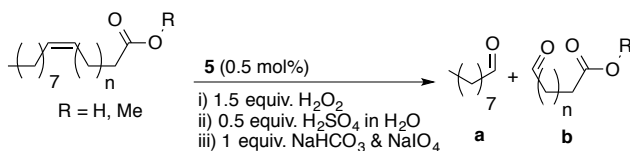
Entry	Substrate	Cat	Time (h)	MeCN:H ₂ O (v/v)	Method	Conversion (%) ^b	Yield (%) ^c
1		2	4	3:1	A	100	94
2		5	4	3:1	A	100	98
3		5	4	3:1	A	90	40
4		5	20	3:1	B	95	41
5		5	20	3:1 → 3:9	C	96	86
6		5	20	3:1 → 3:9	C	73	62
7		5	20	3:1 → 3:9	C	70	63
8		5	20	3:1 → 3:9	C	100	93 ^[d]
9		5	20	3:1 → 3:9	C	100	60 ^[d]
10		5	20	3:1	B	60	44

^a Reaction conditions: Method A: i) 0.18 M alkene in MeCN (3 ml), 0.5 mol% **2** or **5**, 1.5 equiv. H₂O₂ in MeCN (1.08 M) added dropwise, 0 °C, 2.5 h, ii) 0.135 M alkene in MeCN:H₂O (3:1, v/v, 4 ml), RT, 1 h, iii) 1 equiv. NaHCO₃, 1 equiv. NaIO₄, 0.5 h; method B: ii) 16 h; iii) 1.5 h; method C: ii) 16 h, iii) addition of H₂O (8 ml), 0.07 M MeCN:H₂O (3:9, v/v), 1.5 h; ^b Determined by GC; ^c Maximal aldehyde yield set to 100%; ^d Isolated yield.

Next, the attention was turned to the application of the one-pot method in the oxidative cleavage of unsaturated fatty acids and esters. In the oxidative cleavage of non-symmetric substrates such as the unsaturated fatty acids, both a linear aldehyde as well as an ω-1 aldocarboxylic acid are formed. For analytical reasons, the conversion and selectivity of the fatty acid cleavage reactions were determined by monitoring the amounts of linear aldehyde being produced, with the yield of the corresponding ω-1-aldocarboxylic acid assumed to be equal. The difunctionalized molecules are more water-soluble at high temperatures than the monofunctionalized ones and can therefore be separated in hot water. Method A was initially applied for the oxidation of the fatty acid ester methyl oleate, as *cis*-4-octene is readily converted under these conditions into the aldehyde in high yields. Methyl oleate was converted in 93% after 4 h with this method and 78% of nonanal was obtained (Table 3.6, entry 1). As product analysis by ¹H NMR measurements showed that diols were still present after reaction, the reaction time was extended (method B) in order to give excellent yields of nonanal (92%) after 20 h at 94% substrate

conversion (entry 2). In a similar fashion, the reaction was conducted with methyl oleate on a preparative scale, i.e. using a tenfold larger amount of substrate, and obtained a 75% isolated yield of the mono- and difunctionalized product in an equal molar ratio. The reaction of the fatty acid oleic acid in pure MeCN resulted in 95% substrate conversion and 90% nonanal yield (entry 3). In order to illustrate the influence of MeCOOH on the conversion of fatty acid substrates, some reactions were performed in a mixture of MeCOOH and MeCN (1:2, v/v). In the case of methyl oleate, full substrate conversion and 96% yield of nonanal was achieved, which showed a small beneficial effect of the use of acetic acid (entry 4). On the other hand, MeCOOH is required for the efficient conversion of elaidic acid (*trans* isomer of oleic acid), erucic acid (C11 fatty acid), and the methyl ester of erucic acid, as reactions in pure MeCN resulted in mediocre amounts of nonanal. The higher solubility of these substrates in the MeCOOH/MeCN medium is considered to be a crucial factor. The somewhat sluggish reactivity of these three substrates required that the epoxidation, hydrolysis, and diol cleavage were performed for 24 h each. In this way, elaidic acid was completely converted, forming 69% of nonanal (entry 5). Likewise, erucic acid and its methyl ester gave yields of 73% and 70% of nonanal, respectively, at full substrate conversion (entries 6-7). The developed protocol therefore proved to be very efficient for the one-pot oxidative cleavage of various fatty acids and their esters.

Table 3.6. Oxidative cleavage of unsaturated fatty acids and esters.^a



Entry	n	R	MeCOOH (equiv.)	Method	Conversion (%) ^b	Yield a (%) ^b	Yield b (%) ^b
1	6	Me	0	A	93	78	73
2	6	Me	0	B	94	92	86
3	6	H	0	B	95	90	nd ^e
4	6	Me	50	B	100	96	89
5 ^c	6	H	50	B ^d	100	69	nd ^e
6	10	H	50	B ^d	100	73	nd ^e
7	10	Me	50	B ^d	100	70	nd ^e

^a Reaction conditions: Method A i) 0.18 M alkene in organic solvent (MeCN, 3 mL, or MeCN:MeCOOH, 2:1, v/v, 3 mL), 0.5 mol% **5**, 1.5 equiv. H₂O₂ added dropwise (1.08 M in MeCN), 0 ° C, 2.5 h, ii) 0.5 equiv. H₂SO₄ (0.18 M in H₂O, 1 mL), 1 h, RT, iii) 1 equiv. NaHCO₃, 1 equiv. NaIO₄, 0.5 h, Method B: ii) for 16 h, iii) for 1.5 h; ^b Determined by GC; ^c Elaidic acid used, *trans*-double bond; ^d Reaction steps i), ii) and iii) all performed for 24 h; ^e Not determined.

Chapter 3

3.3 Conclusion

A straightforward one-pot protocol for the transformation of internal alkenes into aldehydes has been developed. The protocol relies on the use of iron as the transition metal and a combination of the benign oxidants H_2O_2 (1.5 equiv.) and NaIO_4 (1 equiv.) in MeCN as the sole solvent. The reaction sequence involves the initial epoxidation of the alkene with hydrogen peroxide, mediated by a mixture of iron complexes obtained from an unresolved mixture of isomers of the BPBP ligand. This $[\text{Fe}(\text{OTf})_2(\text{mix-BPBP})]$ catalyst is a cheap and synthetically more straightforward alternative to optically pure FeBPBP complexes, which need chiral resolution of the ligand. Subsequently, epoxide ring opening with diluted sulfuric acid and finally cleavage of the resulting diol into aldehydes by stoichiometric amounts of NaIO_4 occur in the same pot. High yields of the cleavage products can be obtained with catalyst loadings as low as 0.5% and without the need to use acetic acid. The reaction sequence is not hampered by the epoxidation catalyst remaining in the reaction mixture and no over-oxidation of the aldehydes towards carboxylic acids occurs with this system, despite the presence of NaIO_4 and the catalyst. In this way, the subsequent intermediates do not need to be isolated and the reaction can occur in pot. The use of a limited number of reactants, the omission of MeCOOH, and the fact that acid and base neutralize each other enables the aldehydes to be obtained by direct extraction in organic solvent from the reaction mixture, without the need for column chromatography. Cyclic, internal, terminal and trisubstituted aliphatic alkenes as well as terpenes can all be cleaved in high yields within 4-20 h. Furthermore, it was shown that a variety of unsaturated fatty acid (esters) can be cleaved into nonanal and an ω -1 aldocarboxylic acid. The former is an industrially interesting product, nowadays typically produced by hydroformylation of 1-octene, for which this system can be regarded as an alternate process. On the other hand, the latter product could serve as a valuable monomer of a variety of biobased polymers. Our protocol is an alternative to similar processes involving Ru, Os, and W-mediated systems that use additives and less benign oxidants for the oxidative cleavage of unsaturated fatty acids into aldehydes. Furthermore, this system may serve as a substitute for the ozonolysis of oleic acid carried out on large scale in industry.

3.4 Experimental Section

3.4.1 General

Sodium periodate (99%), (*IR*)-(+)- α -pinene (98%), cyclohexene (99%), *trans*- β -methyl styrene (97 %), hydrogen peroxide (35 wt.% in H₂O) and α -methyl styrene (99%) were purchased from Acros Organics. *Trans*-4-octene (90%), 1-decene (94%), styrene (99%, stabilized with 10-15 ppm *p*-*t*-butylcatechol), *cis*-stilbene (96%) and methyl oleate (99%) were purchased from Aldrich. Oleic acid (99%) was obtained from Fluka. *Cis*-4-octene (97%) was purchased from Alfa Aesar. 2-methyl-2-hexene (98%), elaidic acid (98%) and erucic acid methyl ester (90%) were purchased from ABCR. All chemicals were used as received. The reactions were conducted under ambient conditions unless stated otherwise, using demineralized water, pro analysis MeCN, and technical grade ether or CH₂Cl₂. Gas chromatography was carried out on a PerkinElmer Clarus 500 Gas Chromatograph with a Nukol TM fused silica, 15 m \times 0.53 mm \times 0.5 μ m column supplied by Supelco and a PerkinElmer Autosystem XL. Compounds **1-3** were synthesized according to literature procedures.^[30, 35] Compound **4** was prepared using a similar procedure as for the synthesis of **2** and **3**, starting from the commercially available (*R,S*-BPBP) ligand. The synthesis and characterization of compound **5** will be published elsewhere.^[46]

3.4.2 Method A

Alkene substrate (0.72 mmol), pentadecane (0.18 mmol; internal standard) and [Fe(OTf)₂(mix-BPBP)] (3.6 mmol, [Fe(OTf)₂(*R,R*-BPBP)] or [Fe(OTf)₂(*S,S*-BPBP)] can also be used) were dissolved in MeCN (3 mL) at 0 °C. Subsequently, H₂O₂ (1.08 mmol) in MeCN (0.75 mL) was added dropwise to the mixture. After 2.5 h, H₂SO₄ in H₂O (0.72 mmol, 1 mL) was added and the reaction mixture was stirred at RT for 1 h. Next, NaHCO₃ (0.72 mmol) and NaIO₄ were added consecutively, and the solution was stirred for an additional 0.5 h. For analysis, 20 mL of ether was added to the solution in order to precipitate remains of catalyst after which a sample was subjected to GC analysis. The conversion was determined by the consumption of substrate and the product yields were compared with authentic samples of aldehydes. Quantification of aldehydes was based on the partition coefficient in the organic solvent, as the products show a very slight solubility in the water-phase, and it was intended to omit extraction on such small scale. Similar results are obtained when the reaction is performed on 10-fold larger scale and extracted with ether (3 \times 40 mL) prior to analysis with GC.

3.4.3 Method B

Alkene substrate (0.72 mmol), pentadecane (0.18 mmol; internal standard) and [Fe(OTf)₂(mix-BPBP)] (3.6mmol, [Fe(OTf)₂(*R,R*-BPBP)] or [Fe(OTf)₂(*S,S*-BPBP)] can also be used) were dissolved in MeCN (3 mL) at 0 °C. Subsequently, H₂O₂ (1.08 mmol) in MeCN (0.75 mL) was added dropwise to the mixture. After 2.5 h, H₂SO₄ in H₂O (0.72 mmol, 1 mL) was added and it was reacted at RT for 16 h. Next, NaHCO₃ (0.72 mmol) and NaIO₄ were added consecutively and the solution was stirred for an additional 1.5 h. For analysis, 20 mL of ether was added in order to precipitate remains of catalyst after which a sample was subjected to GC analysis. The conversion was determined by the consumption of substrate and the product yields were compared with authentic samples of aldehydes. Quantification of the aldehydes was based on the partition coefficient in the organic solvent, as the products are slightly soluble in the water-phase. In this way, small-scale extractions were omitted. The reaction conducted with methyl oleate on larger scale

Chapter 3

(7.2 mmol) was done in a similar fashion. After extraction with ether (3 × 40 mL) a combined yield of 75% of the mono- and difunctionalized aldehydes was obtained (1.77 g, 5.4 mmol).

3.4.4 Method C

Alkene substrate (0.72 mmol), pentadecane (0.18 mmol; internal standard) and [Fe(OTf)₂(mix-BPBP)] (3.6mmol, [Fe(OTf)₂(*R,R*-BPBP)] or [Fe(OTf)₂(*S,S*-BPBP)]) can also be used) were dissolved in MeCN (3 mL) at 0 °C. Subsequently, H₂O₂ (1.08 mmol) in MeCN (0.75 mL) was added dropwise to the mixture. After 2.5 h, H₂SO₄ in H₂O (0.72 mmol, 1 mL) was added and it was reacted at RT for 16 h. Next, NaHCO₃ (0.72 mmol), NaIO₄ (0.72 mmol) and H₂O (8 mL) were added consecutively, and the solution was stirred for an additional 1.5 h. The reaction mixture was filtered and extracted with 3 times 15 ml of ether. The combined organic fractions were dried over MgSO₄, filtered and subjected to GC analysis. Product yields were compared with authentic samples of aldehydes. Reactions with α -pinene and cyclohexene were done on a larger scale (2.16 mmol) and the isolated yield was determined by extraction with ether (4 times 40 mL) in a similar procedure, omitting the internal standard. The isolated products were characterized with ¹H and ¹³C NMR. The substrate conversion with the latter alkenes was determined in a separate experiment by GC analysis, using the same work-up procedure with internal standard present from the start of the reaction.

3.5 References

- [1] H. Baumann, M. Bühler, H. Fochem, F. Hirsinger, H. Zobelein, J. Falbe *Angew. Chem. Int. Ed.* **1988**, *27*, 41.
- [2] A. Corma, S. Iborra, A. Vely *Chem. Rev.* **2007**, *107*, 2411.
- [3] U. Biermann, U. Bornscheuer, M. A. R. Meier, J. O. Metzger, H. J. Schäfer *Angew. Chem. Int. Ed.* **2011**, *50*, 3854.
- [4] J. R. Henry, S. M. Weinreb *J. Org. Chem.* **1993**, *58*, 4745.
- [5] C. Francavilla, W. Chen, F. R. Kinder Jr. *Org. Lett.* **2003**, *5*, 1233.
- [6] R. E. Taylor, Y. Chen, A. Beatty, D. C. Myles, Y. Zhou *J. Am. Chem. Soc.* **2003**, *125*, 26.
- [7] Z. Wang, M. G. Moloney *Tetrahedron Lett.* **2002**, *43*, 9629.
- [8] B. R. Travis, R. S. Narayan, B. Borhan *J. Am. Chem. Soc.* **2002**, *124*, 3824.
- [9] D. C. Whitehead, B. R. Travis, B. Borhan *Tetrahedron Lett.* **2006**, *47*, 3797.
- [10] S. R. Hart, D. C. Whitehead, B. R. Travis, B. Borhan *Org. Biomol. Chem.* **2011**, *9*, 4741.
- [11] W. Yu, Y. Mei, Y. Kang, Z. Hua, Z. Jin *Org. Lett.* **2004**, *6*, 3217.
- [12] W. A. Herrmann, R. W. Fischer, D. W. Marz *Angew. Chem. Int. Ed. Engl.* **1991**, *30*, 1638.
- [13] H. J. Carlsen, T. Katsuki, V. S. Martin, K. B. Sharpless *J. Org. Chem.* **1981**, *46*, 3936.
- [14] S. Torii, T. Inokuchi, K. Kondo *J. Org. Chem.* **1985**, *50*, 4980.
- [15] K. Kaneda, T. Itoh, N. Kii, K. Jitsukawa, S. Teranishi *J. Mol. Catal.* **1982**, *15*, 349.
- [16] D. Yang, C. Zhang *J. Org. Chem.* **2001**, *66*, 4814.
- [17] V. Piccialli, D. M. A. Smaldone, D. Sica *Tetrahedron* **1993**, *49*, 4211.
- [18] L. Albarella, F. Giordano, M. Lasalvia, V. Piccialli, D. Sica *Tetrahedron Lett.* **1995**, *36*, 5267.
- [19] S. E. Turnwald, M. A. Lorier, L. J. Wright, M. R. Mucalo *J. Mat. Sci. Lett.* **1998**, *17*, 1305.
- [20] Z. P. Pai, A. G. Tolstikov, P. V. Berdnikova, G. N. Kustova, T. B. Khlebnikova, N. V. Selivanova, A. B. Shangina, V. G. Kostrovskii *Russ. Chem. Bull, Int. Ed.* **2005**, *54*, 1847.
- [21] E. Antonelli, R. D'Aloisio, M. Gambaro, T. Fiorani, C. Venturello *J. Org. Chem.* **1998**, *63*, 7190.
- [22] Y. Ishii, K. Yamawaki, T. Ura, H. Yamada, T. Yoshida, M. Ogawa *J. Org. Chem.* **1988**, *53*, 3587.

- [23] T. Oguchi, T. Ura, Y. Ishii, M. Ogawa *Chem. Lett.* **1989**, *18*, 857.
- [24] R. Noyori, M. Aoki, K. Sato *Chem. Commun.* **2003**, 1977.
- [25] J. Freitag, M. Nuchter, B. Ondruschka *Green Chem.* **2003**, *5*, 291.
- [26] B. Zaidman, A. Kisilev, Y. Sasson, N. Garti *J. Am. Oil Chem. Soc.* **1988**, *65*, 611.
- [27] P. Spannring, P. C. A. Bruijninx, B. M. Weckhuysen, R. J. M. Klein Gebbink *RSC Adv.* **2013**, *3*, 6606 (Chapter 2 of this thesis).
- [28] F. N. Khan, R. Jayakumar, C. N. Pillai *J. Mol. Catal. A: Chem.* **2003**, *195*, 139.
- [29] H. J. Schäfer *C. R. Chim.* **2011**, *14*, 745.
- [30] A. Company, L. Gómez, X. Fontrodona, X. Ribas, M. Costas *Chem. Eur. J.* **2008**, *14*, 5727.
- [31] Y. Feng, J. England, L. Que Jr. *ACS Catal.* **2011**, *1*, 1035.
- [32] J. Bautz, P. Comba, C. Lopez de Laorden, M. Menzel, G. Rajaraman *Angew. Chem. Int. Ed.* **2007**, *46*, 8067.
- [33] M. S. Chen, M. C. White *Science* **2007**, *318*, 783.
- [34] O. Y. Lyakin, R. V. Ottenbacher, K. P. Bryliakov, E. P. Talsi *ACS Catal.* **2012**, *2*, 1196.
- [35] I. Garcia-Bosch, L. Gómez, A. Polo, X. Ribas, M. Costas *Adv. Synth. Catal.* **2012**, *354*, 65.
- [36] P. D. Oldenburg, C. Ke, A. A. Tipton, A. A. Shteinman, L. Que Jr. *Angew. Chem. Int. Ed.* **2006**, *45*, 7975.
- [37] P. C. A. Bruijninx, I. L. C. Buurmans, S. Gosiewska, M. A. H. Moelands, M. Lutz, A. L. Spek, G. van Koten, R. J. M. Klein Gebbink *Chem. Eur. J.* **2008**, *14*, 1228.
- [38] R. Mas-Balleste, L. Que Jr. *J. Am. Chem. Soc.* **2007**, *129*, 15964.
- [39] H. Adolfsson, C. Coperet, J. P. Chiang, A. K. Yudin *J. Org. Chem.* **2000**, *65*, 8651.
- [40] J. Rudolph, K. Laxma Reddy, J. P. Chiang, K. B. Sharpless *J. Am. Chem. Soc.* **1997**, *119*, 6189.
- [41] S. Yamazaki *Org. Biomol. Chem.* **2007**, *5*, 2109.
- [42] N. Gharah, S. Chakraborty, A. K. Mukherjee, R. Bhattacharyya *Inorg. Chim. Acta* **2009**, *362*, 1089.
- [43] Y. Nakagawa, K. Kamata, M. Kotani, K. Yamaguchi, N. Mizuno *Angew. Chem. Int. Ed.* **2005**, *44*, 5136.
- [44] A. Rezaeifard, I. Sheikshoae, N. Monadi, M. Alipour *Polyhedron* **2010**, *29*, 2703.
- [45] L. Rebrovic, G. F. Koser *J. Org. Chem.* **1984**, *49*, 2462.
- [46] V. A. Yazerski, P. Spannring, D. Gatineau, C. H. M. Woerde, S. M. Wieclawska, M. Lutz, H. Kleijn, R. J. M. Klein Gebbink, *to be submitted*

Chapter 4

Regioselective cleavage of electron-rich double bonds in dienes with [Fe(OTf)₂(mix-BPBP)] and a combination of H₂O₂ and NaIO₄

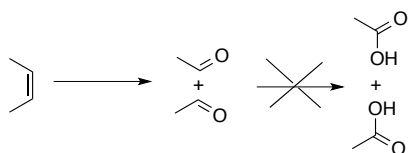
Abstract

A method has been developed that uses the Fe-based catalyst [Fe(OTf)₂(mix-BPBP)] (0.67-0.75 mol%) and an oxidant combination of hydrogen peroxide (1.1-1.5 equiv.) and sodium periodate (1.5 equiv.) to regioselectively cleave the electron-rich double bond in dienes towards aldehydes. In substrates such as geraniol and carvone, which contain double bonds with different electron densities, the more electron-rich double bond is cleaved. Additionally, the reactions are run under mild reaction temperatures (0-50 °C) for 70 minutes in MeCN with 1.5 mol% MeCOOH. The reaction with citronellol and geraniol shows that primary alcohols are tolerated by the system. This first Fe-based regioselective oxidative cleavage method presents an improvement compared to other regioselective cleavage systems in terms of reaction time and low oxidant usage. Also, the system outperforms oxidation methodologies based on simple metal salts including Ru, Os or W, which show no regioselectivity due to their strong oxidizing ability.

Based on: Peter Spannring, Vital A. Yazerski, Pieter C. A. Bruijninx, Bert M. Weckhuysen and Robertus J. M. Klein Gebbink, manuscript in preparation

4.1 Introduction

The oxidative cleavage of alkenes into aldehydes is a reaction of commercial interest, e.g. for the transformation of biomass into valuable products (Scheme 4.1).^[1-3] Ozonolysis is, for example, performed on an industrial scale on a series of alkenes,^[4] including the fatty acid oleic acid. The use of this oxidant comes with significant disadvantages, however, as it is very hazardous due to explosion risks.^[1] Catalytic oxidative cleavage systems using more benign oxidants are typically limited to second- and third-row transition metal complexes such as the RuCl₃/NaIO₄,^[5, 6] Os/NaIO₄^[7] and W/H₂O₂-based^[8] systems that have been applied to a variety of alkenes. First-row metal catalysts for oxidative cleavage reactions would nonetheless be desirable, in particular iron-based ones, as such systems would be cheaper, less toxic and more sustainable alternatives to the second- and third-row metal catalysts.^[9-15] Indeed, the few examples of first-row transition metal catalysts that have been reported are promising and in some cases already outperform the second- and third-row systems OsO₄/NaIO₄^[7, 16] or RuCl₃/NaIO₄ catalysts^[5, 6] in terms of activity or selectivity. The Mn-porphyrine/NaIO₄ cleavage system, for instance, gives higher turnover numbers for styrene cleavage with Mn than the same ligand does with other metals,^[13] and the overall catalyst loading is also much lower than those typically used with the Os-^[7, 16] and Ru-salts.^[5, 6] Nonetheless, examples of catalysts based on first-row transition metals are very scarce, though, with the few reported examples being applied to styrene-type substrates^[9-15] rather than unactivated double bonds such as those found in unsaturated fatty acids. It should furthermore be noted that mild oxidation systems are required if aldehyde products are targeted, as strong oxidizing systems usually over-oxidize the initial aldehyde product to the carboxylic acid.^[17-19] First-row metal catalysts are often milder oxidizing systems than their second- or third-row counterparts and usually have a lower tendency to disproportionate H₂O₂ than Ru and Os (see Chapter 1).

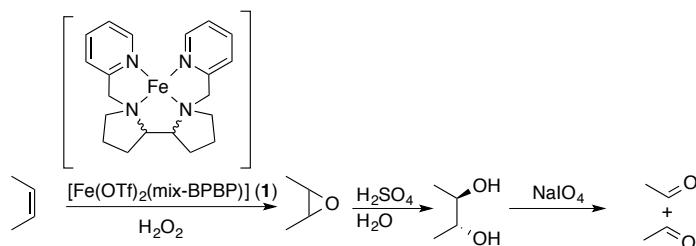


Scheme 4.1. Oxidative cleavage of an alkene into aldehydes without over-oxidation to acids.

Chapter 3 reported on the Fe-based one-pot oxidative cleavage of a number of alkenes and unsaturated fatty acids into aldehydes.^[20] The reaction sequence of this catalytic system involves [Fe(OTf)₂(mix-BPBP)]-catalyzed alkene epoxidation with H₂O₂ (mix-BPBP = mixture of *R,S*-, *R,R*- or *S,S*-isomers of *N,N'*-bis(2-picolyl)-2,2'-bipyrrrolidine),^[21-24] followed by H₂SO₄-induced hydrolysis of the epoxide to the *trans*-diol, and cleavage of the latter species into aldehydes by NaIO₄ (Scheme 4.2). This method can be run with a low catalyst

Chapter 4

loading (0.5 mol%) and uses H_2O_2 (1.5 equiv.) as one of the terminal oxidants in combination with a stoichiometric amount of NaIO_4 (1 equiv.) at ambient temperature, and as such provides a good alternative to Ru, Os or W-based systems. A particular advantage over the latter systems is the ease of product isolation by means of extraction with diethyl ether, requiring no further purification. Additionally, high catalytic activity (180 to 198 TON) at high selectivity (90-99% aldehydes) is observed with substrates containing electron-rich double bonds. Furthermore, a non-enantio-enriched mixture of BPBP ligands was used for the iron catalyst, thus providing a relatively cheap and readily available alternative to enantiopure $[\text{Fe}(\text{OTf})_2(\text{S,S-BPBP})]$.^[34]

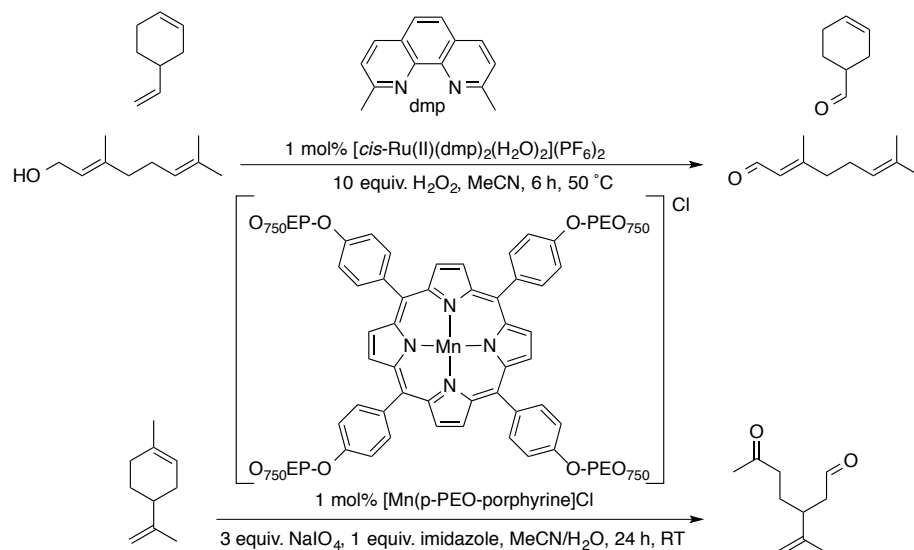


Scheme 4.2. Oxidative cleavage protocol for electron-rich alkenes and unsaturated fatty acids with $[\text{Fe}(\text{OTf})_2(\text{mix-BPBP})]$ reported in Chapter 3.^[20] The coordinating triflate ions are omitted for clarity.

Building on these promising results, the intention was to further investigate the substrate scope and selectivity of the system. A common feature of known cleavage protocols including the ozone, Ru^[5] or Os-based protocols, as well as the previously reported non-metal mediated cleavage with oxone/ NaIO_4 ^[17] (Chapter 2) is the ability to oxidize a wide variety of alkenes. As a result, a common downside of these protocols is the lack of regioselectivity in the oxidation of substrates containing more than one C=C double bond, as all double bonds in polyenes are typically oxidized with these systems. For some purposes, it can be beneficial to selectively cleave one double bond and leave others untouched, to arrive at functionalized alkene products. The formation of, e.g., aliphatic alkene-dialdehydes is challenging but rewarding, as these species can be used as chemical building blocks, for instance for the synthesis of unsaturated primary diamines.^[25]

A known regioselective cleavage method forming such alkenedials uses $[\text{cis-Ru}(\text{dmp})_2(\text{H}_2\text{O})_2](\text{PF}_6)_2$ ^[26] (dmp = 2,9-dimethyl-1,10-phenanthroline, Scheme 4.3 top) with H_2O_2 to cleave only the sterically more accessible double bonds in dienes into the aldehydes.^[27] Using 1 mol% catalyst loading and an excess of H_2O_2 (10 equiv.), the terminal double bonds in limonene and 4-vinyl-1-cyclohexene can be cleaved in 11-21% yield after 6 h at 50 °C. The results obtained with geraniol, which is converted into geranial under these conditions, show that alcohol functional groups are not tolerated and that oxidation of the alcohol to the aldehyde is preferred over alkene cleavage. Other systems have also shown some regioselectivity in the oxidation of dienes. Polymer-supported Mn-

porphyrine complexes selectively catalyze the epoxidation of the more electron-rich C=C bond in 7-methyl-1,6-octadiene (94% epoxide) and limonene (50% epoxide) with 2 equiv. NaIO_4 within 24 h.^[28] Similarly, $[\text{Mn}(p\text{-PEO-porphyrine})]\text{Cl}$ ($(\text{TPP}-(\text{PEO}_{750})_4) = 5,10,15,20\text{-tetrakis}(4\text{-PEO}_{750}\text{-phenyl})\text{porphyrine}$; PEO = polyethylene glycol) with 3 equiv. NaIO_4 (slight excess) and 1 equiv. of imidazole catalyzes the regioselective oxidative cleavage of limonene to 6-oxo-3-isopropylene-heptanal over 24 h in 89% yield (Scheme 4.3 bottom), yet other examples of regioselective cleavage reactions of C=C bonds in dienes are not reported with this system.^[15] Examples of Fe-catalyzed oxidative cleavage reactions of aliphatic monoenes are limited to methods developed in this thesis (see Chapter 2 & 3) and Fe-based regioselective oxidative cleavage reactions of dienes have not yet been reported. Here, it is reported that the method using the catalyst $[\text{Fe}(\text{OTf})_2(\text{mix-BPBP})]$ (**1**) and $\text{H}_2\text{O}_2/\text{H}_2\text{SO}_4/\text{NaIO}_4$ ^[20] can regioselectively form alkenedial by selective cleavage of the electron-rich C=C bonds in various dienes.



Scheme 4.3. Regioselective $[\text{cis-Ru}(\text{dmp})_2(\text{H}_2\text{O})_2](\text{PF}_6)_2$ ^[27] and $[\text{Mn}(p\text{-PEO-porphyrine})]\text{Cl}$ ^[15] catalysts for the cleavage of dienes into alkenedial and the oxidation of geraniol to geranial.

4.2 Results

Initially, the epoxidation of a series of aliphatic alkenes was studied with $[\text{Fe}(\text{OTf})_2(\text{mix-BPBP})]$ (**1**).^[29] In the protocol developed in Chapter 3 for similar substrates, a slight excess of H_2O_2 with respect to the substrate was added to account for disproportionation of the oxidant. Furthermore, reactions were run in pure MeCN, requiring 1.5 h for completion. Acetic acid (MeCOOH), an additive typically used in iron-catalyzed epoxidation reactions, was omitted to enable facile isolation of valuable products from terpenes and unsaturated fatty acids.^[20] Here, it was chosen to use a stoichiometric amount of H_2O_2 with respect to

Chapter 4

the substrate. Although this did lead to incomplete substrate conversion, it did allow for the difference in reactivity between the different substrates to be determined in terms of conversion percentage. Also, MeCOOH (1.5 mol%) was added here in order to speed up the epoxidation,^[30, 31] as in our group it was earlier shown that a trace amount of MeCOOH is sufficient to speed up reactions with **1**.^[29] While the total catalyst loadings were between 0.67-0.75 mol%, note that the catalyst loadings reported in the regioselectivity studies reflect the amount of active catalysts, i. e. the combined amount of [Fe(OTf)₂(*R,R*-BPBP)] and [Fe(OTf)₂(*S,S*-BPBP)], as the 25-33% of the batches of **1** contained inactive [Fe(OTf)₂(*R,S*-BPBP)].^[29] The study of the substrate scope and regioselectivity of the system involved aliphatic alkenes with *cis*- or *trans*-double bonds, various substitution patterns of the double bond and various positions of the C=C bond in the aliphatic chain.

4.2.1.1 Alkene epoxidations

In the catalytic epoxidation protocol (method A), 1 equiv. of substrate, 1.5 mol% MeCOOH and 1.0 equiv. of H₂O₂ were reacted in the presence of **1** (0.5 mol% active catalyst) at 0 °C for 10 minutes (Table 4.1). Near quantitative conversions into the corresponding epoxides were observed for the bis-substituted internal olefins *cis*-4-octene, *trans*-4-octene, *cis*-2-heptene, the tri-substituted internal olefin 2-methyl-hexene and the tetra-substituted internal olefin 2,3-di-methyl-2-butene (entries 1-5). On the contrary, lower conversions were observed for the mono- and bis-substituted terminal olefins 1-octene, 1-dodecene and 2-methyl-1-undecene (63-85%, entries 6-8).

Table 4.1. Epoxidation of electron-rich alkenes.^a

Entry	Substrate	Conversion (%)	Epoxide yield (%)
1		98	97
2		94	94
3		96	95
4 ^b		91	90
5 ^b		>95%	>95%
6		85	85
7		75	66
8		63	54

^a Reaction conditions: Method A: 0.5 mol% active [Fe(OTf)₂(mix-BPBP)] (**1**), 1.5 mol% MeCOOH, 1.0 equiv. H₂O₂ added directly drop wise at 0 °C in MeCN, 10 min., GC yields, ^b Yields determined by NMR.


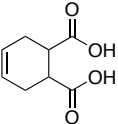
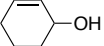

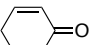
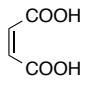
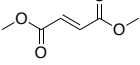
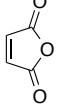
The results indicate that this method can epoxidize any principal type of aliphatic alkene. In terms of activity, it has no preference for *cis*- or *trans*-configurations of the double bond, while the degree of substitution has only a small effect after the allotted reaction time. However, significant differences are observed between terminal and internal alkenes, which are in agreement with our earlier observations for reactions run without MeCOOH.^[20] The lower activity observed in reactions with the 'fatty' substrates 1-dodecene and 2-methyl-1-undecene might be accounted for by their longer chain length, which e. g. leads to a lower solubility. The vast reactivity differences between terminal and internal olefins with this iron catalyst were also recently demonstrated by our group. Competitive epoxidation experiments were conducted between two alkenes,^[29] e. g. *cis*-cyclooctene and 1-decene, in which almost exclusively the internal alkene was oxidized. The aliphatic alkenes reported in Table 4.1 all have a comparable electron-density on the alkene, based on the ¹H chemical shifts of the olefinic hydrogen atoms. Subsequently, it was intended to study the reactivity of substrates with a less electron-rich C=C double bond. A series of cyclohexene derivatives was investigated in order to probe the relation between the electron-density of the alkene and its reactivity in the epoxidation reaction using method A (Table 4.2). Included in Table 4.2 are the ¹H chemical shift values of the olefinic hydrogens of these substrates, with larger chemical shifts reflecting more electron-poor double bonds. Cyclohexene and *cis*-1,2-dicarboxy-4-cyclohexene were quantitatively converted into their epoxides (entries 1-2). Substrate conversion decreased to 90% for 2-cyclohexen-1-ol, and even further for 2-cyclohexen-1-one (60%). Notably, the oxidation of the alcohol group was observed by the formation of 30% 2-cyclohexenone as a side product in the reaction with 2-cyclohexen-1-ol. A mediocre conversion (36%, entry 4) was observed for 3,4-epoxy-1-cyclohexene, despite an electron-density that is comparable to 2-cyclohexenol and 2-cyclohexenone. Finally, the reactions with the electron-deficient substrates maleic acid, dimethyl fumarate, and maleic anhydride gave low conversions (6.37-7.10 ppm, entries 5-7). The reactions are highly selective for all substrates but 2-cyclohexenol, with conversions of almost all entries matching epoxide formation.

The data in Table 4.2 suggest a relation between the epoxide formation and the electron-density on the double bond of the substrate of entries 1-3 and 5-8. The ¹H NMR chemical shift of the olefinic hydrogens does, however, not have a direct relation with the epoxidation reactivity for entry 4. The poor conversion might be explained by the fact that the C=C double bond in 3,4-epoxy-1-cyclohexene is less accessible than in cyclohexene, as probably oxidation only occurs from one side, as opposed to two sites in substrates of entries 1, 2, 3 and 5. Additionally, the functional groups in entries 2, 3 and 4 might also have a directing affect, as they can bind to the iron center and therefore increase the oxidation activity, as commonly occurs in hydroxylations.^[32] Another example where the

Chapter 4

chemical shift cannot directly be related to the epoxide yield is the oxidation of terminal alkenes compared to internal alkenes (see Table 4.1), as the epoxidation reaction of terminal alkenes is slower than with internal alkenes,^[29] despite the higher chemical shift value of the latter.

Table 4.2. Epoxidation of electron-poor alkenes.^a

Entry	Substrate	C=C shift (ppm)	Conversion (%)	Epoxide yield(%)
1		5.66	>95%	>95%
2		5.70	>95%	>95%
3		5.74, 5.80	90	60 ^b
4		5.89, 5.96	36	36
5		5.91, 7.05	60	55
6		6.37	15	15
7		6.86	10	10
8		7.10	10	Nd

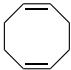
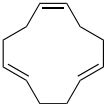
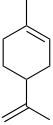
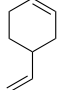
^a Reaction conditions: Method A, yields determined by NMR; ^b 30% 2-Cyclohexenone.

Based on the results of Table 4.2, catalyst **1** is electrophilic. Especially the poor reactivity for dimethyl fumarate, maleic acid and its anhydride is in sharp contrast to the activity observed for other nucleophilic first-row metal-based catalytic oxidation systems.^[33, 34]

Having established the electrophilic nature of the catalyst, the epoxidation of polyenes with dissimilar double bonds was investigated. In a similar protocol as with the monoenes (1 equiv. H₂O₂ with respect to the substrate), 1,5-cyclooctadiene could be converted for 77%, yielding 65% of the monoepoxide and 12% of the diepoxide (Table 4.3). This observation implies that in reactions with dienes a limited amount of oxidant indeed only oxidizes one double bond. The use of a higher amount of oxidant did increase the yield of the diepoxide (not shown). Next, it was examined whether regioselectivity was observed in the epoxidation of polyenes with different double bonds.^[29] Substoichiometric amounts

of oxidant were used to limit diepoxide formation and to obtain a better picture of the inherent reactivity differences between the double bonds.^[28] Reactions of 1,5,9-*cis-trans-trans*-cyclododecatriene and 0.6 equiv. H₂O₂ rendered a mixture of monoepoxides, with a *trans*-epoxide/*cis*-epoxide ratio of 2/1 (entry 2) in 51% yield, consistent with a similar reactivity of the *cis*- and the *trans*-double bonds. On the other hand, reactions with limonene did show the preferential oxidation of one of the double bonds, as the oxidation with 0.75 equiv. H₂O₂ rendered a mixture of monoepoxides with an endocyclic/exocyclic epoxide ratio of (3.4:1) in 54% yield (entry 3), consistent with the preference of the catalytic system to react with internal double bonds. Moreover, the oxidation of 4-vinyl-1-cyclohexene with 0.9 equiv. H₂O₂ showed an even higher selectivity towards internal double bonds than previous entries, with 74% yield of the endocyclic epoxide formed at 79% combined monoepoxide yield (entry 4). Some diepoxide formation was observed for all the substrates.

Table 4.3. Epoxidation of polyenes.^{a[29]}

Entry	Substrate	Reaction Conditions		Mono-epoxide yield (%)	Endo/ <i>trans</i> (%)	Exo/ <i>cis</i> (%)
		H ₂ O ₂ (equiv.)	Conversion (%)			
1		1.0	77	65 ^b	-	-
2 ^c		0.6	Nd	51	34	17
3 ^c		0.75	Nd	54	42	12
4 ^c		0.9	Nd	79	74	5

^a Reaction conditions: Method A, GC yield; ^b 12% diepoxide; ^c 5 mol% MeCOOH, isolated yield of monoepoxides, conversion not determined.

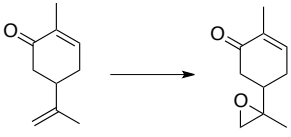
The reactivity differences observed in the oxidation reactions of the aliphatic monoenes (Table 4.1) are thus also reflected in reactions with aliphatic dienes in entries 2-4 in Table 4.3. The observed selectivity towards the monoepoxide in the case of 1,5-cyclooctadiene at the addition of 1.0 equiv. H₂O₂ is remarkable, (entry 1), as statistical factors would predict larger amounts of the diepoxide. Steric aspects that favor the oxidation of 1,5-cyclooctadiene compared to the oxidation of 1,2-epoxy-*cis*-5-cyclooctene probably account for these reactivity differences, as similar observations were made in Table 4.2.

Chapter 4

The epoxidations of 1,5-cyclooctadiene and, especially, of 4-vinyl-1-cyclohexene show that selective cleavage of only one double bond in these substrates is indeed possible and, accordingly, alkene-dials would be accessible with this method.

Finally, the biomass-derived polyene carvone was tested as substrate. This terpenoid contains two C=C double bonds of distinct electron-density as indicated by the ^1H chemical shifts of 6.77 ppm, 4.76 and 4.81 ppm of the olefinic hydrogens, with the electron-rich double bond situated on the exocyclic position. The effect of MeCOOH addition on epoxide formation and selectivity was also assessed for this substrate. Epoxidation of carvone with **1** without MeCOOH gave high epoxide yields and proved highly selective: 88% exocyclic mono-epoxide at 90% substrate conversion was observed after 20 minutes, with the selectivity slightly dropping (82% epoxide) with increased conversion (95%) after 90 minutes (Table 4.4, entries 1-2). The latter observation indicates some over-oxidation of the exocyclic epoxide over time. Likewise, the addition of larger amounts of oxidant (1.2 equiv.) decreased the selectivity towards the exocyclic epoxide (entry 3). To our delight, complete conversion into the exocyclic epoxide was observed with **1** within 10 minutes with as low as 1.5 mol% MeCOOH and 1.0 equiv. H_2O_2 (entries 4-5). Carvone epoxidation reactions were also performed with $[\text{Fe}(\text{OTf})_2(\text{BPMEN})]$ (BPMEN = *N,N'*-dimethyl-*N,N'*-bis(2-pyridylmethyl)-1,2-diaminoethane)^[35] as catalyst in this study, but lower product yields were observed and high amounts of MeCOOH (50 equiv., not shown) were required for substrate conversions to reach over 90%.

Table 4.4. Epoxidation of carvone.^a



Entry ^a	H_2O_2 (equiv.)	MeCOOH (equiv.)	Time (min)	Conversion (%)	8,9-epoxy-carvone yield (%)
1	1.0	0	20	90	88
2	1.0	0	90	95	82
3	1.2	0	70	100	87
4	1.0	50	10	>99	99
5	1.0	0.015	10	99	98

^a Reaction conditions: 0.5 mol% active **1**, 0 °C, MeCN.

The reactivity difference based on the electron-density of the C=C double bond, as observed for the mono-alkenes, can therefore be exploited in the epoxidation of carvone.

Careful control of reaction conditions is crucial though, as absence of MeCOOH, too long reaction times and too much oxidant result in over-oxidation to the diepoxide.

4.2.2 Oxidative cleavage of alkenes

Having established that regioselective epoxidation is possible with **1**, the attention was turned to the regioselective oxidative cleavage, for which the epoxidation is the first step in this protocol. For the oxidative alkene cleavage reactions, Chapter 3 reported substrate-dependent reaction times of 1-12 h.^[20] The overall reaction time depended on the rate of the H₂SO₄-induced hydrolysis step and the subsequent NaIO₄-induced diol cleavage step. Also here, lower reaction rates were observed for the hydrolysis and diol cleavage for some substrates, in particular for *cis*-cycloalkenes and sterically hindered alkenes. In the course of optimizing the reaction, it was observed that for most substrates the combined hydrolysis and cleavage reaction steps were nearly complete after 1 h upon increase of the reaction temperature to 50 °C. Of equal importance was the addition of water upon introducing NaIO₄ to the reaction mixture, yielding a MeCN:H₂O 1:3 (v/v) reaction medium in the last step of the overall reaction. These reaction conditions are similar to the procedure described in Chapter 3 and to the metal-free cleavage procedure described in Chapter 2, which uses a combination of oxone and NaIO₄.^[17] Therefore, the overall cleavage protocol (method B) involved epoxidation of the substrate at 0 °C for 10 min. with **1** (0.5 mol%), H₂O₂ (1.5 equiv.) slight excess to ensure complete conversion), and acetic acid (1.5 mol%), followed by an increase of the reaction temperature to 50 °C and epoxide hydrolysis with H₂SO₄ (0.5 equiv. in H₂O (75 equiv.)) for 30 min. to yield the diol. Finally, 1 equiv. NaHCO₃ was introduced at 50° C to neutralize the reaction mixture, followed by treatment for 30 min. with NaIO₄ (1 equiv. in H₂O (600 equiv.)), dilution with water also observed to be beneficial in Chapter 2) to cleave the diol.

The cleavage method was initially tested on a series of simple alkenes prior to reactions with dienes. A number of aliphatic alkenes could be cleaved in high yields into the corresponding aldehydes (Table 4.5). The industrially relevant suberaldehyde was isolated in 50% from the reaction with *cis*-cyclooctene (entry 1). Furthermore, tri- and tetrasubstituted olefins were cleaved nearly quantitatively to the corresponding aldehydes and ketones (entries 2-3), and the terminal alkenes 1-dodecene and 2-methyl-1-undecene also gave high yields of the corresponding aldehydes at near-quantitative conversions (entries 4-5). Interestingly, the protocol of this chapter rendered significantly higher conversions of terminal alkenes (92-98%) than in Chapter 2 (47%, Table 2.3) and Chapter 3 (70%, Table 3.5). Furthermore, the protocol enabled the oxidative cleavage of the terpenoids citronellol and citronellol acetate with high isolated yields of the aldehydes and full substrate conversion (entries 6-7). These examples show that acetate and alcohol functional groups are tolerated by this procedure. Citronellol oxidation did show trace

Chapter 4

amounts of cyclization product,^[36] which are absent with the acetate derivative (entries 6-7).

Table 4.5. Oxidative cleavage of aliphatic alkenes.^a

Entry	Substrate	Conversion (%)	Product	Yield (%)
1		100		50 ^b
2		100		91
3		100		94
4		92		85 ^c
5		98		88 ^c
6		100		80 ^b
7		100		68 ^{b,d}

^a Reaction conditions: Method B: i) 0.5% active **1**, 0.015 equiv. MeCOOH, 1.5 equiv. H₂O₂ at 0 °C in MeCN, 10 min. ii) 0.5 equiv. H₂SO₄ in 75 equiv. H₂O at 50 °C for 0.5 h, iii) 1 equiv. NaHCO₃, 1.5 equiv. NaIO₄ and 600 equiv. H₂O at 50 °C for 0.5 h, yields determined by NMR; ^b Isolated yield; ^c Additionally analyzed by GC; ^d Traces of hemi-acetal detected.

These reactions show that the oxidative cleavage protocol can be applied to a series of aliphatic alkenes and now has the added advantage of considerably shorter reaction times compared to the protocol described in Chapter 3. The improved protocol does require a small amount of MeCOOH and needs to partially operate at somewhat elevated temperatures. The reactivity observed here for tri- and tetra-substituted alkenes differs from the regioselective catalytic system [*cis*-Ru(dmp)₂(H₂O)₂](PF₆)₂/H₂O₂, for which no activity with trisubstituted alkenes was found.^[27] In addition, although the system prefers internal C=C bonds over terminal ones, high product yields could still be obtained with the terminal alkenes 1-dodecene and 2-methyl-1-undecene. This is in contrast to the Mn-porphyrine/NaIO₄ system, which shows no activity for terminal alkenes.^[15]

Subsequently, the oxidative cleavage of dienes was investigated, again with only 1.0 equiv. of H₂O₂ to limit potential over-oxidation. In this way, alkenedials could indeed be isolated. The oxidation of 1,3-cyclohexadiene gave 49% isolated yield of the *cis*-1,6-hex-2-ene-dial product, while 1,5-cyclooctadiene gave 67% of *cis*-1,8-oct-4-ene-dial (Table 4.6, entries 1-2). With 1,5-cyclooctadiene, trace amounts of 1,4-butanedial were observed, which indicates that over-oxidation to the corresponding diepoxide or the epoxide dialdehyde

intermediate takes place to some extent (also observed in Table 4.3). Notably, the reaction with 4-vinyl-cyclohexene shows that the internal double is preferentially cleaved, yielding 76% of 3-vinyl-adipaldehyde (entry 3). Oxidative cleavage of geraniol resulted in 54% of *trans*-6-hydroxy-4-methyl-hex-4-enal at 70% conversion, indicating that the allylic alcohol group remains predominantly untouched, forming only trace amounts of 4-oxo-1-pentanone (entry 4). Only minor amounts of over-oxidation products were observed for entries 3 and 4. Finally, the oxidative cleavage of carvone was found to be completely regioselective, as only the exocyclic double bond in carvone was affected with 1.1 equiv. of H₂O₂ (a slight excess of oxidant, entry 5).

Not all polyenes could be selectively converted, though, as reactions with limonene and 1,5,9-*cis-trans-trans*-cyclododecatriene gave only poor selectivity to the formation of alkenedial. Other substrates for which the procedure so far did not proceed smoothly are 3-carene (containing a three-membered ring), the triene myrcene, and nopol (containing a four-membered ring and a primary alcohol), as a variety of products was observed.

Table 4.6. Regioselective oxidative cleavage of dienes.^a

Entry	Substrate	Con. (%)	Product	Yield (%)
1		66		49 ^b
2		88		67
3		92		76 ^c
4		70		54 ^d
5		100		99 ^e

^a Reaction conditions: Method B, yet 1.0 equiv. H₂O₂ added, isolated yield; ^b Traces of 1,4-butanedial observed; ^c NMR yield; ^d NMR yield, trace amounts of 4-oxo-1-pentanone; ^e 1.1 equiv. H₂O₂ added, GC yield.

Advantages of this protocol are the short reaction time of only 70 minutes, the application of almost no excess of oxidant and the use of H₂O₂. Moreover, the observed functional group tolerance together with the high selectivities for electron-rich double bonds in

Chapter 4

dienes shows the potential of this protocol for oxidative C=C bond cleavage reactions with more complex dienes, such as some terpenoids.

4.3 Concluding remarks

In summary, an optimized Fe-based oxidative cleavage protocol was developed for the conversion of electron-rich internal and terminal olefins to the corresponding aldehydes and dialdehydes. The protocol involves 0.67-0.75 mol% of the non-heme iron complex [Fe(OTf)₂(mix-BPBP)], which represents a non-resolved mixture of iron BPBP complexes, and uses an oxidant combination of H₂O₂ and NaIO₄ with reaction temperatures ranging from 0 °C to 50 °C. A series of alkenes, comprising different configurations, substitution patterns and locations in the chain of the alkene, can be cleaved in high yields to obtain the corresponding aldehydes and dialdehydes in reasonable to quantitative yields in only 70 minutes. Overall, the protocol shows a high preference for the cleavage of electron-rich alkenes over less electron-rich alkenes and for internal alkenes over external alkenes of similar electron-density. The oxidation of the terpene derivatives citronellol, citronellol acetate, and geraniol to the corresponding aldehydes shows the functional group tolerance of the protocol.

Furthermore, this regioselective oxidative cleavage protocol for electron-rich C=C double bonds is complementary to Ru(dmp)/H₂O₂-based regioselective cleavage systems for terminal alkenes^[27] and outperforms Mn-Porphyrine/NaIO₄-based regioselective cleavage systems for internal alkenes in terms of activity.^[15] The system also outperforms systems using metal oxides of Ru, Os and W, which either do not show regioselectivity, or for which reactions with polyenes have not been reported. The protocol is expected to be useful for the oxidative cleavage of other dienes with significant electron-density differences between the double bonds and for the regioselective cleavage of other terpenoid dienes.

4.4 Experimental

4.4.1 General

Sodium periodate (99%), *trans*-4-octene (90%), (*S*)-(-)-β-citronellol (>99%), citronellyl acetate (99%), (*R*)-(-)-carvone, 2-methyl-1-undecene (97%), 2,3-dimethyl-2-butene (98%), *trans,trans,cis*-1,5,9-cyclododecatriene (98%), 3,4-epoxy-1-cyclohexene (>96%), cyclooctene oxide (99%), maleic anhydride (99%), 1-cyclohexene-1-carboxaldehyde (98%), dimethyl fumarate (97%), *cis*-2-heptene (97%) and 1,3-cyclohexadiene (97%) were purchased from Aldrich. 4-Vinyl-1-cyclohexene (97%), 1-methyl-1-cyclohexene (97%), *cis*-cyclooctene (95%, stabilized), hydrogen peroxide (35 wt.% in H₂O) and 1,5-cyclooctadiene (99%, stabilized) were obtained from Acros Organics. Maleic acid (>99%) was obtained from Fluka. *Cis*-4-octene (97%) was purchased from Alfa. *Cis*-4-cyclohexene-1,2-dicarboxylic acid (98%) and 2-methyl-2-hexene (99%) were purchased from ABCR. (*R*)-(+)-Limonene (97%) was bought from Sigma. Nitrobenzene (99%) was obtained from Sial. All chemicals were used as received. The reactions

were conducted in air, using distilled water, pro analysis MeCN and MeCOOH, and technical grade ether and sulfuric acid. ^1H NMR and ^{13}C NMR measurements were recorded at 298 K using a Varian 400 MHz NMR Spectrometer, using residual solvents peaks as reference. Gas chromatography was carried out on a PerkinElmer Clarus 500 Gas Chromatograph with an Alltech EconocapTM ec TM 53.0 m x 0.0032 mm ID x 0.25 mm, 5% phenyl and 95% methylpolysiloxane column. Conversions were determined by substrate consumption, and the formations of products were compared with authentic samples of the products. The synthesis of $[\text{Fe}(\text{OTf})_2(\text{mix-BPBP})]$ (**1**) was performed according to literature procedures.^[29]

4.4.2 Monoalkene epoxidations, method A

Alkene substrate (0.72 mmol) 0.5% active $[\text{Fe}(\text{OTf})_2(\text{mix-BPBP})]$ (**1**) (thus containing 3.6 mmol of combined $[\text{Fe}(\text{OTf})_2(\text{S,S-BPBP})]$ and $[\text{Fe}(\text{OTf})_2(\text{R,R-BPBP})]$), in a batch commonly containing 0.9-1.2 mmol of inactive $[\text{Fe}(\text{OTf})_2(\text{R,S-BPBP})]$, MeCOOH (0.015 equiv.) and MeCN (3 mL) were mixed at 0 °C. H_2O_2 (1.0 equiv.) in MeCN (0.5 mL) was added dropwise by hand, and the mixture was stirred for 10 minutes prior to addition of diethyl ether (20 mL) and nitrobenzene (1.0 equiv.) in MeCN (1 mL) and subjected to GC analysis to determine the conversion with *cis*-4-octene, *trans*-4-octene, *cis*-4-octene, 1-decene, 2-methyl-1-undecene, 1-carboxyaldehyde-1-cyclohexene and 3,4-epoxy-1-cyclohexene. With other substrates, instead of addition of diethyl ether, CD_3CN (1 mL) and nitrobenzene in MeCN were added and the sample was subjected to NMR analysis. With *cis*-4-octene, the epoxidation was analyzed with both procedures, matching the observed results. With 1-carboxyaldehyde-1-cyclohexene and dimethyl fumarate, the conversion was determined by GC analysis and the epoxide yield by NMR analysis. The monoepoxides from reactions with 1,5,9-*cis-trans-trans*-cyclododecatriene, limonene and 4-vinyl-1-cyclohexene were isolated after the reaction by means of vacuum distillation and analyzed by ^1H NMR to confirm the purity and to determine either the rates of *endo/exo*-epoxide or *cis/trans*-epoxide. For limonene and 4-vinyl-1-cyclohexene, the samples were additionally analyzed with GC and compared with authentic samples of the *endo*- and *exo*-epoxides. Full experimental details on the epoxidations of 1,5,9-*cis-trans-trans*-cyclododecatriene, limonene and 4-vinyl-1-cyclohexene are due to be published.^[29]

4.4.3 Epoxidation of carvone

Method A was applied, with either 0, 0.015 or 50 equiv. of MeCOOH added at the start; reactions were performed for 10, 20, 70 or 90 minutes and either 1.0 equiv. or 1.2 equiv. H_2O_2 was used. The carvone epoxide was isolated in order to obtain an authentic sample for comparison and quantification purposes. The isolation was performed in a similar procedure but without MeCOOH, and with a tenfold increase of the amount of the substrate (7.2 mmol) and 1.5 h reaction time.

4.4.4 Oxidative cleavage aliphatic monoalkenes, method B

The epoxidation protocol described above for the monoalkenes, at the end of the reaction (i.e. 10 min.), the reaction was warmed up to 50 °C and H_2SO_4 (0.5 equiv.) in H_2O (75 equiv.) was added and after which the mixture was stirred for 0.5 h. Then, NaHCO_3 (1 equiv.), NaIO_4 (1.5 equiv.) and H_2O (600 equiv.) were added to the reaction mixture, which was stirred for an additional 0.5 h. Subsequently, CD_3CN was added (1 mL) and nitrobenzene (1 equiv.) in MeCN (1 mL) after which a sample was analyzed with ^1H NMR. For accurate determination of the conversion, after analysis with NMR, 20 mL of diethyl ether were added and a sample subjected to GC analysis. The reactions with *cis*-cyclooctene, citronellol and citronellyl acetate were run on threefold larger scale (2.16 mmol) and the isolated yield was determined by extraction with diethyl ether (3 x 20 mL), drying over MgSO_4 , filtration and concentration in vacuo.

Chapter 4

4.4.5 Oxidative cleavage dienes

For the reaction with dienes, a similar protocol was used as method B, yet 1.0 eq. H₂O₂ were applied. The isolated yields from reactions with 1,3-cyclohexadiene and 1,5-cyclooctadiene were done in the same way as reactions with *cis*-cyclooctene, yet with 1.0 eq. of H₂O₂. The reactions with 4-vinyl-1-cyclohexene and geraniol were analyzed by ¹H NMR, in the same way as the aliphatic monoalkenes were analyzed in method B. For the reaction with carvone, 1.1 equiv. of H₂O₂ was applied. Furthermore, at the end of the reaction, diethyl ether (20 mL) was added, followed by nitrobenzene (1 equiv.) in MeCN and a sample was subjected to GC analysis.

4.5 References

- [1] A. Corma, S. Iborra, A. Vely *Chem. Rev.* **2007**, *107*, 2411.
- [2] U. Biermann, W. Friedt, S. Lang, W. Lühs, G. Machmüller, J. O. Metzger, M. Rüschen, Klaas, H. J. Schäfer, M. P. Schneider *Angew. Chem. Int. Ed.* **2000**, *39*, 2206.
- [3] U. Biermann, U. Bornscheuer, M. A. R. Meier, J. O. Metzger, H. J. Schäfer *Angew. Chem. Int. Ed.* **2011**, *50*, 3854.
- [4] Ozonolysis on industrial scale is performed by Novasep.
- [5] D. Yang, C. Zhang *J. Org. Chem.* **2001**, *66*, 4814.
- [6] C. M. Ho, W. Y. Yu, C. M. Che *Angew. Chem. Int. Ed.* **2004**, *43*, 3303.
- [7] W. Yu, Y. Mei, Y. Kang, Z. Hua, Z. Jin *Org. Lett.* **2004**, *6*, 3217.
- [8] A. Haimov, H. Cohen, R. Neumann *J. Am. Chem. Soc.* **2004**, *126*, 11762.
- [9] H. Mimoun, L. Saussine, E. Davire, M. Postel, J. Fisher, R. Weiss *J. Am. Chem. Soc.* **1983**, *105*, 3101.
- [10] B. M. Choudary, P. N. Reddy *J. Mol. Catal. A: Chem.* **1995**, *103*, L1.
- [11] P. A. Ganeshpure, S. Satish *Tetrahedron Lett.* **1988**, *29*, 6629.
- [12] A. Dhakshinamoorthy, K. Pitchumani *Tetrahedron* **2006**, *62*, 9911.
- [13] H. Chen, H. Ji, X. Zhou, J. Xu, L. Wang *Catal. Commun.* **2009**, *10*, 828.
- [14] Y. F. Li, C. C. Guo, X. H. Yan, Q. Liu *J. Porphyrins Phtalocyanines* **2006**, *10*, 942.
- [15] S. T. Liu, K. V. Reddy, R. Y. Lai *Tetrahedron* **2007**, *63*, 1821.
- [16] S. V. Ley, C. Ramarao, A. L. Lee, N. Ostergaard, S. C. Smith, I. M. Shirley *Org. Lett.* **2003**, *5*, 185.
- [17] P. Spannring, P. C. A. Bruijninx, B. M. Weckhuysen, R. J. M. Klein Gebbink *RSC Adv.* **2013**, *3*, 6606 (Chapter 2 of this thesis).
- [18] B. Borhan, B. R. Travis, J. M. Schomaker, **2003**.
- [19] H. J. Carlsen, T. Katsuki, V. S. Martin, K. B. Sharpless *J. Org. Chem.* **1981**, *46*, 3936.
- [20] P. Spannring, V. A. Yazerski, P. C. A. Bruijninx, B. M. Weckhuysen, R. J. M. Klein Gebbink *Chem. Eur. J.* **2013**, *19*, 15012 (Chapter 3 of this thesis).
- [21] A. Company, L. Gómez, X. Fontrodona, X. Ribas, M. Costas *Chem. Eur. J.* **2008**, *14*, 5727.
- [22] Y. Feng, J. England, L. Que Jr. *ACS Catal.* **2011**, *1*, 1035.
- [23] J. Bautz, P. Comba, C. Lopez de Laorden, M. Menzel, G. Rajaraman *Angew. Chem. Int. Ed.* **2007**, *46*, 8067.
- [24] M. S. Chen, M. C. White *Science* **2007**, *318*, 783.
- [25] E. Artner, R. Haar, F. Hebesberger, E. Kloimstein, C. Kos, E. Lust, *Process for preparing primary amines from aldehydes*, **1995**, US5475141 A.
- [26] A. S. Goldstein, R. H. Beer, R. S. Drago *J. Am. Chem. Soc.* **1994**, *116*, 2424.

- [27] V. Kogan, M. M. Quintal, R. Neumann *Org. Lett.* **2005**, *7*, 5039.
- [28] E. Brulé, Y. R. de Miguel, K. K. Hii *Tetrahedron* **2004**, *60*, 5913.
- [29] V. A. Yazerski, P. Spannring, D. Gatineau, C. H. M. Woerde, S. M. Wieclawska, M. Lutz, H. Kleijn, R. J. M. Klein Gebbink, *to be submitted*.
- [30] O. Y. Lyakin, R. V. Ottenbacher, K. P. Bryliakov, E. P. Talsi *ACS Catal.* **2012**, *2*, 1196.
- [31] I. Garcia-Bosch, L. Gómez, A. Polo, X. Ribas, M. Costas *Adv. Synth. Catal.* **2012**, *354*, 65.
- [32] M. A. Bigi, S. A. Reed, M. C. White *J. Am. Chem. Soc.* **2012**, *134*, 9721.
- [33] T. W. S. Chow, E. L. M. Wong, Z. Guo, Y. Liu, J. S. Huang, C. M. Che *J. Am. Chem. Soc.* **2010**, *132*, 13229.
- [34] J. J. Dong, P. Saisaha, T. G. Meinds, P. L. Alsters, E. G. Ijpeij, R. P. van Summeren, B. Mao, M. Fananas-Mastral, J. W. de Boer, R. Hage, B. L. Feringa, W. R. Browne *ACS Catal.* **2012**, *2*, 1087.
- [35] D. Clemente-Tejeda, A. López-Moreno, F. A. Bermejo *Tetrahedron* **2012**, *68*, 9249.
- [36] M. A. Bigi, S. A. Reed, M. C. White *Nat. Chem.* **2011**, *3*, 216.

Chapter 5

Fe(6-Me-PyTACN)-catalyzed, one-pot oxidative cleavage of methyl oleate and oleic acid into carboxylic acids with H₂O₂ and NaIO₄

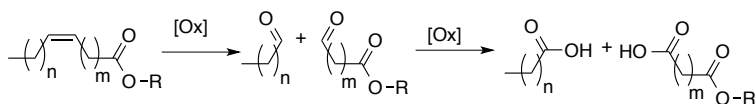
Abstract

The first Fe-based catalytic system for the oxidative cleavage of unsaturated fatty acids and esters to carboxylic acids is reported. The system uses [Fe(OTf)₂(6-Me-PyTACN)] (2) (6-Me-PyTACN = 1-[(6-methyl-2-pyridyl)methyl]-4,7-dimethyl-1,4,7-triazacyclononane) as the catalyst (3 mol%) together with a combination of hydrogen peroxide and NaIO₄ or with exclusively NaIO₄ as the oxidant and operates at 0 °C or ambient temperature. Using these standard conditions (method A), the system yields 50-55% of nonanoic and azelaic acid out of methyl oleate, together with some epoxide and aldehyde byproducts in a one-pot procedure. The addition of sulfuric acid during the procedure (method B) hydrolyzes the epoxide byproducts and forms a mixture of aldehyde and carboxylic acids. A further adjustment of the procedure includes a pH neutralization step and addition of extra catalyst (method C), and enables the transformation of both methyl oleate and oleic acid into high yields of the corresponding carboxylic acids (80-85%). Overall, this catalytic system provides an alternative to the industrial ozonolysis of oleic acid and to catalytic Ru and Os- based systems for the oxidative cleavage of unsaturated fatty acids and esters.

Based on: Peter Spanning, Irene Prat, Miquel Costas, Martin Lutz, Pieter C. A. Bruijninx, Bert M. Weckhuysen, and Robertus J. M. Klein Gebbink, *Catal. Sci. Technol.* revision in progress

5.1 Introduction

Vegetable oils form a renewable resource for the production of sustainable platform chemicals.^[1] Biodiesel, lubricants, surfactants, pharmaceuticals and other chemicals can be produced from this biomass source. Triglycerides can be transformed into fatty acids by hydrolysis and into fatty acid methyl esters by transesterification with methanol. Reactions on the internal C=C double bond in unsaturated fatty acids involve, for example, metathesis in order to obtain terminal double bonds that are susceptible for further reactions.^[2] Furthermore, oxidation reactions on the C=C bond commonly yield epoxides, which can be used for polymerization purposes. Alternatively, oxidations of the internal double bond in unsaturated fatty acids can also involve the oxidative cleavage into aldehydes or carboxylic acids (Scheme 5.1). This transformation can give four potentially interesting products: aliphatic aldehydes, α,ω -aldehyde fatty acids, aliphatic carboxylic acids and α,ω -dicarboxylic acids. The oxidative cleavage route thus provides access to medium chain length aliphatic aldehydes such as nonanal, representing an alternative, renewables-based route for the Rh-mediated hydroformylation of terminal olefins to saturated aldehydes. The α,ω -aldehyde fatty acids and α,ω -dicarboxylic acids can be used as lubricants and are valuable building blocks for the polymer industry. Finally, the long-chain carboxylic acids can find application as emulsifiers.^[1, 3-5]



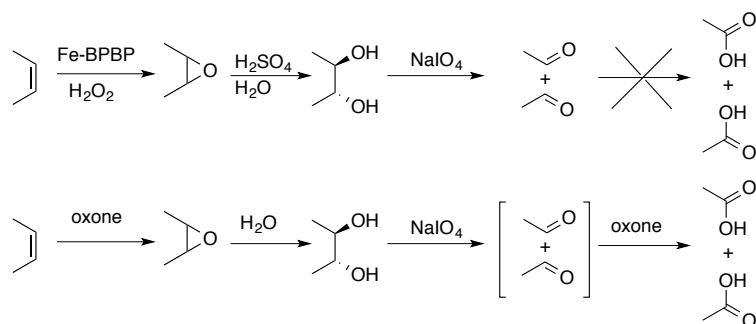
Scheme 5.1. Oxidative cleavage of unsaturated fatty acids into aldehydes and the over-oxidation into carboxylic acids.

Catalytic systems for the oxidative cleavage of alkenes typically comprise transition-metal complexes based on either expensive, toxic or scarce metals such as Ru,^[6-11] W^[12-19] or Os.^[20-27] The use of first-row transition metal-based catalysts would make these reactions more sustainable given their ready availability, low price and low toxicity. Fe-based catalysts particularly stand out in this respect. However, oxidative cleavage reactions with this metal primarily concern activated styrene derivatives that are readily cleaved with complexes based on salen-type^[28, 29] and porphyrine-type^[30-32] ligands. As far as unsaturated fatty acids are concerned, second- and third-row transition-metal systems are mostly used for the catalytic cleavage into aldehydes.^[19, 24, 33]

Currently, the only oxidative cleavage of a fatty acid that is performed on an industrial scale is the oxidative cleavage of oleic acid by ozone.^[34] This process comes with disadvantages as ozone is a dangerous oxidant because of explosion risks and its use is unpractical because of the necessity of preparing the oxidant in-situ prior to reaction.^[3] Alternatives to this process are therefore of interest.

In Chapter 3, the first example of an Fe-catalyzed oxidative fatty acid cleavage was reported.^[35] Iron complexes based on the ligand *N,N'*-bis(2-picoyl)-2,2'-bipyrrolidine (BPBP) in combination with H₂O₂ and NaIO₄ as the oxidants are able to oxidatively cleave unsaturated fatty acids into aldehydes in a one-pot reaction. The reaction involves a sequence of steps, i.e. fatty acid epoxidation catalyzed by the Fe-catalyst, H₂SO₄-catalyzed hydrolysis and subsequent diol cleavage with NaIO₄ (Scheme 5.2, top).^[35] Notably, this catalytic system does not over-oxidize the aldehyde products to carboxylic acids.

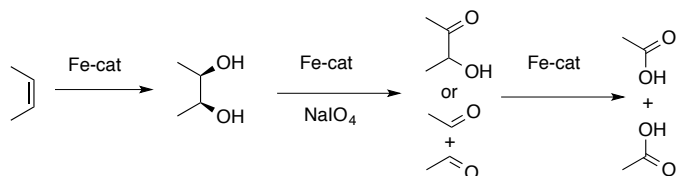
Examples of catalytic oxidative cleavage reactions of unsaturated fatty acids to carboxylic acids exclusively make use of second- and third-row catalysts based on Ru,^[36-39] W^[12-14, 40-45] and Mo.^[12] In Chapter 2, a method towards carboxylic acids from these substrates was reported following a similar, but metal-free approach that uses a combination of oxone and periodate as the sacrificial oxidants (Scheme 5.2, bottom).^[46] In this approach, oxone epoxidizes the double bond of the fatty acid and the acidic nature of this oxidant subsequently induces the hydrolysis of the epoxide to the *trans*-diol. In turn, NaIO₄ oxidizes the *trans*-diol to aldehydes, with oxone then rapidly over-oxidizing the products to carboxylic acids. This protocol requires high reaction temperatures and the use of oxone as oxidant generates a considerable amount of waste. Therefore, catalytic alternatives to oxone that can employ ambient temperatures and generate less waste are of interest.



Scheme 5.2. Previously reported oxidative cleavage of unsaturated fatty acids into aldehydes by Fe-BPBP catalysts with H₂O₂, H₂SO₄ and NaIO₄,^[35] and cleavage into carboxylic acids by oxone/NaIO₄.^[46]

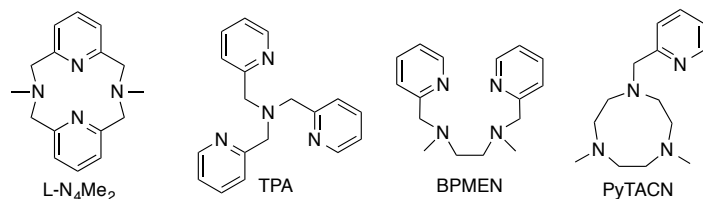
The first step of such a catalytic oxidative cleavage reaction of fatty acids and esters to carboxylic acids may entail an Fe-catalyzed epoxidation or *cis*-dihydroxylation of the double bond. The pathway involving *cis*-dihydroxylation of alkenes is preferred over alkene epoxidation and subsequent acid-catalyzed hydrolysis, in the sense that alkenes can then be transformed to diols without the use of H₂SO₄ (Scheme 5.3). The transformation of the *cis*-diol towards carboxylic acids can either proceed via the Fe-based diol oxidation into hydroxy ketones^[47] or the NaIO₄-mediated oxidation into aldehydes.^[35, 46] Finally, the Fe-catalyst can also mediate the over-oxidation of either species into the

carboxylic acid. NaIO_4 was identified as a convenient oxidant for such a protocol, as the oxidation of the *cis*-diol intermediate into the aldehyde is most efficiently done with this oxidant, which can furthermore be regenerated electrochemically.^[48]



Scheme 5.3. Generalized Fe-catalyzed oxidative cleavage strategy of alkenes into carboxylic acids via *cis*-diol and hydroxy ketones or aldehyde intermediates.

Potential catalysts of interest for the set of reactions described above are Fe-complexes derived from tetradentate ligands, which have labile counter-ions bound in a *cis* fashion. Fe-complexes derived from the ligands dimethyl-diaza-pyridinophane ($\text{L-N}_4\text{Me}_2$),^[49] tris(2-picolyl)amine (TPA),^[50] *N,N'*-dimethyl-*N,N'*-bis(2pyridylmethyl)-1,2-diaminoethane (BPMEN)^[50] and 2-picolyl-di-methyl-triazacyclononane (PyTACN) are known to catalyze the *cis*-dihydroxylation of alkenes (Scheme 5.4).^[51, 52]

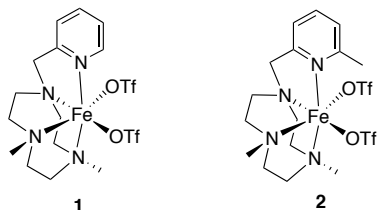


Scheme 5.4. Common ligands for Fe-mediated alkene *cis*-dihydroxylation.

While these catalysts have shown good activity with a variety of different alkenes, these systems have not been widely studied in the oxidation of the internal electron-rich aliphatic double bonds that are found in fatty acids. For example, the use of $[\text{Fe}(\text{L-N}_4\text{Me}_2)(\text{Cl})_2]$ with oxone was optimized primarily for electron-poor alkenes such as dimethyl fumarate (99% diol yield), with *cis*-diol yields of only 36% being obtained with the more electron-rich alkene *cis*-2-heptene.^[49] $[\text{Fe}(\text{OTf})_2(\text{TPA})]$ and $[\text{Fe}(\text{OTf})_2(\text{BPMEN})]$ do catalyze the *cis*-dihydroxylation of electron-rich olefins, e.g. *cis*-2-heptene and *cis*-cyclooctene, with H_2O_2 .^[50] However, epoxides are formed as byproducts particularly under substrate-limiting conditions and significant amounts of diol are only generated at oxidant limiting scale, i.e. in the presence of a large excess of substrate. While the use of $[\text{Fe}(\text{OTf})_2(\text{PyTACN})]$ (**1**) also resulted in a high diol/epoxide ratio under oxidant-limiting conditions,^[51, 52] the recently developed $[\text{Fe}(\text{OTf})_2(6\text{-Me-PyTACN})]$ (6-Me-PyTACN = 1-[(6-methyl-2-pyridyl)methyl]-4,7-dimethyl-1,4,7-triazacyclononane, **2**) showed good chemoselectivity for the formation of diols also under substrate-limiting conditions (Scheme 5.5).^[47] **1** is furthermore capable of converting diols to hydroxy ketones³⁹ and is

known to oxidize substrates with NaIO_4 ,^[47] making **1** and **2** good candidates for the oxidative cleavage of unsaturated fatty acids into carboxylic acids.

Here, the one-pot oxidative cleavage of methyl oleate and oleic acid into carboxylic acids was studied using $[\text{Fe}(\text{OTf})_2(6\text{-Me-PyTACN})]$ (**2**) and a combination of H_2O_2 and NaIO_4 . The reaction sequence involves the *cis*-dihydroxylation of methyl oleate by **2** (also investigated with **1**) and subsequent addition of NaIO_4 to induce over-oxidation to the acids (Scheme 5.3). The investigations reveal that **2** is a suitable catalyst for the oxidative cleavage of fatty acids and fatty acid esters into carboxylic acids.



Scheme 5.5. Fe-catalysts **1** and **2** investigated in this chapter.

5.2 Results and discussion

5.2.1 X-ray crystal structure of **2**

Complexes **1** and **2** were synthesized according to a previously published procedure.^[51] Complex **2** was further characterized by X-ray crystal structure determination (Figure 5.1). Yellow crystals of **2** were obtained by slow vapor diffusion of diethyl ether into a solution of **2** in CH_2Cl_2 . The crystal structure of **1** has been reported before.^[53]

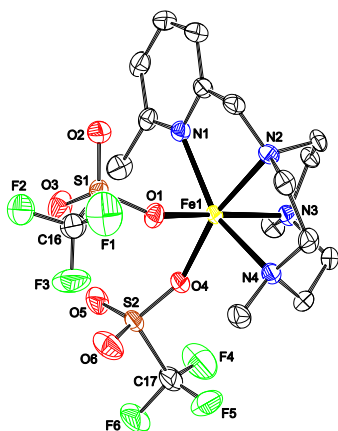


Figure 5.1. Molecular structure of **2** in the crystal (50% probability level). Hydrogen atoms are omitted for clarity.

The molecular structure of **2** shows a six-coordinate iron center with two triflate ions bound to iron in a *cis*-fashion and the 6-Me-PyTACN ligand coordinated through all four nitrogen donors (Figure 5.1). From the overlay plot of the molecular structures of **1** and **2**,

it is evident that the ligands bind to iron in a very similar fashion (Figure 5.2). Small differences are seen for the orientation of the pyridine group, while more significant differences are observed for the orientation of the triflate ligands in the crystal structures, which are exchangeable sites in MeCN solution. In terms of bond distances, the Fe-N (pyridine) distance is 2.165(4) Å in **1** and 2.246(2) in **2**. The Fe-N_{amine} distances are between 2.205(4) and 2.252(4) Å in **1**, and between 2.199(2) and 2.238(2) Å in **2**. Overall, these long distances are indicative of high-spin ferrous centers.^[54, 55] The O-Fe-O angle of 94.90(7)° in **2** is slightly larger than in **1** (91.64(14)°), which might be a consequence of the larger steric demand of the ligand in **2**. Overall, the angular variance in the Fe octahedron (the deviation from perfect octahedral angles) is larger in **2** than in **1** (99.01 deg² vs. 71.07 deg²).^[56] A detailed comparison between **1** and **2** is given in Table 5.1.

Table 5.1. Selected bond lengths [Å] and angles [°] for **1**^[53] and **2**.

Distance (Å)/Angle (°)	(1)	(2)
Fe-O1	2.165(3)	2.1354(17)
Fe-O4	2.055(3)	2.0746(16)
Fe-N1	2.165(4)	2.246(2)
Fe-N2	2.205(4)	2.199(2)
Fe-N3	2.252(4)	2.231(2)
Fe-N4	2.231(4)	2.238(2)
N1-Fe-O1	96.28(13)	89.05(7)
N2-Fe-O1	94.70(14)	93.14(8)
O1-Fe-O4	91.64(14)	94.90(7)

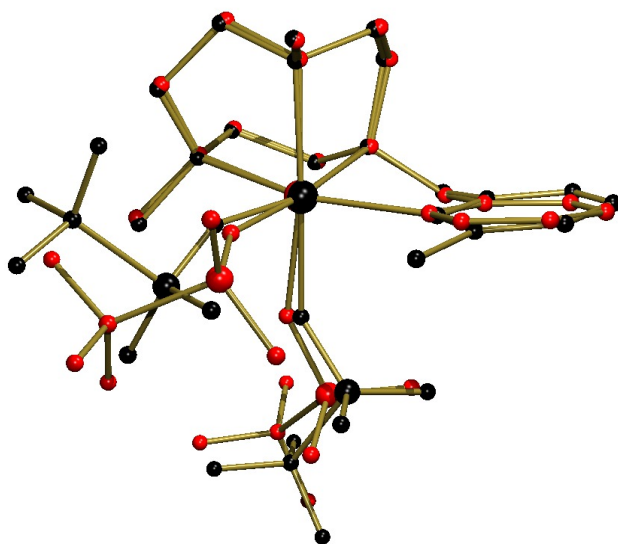


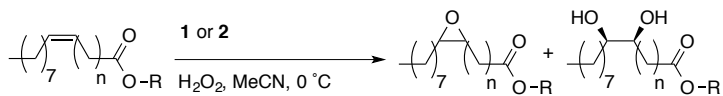
Figure 5.2. Quaternion fit of the molecular structures of **1** (red)^[53] and **2** (black). The fit is based on the metal and its six coordinating atoms.^[57] The hydrogen atoms are omitted for clarity.

5.2.2 *Cis*-dihydroxylation of unsaturated fatty acids

In previous studies, it was shown that for optimal performance of complexes **1** and **2** in the *cis*-dihydroxylation of aliphatic alkenes, a carefully controlled amount of water needs to be added in order to maximize the formation of the proposed, active $[\text{Fe}(\text{O})(\text{OH})(\text{L})]^{2+}$ (L = ligand) oxidant and to facilitate product release from the final ferric hydroglycolate resting state.^[52] A common issue with unsaturated fatty acids and esters is their solubility, which can be of crucial importance, and therefore different conditions than with aliphatic alkenes might be required.^[46] Initially, erucic acid methyl ester was applied as substrate under similar conditions as reported by Prat *et al.* for the *cis*-dihydroxylation of aliphatic alkenes,^[47] i.e. a 3 mol% catalyst loading with 2 equiv. H_2O_2 in MeCN. The only difference is that no H_2O was added because of potential solubility issues with this fatty substrate. As a result, reactions with **1** and **2** almost completely converted the substrate within 15 minutes, yet only the latter rendered a reasonable yield of the diol (48% compared to 12%; Table 5.2, entries 1-2). Likewise, reactions with **2** also yielded a five-fold higher diol/epoxide ratio. Despite the rather small structural differences, the selectivity towards *cis*-dihydroxylation of unsaturated fatty acid esters appears to greatly differ from **1** to **2** in favor of the second. Also, the selectivity difference between the complexes is significantly larger than what was previously observed for aliphatic alkenes.^[47] Therefore, in subsequent reactions only complex **2** was used. Regarding the addition of water, the addition of 15 equiv. H_2O was found not to be beneficial for the oxidation of erucic acid methyl ester, as both conversion and diol yield strongly decreased in contrast to earlier reactions with aliphatic alkenes (entries 3-4).^[47] Nevertheless, as previously documented,^[47] these reactions do induce a higher diol/epoxide ratio.

Next, reactions with methyl oleate were investigated, which is a shorter chain fatty substrate than erucic acid methyl ester. Using a similar protocol, reactions without additional water resulted in 98% methyl oleate conversion and 56% diol yield, values that are both higher than those obtained with erucic acid methyl ester (entry 6). Again, the addition of water decreased the conversion and diol yield, and increased the diol/epoxide ratio. Yet, these differences are less pronounced than with erucic acid methyl ester (entry 7). Optimization attempts other than omitting water failed to further improve the diol yield: neither reactions at $-20\text{ }^\circ\text{C}$ nor experiments with simultaneous addition of H_2O_2 and catalyst (over 12 h) showed a significant improvement (entries 8-9). Over-oxidation of the *cis*-diol into hydroxy ketones is known to occur under the applied conditions^[47] and these byproducts were indeed observed in these reactions and account for 2-6% of the converted substrate.

Table 5.2. *Cis*-dihydroxylation of unsaturated fatty acids and esters with **1** or **2** and H₂O₂^a, forming epoxides as byproduct.



Entry	n	R	Cat	mol %	H ₂ O ₂ (equiv.)	H ₂ O (equiv.)	Conv. (%) ^b	Epoxide yield (%)	Diol yield(%)
1	11	Me	1	3	2	0	89	50	12
2	11	Me	2	3	2	0	96	41 ^c	48 ^c
3	11	Me	2	3	2	15	54	18	29
4 ^d	11	Me	2	2×3	2×1.2	15	63	21	38
5	7	Me	2	3	1	0	68	12	24
6	7	Me	2	3	2	0	98	32	56
7	7	Me	2	3	2	15	80	18	42
8 ^e	7	Me	2	3	2	0	57	14	23
9 ^f	7	Me	2	3	2	0	100	38	50
10	7	H	2	3	2	0	7 ^c	7 ^c	0
11	7	H	2	3	2	15	7 ^c	7 ^c	0

^a Reaction conditions: Alkene in MeCN, H₂O₂ added over 15 minutes, 0 °C, yields determined by GC; ^b Hydroxy ketones detected as byproducts; ^c Determined by NMR; ^d More catalyst and H₂O₂ added after 15 minutes, H₂O₂ added over 15 minutes; ^e Reaction at -20 °C; ^f Catalyst and H₂O₂ added over 12 h.

In contrast to the methyl esters, the oxidation of oleic acid proceeded only to a very limited extent under the standard conditions, with only 7% of epoxide and no diol being obtained regardless of whether H₂O was added or not (entries 10-11). In this respect, it should be noted that the addition of an acid additive such as acetic acid or other aliphatic acids is known to facilitate the formation of the epoxide at the expense of the diol.^[47, 58] Similar effects are therefore anticipated with the use of oleic acid as the substrate. However, the low conversions imply that substrate inhibition may occur or that solubility issues are at stake. The *cis*-dihydroxylation step of this method thus requires unsaturated fatty acid esters and can be achieved in good yields with **2**.

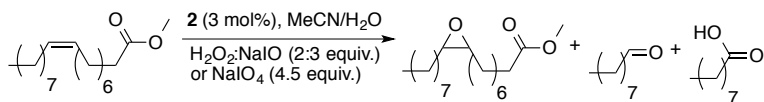
5.2.3 Oxidative cleavage of methyl oleate

Subsequent investigations were aimed at the one-pot cleavage of methyl oleate to carboxylic acids, based on the dihydroxylation activity of **2**. Accordingly, the *cis*-diol was formed using H₂O₂ in the optimized protocol for the methyl oleate *cis*-dihydroxylation (Table 5.2, entry 6), followed by the addition of NaIO₄ to the same reaction mixture in order to induce over-oxidation. After completion of the dihydroxylation (3 mol% **2**, 2 equiv. H₂O₂, 0 °C, 15 minutes), 3 equiv. of NaIO₄ were added at ambient temperature, followed by 150 equiv. of H₂O to dissolve the periodate (yielding a 3:1 (v/v) MeCN:H₂O mixture).^[35, 46] In this way, full substrate conversion and 55% of nonanoic acid yield were obtained after 36 h of reaction (Table 5.3, entry 1, method A). The formation of the corresponding difunctionalized product, monomethyl azelate, is presumed to be equal to the formation of the monoacid,^[35, 46] as the mono- and difunctionalized aldehydes were observed in equal amounts as minor byproducts (10%). The major byproduct observed in this reaction was the epoxide with a 28% yield, which was similar the amount of epoxide product observed in the separate *cis*-dihydroxylation reaction.

Alterations of this protocol involving shorter reaction times, additional amounts of water, and higher reaction temperatures all rendered a lower carboxylic acid yield. As expected, the exclusive use of H₂O₂ (5 or 10 equiv.) in this two-step procedure resulted in low selectivity to the aldehydes (10-12% at 100% conversion) and no carboxylic acids were formed. The yields of methyl 9-oxononanoate were nearly identical to nonanal, indicative that the difunctionalized products form in equal yield as the monofunctionalized ones. In fact, a variety of oxidation products were obtained (data not shown). On the other hand, the exclusive use of NaIO₄ (4.5 equiv.) did yield 50% of nonanoic acid and 33% of epoxide at full conversion in a reaction that was completely carried out at ambient temperatures for 48 h (entry 2). In this case, shorter reaction times gave lower acid yields, which is consistent with the observation that the oxidation steps involving **2** and NaIO₄ are much slower than the *cis*-dihydroxylation with H₂O₂.^[47, 59]

The similar epoxide yields in the dihydroxylation and the cleavage reaction with methyl oleate indicate that the epoxides are inert under the conditions of the cleavage reaction. Notably, the addition of only 1 equiv. of NaIO₄ did not result in selective formation of the aldehyde, but in a mixture of hydroxy ketones and aldehydes. This observation suggests a competition between the direct oxidation of diols by NaIO₄ into aldehydes and the catalyzed oxidation of diols by **2** and NaIO₄ into hydroxy ketones (see Scheme 5.3). Moreover, NaIO₄ does not mediate the oxidation of aldehydes into carboxylic acids by itself,^[35, 46] this reaction is therefore catalyzed by **2**. Accordingly, the catalytic oxidation of *cis*-diols into carboxylic acids with NaIO₄ is proposed to proceed via either hydroxy ketone or aldehyde intermediates.

Table 5.3. Oxidative cleavage of methyl oleate with **2** and H₂O₂/NaIO₄ into aldehydes and acids, forming epoxides as byproduct (method A).^a



Entry	H ₂ O ₂ (equiv.)	NaIO ₄ (equiv.)	Time (h)	Conv. (%) ^b	Epoxide yield (%)	Nonanal yield (%)	Nonanoic acid yield (%)
1	2	3	36	100	28	10 ^c	55
2	0	4.5	48	100	33	8 ^d	50

^a Reaction conditions: Method A: methyl oleate and 3 mol% **2** in MeCN, i) H₂O₂ in MeCN added over 15 min. at 0 °C, 150 equiv. H₂O and 3 equiv. of NaIO₄ added and ambient temperature, 36 h or ii) 4.5 equiv. NaIO₄ and 150 equiv. H₂O added at start, ambient temperature, 48 h; ^b Minor hydroxy ketone byproducts; ^c 10% methyl 9-oxononanoate detected; ^d 7% methyl 9-oxononanoate detected.

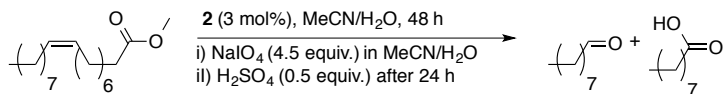
5.2.4 Oxidative cleavage in the presence of H₂SO₄

The significant amount of epoxides formed in the one-pot oxidative cleavage protocol of methyl oleate (method A) prompted us to investigate the addition of H₂SO₄ to the reaction mixture in order to hydrolyze these byproducts towards *trans*-diols (Scheme 5.2).^[35] The formed diols could in turn be further oxidized to carboxylic acids (Scheme 5.3), which would add up to the total amount of cleavage product and thus lead to a higher selectivity of the overall oxidative cleavage reaction.

The oxidative cleavage of methyl oleate in the presence of H₂SO₄ was conducted using a protocol in which the acid was added after both oxidants had been added. Addition of the acid at an earlier stage of the reaction led to lower substrate conversions (not shown). In a similar protocol as the one-pot cleavage using 4.5 equiv. NaIO₄ and 100 equiv. H₂O (see Table 5.3, entry 2), the addition of H₂SO₄ (0.5 equiv.) in H₂O (50 equiv.) after 24 h resulted in complete substrate conversion and the formation of 50% of aldehydes and 42% of carboxylic acids (Table 5.4, entry 1, method B). With this protocol no epoxides were detected. A decrease of the catalyst loading from 3 to 1 mol% in this reaction resulted in incomplete conversion (73%), yet showed 60% of aldehyde formation (entry 2). Methyl 9-oxononanoate was formed in similar yield as nonanal.

Nevertheless, the aldehyde yields obtained from methyl oleate with method B are lower than those previously observed in Chapter 3 with the Fe-BPBP-based protocol,^[35] and the carboxylic acid yields are lower than in the protocol without H₂SO₄ (method A, Table 3). In order to arrive at improved carboxylic acid yields, it was considered to add a mild base in the last stage of the protocol. While it is postulated that **2** catalyzes the oxidation of aldehydes into carboxylic acids, the high aldehyde yields in the protocol using H₂SO₄ indicate a deactivation of the catalyst, likely due to the acidic pH of the reaction medium.

Table 5.4. Oxidative cleavage of methyl oleate with H₂SO₄ into aldehydes and carboxylic acids (method B).^a

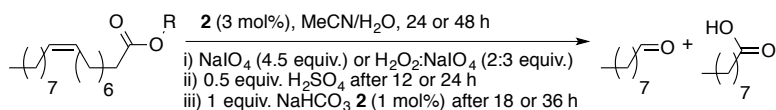


Entry	2 (%)	Conversion (%) ^b	Nonanal yield (%)	Nonanoic acid yield (%)
1	3	100	50 ^c	42
2	1	73	60 ^d	2

^a Reaction conditions: Method B: methyl oleate in MeCN, 4.5 equiv. NaIO₄, 100 equiv. H₂O, 24 h, then 0.5 equiv. H₂SO₄ in 50 equiv. H₂O; ^b Hydroxy ketones as minor byproducts; ^c 44% methyl 9-oxononanoate detected; ^d 55% methyl 9-oxononanoate detected.

Therefore, in a similar protocol as in Table 5.4, entry 1 (3 mol% **2**, 4.5 equiv. NaIO₄, 48 h total reaction time, H₂SO₄ after 24 h), NaHCO₃ was added after 36 h to neutralize the reaction medium and an additional amount of **2** (1 mol%) was added to drive the oxidation of the remaining aldehydes into carboxylic acids (method C). Indeed, high carboxylic acid yields (82%) were observed in this way at full conversion of methyl oleate (Table 5.5, entry 1). This protocol was also successfully applied to oleic acid: in this case full conversion and 85% formation of nonanoic acid was observed (entry 2). As discussed above for method A, H₂O₂:NaIO₄ (2:3 equiv.) can be applied instead of NaIO₄, resulting in full methyl oleate conversion into 80% carboxylic acid and 16% nonanal (15% methyl 9-oxononanoate) after only 24 h.

Table 5.5. Oxidative cleavage of methyl oleate and oleic acid with **2** and H₂O₂/NaIO₄ towards carboxylic acids with the aid of H₂SO₄ (method C).^a



Entry	R	H ₂ O ₂ (equiv.)	NaIO ₄ (equiv.)	Time (h)	Conversion (%) ^b	Nonanal (%)	Nonanoic acid (%)
1	Me	0	4.5	48	100	9 ^c	82
2	H	0	4.5	48	100	5	85
3	Me	2	3	24	100	16 ^d	80

^a Reaction conditions: Method C: substrate in MeCN, 3 mol% **2**, i) 4.5 equiv. NaIO₄, 100 equiv. H₂O, 24 h, then H₂SO₄ (0.5 equiv.) in H₂O (50 equiv.), 12 h, and NaHCO₃ (1 equiv.) and **2** (1 mol%) or ii) 2 equiv. H₂O₂ added over 15 minutes at 0 °C, then 3 equiv. of NaIO₄ in 100 equiv. H₂O added at ambient temperature, 12 h, H₂SO₄ (0.5 equiv.) in H₂O (50 equiv.), 6 h, then NaHCO₃ (1 equiv.) and **2** (1 mol%), 6 h; ^b Hydroxy ketones as minor byproducts; ^c 6% methyl 9-oxononanoate detected; ^d 15% methyl 9-oxononanoate detected.

5.3 Conclusions

The first Fe-based catalytic system for the oxidative cleavage of unsaturated fatty acids and their esters into carboxylic acids was developed. The system is based on $[\text{Fe}(\text{OTf})_2(6\text{-Me-PyTACN})]$ (**2**) as catalyst, which showed a superior performance compared to the non-methyl substituted $[\text{Fe}(\text{OTf})_2(\text{PyTACN})]$ (**1**). **2** can be used in a number of different one-pot procedures that each uses a different combination of oxidants and additives, and each provide a different substrate conversion and product distribution.

Method A uses H_2O_2 (2 equiv., 0 °C) to *cis*-dihydroxylate methyl oleate (56%), after which the addition of NaIO_4 (3 equiv.) at ambient reaction temperature induces the subsequent over-oxidation steps towards the acids in good yields after 36 h (55%) with epoxides as byproducts. The exclusive use of NaIO_4 (4.5 equiv.) in this method for 48 h under ambient conditions allows one to obtain similar acid yields (50%). In method B, the addition of H_2SO_4 at intermediate reaction stages hydrolyzes the epoxide byproducts and eventually forms a mixture of aldehydes and carboxylic acids. Finally, method C includes the additional insertion of NaHCO_3 for pH neutralization, followed by the addition of a small additional amount of catalyst to render almost exclusively carboxylic acids from both methyl oleate and oleic acid in high yields (80-85%), which can again be achieved with a combination of $\text{H}_2\text{O}_2/\text{NaIO}_4$ or exclusively NaIO_4 .

These methods using the new catalyst system involve one-pot procedures with low catalyst loadings (3-4 mol%), almost stoichiometric use of oxidants (4.5-5 equiv.), and convenient reaction temperatures (0-25 °C). The high selectivity to the carboxylic acid products found with method C is complementary to the protocol of Chapter 3 (based on Fe-BPBP systems), which is selective to the formation of the corresponding aldehydes rather than the carboxylic acids.^[35] Furthermore, these methods improve on the oxone/ NaIO_4 -based method^[46] of Chapter 2 in the sense that ambient temperatures can be applied and significantly less waste is generated.

Overall, it is believed that the new catalytic system is of general synthetic interest. More specially, it represents an effective system for the production of medium length aliphatic aldehydes and carboxylic acids, as well as medium length α,ω -diacids and aldehydes acids from unsaturated fatty acids and esters. The system may accordingly find application in general organic syntheses as well as in the valorization of plant oils for the production of a number of interesting fine chemicals.

5.4 Experimental section

5.4.1 General

Sodium periodate (99%), hydrogen peroxide (35% in water), *trans*-4-octene (90%) and methyl oleate (99%) were purchased from Aldrich. Oleic acid (99%) was obtained from Fluka. *Cis*-4-octene (97%) was purchased from Alfa Aesar. Erucic acid methyl ester (90%) was purchased from ABCR. All chemicals were used as received. The reactions were conducted under ambient conditions, using distilled water, pro analysis MeCN, and technical grade ethyl acetate. ¹H NMR and ¹³C NMR measurements were recorded in CDCl₃ at 298 K on a Varian 400 MHz NMR Spectrometer, using residual solvent peaks as reference. Gas chromatography was carried out on an Agilent 7820A gas chromatograph (HP5 column, 30 m) and a flame ionization detector. The syntheses of [Fe(OTf)₂(PyTACN)] (**1**) and [Fe(OTf)₂(6-Me-PyTACN)] (**2**) were performed according to literature procedures.^[47]

5.4.2 X-ray crystal structure determination of [Fe(OTf)₂(6-Me-PyTACN)] (**2**)

C₁₇H₂₆F₆FeN₄O₄S₂, Fw = 616.39, pale yellow needle, 0.38 × 0.11 × 0.05 mm³, orthorhombic, P2₁2₁2₁ (no. 19), a = 8.9413(6), b = 15.7005(10), c = 17.7436(11) Å, V = 2490.9(3) Å³, Z = 4, D_x = 1.644 g/cm³, μ = 0.86 mm⁻¹. 16042 Reflections were measured on a Bruker Kappa ApexII diffractometer with sealed tube and Triumph monochromator (λ = 0.71073 Å) at a temperature of 150(2) K up to a resolution of (sin θ/λ)_{max} = 0.60 Å⁻¹. Intensity data were integrated with the Saint software.^[60] The absorption correction and scaling was performed with SADABS^[61] (correction range 0.64-0.75). 4381 Reflections were unique (R_{int} = 0.019), of which 4105 were observed [I > 2σ(I)]. The structure was solved with the program SHELXT.^[62] The least-squares refinement was performed with SHELXL-97^[63] against F² of all reflections. Non-hydrogen atoms were refined freely with anisotropic displacement parameters. All hydrogen atoms were located in difference Fourier maps and refined with a riding model. 329 Parameters were refined with no restraints. R1/wR2 [I > 2σ(I)]: 0.0250 / 0.0559. R1/wR2 [all refl.]: 0.0290 / 0.0576. S = 1.096. Flack parameter^[64] x = 0.007(13). The residual electron density was between -0.30 and 0.53 e/Å³. Geometry calculations and checking for higher symmetry was performed with the PLATON program.^[65]

5.4.3 *Cis*-dihydroxylation of alkenes

Alkene substrate (0.09 mmol), **1** or **2** (2.7 μmol), H₂O (0-0.135 mmol) were dissolved in MeCN (1 mL) at 0 °C. Then, H₂O₂ in MeCN (67.5-180 mmol in 1.44 M) was added over 15 minutes. Biphenyl (22.5 μmol, internal standard) in MeCN (125 mL) and ethyl acetate (4 mL) were added, and the sample was filtered over a short silica column before being subjected to GC analysis.

5.4.4 Oxidative cleavage methyl oleate into epoxides and carboxylic acids (method A)

Alkene substrate (0.09 mmol), **2** (2.7 μmol), H₂O (0-1.35 mmol) were dissolved in MeCN (1 mL) at 0 °C. Then, H₂O₂ in MeCN (67.5-180 mmol in 1.44 M) was added over 15 minutes. NaIO₄ (27 mmol) and H₂O (13.5 mmol) were added at ambient temperature and stirred for 36 h. In case no H₂O₂ was used, NaIO₄

(405 mmol) was added under ambient conditions and stirred for 48 h. Subsequently, biphenyl (22.5 μmol , internal standard) in MeCN (125 mL) and ethyl acetate (4 mL) were added and the sample was subjected to GC analysis. The catalyst precipitated under these conditions and needed no separation from the mixture. In the analytic protocol, monomethyl azelate was observed as well, yet the quantification was not reproducible by GC monitoring. As the yields of nonanal and methyl 9-oxononanoate match, only the yields of nonanal, nonanoic acid and methyl 9-oxononanoate are given in Table 5.3.

5.4.5 Oxidative cleavage methyl oleate into aldehydes and carboxylic acids (method B)

Alkene substrate (0.09 mmol), **2** (2.7 μmol), sodium periodate (0.45 mmol) and H_2O (75 equiv.) were stirred in MeCN (1 mL) for 24 h. Then, H_2SO_4 (0.5 equiv.) in H_2O (75 equiv.) was added and stirred for additional 24 h. Subsequently, biphenyl (22.5 μmol , internal standard) in MeCN (125 mL) and ethyl acetate (4 mL) were added and the sample was subjected to GC analysis. The catalyst precipitated under these conditions and needed no separation from the mixture. In the analytic protocol, monomethyl azelate was observed as well, yet the quantification was not reproducible by GC monitoring. As the yields of nonanal and methyl 9-oxononanoate match, only the yields of nonanal, nonanoic acid and methyl 9-oxononanoate are given in Table 5.4.

5.4.6 Oxidative cleavage methyl oleate into carboxylic acids (method C)

Alkene substrate (0.09 mmol), **2** (2.7 μmol), sodium periodate (0.45 mmol) and H_2O (100 equiv.) were stirred in MeCN (1 mL) for 24 h. Then, H_2SO_4 (0.045 mmol) in H_2O (75 equiv.) was added and stirred for additional 12 h. Subsequently, NaHCO_3 (0.09 mmol) and **2** were added (0.9 μmol) and stirred for additional 12 h. Biphenyl (22.5 μmol , internal standard) in MeCN (125 mL) and ethyl acetate (4 mL) were added and the sample was subjected to GC analysis. The catalyst precipitated under these conditions and needed no separation from the mixture. In the analytic protocol, monomethyl azelate was observed as well, yet the quantification was not reproducible by GC monitoring. As the yields of nonanal and methyl 9-oxononanoate match, only the yields of nonanal, nonanoic acid and methyl 9-oxononanoate are given in Table 5.5. In reactions performed with H_2O_2 , the same conditions as for *cis*-dihydroxylations are applied at start. After 15 minutes of reaction, NaIO_4 (27 mmol) and H_2O (100 equiv.) are added and stirred for 12 h. In a similar fashion as for reactions with 4.5 equiv. NaIO_4 , H_2SO_4 was added, stirred for 6 h, and NaHCO_3 and NaIO_4 were added and reacted for additional 6 h.

5.5 Acknowledgement

COST action CM1003 is acknowledged for providing funding for a research stay in the group of prof. M. Costas at the University of Girona.

5.6 References

- [1] A. Corma, S. Iborra, A. Vely *Chem. Rev.* **2007**, *107*, 2411.
- [2] A. Köckritz, A. Martin *Eur. J. Lipid Sci. Technol.* **2008**, *110*, 812.
- [3] H. Baumann, M. Bühler, H. Fochem, F. Hirsinger, H. Zobebelein, J. Falbe *Angew. Chem. Int. Ed.* **1988**, *27*, 41.
- [4] U. Biermann, U. Bornscheuer, M. A. R. Meier, J. O. Metzger, H. J. Schäfer *Angew. Chem. Int. Ed.* **2011**, *50*, 3854.
- [5] U. Biermann, W. Friedt, S. Lang, W. Lühs, G. Machmüller, J. O. Metzger, M. Rüschen, Klaas, H. J. Schäfer, M. P. Schneider *Angew. Chem. Int. Ed.* **2000**, *39*, 2206.
- [6] H. J. Carlsen, T. Katsuki, V. S. Martin, K. B. Sharpless *J. Org. Chem.* **1981**, *46*, 3936.
- [7] S. Torii, T. Inokuchi, K. Kondo *J. Org. Chem.* **1985**, *50*, 4980.
- [8] A. Behr, N. Tenhumberg, A. Wintzer *RSC Adv.* **2013**, *3*, 172.
- [9] D. Yang, C. Zhang *J. Org. Chem.* **2001**, *66*, 4814.
- [10] V. Piccialli, D. M. A. Smaldone, D. Sica *Tetrahedron* **1993**, *49*, 4211.
- [11] L. Albarella, F. Giordano, M. Lasalvia, V. Piccialli, D. Sica *Tetrahedron Lett.* **1995**, *36*, 5267.
- [12] S. E. Turnwald, M. A. Lorier, L. J. Wright, M. R. Mucalo *J. Mat. Sci. Lett.* **1998**, *17*, 1305.
- [13] Z. P. Pai, A. G. Tolstikov, P. V. Berdnikova, G. N. Kustova, T. B. Khlebnikova, N. V. Selivanova, A. B. Shangina, V. G. Kostrovskii *Russ. Chem. Bull, Int. Ed.* **2005**, *54*, 1847.
- [14] E. Antonelli, R. D'Aloisio, M. Gambaro, T. Fiorani, C. Venturello *J. Org. Chem.* **1998**, *63*, 7190.
- [15] Y. Ishii, K. Yamawaki, T. Ura, H. Yamada, T. Yoshida, M. Ogawa *J. Org. Chem.* **1988**, *53*, 3587.
- [16] T. Oguchi, T. Ura, Y. Ishii, M. Ogawa *Chem. Lett.* **1989**, *18*, 857.
- [17] R. Noyori, M. Aoki, K. Sato *Chem. Commun.* **2003**, 1977.
- [18] J. Freitag, M. Nuchter, B. Ondruschka *Green Chem.* **2003**, *5*, 291.
- [19] A. Haimov, H. Cohen, R. Neumann *J. Am. Chem. Soc.* **2004**, *126*, 11762.
- [20] J. R. Henry, S. M. Weinreb *J. Org. Chem.* **1993**, *58*, 4745.
- [21] C. Francavilla, W. Chen, F. R. Kinder Jr. *Org. Lett.* **2003**, *5*, 1233.
- [22] R. E. Taylor, Y. Chen, A. Beatty, D. C. Myles, Y. Zhou *J. Am. Chem. Soc.* **2003**, *125*, 26.
- [23] Z. Wang, M. G. Moloney *Tetrahedron Lett.* **2002**, *43*, 9629.
- [24] B. R. Travis, R. S. Narayan, B. Borhan *J. Am. Chem. Soc.* **2002**, *124*, 3824.
- [25] D. C. Whitehead, B. R. Travis, B. Borhan *Tetrahedron Lett.* **2006**, *47*, 3797.
- [26] S. R. Hart, D. C. Whitehead, B. R. Travis, B. Borhan *Org. Biomol. Chem.* **2011**, *9*, 4741.
- [27] W. Yu, Y. Mei, Y. Kang, Z. Hua, Z. Jin *Org. Lett.* **2004**, *6*, 3217.
- [28] A. Dhakshinamoorthy, K. Pitchumani *Tetrahedron* **2006**, *62*, 9911.
- [29] P. A. Ganeshpure, S. Satish *Tetrahedron Lett.* **1988**, *29*, 6629.
- [30] Y. F. Li, C. C. Guo, X. H. Yan, Q. Liu *J. Porphyrins Phtalocyanines* **2006**, *10*, 942.
- [31] H. Chen, H. Ji, X. Zhou, J. Xu, L. Wang *Catal. Commun.* **2009**, *10*, 828.
- [32] S. T. Liu, K. V. Reddy, R. Y. Lai *Tetrahedron* **2007**, *63*, 1821.
- [33] C. M. Ho, W. Y. Yu, C. M. Che *Angew. Chem. Int. Ed.* **2004**, *43*, 3303.
- [34] Ozonolysis on industrial scale is performed by Novasep
- [35] P. Spannring, V. Yazerski, P. C. A. Bruijninx, B. M. Weckhuysen, R. J. M. Klein Gebbink *Chem. Eur. J.* **2013**, *19*, 15012 (Chapter 3 of this thesis).
- [36] Y. Nakano, T. A. Foglia *J. Am. Oil Chem. Soc.* **1982**, *59*, 163.
- [37] F. Zimmermann, E. Meux, J. L. Mieloszynski, J. M. Lecuire, N. Oget *Tetrahedron Lett.* **2005**, *46*, 3201.

- [38] S. Rup, F. Zimmermann, E. Meux, M. Schneider, M. Sindt, N. Oget *Ultrason. Sonochem.* **2009**, *16*, 266.
- [39] S. Rup, M. Sindt, N. Oget *Tetrahedron Lett.* **2010**, *51*, 3123.
- [40] H. Nouredini, M. Kanabur *J. Am. Oil Chem. Soc.* **1999**, *76*, 305.
- [41] M. A. Oakley, S. Woodward, K. Coupland, D. Parker, C. Temple-Heald *J. Mol. Catal. A: Chem.* **1999**, *150*, 105.
- [42] A. T. Herrmann, S. Warwel, M. Rüschen, Klaas, **1997**.
- [43] E. Santacesaria, A. Sorrentino, F. Rainone, M. Di Serio, F. Speranza *Ind. Eng. Chem. Res.* **2000**, *39*, 2766.
- [44] E. Santacesaria, M. Ambrosio, A. Sorrentino, R. Tesser, M. Di Serio *Catal. Tod.* **2003**, *79-80*, 59.
- [45] T. B. Khlebnikova, Z. P. Pai, L. A. Fedoseeva, Y. V. Matsat *React. Kinet. Catal. Lett.* **2009**, *98*, 17.
- [46] P. Spanring, P. C. A. Bruijninx, B. M. Weckhuysen, R. J. M. Klein Gebbink *RSC Adv.* **2013**, *3*, 6606 (Chapter 2 of this thesis).
- [47] I. Prat, D. Font, A. Company, K. Junge, X. Ribas, M. Beller, M. Costas *Adv. Synth. Catal.* **2013**, *355*, 947.
- [48] U. S. Bäumer, H. J. Schäfer *Electroch. Acta* **2003**, 489.
- [49] T. W. S. Chow, E. L. M. Wong, Z. Guo, Y. Liu, J. S. Huang, C. M. Che *J. Am. Chem. Soc.* **2010**, *132*, 13229.
- [50] A. Company, Y. Feng, M. Güell, X. Ribas, J. M. Luis, L. Que Jr., M. Costas *Chem. Eur. J.* **2009**, *15*, 3359.
- [51] A. Company, L. Gómez, X. Fontrodona, X. Ribas, M. Costas *Chem. Eur. J.* **2008**, *14*, 5727.
- [52] I. Prat, J. S. Mathieson, M. Güell, X. Ribas, J. M. Luis, L. Cronin, M. Costas *Nat. Chem* **2011**, *3*, 788.
- [53] A. Company, L. Gaez, M. Güell, X. Ribas, J. M. Luis, L. Que Jr., M. Costas *J. Am. Chem. Soc.* **2007**, *129*, 15766.
- [54] A. Bousseksou, G. Molnar, L. Salmon, W. Nicolazzi *Chem. Soc. Rev.* **2011**, *40*, 3313.
- [55] K. Chen, M. Costas, J. Kim, A. K. Tipton, L. Que Jr. *J. Am. Chem. Soc.* **2002**, *124*, 3026.
- [56] K. Robinson, G. V. Gibbs, P. H. Ribbe *Science* **1971**, *172*, 567.
- [57] A. L. Mackay *Acta Crystallograph. Sect. A* **1984**, *40*, 165.
- [58] O. Y. Lyakin, R. V. Ottenbacher, K. P. Bryliakov, E. P. Talsi *ACS Catal.* **2012**, *2*, 1196.
- [59] J. L. Filloi, Z. Codola, I. Garcia-Bosch, L. Gomez, J. J. Pla, M. Costas *Nat. Chem.* **2011**, *3*, 807.
- [60] Bruker, *2001, SAINT-Plus*. Bruker AXS Inc., Madison, Wisconsin, USA.
- [61] G. M. Sheldrick, **SADABS**: Area-Detector Absorption Correction, Universität Göttingen, Germany.
- [62] G. M. Sheldrick, **SHELXT**, Universität Göttingen, Germany.
- [63] G. M. Sheldrick *Acta Crystallograph. Sect. A* **2008**, *64*, 112.
- [64] H. D. Flack *Acta Crystallograph. Sect. A* **1983**, *39*, 876.
- [65] A. L. Spek *Acta Crystallograph. Sect. D* **2009**, *65*, 148.

Design of non-heme iron catalysts for alkene oxidations

Chapter 6

Synthesis, characterization and catalytic properties of non-heme [Fe(OTf)₂(bapbpy)] and [Fe(OTf)₂(*o,p*-di-Me-bapbpy)]

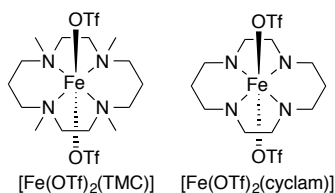
Abstract

From the neutral tetradentate ligands *N*⁶,*N*^{6'}-bis(pyridine-2-yl)-[2,2'-bipyridine]-6,6'-diamine (bapbpy) and *N*⁶,*N*^{6'}-bis(4,6-di-methyl-pyridine-2-yl)-[2,2'-bipyridine]-6,6'-diamine (*o,p*-di-Me-bapbpy), the neutral non-heme iron complexes [Fe(II)(OTf)₂(bapbpy)] (**1**) and [Fe(II)(OTf)₂(*o,p*-di-Me-bapbpy)] (**2**) were synthesized. **1** and **2** were fully characterized by single crystal X-ray diffraction and spectroscopic means. Both complexes adopt a temperature-independent high-spin state in the solid state and exhibit thermal spin crossover behavior in acetonitrile solution. DFT calculations revealed a low reaction barrier for propene epoxidation by a putative [Fe(IV)(bapbpy)(MeCN)(O)]²⁺ species of *S* = 1 and a negligible barrier for the *S* = 2 species, which suggests that this species could be a good epoxidation agent. The reaction of **1** with different peracids resulted in the rapid formation of Fe(III)-μ-oxo dimers. [Fe₂(μ-O)(OTf)₂(bapbpy)₂](OTf)₂ (**3**) was isolated and characterized by single crystal X-ray diffraction and spectroscopic means. Reactions with peracids at -40 °C allowed the detection of [Fe(IV)(O)(bapbpy)]²⁺ (**1b**) by ESI-MS in the same reaction mixture. Based on these observations, **1** is postulated to be oxidized after coordination of the oxidant in a heterolytic fashion to directly yield **1b**, which subsequently reacts with **1** to form **3**. Reactivity studies showed that **1** and **2** display some catalytic activity in *cis*-cyclooctene epoxidation with H₂O₂ under oxidant-limiting conditions at 50-70 °C. The system is one of few non-heme Fe-based systems with *trans*-vacant sites to perform *cis*-cyclooctene epoxidations.

Based on: Peter Spannring, Elier Hernando Martinez, Laura Gómez Martin, Miquel Costas, Apparao Draksharapu, Wesley R. Browne, Sipeng Zheng, Sylvestre Bonnet, Martin Lutz, Matthew G. Quesne, Sam P. de Visser, Pieter C. A. Bruijninx, Bert M. Weckhuysen and Robertus J. M. Klein Gebbink, manuscript in preparation

6.1 Introduction

Mononuclear non-heme iron centers are found in the active site of several enzymes that are able to activate dioxygen.^[1] Most of these enzymes are believed to operate through a mechanistic scheme that involves a high-valent iron-oxo species, which is postulated to be the active species for a series of oxidation reactions, e. g. C-H bond hydroxylation.^[2] The oxidative power of these intermediates has triggered the study of synthetic high-valent iron-oxo complexes using various ligands able to stabilize such Fe=O moieties. One of the first non-heme ligands that allowed the successful isolation of such species is the 1,4,8,11-tetramethyl-1,4,8,11-tetraazacyclotetradecane (TMC) ligand.^[3] The neutral, tetradentate N,N,N,N ligand TMC typically occupies four equatorial positions around iron to form octahedral iron complexes with two axial positions available for further chemistry, such as in $[\text{Fe}(\text{OTf})_2(\text{TMC})]$ (Scheme 6.1). Ligands bound in the axial position *trans* to the Fe-oxo moiety in $[\text{Fe}(\text{O})(\text{TMC})]^{2+}$ species are known to increase the overall stability of this transient species for characterization purposes or conversely decrease its stability for oxidation purposes.^[4, 5] Notably, the $[\text{Fe}(\text{OTf})_2(\text{TMC})]$ complex does not tend to form binuclear dimers, which are often regarded as a dead end in catalysis.^[2, 6] $[\text{Fe}(\text{OTf})_2(\text{TMC})]$ catalyzes the epoxidation of *cis*-cyclooctene under oxidant-limiting conditions with hydrogen peroxide.^[7] A number of TMC derivatives have been synthesized to include fifteen-membered macrocyclic ligands,^[8] a fifth, axial ligand^[9] or to enforce two *cis*-labile sites.^[7] The non-methylated analogue of TMC, $[\text{Fe}(\text{OTf})_2(\text{cyclam})]$ (cyclam = 1,4,8,11-tetraazacyclotetradecane) does not allow for the isolation of Fe=O reactive intermediates, it normally forms dimeric species upon oxidation and shows a higher catalytic strength than $[\text{Fe}(\text{OTf})_2(\text{TMC})]$; alkene epoxidations under substrate-limiting conditions can be performed with H_2O_2 as the oxidant.^[2, 10, 11]



Scheme 6.1. Structures of $[\text{Fe}(\text{OTf})_2(\text{TMC})]$ ^[3] and $[\text{Fe}(\text{OTf})_2(\text{cyclam})]$,^[10] which contain non-heme neutrally coordinating tetradentate ligands and *trans*-vacant sites.

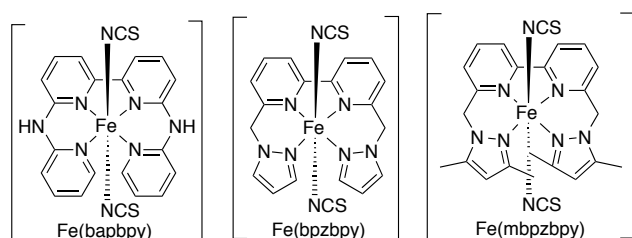
The non-heme complex $[\text{Fe}(\text{H}_2\text{O})(\text{TAML})]\text{Li}$ and its derivatives (TAML = tetraamido macrocyclic ligand, $[\text{C}_6\text{H}_4-1,2-(\text{NCOCMe}_2\text{NCO})_2\text{CMe}_2]$) also contain tetradentate, all-N ligands that bind to the metal in a square-planar fashion and enable the formation of high-valent Fe-oxo species.^[12, 13] Differences with $[\text{Fe}(\text{OTf})_2(\text{TMC})]$ or $[\text{Fe}(\text{OTf})_2(\text{cyclam})]$ are that the ligands are tetraanionic, that the metal center is electron-rich and that Fe-

Chapter 6

complexes generally adopt a pentadentate coordination, therefore lacking an axial donor upon formation of Fe-oxo species making the oxo group relatively basic. The complexes have not been reported to be suitable epoxidation catalysts, but are rather used for degradation of chlorophenols or carbohydrate alcohols with H_2O_2 ,^[14] showing resistance to oxidation as a result of careful ligand design. New non-heme Fe-based complexes with square-planar ligands intended for alkene epoxidations should therefore be more similar to complexes of Scheme 6.1. Most other neutral, tetradentate all-nitrogen ligands that have been reported to stabilize high-valent Fe-species result in coordination geometries around iron with the two labile sites oriented *cis* rather than *trans* to each other.^[2]

6.1.1 Bapbpy-type ligand complexes

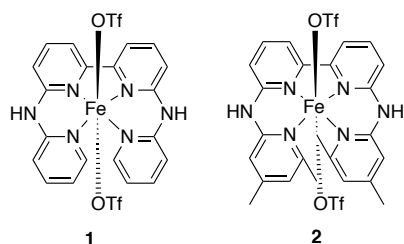
The tetradentate polypyridine ligand $N^6,N^{6'}$ -bis(pyridine-2-yl)-[2,2'-bipyridine]-6,6'-diamine (bapbpy) coordinates as a neutral ligand to a transition metal ion in a pseudo-square planar fashion, thus showing structural similarities to, for instance, the TMC or the cyclam ligand family. Complexation of metal ions to the bapbpy ligand manifold can lead to an overall penta-coordinated metal center as in $[\text{ZnCl}(\text{bapbpy})]\text{Cl}\cdot 2\text{H}_2\text{O}$ ^[15] or $[\text{Cu}(\text{H}_2\text{O})(\text{bapbpy})]\text{Cl}_2\cdot \text{H}_2\text{O}$,^[16] or to an overall hexa-coordinated metal environment as in $[\text{Fe}(\text{NCS})_2(\text{bapbpy})]$ (Scheme 6.2).^[17, 18] Structural variations on the latter complex, bearing methyl substituents on the ligand, have also been reported.^[19] These iron-thiocyanate complexes were initially studied for their spin crossover behavior (SCO),^[20-30] and are related to the $\text{Fe}(\text{NCS})_2$ -complexes derived from the bpzbp (bpzbp = 6,6'-bis(*N*-pyrazolylmethyl)-2,2'-bipyridine) and mbpzbpy ligands (mbpzbpy = 6,6'-bis-(3,5-dimethyl-*N*-pyrazolylmethyl)-2,2'-bipyridine),^[31] which adopt a similar coordination geometry and show similar SCO behavior (Scheme 6.2). More labile counter-ions were introduced in the two apical positions of these complexes by replacement of the thiocyanate anions for triflate anions to give the complexes $[\text{Fe}(\text{OTf})_2(\text{bpzbp})]$ and $[\text{Fe}(\text{OTf})_2(\text{mbpzbpy})]$.^[31]



Scheme 6.2. Structures of $[\text{Fe}(\text{NCS})_2(\text{bapbpy})]$,^[17] $[\text{Fe}(\text{NCS})_2(\text{bpzbp})]$ ^[31] and $[\text{Fe}(\text{NCS})_2(\text{mbpzbpy})]$.^[31]

Given the similarity of the bapbpy ligand to some of the ligands used for the generation of high-valent iron-oxo species and for the development of new iron-based oxidation

catalysts, the properties of bapbpy-derived iron complexes bearing labile counter-ions in oxidation chemistry were explored. In this chapter, the synthesis of $[\text{Fe}(\text{OTf})_2(\text{bapbpy})]$ (**1**) and $[\text{Fe}(\text{OTf})_2(o,p\text{-di-Me-bapbpy})]$ (**2**, *o,p*-di-Me-bapbpy = *N*⁶,*N*^{6'}-bis(4,6-di-methylpyridine-2-yl)-2,2'-bipyridine-6,6'-diamine) is reported (Scheme 6.3), as well as their full characterization by single crystal X-ray diffraction and by various spectroscopic techniques. Furthermore, the thermal spin crossover behavior of **1** and **2** were investigated in both the solid state and in MeCN solution. Finally, reactions with peracids were investigated at low temperature with the aim of detecting high-valent intermediates. Catalytic alkene epoxidations using these complexes have been assessed by computational and experimental means.



Scheme 6.3. Structure of $[\text{Fe}(\text{OTf})_2(\text{bapbpy})]$ (**1**) and $[\text{Fe}(\text{OTf})_2(o,p\text{-di-Me-bapbpy})]$ (**2**).

6.2 Results

6.2.1 Synthesis

The syntheses of $[\text{Fe}(\text{OTf})_2(\text{bapbpy})]$ (**1**) and $[\text{Fe}(\text{OTf})_2(o,p\text{-di-Me-bapbpy})]$ (**2**) complexes involved the reaction of equimolar amounts of bapbpy or *o,p*-di-Me-bapbpy with $[\text{Fe}(\text{OTf})_2(\text{MeCN})_2]$ in a minimal amount of THF under inert atmosphere for 16 h. The complexes were obtained by recrystallization of the crude product from a MeCN/diethyl ether mixture. The resulting yellow powders (85% for **1** and 89% for **2**) were analyzed by elemental analysis to confirm their purity.

6.2.2 Structural features

Single crystals of **1** and **2** suitable for X-ray diffraction studies were obtained by vapor diffusion of diethyl ether into a concentrated solution of the complexes in MeCN. In one of the attempts to crystallize **1** from a concentrated solution in MeCN at $-20\text{ }^\circ\text{C}$, after a week crystals of the acetonitrile adduct $[\text{Fe}(\text{MeCN})_2(\text{bapbpy})](\text{OTf})_2$ (**1**^{*}(MeCN)₂) were obtained. All complexes show the coordination of the bapbpy-type ligand to iron through all four of its pyridine residues and adopt a distorted octahedral geometries around the metal center (Figure 6.1). Complexes **1** and **2** contain triflate molecules in the axial positions, whereas MeCN ligands occupy the axial positions in **1**^{*}(MeCN)₂, with the

Chapter 6

triflates acting as non-coordinating counter-ions. The molecular structure of the latter complex showed C_2 symmetry, which was not observed for **1** and **2**.

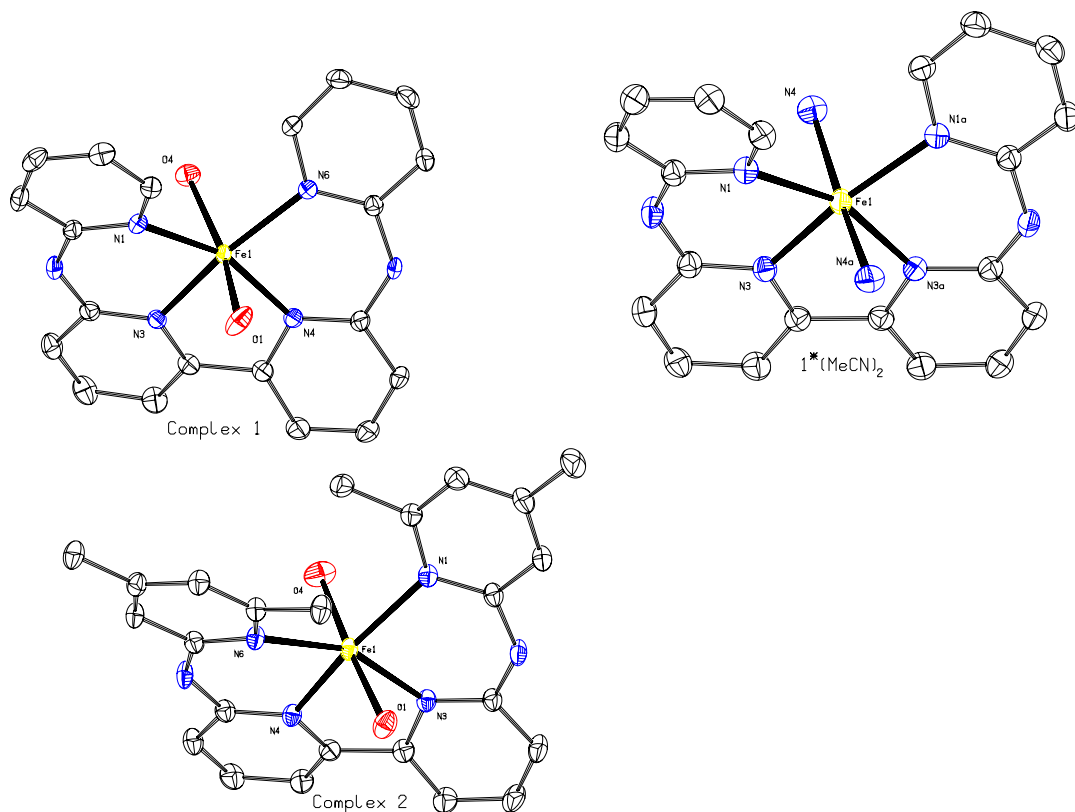


Figure 6.1. ORTEP plots at 50% probability of **1**, **1*(MeCN)₂** and **2**. Hydrogen atoms and non-coordinating anions are omitted for clarity, and only the axially coordinating O and N atoms are shown of the coordinating triflate ions and MeCN molecules, respectively.

The Fe-N_{pyridine} distances in these complexes vary between 2.1147(15)-2.2129(16) Å and are consistent with high-spin Fe(II) complexes (Table 6.1).^[32, 33] The Fe-N1 (2.2111(17)) and Fe-N6 (2.2129(16)) bond lengths are larger in **2**, which points at a weaker binding of the terminal pyridines and can be attributed to the more sterically demanding methyl groups in their ortho-positions. Considering the intermolecular angles, the O1-Fe-O4 angle in **1** deviates significantly from a perfect octahedron with a value of 165.70(5)°. A smaller distortion is observed for the corresponding angles in **1*(MeCN)₂** and **2** with values of 176.68(6)° and 170.87(7)°, respectively. The bipyridine moieties are nearly planar in **1*(MeCN)₂** with an interplanar dihedral angle between the two pyridine rings of 1.04(7)°, as opposed to the considerably larger distortion found in **1** and **2** with dihedral angles of 23.11(9)° and 21.53(11)°, respectively. The babpy ligand framework was found to be

twisted in all complexes, the extent of which can be expressed as the interplanar angle of the terminal pyridines. Twisting values of 34.47(9)°, 29.26(7)° and 30.97(11)° are found for **1**, **1***(MeCN)₂, and **2** respectively. The angular variance^[34] of **1**, **1***(MeCN)₂ and **2** is 105.77 deg², 88.59 deg² and 96.76 deg², respectively. In all complexes, the Fe center is almost exactly in the N,N,N,N least-squares plane of the ligand.

Table 6.1. Bond distances and angles in **1**, **1***(MeCN)₂ and **2**.

Distance/Angle ^a	1	1 *(MeCN) ₂	2
Fe-N1	2.1229(15)	2.1306(12)	2.2111(17)
Fe-N3	2.1147(15)	2.1354(12)	2.1431(16)
Fe-N4	2.1277(15)	2.2260(13)	2.1392(17)
Fe-N6	2.1184(15)	-	2.2129(16)
Fe-O1	2.2248(14)	-	2.2151(19)
Fe-O4	2.2352(13)	-	2.184(2)
N3-Fe-N4	78.43(6)	85.74(4)	77.36(6)
N3-Fe-N3a	-	77.51(6)	-
N1-Fe-N6	111.28(6)	-	112.04(6)
N1-Fe-N1a	-	111.43(5)	-
O1-Fe-O4	165.70(5)	-	176.68(6)
N4-Fe-N4a	-	170.87(7)	-
Bipyridine dihedral ^b	23.11(9)	1.04(7)	21.53(11)
Pyridine twist ^c	34.47(9)	29.26(7)	30.97(11)
Fe-N,N,N,N ^d	0.0019(2)	0	0.0178(4)

^a Distances are reported in Å, angles in (°); ^b Interplanar angle between the least square-planes of N3, C6, C7, C8, C9, C10 with N4, C11, C12, C13, C14, C15, or N3a, C6a, C7a, C8a, C9a, C10a or N4, C11, C12, C13, C14, C15; ^c Interplanar angle between the least square-planes of N1, C1, C2, C3, C4, C5 with N6, C20, C19, C18, C17, C16 or N1a, C1a, C2a, C3a, C4a, C5a or N6, C16, C17, C18, C19, C20; ^d Distance of the least square plane of N1, N3, N4, N6 or N1, N3, N1a, N3a with Fe.

The similarity in structure of **1** with **2** is remarkable and indicates that the two methyl groups on each of the terminal pyridines of the bapbpy ligand framework have only a minor effect on the overall sterics of the ligand. The only clear difference is the more linear apical axis observed for **2** with respect to **1** (O-Fe-O of 176.68(6)° in **2** compared to 165.70(5)° in **1**), potentially resulting in a stronger ligand-field strength of the axial ligands for **2**, as observed elsewhere.^[18, 31] A comparison of the structural features of [Fe(OTf)₂(bpzbpby)] and [Fe(OTf)₂(mbpzbpby)]^[31] showed that the methyl substituents in this case caused a more pronounced deviation of the O-Fe-O angle from the ideal geometry. The structure of **1***(MeCN)₂ provides insight into the structure of **1** in acetonitrile solution, as the coordinated triflate ions in **1** are expected to exchange for MeCN molecules in solution.

6.2.3 Spectroscopic features

In the solid state, a comparison of the FT-IR spectra of **1** and **2** with the free ligand showed a shift of the C-N vibration from 1608 cm⁻¹ to 1638 cm⁻¹ for **1** and from 1611 to 1648 cm⁻¹ for **2** upon complexation, indicating not only binding of the pyridine to the metal but also differences in binding strength between the two ligands. The vibrations at 1221, 1162, 1028 and 1010 cm⁻¹ are furthermore characteristic of coordinated triflate anions.^[35]

Electronic absorption spectra of **1** (Figure 6.10 and Figure 6.4) and **2** (see Figure 6.4) dissolved in MeCN exhibit ligand-based π - π^* bands at 264-270 nm and at 305-313 nm, and MLCT^[36] features around 364-380 nm (vide infra).

Solid state Raman spectra were recorded at 785 nm of **1** and **2**, and showed strong bands at around 1600, 1480 and 1370 cm⁻¹, characteristic for pyridine-based transitions.^[37] Triflate-based vibrations are present between 1000-1200 cm⁻¹.^[36] In MeCN solution, Raman spectra recorded at 355 and 473 nm show similar pyridine-based vibrations between 1400-1600 cm⁻¹. The coordination of MeCN (commonly observed at 2300 cm⁻¹) was not observed at the recorded concentrations.

¹H NMR measurements of solutions of **1** and **2** in CD₃CN showed typical paramagnetic NMR spectra for both compounds, corroborating the high-spin Fe(II) assignment based on the X-ray crystal structures. A total of 8 signals were observed for each complex in the range of 7 to 77 ppm for **1** (Figure 6.5) and -20 to 60 ppm for **2** (Figure 6.6). 2D COSY measurements for **1** in CD₃CN, did not allow for further assignment of the peaks. ¹H NMR of **1** in *d*DMSO showed a similar set of signals in the same paramagnetic range as in the spectrum in CD₃CN. The arrangement order of the peaks for **1** (based on line shape analysis) is different though in the two spectra, which indicates that the assignment of the signals is not straightforward and the signals observed in the spectrum of the ligand cannot be simply extrapolated to the complexes. ¹⁹F NMR of **1** in CD₃CN showed one peak at $\delta = -77$ ppm, corresponding to non-coordinated triflate ions,^[38] which supports binding of MeCN molecules to the metal upon dissolution of **1** in MeCN.

6.2.4 Electrochemistry

The redox chemistry of complexes **1** and **2** in MeCN was studied by cyclic voltammetry in order to investigate their one-electron oxidations. **1** displayed a quasi-reversible one-electron oxidation (Fe(III)/Fe(II)) with a midpoint potential of 1.09 V vs. SCE with $\Delta E_p = 91$ mV (Figure 6.2). This midpoint potential is similar to the one observed for the oxidation of $[\text{Fe}(\text{N4PY})(\text{MeCN})](\text{ClO}_4)_2$ in MeCN (1.010 V, N4Py = 1,1-bis(pyridine-2-yl)-N,N-bis(pyridine-2-ylmethyl)methanamine), which also contains four coordinating pyridine groups, and is typical for the high potential required for a 1-electron oxidation of $\text{Fe(II)L}(\text{MeCN})_2$ complexes in solution.^[36, 39] Under similar conditions, the midpoint potential of **1** is in between the values of $[\text{Fe}(\text{TPA})(\text{MeCN})_2](\text{ClO}_4)$ (860 mV, TPA = tris(2-picolyl)amine),^[40] $[\text{Fe}(\text{OTf})_2(\text{TACN})]$ (0.902 V, TACN = 1,4,7-triazacyclononane) and $[\text{Fe}(\text{Py5})(\text{MeCN})](\text{ClO}_4)_2$ (1.210 V, Py5 = 2,6-bis(methoxy(di(2-pyridyl)methyl)pyridine), which have no, fewer or more coordinating pyridines, respectively.^[41] Fe-TMC derivatives are generally irreversibly oxidized at potentials between 0.54 to 0.57 V vs. SCE.^[42]

In the voltammogram of **1**, an irreversible reduction wave was observed at 0.2 V, as well as additional reduction/oxidation couples between 0.4-0.8 V. These are assigned to electrochemical processes induced by the presence of trace amounts of water within the electrochemical set-up, causing the exchange of MeCN ligands for water ligands. Because these exchanges are especially favorable in the Fe(III) state,^[36, 43] these features are assigned to the reduction/oxidation of Fe(III)(OH)(L) (between 0.2-0.4 V) and $\text{Fe(III)(L)(H}_2\text{O)}_2$ (0.4-0.8 V) species. The multiple features in the latter couple are likely due to the existence of two vacant sites where MeCN can be exchanged for H_2O . The single exchange of MeCN by H_2O was observed at addition of 1 vol% of water (Figure 6.2 bottom left), giving rise to the $\text{Fe(III/II)(L)(H}_2\text{O)(MeCN)}$ couple with a poor reduction wave, a midpoint potential of 0.96 V and $\Delta E_p = 115$ mV. The electrochemical features involving double coordination of H_2O increase in intensity when more water (10 vol%) is added (Figure 6.2 bottom right), with concomitant disappearance of the features associated with Fe(III/II)(MeCN) species.

Complex **2** displayed a single quasi-reversible redox feature with a midpoint potential at 0.87 vs. SCE ($\Delta E_p = 181$ mV), assigned to the Fe(III)/Fe(II) redox couple (Figure 6.2 top right). This midpoint potential is lower than with iron-based complexes bearing the TPA- or N4PY derivatives $[\text{Fe}(6\text{-Me}_2\text{TPA})(\text{CH}_3\text{CN})_2](\text{ClO}_4)_2$, $[\text{Fe}(6\text{-Me}_3\text{TPA})(\text{CH}_3\text{CN})_2](\text{ClO}_4)_2$ (both at 940 mV)^[40] or $[\text{Fe}(5\text{-(MeO)}_2\text{N4PY})(\text{MeCN})](\text{ClO}_4)_2$ (996mV).^[41] The lower midpoint potential for the oxidation of **2** compared to **1** could be explained by the electron-donating effect of the methyl groups in **2** (Table 6.1), and is consistent with the fact that a more electron-rich Fe-center is oxidized easier.^[41]

Chapter 6

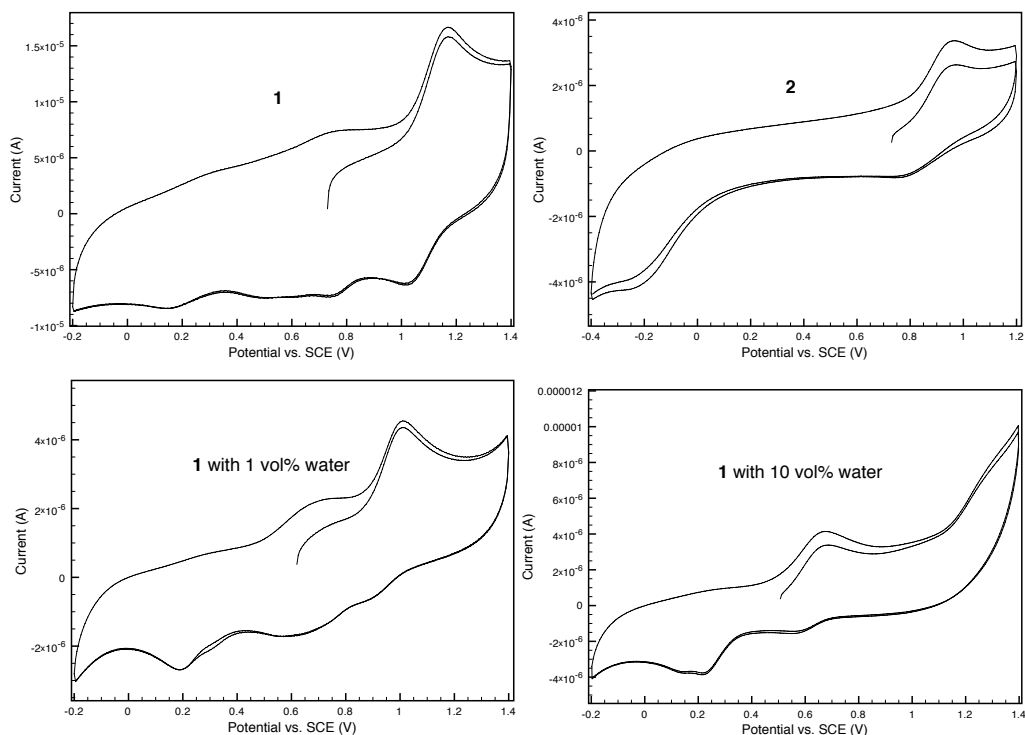


Figure 6.2. Cyclic voltammograms (CV) for the oxidation and subsequent reduction of **1** (top left) and **2** (top right) in MeCN. Bottom: CV of **1** with 1 vol% (left) and 10 vol% (right) of water.

6.2.5 Spin crossover features

Magnetic susceptibility measurements were conducted in the solid state to determine the evolution with temperature of the $\chi_m T$ product of **1** and **2**, where χ_m is the molar magnetic susceptibility and T is the temperature. The $\chi_m T$ value of **1** and **2**, measured in the heating and cooling mode over a temperature range of -223 to 77 °C, were found not to vary significantly from their value at ambient temperature (3.13 and 4.57 ($\text{cm}^3 \times \text{mol}^{-1} \times ^\circ\text{C}$), respectively) (Figure 6.3). The $\chi_m T$ value of **1** at ambient temperature of 3.13 is comparable with the spin-only value calculated for a 5T_2 ground state ($S = 2$) in an octahedral coordination environment,^[18] and similar to those of $[\text{Fe}(\text{OTf})_2(\text{bpzbp})]$ (3.03).^[31] The $\chi_m T$ value for **2** at ambient temperature is similar to that of a recrystallized sample of $[\text{Fe}(\text{NCS})_2(\text{bapbpy})]$ at room temperature ($\chi_m T = 4.34$ $\text{cm}^3 \times \text{mol}^{-1} \times ^\circ\text{C}$),^[18] and slightly higher than the theoretical value for a spin-only high-spin state. Next to paramagnetic impurities, other factors might influence the $\chi_m T$ value, such as orientational effects in the solid state that are known to result in effective magnetic moments that do not correspond to the real average magnetic moment.^[18] Overall,

magnetic susceptibility data show the absence of spin crossover for compound **1** and **2** in the solid state.

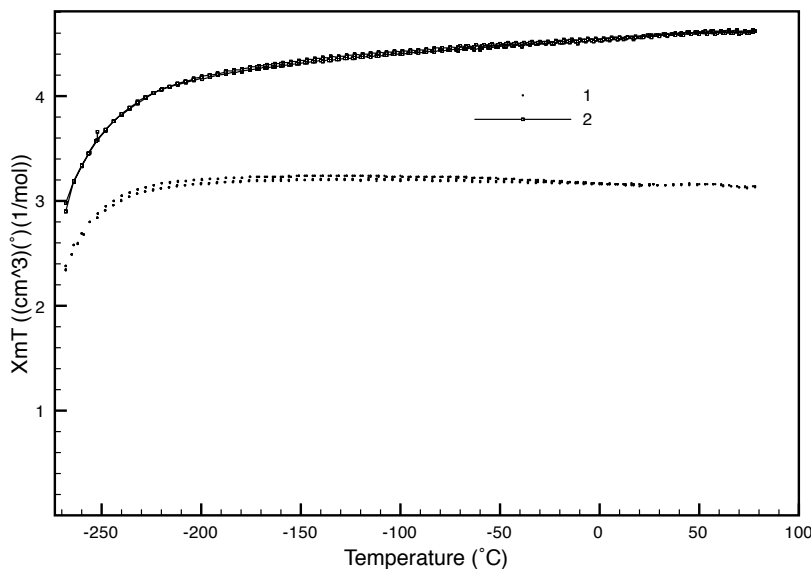


Figure 6.3. $\chi_m T$ vs. T plot for **1** and **2** in both heating and cooling modes.

In MeCN solution, however, the electronic absorption spectra of **1** recorded at different temperatures showed a change of the MLCT transition at 365 nm (see Figure 6.4 top). At ambient temperature, the MLCT transition has a maximum at 357 nm ($\epsilon = 11.05 \text{ (mM} \times \text{cm)}^{-1}$). At $-40 \text{ }^\circ\text{C}$, two peaks were observed: next to the absorption at 357 nm ($\epsilon = 11.05 \text{ (mM} \times \text{cm)}^{-1}$) another absorption was observed at 372 nm ($\epsilon = 10.53 \text{ (mM} \times \text{cm)}^{-1}$). The π - π^* transition also has a higher absorption at $-40 \text{ }^\circ\text{C}$ (306 nm, $\epsilon = 30.81 \text{ (mM} \times \text{cm)}^{-1}$) than at ambient temperature at (309 nm, $\epsilon = 26.03 \text{ (mM} \times \text{cm)}^{-1}$).

The electronic absorption spectra of **2** recorded in MeCN showed a temperature-dependent ϵ for the MLCT transition at around 371 nm (Figure 6.4 bottom), showing higher absorptions at $-40 \text{ }^\circ\text{C}$ ($\epsilon = 10.16 \text{ (mM} \times \text{cm)}^{-1}$) than at ambient temperature ($\epsilon = 8.16 \text{ (mM} \times \text{cm)}^{-1}$). As with **1**, the π - π^* transition also showed a higher absorption at $-40 \text{ }^\circ\text{C}$ (at 312 nm, $\epsilon = 23.85 \text{ (mM} \times \text{cm)}^{-1}$) than at ambient temperature (at 308 nm $\epsilon = 21.34 \text{ (mM} \times \text{cm)}^{-1}$). Fe(II) species that display higher ϵ for low-spin species than high-spin species are, for example, complexes of type $[\text{Fe}(\text{tpen})](\text{ClO}_4)_2$ (tpen = tetrakis(2-pyridylmethyl)ethylenediamine),^[44] which is also observed in the changes of the MLCT transitions for **2**.

Chapter 6

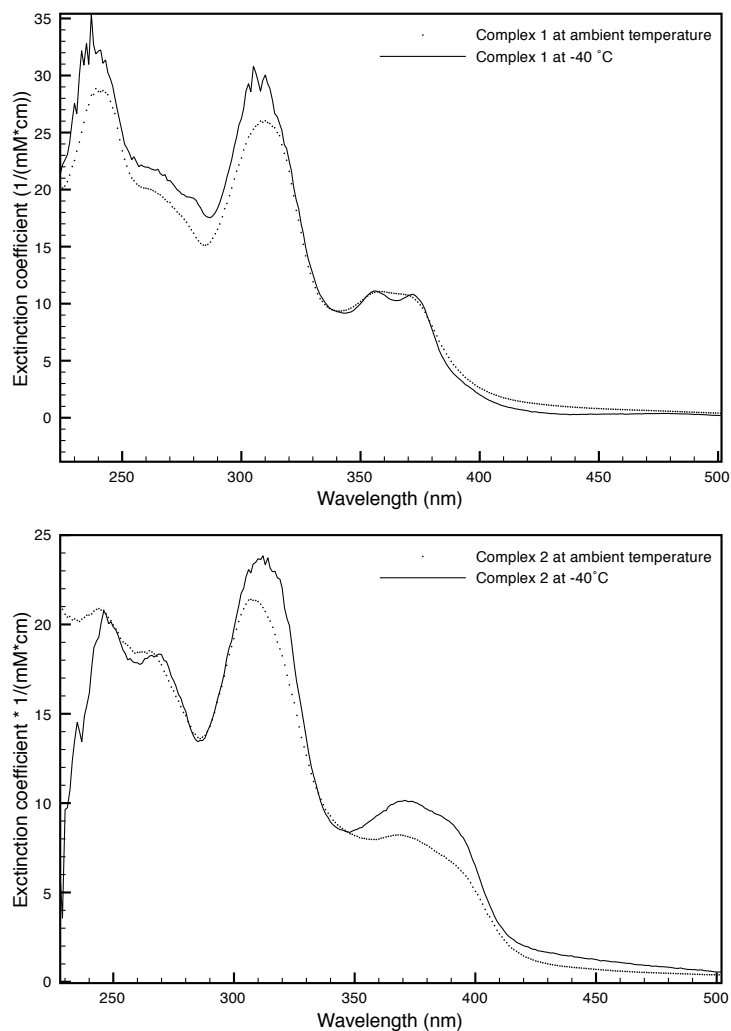


Figure 6.4. Electronic absorption spectrum of **1** (top) and **2** (bottom) in MeCN at ambient temperature (dotted line) and $-40\text{ }^{\circ}\text{C}$ (solid line).

The temperature-dependent electronic absorption spectra of **1** and **2** in MeCN solution triggered the investigation of their ^1H NMR spectra in CD_3CN at different temperatures as well. The variable-temperature (VT) ^1H NMR spectra of **1** showed similar features at $50\text{ }^{\circ}\text{C}$ and $25\text{ }^{\circ}\text{C}$ (Figure 6.5) with the signals spanning a range between 7 to 77 ppm, which is not consistent with a Curie behavior of paramagnetic Fe(II) complexes (more downfield shift with higher temperature), e. g. $[\text{Fe}(\text{OTf})_2(\text{MCP})]$ (MCP = *N,N'*-dimethyl-*N,N'*-bis(2-pyridylmethyl)-cyclohexane-*trans*-1,2-diamine).^[45] Measurements at $-20\text{ }^{\circ}\text{C}$ caused the signals to shift dramatically and the spectral range now only spanned a range between 8 to 58 ppm. A more drastic shift is observed at $-40\text{ }^{\circ}\text{C}$, with the paramagnetic signal observed between 8 to 37 ppm. The increasing fraction of low-spin molecules at lower

temperatures probably caused the averaged signal of the two spin states to continuously span a smaller and more upfield range in the ^1H NMR spectrum.

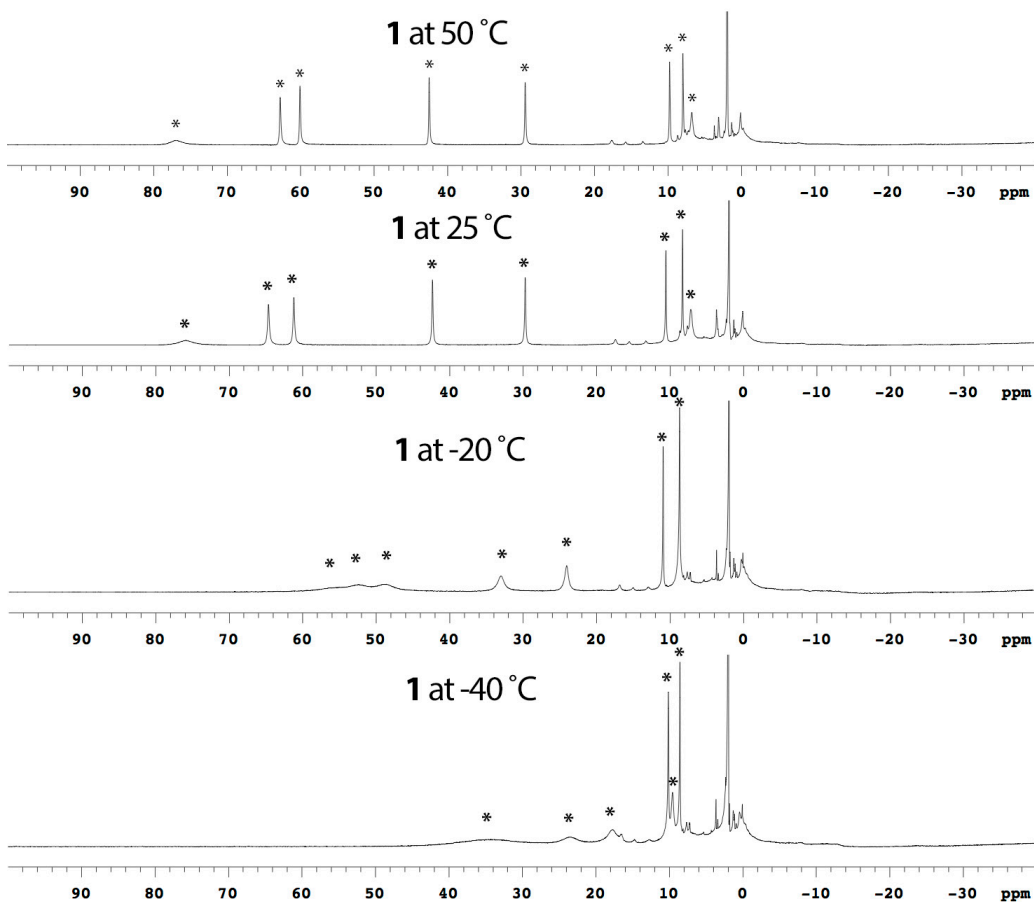


Figure 6.5. VT ^1H NMR measurements of **1** in CD_3CN . Peaks assigned to **1** are denoted with (*).

The VT ^1H NMR measurements of **2** showed a different behavior compared to **1**. The paramagnetic signals span a range of -17 to 57 ppm at 50 °C, -20 to 60 ppm at 25 °C, -28 to 68 ppm at -20 °C and -34 to 70 ppm at -40 °C, which is opposite to a Curie behavior of a paramagnetic complex with a temperature-independent spin state.^[45] Interestingly, at temperatures of -20 °C and -40 °C diamagnetic signals become visible, which are predominantly absent at 50 °C. The increasing amounts of low-spin species at -20 °C and -40 °C probably enabled diamagnetic impurities to be better visible at these temperatures.

Chapter 6

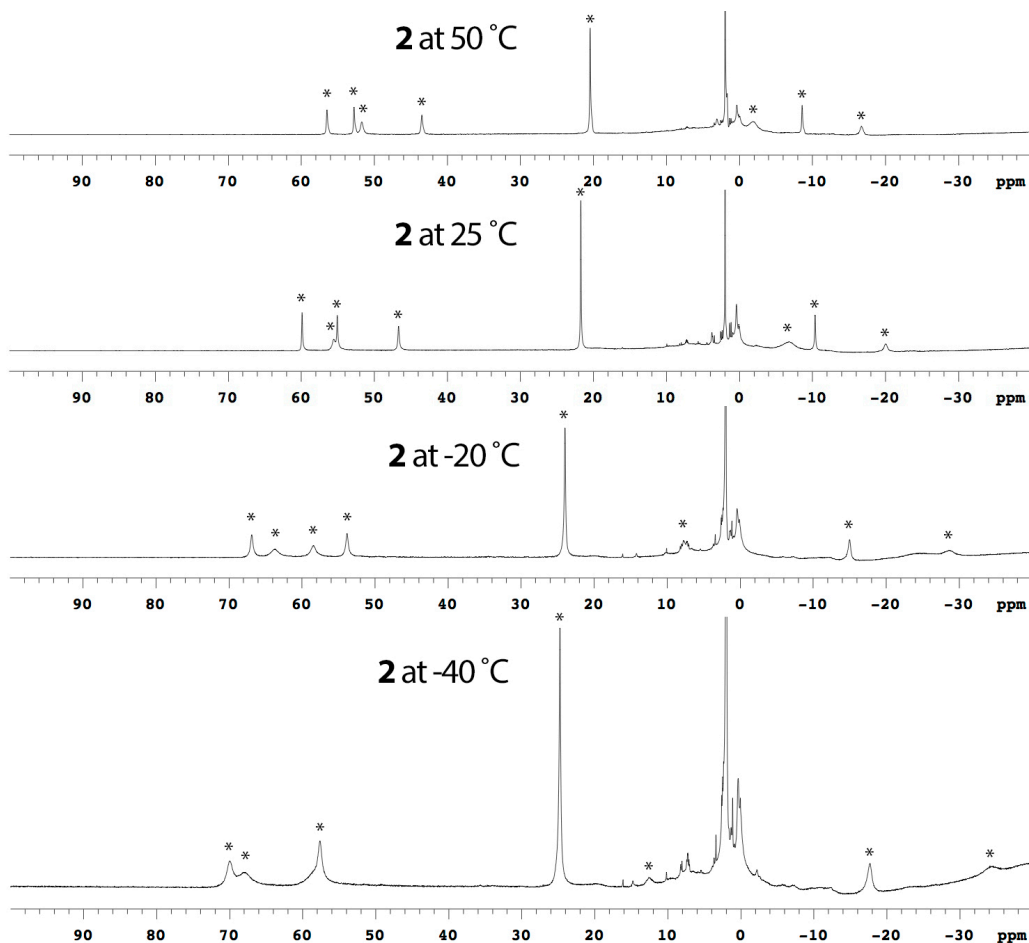


Figure 6.6. VT ¹H NMR measurement of **2** in CD₃CN. Peaks assigned to **2** are denoted with (*).

The evolution of the average magnetic moments (μ_{eff}) of complexes **1** and **2** as a function of the temperature were measured in MeCN solution using Evan's method. At ambient temperatures, the μ_{eff} of **1** and **2** was found to be 4.33 and 4.77 μ_{B} , respectively, which is somewhat lower than the theoretical value of 4.90 μ_{B} for a high-spin $S = 2$ Fe(II) species. Increasing the temperature to 50 °C led to an increase of the μ_{eff} for both complexes, to reach a value of 4.55 μ_{B} for **1** and 4.95 μ_{B} for **2** at 50 °C (Figure 6.7). While at higher temperatures saturation behavior of the μ_{eff} was observed, a decrease in temperature from 0 °C to -40 °C showed a more or less linear decrease of the μ_{eff} , with values of 2.76 and 3.04 μ_{B} at -40 °C for **1** and **2**, respectively. According to these data, it can be concluded that spin crossover occurs with **1** and **2** in MeCN solution.

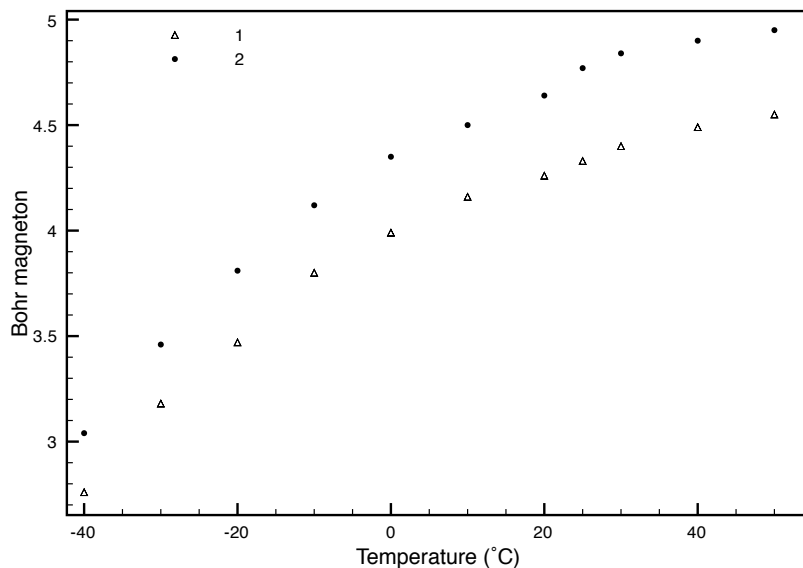


Figure 6.7. Plot of the μ_{eff} of **1** and **2** in MeCN against temperature by Evan's method.

The magnetic susceptibility data for **1** and **2** suggest an $S = 2$ high-spin state in the solid state and spin crossover in MeCN solution. The axial positions in these complexes will be occupied differently in the solid state than in solution. In the solid state triflates will be bound, whereas in acetonitrile solution the coordinating MeCN molecules will bind to iron(II). Due to the much better coordinating properties of MeCN ligands compared to triflate anions, the low-spin state is stabilized for the FeN6 coordination sphere of **1** and **2** in MeCN solution, which allows SCO to occur, as also reported in the solid state for $[\text{Fe}(\text{NCS})_2(\text{bpzbp})]$ ^[31] and $[\text{Fe}(\text{NCS})_2(\text{bapbp})]$.^[18] On the contrary, the temperature-independent spin state of **1** and **2** in the solid state correlates to observations for similar FeN4O2 coordination surroundings in $[\text{Fe}(\text{OTf})_2(\text{bpzbp})]$ and $[\text{Fe}(\text{OTf})_2(\text{mbpzbp})]$,^[31] where the ligand field splitting is lower and the compounds remain in high-spin state.^[46] The observed SCO for **2** in MeCN contrasts with observations made for $[\text{Fe}(\text{NSC})_2(\text{mbpzbp})]$, where the dimethyl-substituted complex has a constant $\chi_{\text{m}}T$ (2.95-3.05) in the temperature range of -223 °C to 77 °C and thus showed no SCO, as opposed to the unsubstituted derivative $[\text{Fe}(\text{NSC})_2(\text{bpzbp})]$ ($\chi_{\text{m}}T$ between 1.18 and 3.12).^[31] Comparing the magnetic moments in MeCN of the two complexes, **2** showed a slightly higher occupation of high-spin states than **1** at all temperatures. Complex **2** also gave a higher $\chi_{\text{m}}T$ in solid state. Overall, both complexes showed temperature-dependent SCO in MeCN solution with a relatively high μ_{eff} at ambient temperatures.

6.2.6 DFT calculations

Prior to attempts to study the activity of **1** and **2** in oxidation reactions, the structure and stability of a putative iron-oxo species $[\text{Fe}^{\text{IV}}(\text{O})(\text{bapbpy})(\text{MeCN})]^{2+}$ and its potential for olefin epoxidation was studied by computational means, i.e. through DFT calculations at the B3LYP level. Considering the high-spin state of complexes **1** and **2** at ambient temperature in MeCN solution and their potential spin change, the calculations were run in both the $S = 2$ (^5R , quintet, high-spin) and the $S = 1$ (^3R , triplet, intermediate-spin) state. Based on the X-ray crystal structure of **1**, a geometry optimization in the gas-phase for the triplet and the quintet state was carried out for $[\text{Fe}(\text{O})(\text{bapbpy})(\text{MeCN})]^{2+}$, where the triflate atoms in **1** were replaced by one MeCN molecule (as expected to occur in solution) and one oxo moiety, with Fe-N7 and Fe-O1 distances set to 2.20 and 1.76 Å prior to the geometry optimization. In this way, stable configurations could be obtained (Figure 6.8 top), showing that such species should in principle be accessible.

For ^3R and ^5R (R = reactant), the Fe1-O1 distances of 1.651 Å in the triplet state and of 1.642 Å in the quintet state are indicative of an Fe=O double bond (Table 6.2). The calculated iron-oxo moiety is therefore more labile than in $[\text{Fe}(\text{O})(\text{TMC})(\text{MeCN})](\text{OTf})_2$ (Fe=O is 1.646(3) Å at $S = 1$),^[3] is more similar to the bond length measured for $[\text{Fe}(\text{O})(\text{TPA})(\text{MeCN})](\text{OTf})_2$ (Fe=O = 1.67 Å according to EXAFS),^[47] yet significantly shorter than observed for $[\text{Fe}(\text{IV})(\text{O})(\text{TAML})]^{2-}$ (Fe=O length of 1.69 Å according to EXAFS).^[13] The Fe-TPA species is known to be a better oxidant than $[\text{Fe}(\text{O})(\text{TMC})(\text{MeCN})](\text{OTf})_2$.^[7, 47] The MeCN ligand was found to be bound at 2.136 and 2.139 Å (Fe-N7) in the triplet and quintet state, respectively. The Fe-N distances of the bapbpy ligand in the triplet state are consistent with typical intermediate-spin bond distances with values of between 1.975 to 2.034 Å. Likewise, The Fe-N distances in the quintet state are consistent with high-spin bond distances with values ranging from 2.084 to 2.152 Å. The angles of the axial ligands with Fe are close to values in a perfect octahedron with O1-Fe-N7 of 179.4° and 174.4° in the triplet and quintet state, respectively. These angles are larger than those determined for **1** and **1***(MeCN)₂ by single crystal X-ray diffraction (Table 6.1). The dihedral angles of the bipyridines are rather in-plane, with small values of 9.3° and 13.0° for the triplet and quintet state, respectively. On the other hand, the interplanar angles of the pyridines are larger than in **1** and **2** with 46.2° and 41.8°. The Fe atom is almost in the N,N,N,N least-squares plane of the ligand.

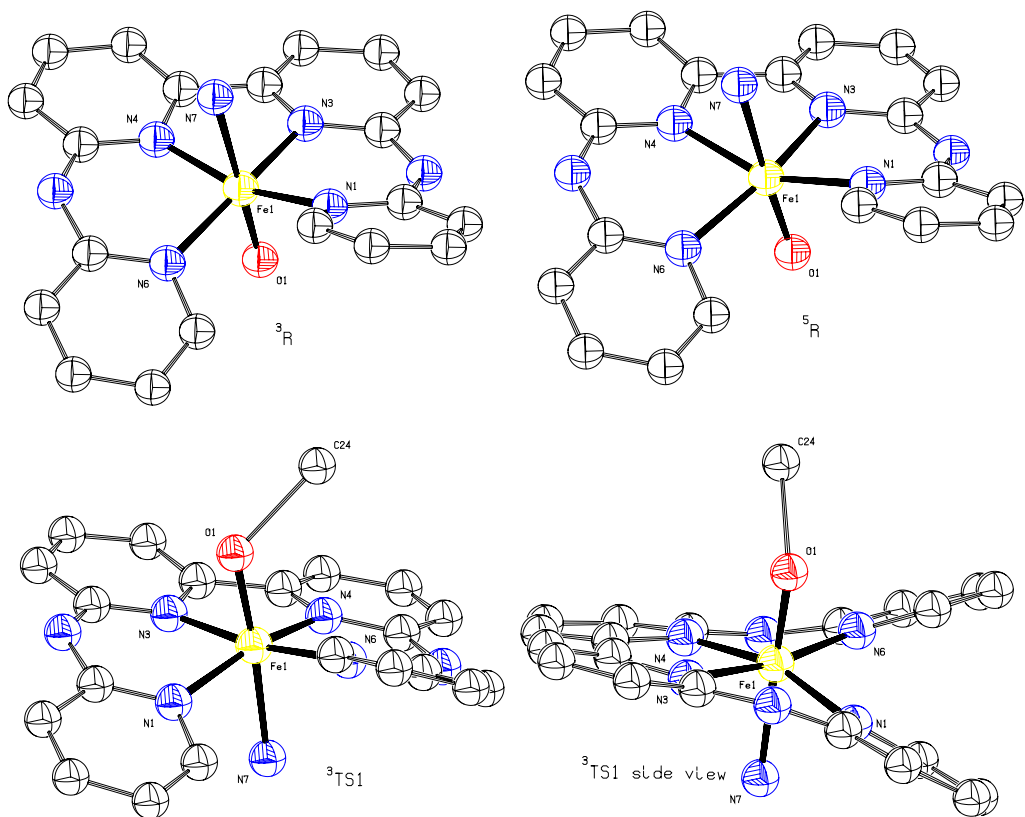


Figure 6.8. Calculated structures of $[\text{Fe}(\text{O})(\text{bapbpy})(\text{MeCN})]^{2+}$ in the triplet state (3R , top left) and quintet state (5R , top right), and of transition state $[\text{Fe}(\text{OCH}_2\text{CHCH}_3)(\text{bapbpy})(\text{MeCN})]^{2+}$ in the triplet state ($^3\text{TS1}$) from top view (bottom left) and from side view (bottom right), where only the alkoxy C-atom is shown for clarity. In all structures the hydrogen atoms are omitted, and only the coordinating N-atom from MeCN is shown for clarity.

Overall, the calculated potential energy curve for the oxygen transfer of $[\text{Fe}(\text{O})(\text{bapbpy})(\text{MeCN})]^{2+}$ to the model substrate propene in the gas phase in the triplet and in the quintet state is shown in Figure 6.9. For 3R , the reaction of the $\text{Fe}=\text{O}$ with the double bond in propene goes through a $[\text{Fe}(\text{OCH}_2\text{CHCH}_3)(\text{bapbpy})(\text{MeCN})]^{2+}$ transition state $^3\text{TS1}$ (Figure 6.8 bottom) that is 7.9 kcal/mol higher in energy than 3R . In this state, the ligand is wrapped oppositely around the Fe compared to 3R (O1 on top with $^3\text{TS1}$), probably induced by a twist of the ligand upon approach of the substrate. In $^3\text{TS1}$, the Fe1-O1 distance elongates to 1.742 Å, while the O1-C24 distance (binding of the substrate to the oxide) is 2.030 Å (Table 6.2). The Fe1-N7 distance for the coordinating MeCN is 2.095 Å, which is shorter than the distance in 3R and 5R . Notable angles are the O1-Fe1-N7 angle of 175.5°, which is close to a perfect octahedral angle, as opposed Fe1-O1-C24 , which has a

Chapter 6

value of 124.0° and indicates that the propene does not approach the Fe-oxide in an axial manner in ³TS1.

Table 6.2. Bond distances (Å) and bond angles (°) of [Fe(O)(bapbpy)(MeCN)]²⁺ in the triplet (³R) and quintet state (⁵R), and of [Fe(OCH₂CHCH₃)(bapbpy)(MeCN)]²⁺ in the triplet state (³TS1).^a

Assignment	³ R	⁵ R	³ TS1
Fe1-O1	1.651	1.642	1.742
Fe1-N7	2.136	2.139	2.095
Fe1-N1	2.018	2.125	2.035
Fe1-N3	1.980	2.098	1.989
Fe1-N4	1.975	2.153	1.980
Fe1-N6	2.034	2.084	2.020
O1-C24	-	-	2.030
O1-Fe1-N7	179.4	174.4	175.5
Fe1-O1-C24	-	-	124.0
N3-Fe1-N4	82.7	78.0	82.8
N1-Fe1-N6	96.1	107.4	96.7
Bipyridine dihedral ^b	9.3	13.0	10.5
Pyridine twisting ^c	46.2	41.8	43.2
Fe-N,N,N,N ^d	-0.069	-0.097	0.076

^a Distances are reported in Å, angles in (°); ^b Interplanar angle between the least square-planes of N4, C16, C17, C18, C19, C20 with N3, C6, C7, C8, C9, C10; ^c Interplanar angle between the least square-planes of N6, C15, C14, C13, C12, C11 with N1, C1, C2, C3, C4, C5; ^d Distance of the least square planes of N1, N3, N4 and N6 with Fe1.

After formation of ³TS1, a propyl-oxyl radical is released (³I) that eventually ring-closes to form propene oxide (³P). The energy of the Fe-bound propyl-oxyl radical intermediate state ³I amounts to the sum of the energies of [Fe(bapbpy)(MeCN)]²⁺ and the 1-propyl-oxyl radical, which is 6.6 kcal/mol lower in energy than ³R. The final state ³P comprises the epoxide product separated from the [Fe(bapbpy)(MeCN)]²⁺ fragment and the combined energies are found at 37.4 kcal/mol lower than ³R (Figure 6.9).

In the high-spin state, ⁵R was found to be 5.8 kcal/mol higher in potential energy than the triplet state species ³R (Figure 6.9). This spin state ordering is characteristic for biomimetic non-heme Fe(IV)(O) species.^[48-50] Remarkably, no ⁵TS1 transition state could be found, with rather the epoxide being directly obtained instead. The ⁵I (-15.7 kcal/mol) and the ⁵P (-46.7 kcal/mol) states were found to be lower in energy than in the corresponding triplet states. However, the absence of any sort of transition state at all in the conversion from reactant ⁵R to product ⁵P indicates no actual formation of the Fe-alkyloxide intermediate ⁵I. Despite the ⁵R state being of higher energy than the ³R state, the epoxidation of propene with the quintet state thus seems to occur with a negligible energetic barrier.

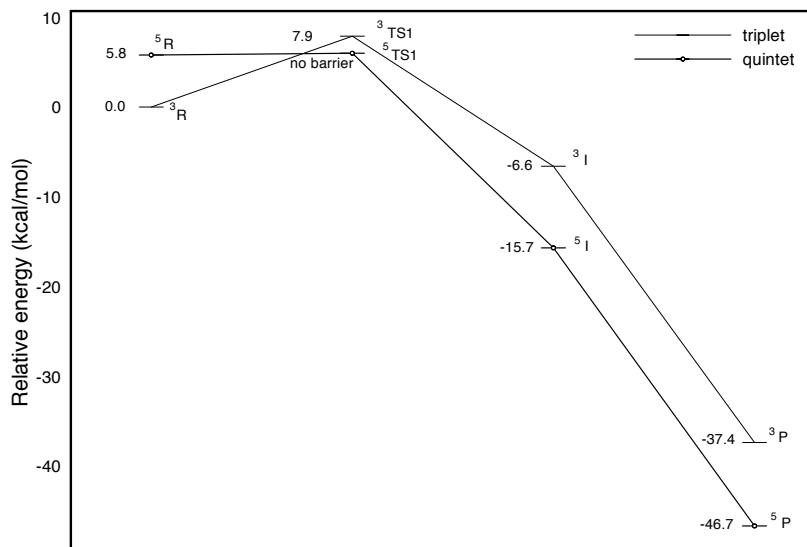


Figure 6.9. Potential energy curve of the propene epoxidation by $[\text{Fe}(\text{O})(\text{bapbpy})(\text{MeCN})]^{2+}$ in the gas phase in the triplet and quintet state with relative energies ($\Delta E + \text{ZPE}$) given in kcal/mol.

The preliminary results reported here refer to gas-phase data only. As it is dealt with a system with overall charge of +2, a full set of calculations in solvent are required. However, the current DFT results suggest that a $[\text{Fe}(\text{O})(\text{bapbpy})(\text{MeCN})]^{2+}$ species is in principle stable and that its formation should therefore be feasible. Furthermore, the low energy barriers observed for the propene epoxidation in either one of the spin state manifolds show that it could be a competent epoxidation agent. Finally, due to the negligible barrier at the $S = 2$ state, it seems likely that the high-spin state is more favorable in such epoxidations than the $S = 1$ state, although the $S = 1$ state is lower in energy in the formal ground state.

6.2.7 Reactions with peracids

Following up on the DFT calculations, complexes **1** and **2** were reacted with stoichiometric amounts of the 2-electron oxidants *m*-chloroperbenzoic acid (mcpba) and peracetic acid (AcOOH), which are common oxidants for the formation of high-valent Fe-oxo species.^[2] The titration of **1** with mcpba at ambient temperature showed a red-shift of the MLCT absorption at 360 nm to 380 nm and a slight blue-shift of the $\pi\text{-}\pi^*$ transitions from 311 to 305 nm along with a decrease of the absorption (Figure 6.10). These spectral features coincide with those of commonly reported μ -oxo dimers.^[51-53] At this temperature, no evidence was found for the formation of mononuclear peroxy or oxo species, which should exhibit spectroscopic signatures at higher wavelengths.^[2] Similar observations were made for the titration of **2** with mcpba, in titrations of both complexes with AcOOH, as well as

Chapter 6

for titrations conducted at $-40\text{ }^{\circ}\text{C}$. The electronic absorption spectra indicate that μ -oxo dimers are formed as the major species in these reactions and that their formation is rapid.

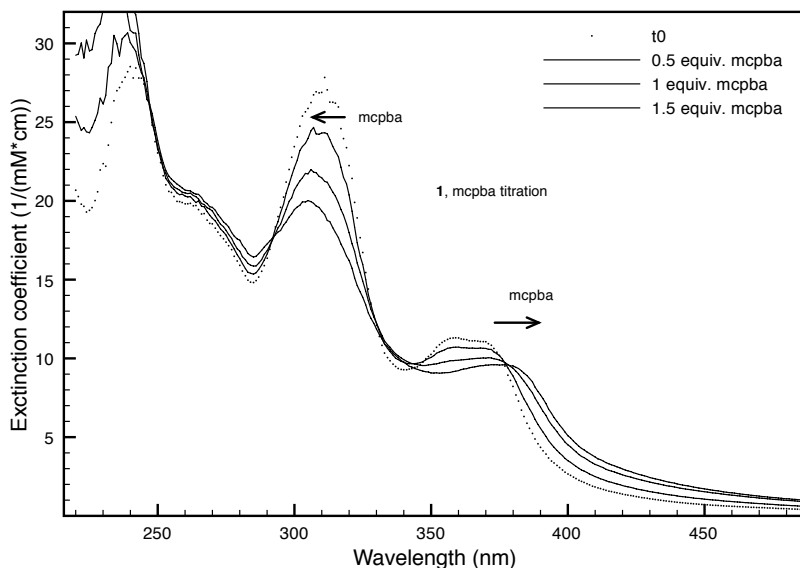
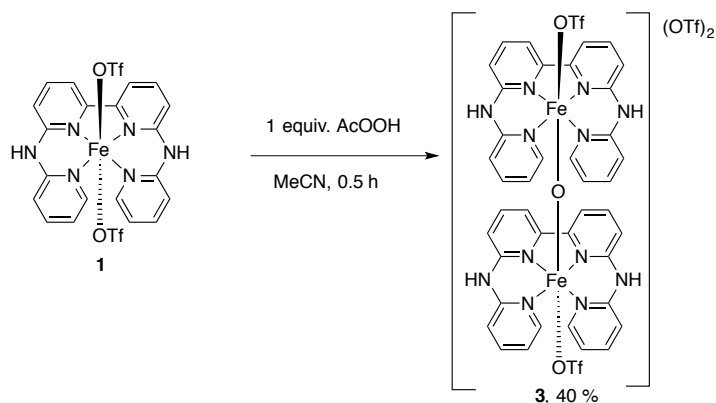


Figure 6.10. Electronic absorption spectra in MeCN of the titration of **1** with mcpba.

6.2.8 Synthesis and characterization of the non-heme complex $[\text{Fe}_2(\mu\text{-O})(\text{OTf})_2(\text{bapbpy})_2](\text{OTf})_2$ (**3**)

To unambiguously assign the identity of the μ -oxo dimers and to determine their spectroscopic signature, $[\text{Fe}(\text{OTf})_2(\text{bapbpy})]$ (**1**) was reacted on a preparative scale with 1 equiv. of AcOOH in MeCN for 0.5 h (Scheme 6.4). The dimer product was subsequently obtained upon recrystallization by vapor diffusion of diethyl ether in a MeCN solution of the crude reaction product, yielding black needle-like crystals of $[\text{Fe}_2(\mu\text{-O})(\text{OTf})_2(\text{bapbpy})_2](\text{OTf})_2$ (**3**) in 40% yield.



Scheme 6.4. Synthesis of $[\text{Fe}_2(\mu\text{-O})(\text{OTf})_2(\text{bapbpy})_2](\text{OTf})_2$ (**3**).

The crystal structure determination of **3** confirmed the formation of an Fe(III)-(μ -O)-Fe(III) dimer (Figure 6.11). The structure shows π -stacking between the aromatic ligands and both iron centers in a distorted octahedral geometry. Two of the triflate anions are bound in the axial positions and two triflate anions are found as non-coordinating counter-ions.

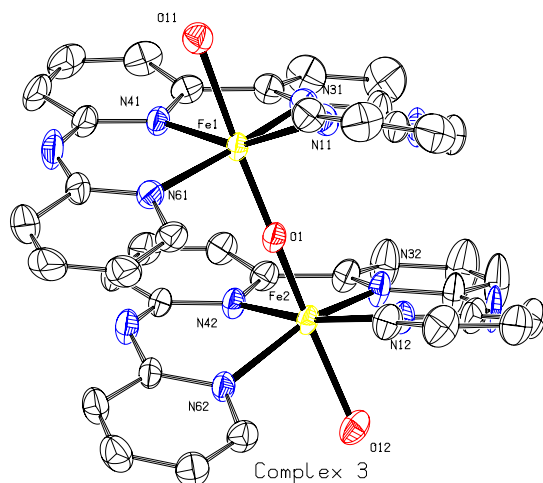


Figure 6.11. ORTEP plot at 50% probability of **3**, hydrogen atoms are omitted and only the O-atom of the two axial coordinating triflate molecules are shown for clarity. The two non-coordinating triflates are not shown.

The Fe1-N bond lengths of 2.099(5)-2.126(5) Å, the Fe1-O1 distance of 1.790(4) Å, the Fe-O-Fe angle of 163.2(3)° and the O1-Fe1-O11 and O1-Fe1-O12 angles of 170.40(18)° and 165.38(19)° are characteristic of high-spin Fe(III) centers^[54] and are similar to common monobridged Fe(III)-oxo dimers of coordination number 6 (Table 6.3).^[6, 53] These bond lengths and angles are similar with the ligand bound to Fe2. The characteristic twisting of

Chapter 6

the bapbpy ligand in **1** and **2** is also observed in **3**, as indicated by the interplanar angles of the terminal pyridines of 37.1(4)° and 36.5(4)° and the dihedral bipyridine angles of 14.9(4)° and 12.9(4)°. Fe1 and Fe2 are displaced from the least square plane of the coordinating N atoms by 0.1691(8) and 0.1678(8) Å, which is a larger distortion from planarity than observed with **1** and **2** (see Table 6.1).

Table 6.3. Bond distances and angles of **3**.

Bond distances (Å)/ angles (°)		Bond distances (Å)/ angles (°)	
Fe1-N11	2.099(5)	Fe2-N12	2.130(6)
Fe1-N31	2.101(5)	Fe2-N32	2.114(5)
Fe1-N41	2.126(5)	Fe2-N42	2.111(5)
Fe1-N61	2.109(5)	Fe2-N62	2.123(5)
Fe1-O11	2.196(4)	Fe2-O12	2.159(4)
Fe1-O1	1.790(4)	Fe2-O1	1.787(4)
N31-Fe1-N41	77.5(2)	N31-Fe2-N41	77.22(19)
N11-Fe1-N61	108.8(2)	N11-Fe2-N61	109.6(2)
O1-Fe1-O11	170.40(18)	O1-Fe2-O12	165.38(19)
Fe1-O1-Fe2	163.2(3)		
Fe1 Bipyridine angle ^a	14.9(4)	Fe2 Bipyridine angle ^a	12.9(4)
Fe1 Pyridine angle ^b	37.1(4)	Fe2 Pyridine angle ^b	36.5(4)
Fe1-N11, N31, N41, N61 ^c	-0.1691(8)	Fe2-N11, N31, N41, N61 ^c	0.1678(8)

^a Interplanar angle (°) of least square planes of N41, C151, C141, C131, C121, C111 with N31, C101, C91, C81, C71, C61 or N42, C152, C142, C132, C122, C112 with N32, C102, C92, C82, C72, C62; ^b Interplanar angle (°) of least square planes of N61, C161, C171, C181, C191, C201 with N11, C11, C21, C31, C41, C51 or N62, C162, C172, C182, C192, C202 with N12, C12, C22, C32, C42, C52; ^c Distance of the least square planes of the N11, N31, N41, N61 with Fe1 or N12, N32, N42, N62 with Fe2.

The electronic absorption spectrum of the isolated complex **3** dissolved in MeCN showed an MLCT band at 380 nm and π - π^* transitions at 270 and 305, which is in accordance with the species observed in the titration of **1** with mcpsa (*vide supra*), and with reported oxo-dimers.^[53] The ¹H NMR spectrum shows 8 signals in the region between -11 and 31 ppm, which is typical for antiferromagnetically coupled (μ -oxo)diiron(III) species.^[55, 56] ¹H NMR spectra of **3** recorded at different temperatures (-40 °C to ambient temperature) showed a comparable spectral width, which is indicative of a temperature-independent spin state.

Further investigations on the temperature dependence of the spin state of **3** by Evan's method showed a μ_{eff} of 2.22 μ_{B} at -40 °C and 2.64 μ_{B} at 50 °C (not shown). These values show the relative independence of the magnetic moment of **3** in this temperature range and are close to those reported for other non-heme and heme oxo-bridged Fe(III/III)-dimers in solution (1.89-2.18 μ_{B} at ambient temperatures).^[6, 51] Furthermore, **3** is EPR-silent, consistent with an antiferromagnetically coupled species.

The cyclic voltammogram of complex **3** shows no oxidation features up to a potential of 1.4 V vs. SCE, which is consistent with the oxidation to Fe(IV) generally occurring sluggish

under CV conditions. An irreversible reductive feature is observed at a midpoint potential at 0.69 V vs SCE (Fe(III)/Fe(II)) with a $\Delta E = 578$ mV. The midpoint potential is higher than with $[\text{Fe}_2(\text{N4Py})_2\text{O}]^{4+}$ ($E_{1/2} = 590$ mV),^[55] yet lower than common Fe-TPA dimers (around 1 V vs. SCE).^[6] The spectroscopic and electrochemical data of **3** confirm the formation of a stable and relatively inert μ -oxo dimer upon reaction of **1** and **2** with peracid oxidants.

6.2.9 Formation of mononuclear oxygenated species

As monomeric oxygenated Fe-species are expected to be formed prior to the formation of dimeric species such as **3**, it was investigated whether these could indeed be observed. A number of spectroscopic techniques have been applied to monitor the reaction of **1** with 1 equiv. of either mcpba or AcOOH at -40 °C. Neither electronic absorption and resonance Raman spectroscopic measurements (355 and 473 nm lasers) in MeCN of the reaction of **1** and **2** with mcpba or AcOOH, nor ^1H NMR titration experiments of the reaction of **1** with mcpba provided any evidence for any intermediate, but rather showed rapid formation of the dimer **3**.

On the other hand, EPR spectra recorded at -196 °C of a frozen sample of the reaction between **1** and mcpa at -40 °C showed the formation of a low-spin Fe(III) species^[1] at $g = 2.00$ upon addition of mcpba to **1** (Figure 6.12). This species was not observed in reactions carried out at 0 °C. Under similar conditions, **2** showed similar mononuclear species ($g = 2.00$), but with a much less intense signal intensity even after addition of 3 equiv. of mcpba (not shown). With both **1** and **2**, trace amounts of an high-spin Fe(III) species were observed ($g = 4.28$).^[50] The observed mononuclear low-spin species point either at the formation of $[\text{Fe}(\text{OO}(3\text{-chlorobenzoyl}))_2]^{2+}$ ^[50] or $[\text{Fe}(\text{OH})\text{L}]^{2+}$ for both **1** and **2**.^[57] Note that these species were not observed by EPR after the addition of H_2O_2 .

Chapter 6

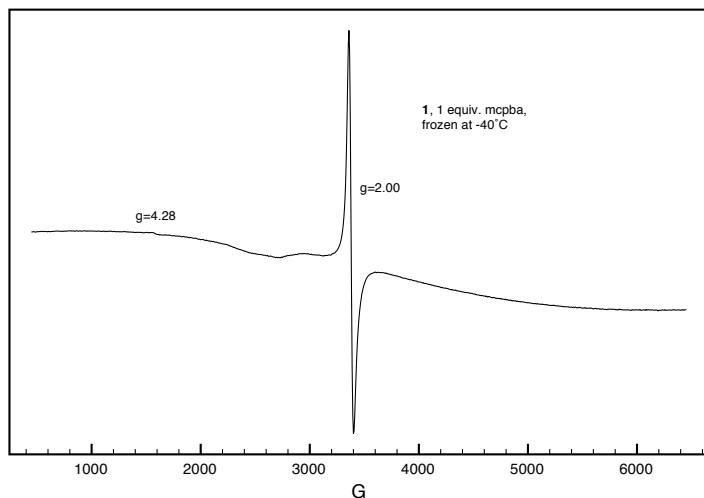


Figure 6.12. EPR spectrum of **1** with 1 equiv. AcOOH at $-40\text{ }^{\circ}\text{C}$ in MeCN, recorded at $-196\text{ }^{\circ}\text{C}$, indicating a low-spin Fe(III) species.

Low-temperature ESI-MS measurements at $-40\text{ }^{\circ}\text{C}$ of the reaction of **1** with oxidants mcpba, AcOOH or H_2O_2 showed similar traces. The reaction with 1 equiv. of AcOOH at $-40\text{ }^{\circ}\text{C}$ resulted in the formation of both $[\text{Fe}(\text{O})(\text{bapbpy})]^{2+}$ (**1b**) and $[\text{Fe}(\text{OH})(\text{bapbpy})]^{2+}$ (**1c**) (Figure 6.13) species, both of which are lower in intensity than $[\text{Fe}_2(\mu\text{-O})(\text{bapbpy})_2]^{2+}$ (**3**) (Figure 6.14, top right, m/z 404). Complete disappearance of the starting material **1** was observed, except for reactions with H_2O_2 , where a significant amount of **1** was still present (not shown). The observed pattern for **1b** (m/z 206.0385 calculated, m/z 206.0379 found) matches with the calculated isotope pattern (top). The pattern for **1c** also matches with the isotope pattern (m/z 206.5385 calculated, m/z 206.5403 found); the slight deviation from to the calculated value is thought to result from overlapping isotopes of **1b** (m/z 206.5425 calculated). The monomeric species **1b** and **1c** were observed at various collision rates, indicating that the species are indeed present in solution and do not stem from cleavage of the dimer. Additional proof for the existence of these monomeric species is that both species incorporated ^{18}O -labeled oxygen upon addition of 500 equiv. of H_2^{18}O prior to oxidant addition. The incorporation of ^{18}O into $[\text{Fe}(\text{O})(\text{bapbpy})]^{2+}$ (**1b**) was observed by the increase of the signal at m/z 207.0450 (calculated m/z 207.0440, see Figure 6.13 bottom), which is assigned to $[\text{Fe}(^{18}\text{O})(\text{bapbpy})]^{2+}$, in relative intensity to the signal at m/z 206.0379 (**1b**). Additional indication is the decrease in intensity of the signals at m/z 205.044 and m/z 205.5361 (Figure 6.13, third figure). Also, $[\text{Fe}(\text{OH})(\text{bapbpy})]^{2+}$ (**1c**) incorporated ^{18}O , indicated by the increase in intensity of the peak at m/z 207.5391 and appearance of m/z 208.0530. About 6% ^{18}O was incorporated into **1b** and 16% ^{18}O into **1c**, based on fitting a simulated spectrum with the experimental one (Figure 6.13, fourth figure).

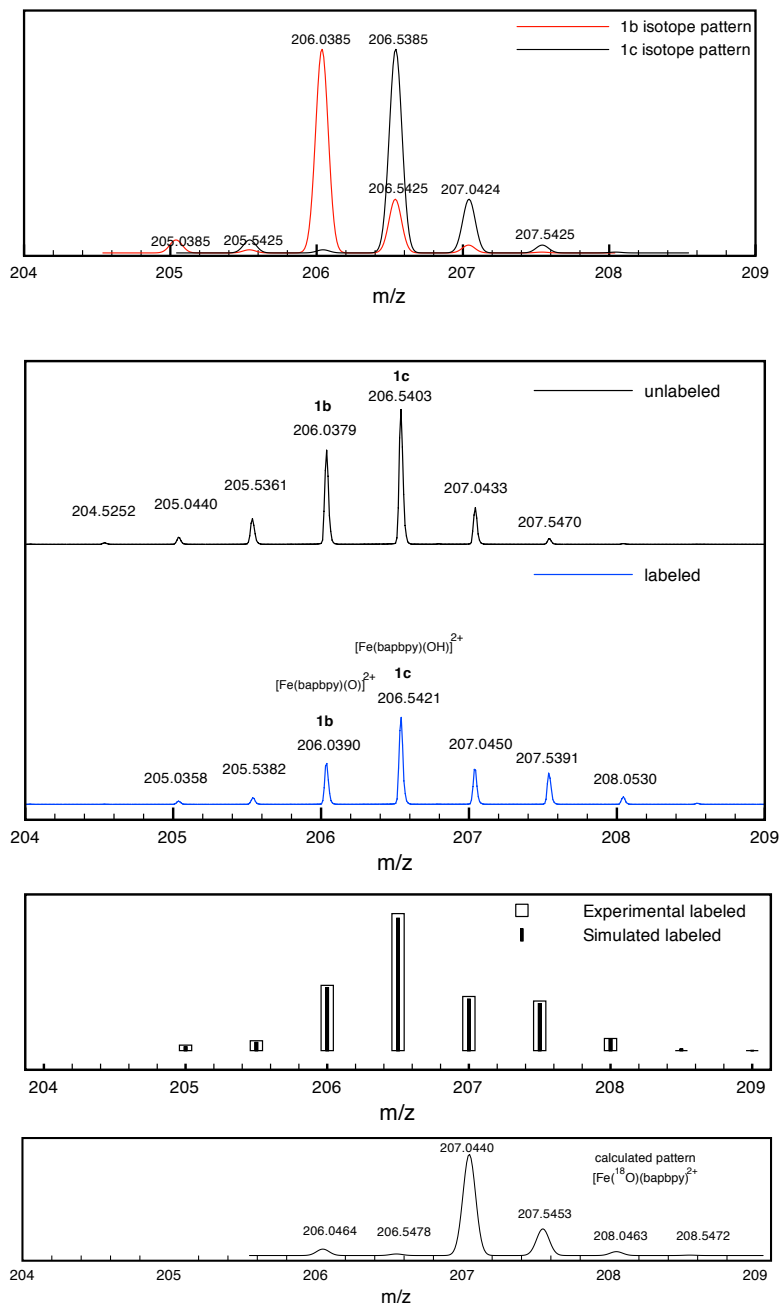


Figure 6.13. Top: Calculated isotope patterns for $[\text{Fe}(\text{O})(\text{bapbpy})]^{2+}$ (**1b**) and $[\text{Fe}(\text{OH})(\text{bapbpy})]^{2+}$ (**1c**). Second figure: reaction of **1** with 1 equiv. AcOOH at -40°C , showing both **1b** and **1c**. Third figure: similar reaction in the presence of 500 equiv. $\text{H}_2(^{18}\text{O})$ at start, showing the appearance of $[\text{Fe}(^{18}\text{O})(\text{bapbpy})]^{2+}$. Fourth figure: Y-stick plot of 9 crucial points from third figure (experimental labeled), and the simulated spectrum (simulated labeled) of **1b** with 6% incorporated ^{18}O and **1c** with 16% incorporated ^{18}O . Bottom: calculated isotope pattern for $[\text{Fe}(^{18}\text{O})\text{bapbpy}]^{2+}$.

Chapter 6

Investigations of the lifetime of **1b** and **1c** with AcOOH as oxidant showed that warming up the sample to ambient temperature over 15 minutes resulted in the almost complete disappearance of the monomeric species (Figure 6.14, bottom left) and an increase of the signals of the dimeric species **3** (Figure 6.14, bottom right). These are indications that **1b** and **1c** are indeed labile species. The same experiments carried out with **2** did not provide any evidence for the formation of a similar mononuclear oxygenated Fe-species; only dimeric species could be detected.

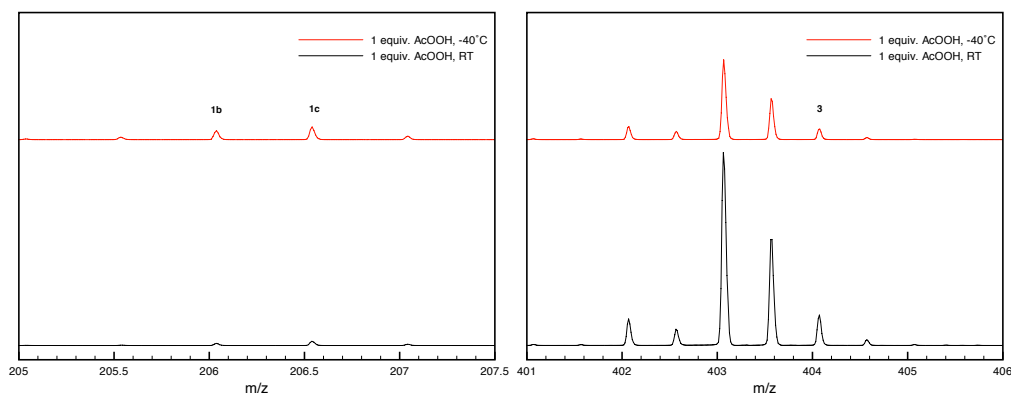
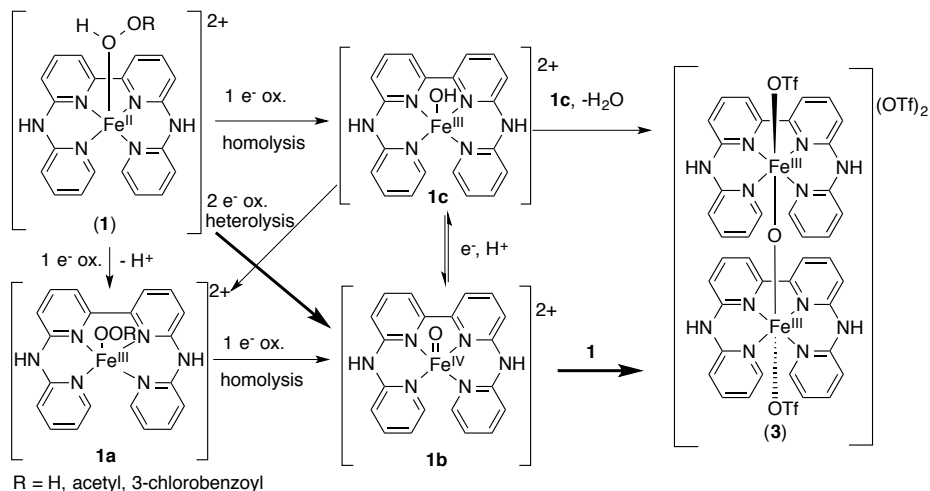


Figure 6.14. ESI-MS traces of the reaction of **1** with 1 equiv. AcOOH at $-40\text{ }^{\circ}\text{C}$ (top), forming (**1b**) and (**1c**) (left) and $[\text{Fe}(\mu\text{-O})(\text{bapbpy})_2]^{2+}$ (**3**) (right), with relative intensities. Bottom: heating up the sample to ambient temperature.

Mechanistic considerations (Scheme 6.5) starting from the simple coordination of the oxidant HOOR to **1** ($\text{R} = \text{H}$, acetyl or 3-chlorobenzoyl) enable the possibility of one-electron oxidation and subsequent loss of H^+ to yield **1a** (postulated observed species^[50] in Figure 6.12). Homolysis of this species then forms **1b**, which can react to **1c** upon addition of an electron and H^+ , as occurs with Fe-porphyrine systems.^[58] Either condensation of two molecules of **1c** or addition of **1** to **1b** eventually forms **3**. In an alternative pathway, **1** can react with the oxidant in a Fenton reaction (homolysis) to form **1c**. Ligand exchange with the peroxide then forms **1a**.^[50] This pathway is common with Fe(II)-complexes with *cis*-vacant sites, such as $[\text{Fe}(\text{OTf})_2(\text{BPBP})]$ (BPBP = *N,N'*-bis(2-picolyl)-2,2'-bipyrrrolidine),^[57] $[\text{Fe}(\text{OTf})_2(\text{BPMEN})]$ (BPMEN = *N,N'*-dimethyl-*N,N'*-bis(2-pyridylmethyl)-1,2-diaminoethane) or $[\text{Fe}(\text{OTf})_2(\text{TPA})]$. Decay of the peroxide or high-valent species may involve oxidation of organic moieties in a non-identified manner. It is proposed that the pathways involving the Fe(III)-intermediates occur only to a minor extent, as no Fe(III) species were observed by EPR with reactions with H_2O_2 , only with mcpba (Figure 6.12). The absence of any hydroxylation activity (see section 6.2.10) also disfavors these pathways.^[59] The proposed major pathway (in bold) is that **1** undergoes heterolysis to directly form **1b** by a 2-electron oxidation, which has been postulated to

occur with $[\text{Fe}(\text{OTf})_2(\text{TMC})]$ complexes,^[60, 61] and with Fe-porphyrine complexes.^[58, 59, 62, 63] Oxidation reactions of **2** are likely to proceed via a similar mechanism.



Scheme 6.5. Postulated reaction sequence of peroxides with **1**. The pathway in bold is proposed to be the major pathway.

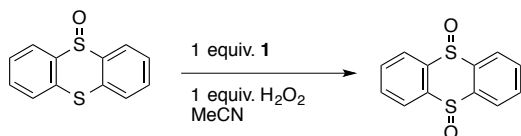
The oxygenation reactions of complex **1** and **2** indicate that the formation of the anticipated high-valent Fe-oxo species does indeed take place, but that the species has a very short lifetime. While related Fe-oxo species have shown to be very powerful oxidizing species,^[2, 64] oxo-bridged Fe(III) dimers are not generally considered as good oxidants.^[6, 56] In order to use complexes **1** and **2** as catalyst precursors for oxidation reactions, conditions and reagents that enable the formation of **1b** and/or disfavor the formation of **3** will therefore have to be found.

6.2.10 Reactivity

The low energy-barriers observed by DFT for the reaction of $[\text{Fe}(\text{O})(\text{bapby})(\text{MeCN})]^{2+}$ with propene and the detection of **1b** by ESI-MS lead to the investigation of the reactivity of **1** and **2** in oxidation reactions, with epoxidation reactions in particular. Catalytic reactions were carried out with H_2O_2 as the terminal oxidant.

The oxidation of thianthrene oxide, a common substrate to determine if oxidizing species have a more electrophilic or nucleophilic character,^[65] was tested in MeCN with 1 equiv. of **1** and 1 equiv. of H_2O_2 to afford thianthrene 5,10-dioxide (Scheme 6.6). This indicates that the active oxidizing species of **1** with H_2O_2 is electrophilic, i.e. prone to oxidize more electron-rich substrates.

Chapter 6



Scheme 6.6. Oxidation of thianthrene oxide with stoichiometric amounts of **1** and H₂O₂ in MeCN.

The extent to which **1** and **2** are active in hydrogen peroxide disproportionation was determined by iodometric titrations.^[66, 67] A solution of 3 mol% of iron complex in MeCN was titrated with sodium thiosulphate 1 minute after the addition of aqueous H₂O₂ to quantify the remaining amount of H₂O₂. Both catalysts induce the disproportionation of H₂O₂ to a similar extent as [Fe(OTf)₂(MeCN)₂] does (12-20%) (Table 6.4). The absolute amount of disproportionation at this timescale is similar to values observed for iron-corrole complexes.^[68] These results are indicative that this unwanted side-reaction can indeed occur with both complexes within short time scales.

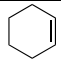
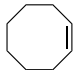
Table 6.4. Disproportionation of H₂O₂ by **1** and **2**.

Entry	Catalyst	H ₂ O ₂ disproportionation (%)
1	1	12
2	2	20
3	[Fe(OTf) ₂ (MeCN) ₂]	13

^a Reaction conditions: 3 mol% catalyst, H₂O₂ in H₂O, MeCN, 1 min, amount of H₂O₂ determined by iodometric titration.

Epoxidation reactions were then run under substrate-limiting conditions with a slight excess of H₂O₂ (2 equiv.), at 1 mol% catalyst loading. A small amount of acetic acid (3 mol%) was added to these reactions in order to increase the overall activity (Table 6.5).^[57, 69] No reaction occurred with cyclohexene with either of the complexes **1** or **2**, while *cis*-cyclooctene gave very small amounts of epoxide with **1** at ambient temperature. Increase of the reaction temperature to 50 °C resulted in an increase in activity, with significant amounts of the epoxide (16%) being formed, albeit slowly (27% substrate conversion in 16 h). Blank experiments showed negligible amounts of epoxide product in the absence of **1** or **2**.

Table 6.5. Alkene epoxidation with H₂O₂ under substrate-limiting conditions.^a

Ent.	Sub.	Cat	T (°C)	Time (h)	Conv. (%)	Epoxide yield (%)
1		1	25	0.25	0	0
2	Idem	2	25	0.25	0	0
3		1	0	0.25	0	0
4	Idem	1	25	0.25	3	2
5	Idem	1	25	16	10	7
6	Idem	1	50	16	27	16
7	Idem	[Fe(OTf) ₂ (MeCN) ₂]	50	16	34	1
8	Idem	-	50	16	4	1

^a Reaction conditions: 2 equiv. H₂O₂, 3 mol% MeCOOH, 1 mol% **1**, **2** or [Fe(OTf)₂(MeCN)₂] in MeCN.

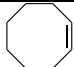
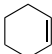
Because a number of simple Fe-salts are capable of slowly oxidizing *cis*-cyclooctene at high temperatures using O₂ as the oxidant,^[70] the catalytic activity of **1** with H₂O₂ under substrate-limiting conditions is considered rather poor. Indeed, [Fe(OTf)₂(cyclam)] catalyzes the cyclohexene epoxidation with H₂O₂ in only 20 min,^[10, 11] and several Fe-complexes with *cis*-vacant sites show high activity at under these conditions.^[32, 57, 71-74]

The limited activity of **1** and **2** under substrate-limiting conditions is not unexpected given the rapid formation of μ -oxo dimers with **1** and **2**. Better results in terms of catalyst activity might therefore be expected if a significant excess of substrate is used in order to force the catalytic reaction to occur prior to the dimerization of the complexes. Therefore, *cis*-cyclooctene epoxidation reactions were carried out under oxidant-limiting conditions with a catalyst : oxidant : substrate ratio of 1 : 10 : 1000 and H₂O₂ again being added slowly over 15 minutes to the MeCN solution (Table 6.6). While no epoxidation occurred with **1** at ambient temperature, 12% of the epoxide with respect to added H₂O₂ was formed at 50 °C, which was not observed in blank runs (entries 2-4). Dimer **3** was not able to bring about substantial oxidation under these conditions (entry 6), while the use of **2** gave the highest epoxide yield (17%, entry 5). Interestingly, a further increase of the reaction temperature to 70 °C led to an increase in epoxide yield to 26% with **1**, resulting in a TON of 2.6 per iron and a TOF of 10.8 h⁻¹. Under the same conditions, cyclohexene was converted into 14% of epoxide at 50 °C. The epoxide was exclusively observed in the catalytic runs, whereas blank reactions (no catalyst, H₂O₂) or aerobic oxidations (catalyst,

Chapter 6

no H₂O₂) only resulted in allylic oxidation products. Furthermore, no activity in the hydroxylation of cyclohexane was observed for any of the iron complexes (not shown).

Table 6.6. Oxidation of substrates with H₂O₂ under oxidant-limiting conditions.

Entry	Substrate	Catalyst	T (°C)	Epoxide yield (%)
1		1	25	0
2	Idem	1	50	13
3	Idem	[Fe(OTf) ₂ (MeCN) ₂]	50	3
4	Idem	-	50	3
5	Idem	2	50	17
6	Idem	3	50	3
7	Idem	1	70	26
8		1	50	14 ^b
9	Idem	[Fe(OTf) ₂ (MeCN) ₂]	50	-
10	Idem	-	50	-

^a Reaction conditions: **1**, **2**, [Fe(OTf)₂(MeCN)₂] or **3** with H₂O₂, cat.:oxidant:substrate 1:10:1000, H₂O₂ added over 15 minutes, MeCN, the epoxide yields are expressed compared to the addition of H₂O₂; ^b Yield of the epoxide, other oxidation products were allylic oxidation at almost equimolar ratio.

As higher epoxide yields are achieved at increased temperatures, the oxidant dismutation does not likely hamper the reactions to a large extent. It is postulated that **1b** is the active epoxidation species, and radical pathways or the involvement of **1c**^[59] or **1a** do not take place in the epoxidations.^[11] Assuming that high-spin states favor substrate oxidations, the inactivity at ambient temperature (high-spin in MeCN, Figure 6.7) is remarkable, as **1** and **2** occupy a significant amount of high-spin state at that temperature according to their μ_{eff} values. The change in spin state with temperature (Figure 6.7) could be related to the increase in catalytic activity with temperature Table 6.6, yet the SCO behavior between 25-50 °C is rather small to unambiguously correlate one with another.

Even though the catalytic performances of **1** and **2** are not outstanding, the observed TON of 2.6 for **1** at 70 °C is within the same order of magnitude as the TONs of 7.5, 8.0 and 0.5 reported under similar conditions for [Fe(OTf)₂(TPA)], [Fe(OTf)₂(BPMEN)] and [Fe(OTf)₂(N4PY)], respectively.^[72] However, the optimal temperature range of these systems is 0-25 °C, which is quite different from the optimal conditions for **1** and **2**. Also, *cis*-diols are formed as byproducts with these complexes. It is perhaps more fair to

compare the catalytic performances of **1** and **2** to structurally more related complexes, which also have the two labile coordination sites located in *trans*-positions and which form primarily epoxides. [Fe(OTf)₂(TMC)] yields a TON of 1.0 at ambient temperature.^[7] Similarly, [Fe(OTf)₂(cyclam)], [FeCl(TMP)] (TMP = tetramesitylporphinato dianion) and [FeCl(F₂₀TPP)] (F₂₀TPP = tetrakis(pentafluorophenyl)porphinato dianion) yield TONs of 4, 0.2 and 8.6, respectively.^[32] The iron-babppy complexes thus constitute a new member of the small family of non-heme Fe(OTf)₂ systems with two *trans*-vacant sites that give significant TONs in epoxidation reactions.

6.3 Concluding remarks

Summarizing, the neutral N,N,N,N ligands babppy and *o,p*-di-Me-babppy have been used to generate the non-heme Fe(II) complexes [Fe(OTf)₂(babppy)] (**1**) and [Fe(OTf)₂(*o,p*-di-Me-babppy)] (**2**), which have been isolated and fully characterized by single crystal X-ray diffraction and spectroscopic means. The complexes occupy a temperature-independent high-spin state in the solid state and showed spin-crossover phenomena in MeCN solution. DFT investigations have pointed out that the formation of high-valent iron-oxo species such as [Fe(O)(babppy)(MeCN)]²⁺ is viable starting from complexes **1** and **2**. Most interestingly, these calculations have pointed out a close-to-barrierless epoxidation of propene through a high-spin *S* = 2 manifold by this high-valent species. Attempts to form such species through the reaction of either **1** or **2** with peracids have shown the high propensity of these complexes to form μ-oxo dimers, which was substantiated by the isolation and full characterization of [Fe₂(μ-O)(OTf)₂(babppy)₂](OTf)₂ (**3**). However, a detailed spectroscopic investigation of these oxygenation reactions at lower temperatures did show the transient formation of the high-valent iron-oxo species **1b**, which is most likely formed via heterolytic cleavage of the oxidant coordinated to **1**. Finally, reactivity studies showed that **1** and **2** have some catalytic activity in the epoxidation of *cis*-cyclooctene with H₂O₂ under oxidant-limiting conditions at temperatures above 50 °C, for which **1b** is postulated to be the active oxidizing species. The catalytic results show that the synthesized complexes are one of few non-heme Fe(OTf)₂ systems with two *trans*-vacant sites with significant epoxidation activity.

6.4 Experimental

6.4.1 General

6,6'-Dibromobipyridine,^[75] babppy,^[17, 18] [Fe(OTf)₂(MeCN)₂]^[76] and thianthrene oxide^[65, 77] were all synthesized according to literature procedures. All other chemicals were used without further purification unless stated otherwise. Dry MeCN and diethyl ether were obtained from a MBraun MB SPS-800 solvent purification setup. Hydrogen peroxide (35 wt% in H₂O), 3-chloroperbenzoic acid (70-75%) in 3-

Chapter 6

chlorobenzoic acid and H₂O), ammonium molybdate (VI) tetrahydrate (99+%), cyclohexene (99%), cyclohexane (99+%) and *cis*-cyclooctene (95%) were purchased from Acros Organics. Dimethyl fumarate (97%) was obtained from Aldrich. Peracetic acid (32 wt.% in acetic acid) was ordered at Sial. CD₃CN (d, 99.8%) and *d*DMSO (d, 99.9%) were purchased from Cambridge Isotope Laboratories.

6.4.2 Physical methods

Electronic absorption spectra were obtained using a Varian Cary 50 scan UV-Visible spectrometer at ambient temperature and at -40 °C. Magnetic susceptibility measurements were recorded on a Quantum Design MPMS-XL SQUID magnetometer. DC magnetization measurements were performed in a field of 0.1 T, from 5 to 350 K (heating mode) and from 350 to 5 K (cooling mode) with a rate of ± 0.3 - 1.1 K min⁻¹. The measuring time was 20 h, corrections for the diamagnetism were calculated using Pascal's constants. Evan's method experiments for determination of the effective magnetic moment were performed according to literature procedures.^[78] Raman spectra were recorded at λ_{exc} 785 nm using a Perkin Elmer Raman Station at room temperature. Raman spectra were obtained with excitation at 400.8 (50 mW at source, PowerTechnology), 449 nm (35 mW at source, PowerTechnology), 473 (100 mW at source, Cobolt Lasers), and 355 nm (10 mW, Cobolt Lasers) to the sample through a 5 cm diameter planoconvex lens ($f = 6$ cm) and Raman scattering collected in a 180° backscattering arrangement. The collimated Raman scattering was focused by a second 5 cm diameter plano convex lens ($f = 6$ cm) through an appropriate long pass edge filter (Semrock) into a Shamrock300i spectrograph (Andor Technology) with a 1200 L/mm grating blazed at 500 nm, or 2400 L/mm blazed at 400 nm and acquired with an DV420A-BU2 CCD camera (Andor Technology). The spectral slit width was set to 10 or 20 μ m. Each spectrum was accumulated, typically 60 or 120 times with 5 s acquisition time, resulting in a total acquisition time of between 5 to 10 min per spectrum. Data were recorded and processed using Solis (Andor Technology) with spectral calibration performed using the Raman spectrum of acetonitrile/toluene 50:50 (v:v). Samples were held in quartz 10 mm path length cuvettes. Baseline correction was performed for all spectra. The concentrations used for resonance Raman studies were 0.05-0.5 mM for all samples in acetonitrile and water. Electrochemical measurements were carried out on a model CHI760B Electrochemical Workstation (CH Instruments). Analyte concentrations were typically 0.25–0.5 mM in water containing 10 mM potassium nitrate and in acetonitrile containing 0.1 M tetrabutylammonium hexafluorophosphate. A 3-mm-diameter Teflon-shrouded glassy carbon working electrode (CH Instruments), a Pt wire auxiliary electrode, and an saturated calomel reference electrode (SCE) were employed. Cyclic voltammograms were obtained at sweep rates between 10 mV s⁻¹ and 1 V s⁻¹. All potential values are quoted with respect to the SCE. Redox potentials are reported ± 10 mV. NMR spectra were recorded on a Varian VNMRS400 (400 MHz), chemical shifts (δ) are given in ppm referenced to the residual solvent peak. Infrared spectra were recorded using a Perkin-Elmer Spectrum One FT-IR spectrometer in the range of 650-4000 cm⁻¹. ESI-MS spectra were recorded using a Waters LCT Premier XE instrument in MeCN solvent. Low-temperature high resolution mass spectra (HRMS) were recorded on a Bruker MicrOTOF-Q IITM instrument at Serveis Tècnics of the University of Girona. A cryospray attachment was used for CSI-MS (cryospray injection mass spectrometry). The temperature of the nebulizing and drying gases was set at -40°C. Samples were introduced into the mass spectrometer ion source by direct infusion using a syringe pump and were externally calibrated using sodium formate. The instrument was operated in the positive ion mode. Hydrogen peroxide disproportionation was titrated with a Piston Burette TITRONIC basic. Gas chromatography was carried out on a PerkinElmer Clarus 500 Gas Chromatograph with an Alltech EconocapTM ec TM 53.0 m x 0,0032 mm ID x 0.25 mm, 5% phenyl and 95% methylpolysiloxane column. Elemental microanalyses were carried out by the Mikroanalytisches Laboratorium Kolbe, Mülheim an der Ruhr, Germany.

6.4.3 Synthesis of *o,p*-di-Me-bapbpy

6,6'-dibromo-2,2'-bipyridine (302 mg, 0.96 mmol), Pd(dba)₂ (10.3 mg, 0.019 mmol), (*S*)-BINAP (11.9 mg, 0.019 mmol) and KO*t*-Bu (226 mg, 2.0 mmol) were weighed in a two-neck round-bottom flask, and placed under argon atmosphere, then suspended in distilled and degassed toluene (20 mL). The red colour suspension was stirred under argon for 20 mins before 2-amino-4,6-dimethylpyridine (246 mg, 2.0 mmol) was added. The dark brown suspension was heated to 80 °C and stirred under argon for 3 days. The reddish brown suspension was cooled to room temperature after 3 days, and demineralized water (20 mL) was added. The mixture was stirred vigorously for 1.5 hours, filtered, and washed with water (5 mL × 3), diethyl ether (5 mL × 3), and hexanes (5 mL × 3). The yellow powder was collected, dried in vacuo for two hours, to yield 82% of compound *o,p*-di-Me-bapbpy (313 mg, 0.79 mmol). Anal. Calcd for C₂₄H₂₄N₆ + H₂O: Calc: C, 69.53; H, 6.33; N, 20.28. Found: C, 69.7; H, 4.7; N, 19.8. ¹H NMR (300 MHz, *d*DMSO): δ = 9.65 (s, 2H, NH), 7.87 – 7.74 (m, 6H), 7.63 – 7.51 (m, 2H, CqCHCH₃), 6.63 (s, 2H, CCH₃CHCCH₃), 2.37 (s, 6H, NCqCH₃), 2.29 (s, 6H, CHCH₃CH). ¹³C-NMR (300 MHz, *d*DMSO): 21.00(CH₃), 23.69(CH₃), 108.97(CH), 111.98(CH), 112.09(CH), 116.44(CH), 132.04(C), 138.26(CH), 148.25(C), 153.54(C), 153.78(C), 154.14(C), 155.55(C). ESI-MS in DMF (m/z): 396.52 ([M + H]⁺ calcd.: 396.21). FTIR (cm⁻¹): 1575.5, 1564.0, 557.6, 1515.9, 1435.7, 1417.9, 1368.4, 1259.0, 1229.5, 1147.57, 989.9, 865.9, 825.8, 784.1, 736.2, 667.9, 611.4, 534.4, 519.2, 457.4, 327.9.

6.4.4 [Fe(OTf)₂(bapbpy)] (1)

Equimolar amounts of bapbpy (310 mg) and [Fe(MeCN)₂(OTf)₂] (400 mg) were stirred in THF (2 mL) under inert atmosphere. A pale yellow suspension immediately formed. After 16 h of stirring, the solids were allowed to sediment and the supernatant was decanted. The remaining precipitate was repetitively suspended and sedimented in THF (2 mL), THF:diethyl ether (2 × 3 mL) and diethyl ether (2 × 3 mL). After drying in vacuo for 0.5 h, a yellow powder was formed which was additionally dried overnight under high vacuum and subjected to elemental analysis (537 mg, 85%). Anal. Calcd. for [Fe(OTf)₂(bapbpy)]·0.5H₂O: C, 37.57, H, 2.44; N, 11.95; Found: C, 37.65; H, 2.65; N, 11.78. Yellow rod-like crystals, suitable for single crystal X-ray analysis were obtained by recrystallization from MeCN/diethyl ether by vapor diffusion overnight. Electronic absorption in MeCN (λ, ε (mM × cm)⁻¹): 364 (12), 311 (32), 264 (32). Solid state Raman, 785 nm (cm⁻¹): 1636, 1614, 1586, 1536, 1446, 1418, 1326, 1280, 1032, 1014. FTIR (cm⁻¹): 3320, 3252, 3215, 3154, 1639, 1587, 1538, 1488, 1466, 1448, 1433, 1374, 1294, 1222, 1182, 1162, 1028, 1010, 774. ¹H NMR (CD₃CN, ppm, 400 MHz): 7.2 (s), 8.3 (s), 10.5 (s), 29.7 (s), 42.4 (s), 61.2 (s), 64.7 (s), 76.2 (b). ¹⁹F NMR (CD₃CN, ppm, 400 MHz): -77.03. Solution effective magnetic moment (Evan's method) (value, T (°C)): 2.76, -40; 3.18, -30; 3.47, -20; 3.80, -10; 3.99, 0; 4.16, 10; 4.26, 20; 4.33, 25; 4.40, 30; 4.49, 40; 4.55, 50. ESI-MS in MeCN (m/z): 545.033 ([M-OTf]⁺ calcd.: 545.031).

6.4.5 [Fe(OTf)₂(*o,p*-di-Me-bapbpy)] (2)

A similar procedure was followed for the synthesis of **2** as for **1**. A yellow powder was formed which was dried overnight in vacuo and subjected to elemental analysis (325 mg, 89%). Anal. Calcd for [Fe(*o,p*-di-Me-bapbpy)(OTf)₂] (C₂₆H₂₄F₆FeN₆O₆S₂): C, 41.61; H, 3.22; N, 11.20; Found: C, 41.52; H, 3.32, N, 11.15. Yellow rod-like crystals, suitable for single crystal X-ray analysis were obtained by recrystallization in MeCN/diethyl ether by vapor diffusion overnight. Electronic absorption in MeCN (λ, ε (mM × cm)⁻¹): 370, (10); 313, (31); 268, (20). Solid state Raman, 785 nm (cm⁻¹): 2938, 2904, 1646, 1614, 1584, 1536,

Chapter 6

1454, 1392, 1340, 1286, 1268, 1234, 1034, 1006, 762. FTIR (cm^{-1}): 3336, 3233, 3166, 1649, 1605, 1585, 1541, 1476, 1455, 1370, 1285, 1248, 1223, 1174, 1159, 1028, 1004, 843, 798. ^1H NMR (CD_3CN , ppm, 400 MHz): -20.4 (s), -10.3 (s), -7.5 (s), 22.2 (b), 47.1 (s), 55.0 (s), 56.6 (s), 59.9 (s). Solution effective magnetic moment (Evan's method) (value, T ($^\circ\text{C}$)): 3.04, -40 ; 3.46, -30 ; 3.81, -20 ; 4.12, -10 ; 4.35, 0; 4.50, 10; 4.61, 20; 4.77, 25; 4.84, 30; 4.90, 40; 4.95, 50. ESI-MS in MeCN (m/z): 601.085 ($[\text{M-OTf}]^+$ calcd.: 601.093).

6.4.6 $[\text{Fe}_2(\mu\text{-O})(\text{OTf})_2(\text{bapbpy})_2](\text{OTf})_2$ (**3**)

To solution of **1** (70 mg) in MeCN (2 mL), 1 equiv. of AcOOH in MeCN (0.5 mL) was added and stirred for 0.5 h. To this solution, diethyl ether was added via vapor diffusion over 16 h to yield rod-like crystals, suitable for single crystal X-ray analysis (28 mg, 40%). Electronic absorption in MeCN (λ , ϵ ($\text{mM} \times \text{cm}$) $^{-1}$): 380, (11); 305, (19); 270, (18). Solid state Raman, 785 nm (cm^{-1}): 3084, 1618, 1588, 1548, 1456, 1420, 1336, 1284, 1250, 1036, 1016, 760. FTIR (cm^{-1}): 3312, 3256, 3210, 3151, 3106, 3052, 1641, 1586, 1541, 1490, 1469, 1450, 1434, 1279, 1225, 1162, 1027, 1012, 817, 796, 770. ^1H NMR (CD_3CN , ppm, 400 MHz): -12.5 (b), 5.1 (s), 7.2 (s), 8.8 (s), 13.1 (s), 15.5 (s), 16.3 (s), 30.8 (b). Solution effective magnetic moment (Evan's method) (value, T ($^\circ\text{C}$)): 2.22, -40 ; 2.25, -30 ; 2.30, -20 ; 2.36, -10 ; 2.39, 0; 2.42, 10; 2.44, 20; 2.46, 20; 2.48, 30; 2.57, 40; 2.64, 50. ESI-MS in MeCN (m/z): 1254.986 ($[\text{M-OTf}]^+$ calcd.: 1255.008), 553.024 ($[\text{M-OTf}]^{2+}$ calcd.: 553.028).

6.4.7 X-ray crystal structure determinations

Reflections were measured on a Bruker Kappa ApexII diffractometer with sealed tube and Triumph monochromator (compounds **1** and **3**) or on a Nonius KappaCCD diffractometer with rotating anode and graphite monochromator ($\mathbf{1}^*(\text{MeCN})_2$ and **2**). Software packages for intensity integration were Eval15^[79] (**1**, **2**, and **3**) and HKL2000^[80] ($\mathbf{1}^*(\text{MeCN})_2$). Absorption correction was performed with SADABS^[81] (**1** and **3**), TWINABS^[81] (**2**), or SORTAV^[82] ($\mathbf{1}^*(\text{MeCN})_2$). The structures were solved with Direct Methods using SHELXS-97^[83]. Least-squares refinement was performed with SHELXL-97^[83] (**1**, $\mathbf{1}^*(\text{MeCN})_2$, and **2**) or SHELXL-2013^[83] (**3**) against F^2 of all reflections. Non-hydrogen atoms were refined freely with anisotropic displacement parameters. Hydrogen atoms were located in difference Fourier maps (**1**, $\mathbf{1}^*(\text{MeCN})_2$, and **2**) or introduced in calculated positions (**3**). N-H hydrogen atoms in **1**, $\mathbf{1}^*(\text{MeCN})_2$, and **2** were refined freely with isotropic displacement parameters. All other hydrogen atoms were refined with a riding model. The crystal of **2** was cracked into two fragments and therefore integrated with two orientation matrices. Refinement was performed on a HKLF5 type of reflection file. In **3**, the non-coordinated triflate anions were refined with a disorder model using restraints for distances, angles and isotropic behavior. Geometry calculations and checking for higher symmetry was performed with the PLATON program.^[84]

6.4.8 DFT calculations

The calculations were done using density functional theory methods as employed in the *Gaussian-03* program package. The unrestricted B3LYP hybrid density functional method for all calculations was selected. All geometries were fully optimized (without geometric constraints) using a mixed basis set containing LACVP on Fe that includes a core potential and 6-31G on the rest of the atoms: basis set B1.3 This basis set gave adequate structures for the investigation of a potential energy profile of a chemical reaction by an iron(IV)-oxo species. A subsequent frequency calculation characterized the local minima with real frequencies only and the transition states with one imaginary frequency for the correct mode. To

improve the energetics, single point calculations using a triple- ζ _quality LACV3P+ basis set on Fe (with core potential) and 6-311+G* on the rest of the atoms were performed: basis set B2. Energies reported in here are taken from the UB3LYP/B2 results and are corrected for zero-point energies at UB3LYP/B1. Free energies use UB3LYP/B2 energies and UB3LYP/B1 zero-point energies, thermal and entropic corrections.

6.4.9 Oxidation of thianthrene oxide

Catalyst (7.2 μmol), thianthrene oxide and H_2O_2 were mixed in CD_3CN (1 mL) and the product was analyzed by ^{13}C NMR (CD_3CN , 400 MHz): 130.9, 129.1, 128.6.

6.4.10 Disproportionation of hydrogen peroxide

The iodometric titration of H_2O_2 was conducted in a similar fashion to a literature procedure.^[67] 7.2 μmol catalyst and H_2O_2 (33 equiv.) were dissolved in MeCN (5 mL). The mixture was stirred for 2 minutes, prior to addition of potassium iodide (45 equiv. in 1 ml H_2O), sulfuric acid (22 equiv. in 0.5 mL H_2O) and trace amounts of ammonium molybdate (VI) tetrahydrate. The mixture was titrated with 0.1 M sodium thiosulfate. The experiments were conducted twice and results averaged.

6.4.11 Oxidation at substrate-limiting scale

Alkene substrate (0.72 mmol), catalyst (0.01 equiv.), and MeCOOH (0.03 equiv.) were mixed in MeCN (3 mL). H_2O_2 (2 equiv.) in MeCN (1 mL) was added drop wise by hand and stirred until completion of the reaction. Diethyl ether (20 mL) and PhNO_2 as internal standard (1 equiv. in 1 mL MeCN) were added and the sample was subjected to GC analysis. The epoxide yields were compared with authentic samples.

6.4.12 Oxidation at oxidant-limiting scale

Alkene substrate (7.2 mmol) and catalyst (0.001 equiv.) were mixed in MeCN (3 mL). H_2O_2 (0.01 equiv.) in MeCN (0.5 mL) was added via syringe pump and stirred until completion of the reaction. Diethyl ether (3 mL) and nitrobenzene as internal standard (0.001 equiv. in 1 mL MeCN) were added and the sample was subjected to GC analysis. The epoxide yields were compared with authentic samples and expressed compared to the addition of oxidant.

6.5 Acknowledgements

The work described in this chapter was supported by the COST action CM1003; the Costas group at the University of Girona is acknowledged for low-temperature ESI-MS experiments and the Brown group at the University of Groningen is acknowledged for a series of Raman, EPR, and electrochemistry experiments. The EU ITN program Nanohost is thanked for supporting the time Dr. Sam de Visser spent time in Utrecht as a visiting professor.

Chapter 6

6.6 References

- [1] M. Costas, M. P. Mehn, M. P. Jensen, L. Que Jr. *Chem. Rev.* **2004**, *104*, 939.
- [2] A. R. McDonald, L. Que Jr. *Coord. Chem. Rev.* **2013**, *257*, 414.
- [3] J. Rohde, J. In, M. H. Lim, W. W. Brennessel, M. R. Bukowski, A. Stubna, E. Münck, W. Nam, L. Que Jr. *Science* **2003**, *299*, 1037.
- [4] C. V. Sastri, M. J. Park, T. Ohta, T. A. Jackson, A. Stubna, M. S. Seo, J. Lee, J. Kim, T. Kitagawa, E. Münck *J. Am. Chem. Soc.* **2005**, *127*, 12494.
- [5] T. A. Jackson, J. Rohde, M. S. Seo, C. V. Sastri, R. DeHont, A. Stubna, T. Ohta, T. Kitagawa, E. Münck, W. Nam, L. Que Jr. *J. Am. Chem. Soc.* **2008**, *130*, 12394.
- [6] D. M. Kurtz *Chem. Rev.* **1990**, *90*, 585.
- [7] Y. Feng, J. England, L. Que Jr. *ACS Catal.* **2011**, *1*, 1035.
- [8] Y. Suh, M. S. Seo, K. M. Kim, Y. S. Kim, H. G. Jang, T. Tosha, T. Kitagawa, J. Kim, W. Nam *J. Inorg. Biochem.* **2006**, *100*, 627.
- [9] M. R. Bukowski, K. D. Koehntop, A. Stubna, E. L. Bominaar, J. A. Halfen, E. Münck, W. Nam, L. Que Jr. *Science* **2005**, *310*, 1000.
- [10] W. Nam, R. Ho, J. S. Valentine *J. Am. Chem. Soc.* **1991**, *113*, 7052.
- [11] W. Nam, H. J. Kim, S. H. Kim, R. Y. N. Ho, J. S. Valentine *Inorg. Chem.* **1996**, *35*, 1045.
- [12] A. Chanda, X. Shan, M. Chakrabarti, W. C. Ellis, D. L. Popescu, F. Tiago de Oliveira, D. Wang, L. Que Jr., T. J. Collins, E. Münck, E. L. Bominaar *Inorg. Chem.* **2008**, *47*, 3669.
- [13] D. Popescu, M. Vrabel, A. Brausam, P. Madsen, G. Lente, I. Fabian, A. D. Ryabov, R. van Eldik, T. J. Collins *Inorg. Chem.* **2010**, *49*, 11439.
- [14] E. S. Beach, J. L. Duran, C. P. Horwitz, T. J. Collins *Ind. Eng. Chem. Res.* **2009**, *48*, 7072.
- [15] E. Molenbroek, N. Straathof, S. Duck, Z. Rashid, J. H. van Lenthe, M. Lutz, A. Gandubert, R. J. M. Klein Gebbink, L. De Cola, S. Bonnet *Dalton Trans.* **2013**, *42*, 2973.
- [16] I. Gamba, I. Mutikainen, E. Bouwman, J. Reedijk, S. Bonnet *Eur. J. Inorg. Chem.* **2013**, *2013*, 115.
- [17] S. Bonnet, M. A. Siegler, J. S. Costa, G. Molnar, A. Bousseksou, A. L. Spek, P. Gamez, J. Reedijk *Chem. Commun.* **2008**, 5619.
- [18] S. Bonnet, G. Molnar, J. Sanchez Costa, A. L. Spek, A. Bousseksou, W. T. Fu, P. Gamez, J. Reedijk *Chem. Mater.* **2009**, *21*, 1123.
- [19] Z. Arcis-Castillo, S. Zheng, M. A. Siegler, O. Roubeau, S. Bedoui, S. Bonnet *Chem. Eur. J.* **2011**, *17*, 14826.
- [20] J. A. Real, A. B. Gaspar, M. C. Muñoz *Dalton Trans.* **2005**, 2062.
- [21] A. Bousseksou, G. Molnar, L. Salmon, W. Nicolazzi *Chem. Soc. Rev.* **2011**, *40*, 3313.
- [22] B. Weber *Coord. Chem. Rev.* **2009**, *253*, 2432.
- [23] O. Sato, J. Tao, Y. Zhang *Angew. Chem. Int. Ed.* **2007**, *46*, 2152.
- [24] H. A. Goodwin *Coord. Chem. Rev.* **1976**, *18*, 293.
- [25] P. Gütllich, A. Hauser *Coord. Chem. Rev.* **1990**, *97*, 1.
- [26] P. Gütllich, A. Hauser, H. Spiering *Angew. Chem. Int. Ed.* **1994**, *33*, 2024.
- [27] P. Gamez, J. S. Costa, M. Quesada, G. Aromi *Dalton Trans.* **2009**, 7845.
- [28] M. Kepenekian, J. S. Costa, B. Le Guennic, P. Maldivi, S. Bonnet, J. Reedijk, P. Gamez, V. Robert *Inorg. Chem.* **2010**, *49*, 11057.
- [29] H. J. Shepherd, S. Bonnet, P. Guionneau, S. Bedoui, G. Garbarino, W. Nicolazzi, A. Bousseksou, G. Molnar *Phys. Rev. B* **2011**, *84*, 144107.
- [30] S. Pillet, E. Bendeif, S. Bonnet, H. J. Shepherd, P. Guionneau *Phys. Rev. B* **2012**, *86*, 064106.

- [31] J. S. Costa, K. Lappalainen, G. de Ruiter, M. Quesada, J. Tang, I. Mutikainen, U. Turpeinen, C. M. Grunert, P. Gütlich, H. Z. Lazar, J. Letard, P. Gamez, J. Reedijk *Inorg. Chem.* **2007**, *46*, 4079.
- [32] K. Chen, M. Costas, J. Kim, A. K. Tipton, L. Que Jr. *J. Am. Chem. Soc.* **2002**, *124*, 3026.
- [33] M. Costas, L. Que Jr. *Angew. Chem. Int. Ed.* **2002**, *41*, 2179.
- [34] K. Robinson, G. V. Gibbs, P. H. Ribbe *Science* **1971**, *172*, 567.
- [35] M. A. H. Moelands, S. Nijse, E. Folkertsma, B. de Bruin, M. Lutz, A. L. Spek, R. J. M. Klein Gebbink *Inorg. Chem.* **2013**, *52*, 7394.
- [36] A. Draksharapu, Q. Li, H. Logtenberg, van den Berg, T. A., A. Meetsma, J. S. Killeen, B. L. Feringa, R. Hage, G. Roelfes, W. R. Browne *Inorg. Chem.* **2012**, *51*, 900.
- [37] S. McClanahan, J. Kincaid *J. Raman Spectrosc.* **1984**, *15*, 173.
- [38] P. C. A. Bruijninx, I. L. C. Buurmans, S. Gosiewska, M. A. H. Moelands, M. Lutz, A. L. Spek, G. van Koten, R. J. M. Klein Gebbink *Chem. Eur. J.* **2008**, *14*, 1228.
- [39] M. Lubben, A. Meetsma, E. C. Wilkinson, B. Feringa, L. Que Jr. *Angew. Chem. Int. Ed.* **1995**, *34*, 1512.
- [40] Y. Zang, J. Kim, Y. Dong, E. C. Wilkinson, E. H. Appelman, L. Que Jr. *J. Am. Chem. Soc.* **1997**, *119*, 4197.
- [41] G. Roelfes, V. Vrajmasu, K. Chen, R. Y. N. Ho, J. Rohde, C. Zondervan, R. M. la Crois, E. P. Schudde, M. Lutz, A. L. Spek, R. Hage, B. L. Feringa, E. Münck, L. Que Jr. *Inorg. Chem.* **2003**, *42*, 2639.
- [42] A. T. Fiedler, H. L. Halfen, J. A. Halfen, T. C. Brunold *J. Am. Chem. Soc.* **2005**, *127*, 1675.
- [43] M. J. Collins, K. Ray, L. Que Jr. *Inorg. Chem.* **2006**, *45*, 8009.
- [44] H. R. Chang, J. K. McCusker, H. Toftlund, S. R. Wilson, A. X. Trautwein, H. Winkler, D. N. Hendrickson *J. Am. Chem. Soc.* **1990**, *112*, 6814.
- [45] L. Gómez, I. Garcia-Bosch, A. Company, J. Benet-Buchholz, A. Polo, X. Sala, X. Ribas, M. Costas *Angew. Chem. Int. Ed.* **2009**, *48*, 5720.
- [46] L. J. Wilson, D. Georges, M. A. Hoselton *Inorg. Chem.* **1975**, *14*, 2968.
- [47] M. H. Lim, J. Rohde, A. Stubna, M. R. Bukowski, M. Costas, R. Y. N. Ho, E. Münck, W. Nam, L. Que Jr. *PNAS* **2003**, *100*, 3665.
- [48] S. P. de Visser *J. Am. Chem. Soc.* **2006**, *128*, 15809.
- [49] D. Kumar, G. N. Sastry, S. P. de Visser *J. Phys. Chem. B* **2012**, *116*, 718.
- [50] J. Bautz, P. Comba, C. Lopez de Laorden, M. Menzel, G. Rajaraman *Angew. Chem. Int. Ed.* **2007**, *46*, 8067.
- [51] J. H. Helms, L. W. Ter Haar, W. E. Hatfield, D. L. Harris, K. Jayaraj, G. E. Toney, A. Gold, T. D. Mewborn, J. E. Pemberton *Inorg. Chem.* **1986**, *25*, 2334.
- [52] A. Ikezaki, M. Nakamura *J. Inorg. Biochem.* **2001**, *84*, 137.
- [53] M. M. Monzyk, *Characterization of some mu-oxo homonuclear dimers containing the metals iron and manganese*, Source Graduate Faculty of Texas Tech University, Dissertation, **1997**.
- [54] R. Mayilmurugan, H. Stoeckli-Evans, E. Suresh, M. Palaniandavar *Dalton Trans.* **2009**, 5101.
- [55] G. Roelfes, M. Lubben, K. Chen, R. Y. N. Ho, A. Meetsma, S. Genseberger, R. M. Hermant, R. Hage, S. K. Mandal, V. G. Young Jr., Y. Zang, H. Kooijman, A. L. Spek, L. Que Jr., B. L. Feringa *Inorg. Chem.* **1999**, *38*, 1929.
- [56] R. E. Norman, R. C. Holz, S. Menage, L. Que Jr., J. H. Zhang, C. J. O'Connor *Inorg. Chem.* **1990**, *29*, 4629.
- [57] O. Y. Lyakin, R. V. Ottenbacher, K. P. Bryliakov, E. P. Talsi *ACS Catal.* **2012**, *2*, 1196.

Chapter 6

- [58] J. T. Groves *J. Inorg. Biochem.* **2006**, *100*, 434.
- [59] W. Nam, H. J. Han, S. Y. Oh, Y. J. Lee, M. H. Choi, S. Y. Han, C. Kim, S. K. Woo, W. Shin *J. Am. Chem. Soc.* **2000**, *122*, 8677.
- [60] J. Rohde, A. Stubna, E. L. Bominaar, E. Münck, W. Nam, L. Que Jr. *Inorg. Chem.* **2006**, *45*, 6435.
- [61] J. Rohde, L. Que Jr. *Angew. Chem.* **2005**, *117*, 2295.
- [62] T. G. Traylor, C. Kim, W. Fann, C. L. Perrin *Tetrahedron* **1998**, *54*, 7977.
- [63] T. G. Traylor, S. Tsuchiya, Y. S. Byun, C. Kim *J. Am. Chem. Soc.* **1993**, *115*, 2775.
- [64] A. R. McDonald, L. Que Jr. *Nat. Chem.* **2011**, *3*, 761.
- [65] K. Sato, M. Hyodo, M. Aoki, X. Zheng, R. Noyori *Tetrahedron* **2001**, *57*, 2469.
- [66] G. B. Payne, P. H. Deming, P. H. Williams *J. Org. Chem.* **1961**, *26*, 659.
- [67] A. I. Vogel, *A textbook of quantitative inorganic analysis*, Longmans, London, **1962**.
- [68] B. Zyska, M. Schwalbe *Chem. Commun.* **2013**, *49*, 3799.
- [69] R. V. Ottenbacher, D. G. Samsonenko, E. P. Talsi, K. P. Bryliakov *Org. Lett.* **2012**, *14*, 4310.
- [70] M. Bonchio, M. Carraro, A. Farinazzo, A. Sartorel, G. Scorrano, U. Kortz *J. Mol. Catal. A: Chem.* **2007**, *262*, 36.
- [71] P. Spanning, V. Yazerski, P. C. A. Bruijninx, B. M. Weckhuysen, R. J. M. Klein Gebbink *Chem. Eur. J.* **2013**, *19*, 15012 (Chapter 3 of this thesis).
- [72] R. Mas-Ballesté, L. Que Jr. *J. Am. Chem. Soc.* **2007**, *129*, 15964.
- [73] M. S. Chen, M. C. White *Science* **2007**, *318*, 783.
- [74] M. Fujita, L. Que Jr. *Adv. Synth. Catal.* **2004**, *346*, 190.
- [75] X. L. Bai, X. D. Wang, C. Q. Kang, L. X. Gao *Synthesis* **2005**, *3*, 458.
- [76] K. S. Hagen *Inorg. Chem.* **2000**, *39*, 5867.
- [77] K. Amani, M. Zolfigol, A. Ghorbani-Choghamarani, M. Hajjami *Monatsh. Chem.* **2009**, *140*, 65.
- [78] D. F. J. Evans *J. Chem. Soc.* **1959**, 2003.
- [79] A. M. M. Schreurs, X. Xian, L. M. J. Kroon-Batenburg *J. Appl. Cryst.* **2010**, *43*, 70.
- [80] Z. Otwinowski, W. Minor, *Methods in Enzymology, Volume 276*, **1997**, 307-326.
- [81] G. M. Sheldrick, SADABS and TWINABS: Area-Detector Absorption Correction, **1999**, Universität Göttingen, Germany.
- [82] R. H. Blessing *Acta Crystallograph. Sect. A* **1995**, *51*, 33.
- [83] G. M. Sheldrick *Acta Crystallograph. Sect. A* **2008**, *64*, 112.
- [84] A. L. Spek *Acta Crystallograph. Sect. D* **2009**, *65*, 148.

Addendum

Synthesis and structure of $[\text{Mn}(\text{OTf})_2(\text{bapbpy})]$ and $[\text{Mn}(\text{OTf})_2(o,p\text{-di-Me-bapbpy})]$

Based on: Peter Spanring, Martin Lutz, Pieter C. A. Bruijninx, Bert M. Weckhuysen, and Robertus J. M. Klein Gebbink, manuscript in preparation

As part of the investigations on the coordination chemistry of bapbpy ligands and the development of first-row transition metal complexes for catalytic oxidative transformations, some bapbpy-derived manganese complexes were studied. The syntheses of the $[\text{Mn}(\text{OTf})_2(\text{bapbpy})]$ (**1**) and $[\text{Mn}(\text{OTf})_2(o,p\text{-di-Me-bapbpy})]$ (**2**) complexes involved the reaction of equimolar amounts of the bapbpy or *o,p*-di-Me-bapbpy ligand with $[\text{Mn}(\text{OTf})_2(\text{MeCN})_2]$ in a minimal amount of MeCN under inert conditions for 16 h and recrystallization of the crude product from MeCN/ether (Figure 1). The resulting yellow powders (yields: 81% for **1** and 80% for **2**) were analyzed by elemental analysis to confirm their purity.

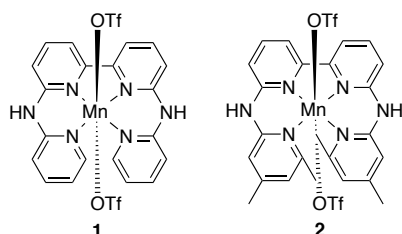


Figure 1. Structures of $[\text{Mn}(\text{OTf})_2(\text{bapbpy})]$ (**1**) and $[\text{Mn}(\text{OTf})_2(o,p\text{-di-Me-bapbpy})]$ (**2**).

Crystals suitable for X-ray diffraction of **1** were obtained from a concentrated solution of **1** in MeCN at $-20\text{ }^\circ\text{C}$. Single crystals of **2** were obtained by slow evaporation of a concentrated solution of **2** in MeCN. Both complexes show a distorted octahedral geometry in the solid state. In both molecules, the Mn center is close to the N,N,N,N least-squares plane of the ligand ($<0.03\text{ \AA}$). Although $[\text{Cu}(\text{II})(\text{bapbpy})(\text{H}_2\text{O})]\text{Cl}_2\cdot\text{H}_2\text{O}$,^[1] $[\text{Zn}(\text{II})\text{Cl}(\text{bapbpy})]\text{Cl}\cdot\text{H}_2\text{O}$ ^[2] and $[\text{Mn}(\text{II})\text{Cl}(\text{tmc})]\text{BPh}_4\cdot\text{MeCN}$ ^[3] (tmc = 1,4,8,11-tetraazacyclotetradecane) show a pentacoordination environment around the metal, a hexa-coordinated Mn(II) center is observed in **1** and **2**, with the two triflate anions binding in the axial positions (Figure 2). The characteristic twisting of the bapbpy ligand around the metal center is also observed for these Mn(II) complexes.^[4-6] The overall symmetry of the complexes is C_1 , which is similar to the iron complexes described in Chapter 6. Bond angles and distances in **1** and **2** are listed in Table 1. Complex **2** and $[\text{Fe}(\text{OTf})_2(o,p\text{-di-Me-bapbpy})]$ (Chapter 6) are isostructural. The slight differences in the geometries can be attributed to the difference in atomic radii of Fe and Mn. On the other hand, **1** and $[\text{Fe}(\text{OTf})_2(\text{bapbpy})]$ (Chapter 6) crystallize in a different space group as a consequence of a different packing.

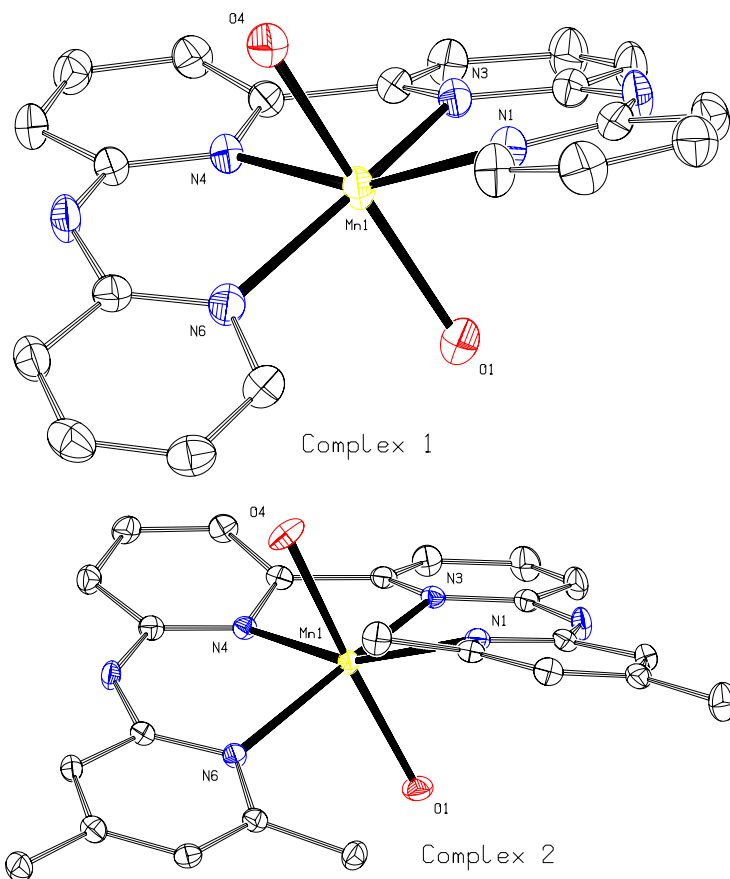


Figure 2. ORTEP plots of $[\text{Mn}(\text{OTf})_2(\text{bapbpy})]$ (**1**) and $[\text{Mn}(\text{OTf})_2(o,p\text{-di-Me-bapbpy})]$ (**2**) at 50% probability. Hydrogen atoms are omitted and only the coordinating O atoms from the triflate anions are shown for clarity.

The Mn-N bond distances have values between 2.1801(16) to 2.1976(15) Å for **1** and 2.2050(16) to 2.2520(16) Å for **2**. These are in conjunction with high-spin Mn(II) centers,^[7, 8] like for $[\text{Mn}(\text{II})\text{Cl}(\text{tmc})]\text{BPh}_4\cdot\text{MeCN}$ (2.283(3)-2.281(3) Å).^[3] These bond distances are significantly larger than Mn-N distances in Mn(III)(cyclam) complexes (2.03 Å; cyclam = 1,4,8,11-tetraaza-cyclotetradecane),^[9] or the Mn-N distances in Mn(II)-porphyrine derivatives of intermediate spin (1.93-1.94 Å).^[10] With **1**, the Mn-N3 and Mn-N4 distances (stemming from the bipyridine moiety) are almost identical, whereas the Mn-N1 and Mn-N6 distances are significantly different (stemming from the terminal pyridines). This is opposite to the Fe-N distances in $[\text{Fe}(\text{OTf})_2(\text{bapbpy})]$. The Mn-N3 and Mn-N4, and the Mn-N1 and Mn-N6 distances are more similar to the corresponding Fe-N distances in **2**. Considering the intramolecular O-Mn-O angles, the value of 177.36(6)° is more linear in **2** than in **1** (168.30(5)°). These values are similar to the ones described for

the Fe-complexes (Chapter 6). As with the Fe-complexes, the ligand twisting, as indicated by the interplanar angles of the terminal pyridines, is larger in **1** (37.54(10)°) than in **2** (29.45(11)°). On the other hand, the bipyridine moieties are more in-plane in **1** (17.45(9)° interplanar angle) than in **2** (23.20(11)°), which is opposite to the observation made for the Fe derivatives. The angular variance^[11] of **1** and **2** is 141.49 deg² and 128.12 deg², respectively, indicate that the angles in **1** are more distorted from perfect octahedral angles than in **2**.

Table 1. Bond distances and angles of **1** and **2**. Distances are reported in Å, angles in °.

	1	2
Mn1-N1	2.1801(16)	2.2565(16)
Mn1-N3	2.1976(15)	2.2132(16)
Mn1-N4	2.1952(15)	2.2050(16)
Mn1-N6	2.1964(16)	2.2520(16)
Mn1-O1	2.2336(14)	2.2500(14)
Mn1-O4	2.2710(14)	2.2202(15)
N3-Mn1-N4	75.89(6)	75.60(6)
N1-Mn1-N6	116.01(6)	116.94(6)
O1-Mn1-O4	168.30(5)	177.36(6)
Bipyridines ^a	18.45(9)	23.20(11)
Pyridines ^b	37.54(10)	29.45(11)
Mn-N,N,N,N ^c	0.0306(3)	-0.0187(4)

^a Interplanar angle between the least square-planes of N3, C6, C7, C8, C9, C10 with N4, C11, C12, C13, C14, C15; ^b Interplanar angle between the least square-planes of N1, C1, C2, C3, C4, C5 with N6, C16, C17, C18, C19, C20; ^c Distance of the least square plane of N1, N3, N4, N6 with Mn1.

Unlike bapbpy-complexes with Zn or Cu that form a pentacoordination environment, the Mn derivatives form octahedral structures around the metal. The similar structural features between **1** and **2** are remarkable and indicate that the additional methyl groups only have a minor sterical influence. The Mn-complexes are thus very similar to their iron counterparts, and can be expected to be suitable oxidizing agents as well.

Experimental Section

General

Dry MeCN and diethyl ether were obtained from MBraun MB SPS-800 solvent purification system. Reactions were performed under inert conditions. The ligand bapbpy^[4, 5] was synthesized according to literature procedures, the ligand *o,p*-di-Me-bapbpy was synthesized as in Chapter 6. [Mn(OTf)₂(MeCN)₂] was synthesized according to a literature procedure of similar precursors.^[12, 13] Electronic absorption spectra were obtained using a Varian Cary 50 scan UV-Visible spectrometer at ambient temperature. Infra-red spectra were recorded using a Perkin-Elmer Spectrum One FT-IR spectrometer in the range of 650-4000 cm⁻¹. ESI-MS spectra were recorded using a Waters LCT

Premier XE instrument in MeCN solvent. Elemental microanalyses were carried out by the Mikroanalytisches Laboratorium Kolbe, Mülheim an der Ruhr, Germany.

[Mn(OTf)₂(bapbpy)] (1)

Equimolar amounts of bapbpy (310 mg, 0.91 mmol) and [Mn(OTf)₂(MeCN)₂] (398 mg, 0.91 mmol) were combined in MeCN (2 mL). A pale yellow suspension immediately formed. After 16 h, the solids were allowed to settle and the supernatant was decanted. The remaining precipitate was repetitively suspended and settled in THF (2 mL), THF/ether (1/1 (v/v), 6 mL) and ether (2 x 3 mL). After drying in vacuo, a yellow powder was isolated (511 mg, 81%). Anal. Calcd for 1.0.5(H₂O).0.5(MeCN): C, 38.21, H, 2.58; N, 12.59; Found: C, 38.27; H, 2.87; N, 12.55. Yellow rod-like crystals, suitable for X-ray analysis were obtained from a concentrated solution in MeCN at -20 °C after one week. UV-Vis (MeCN, λ (ε ((mM×cm)⁻¹): 275 (18), 315 (25), 366 (10). FTIR (cm⁻¹): 3351.97, 3327.90, 3222.39, 3158.80, 1640.86, 1586.72, 1540.64, 1492.52, 1464.86, 1448.26, 1434.55, 1377.24, 1285.06, 1221.51, 1191.65, 1181.73, 1163.82, 1025.59, 1008.44, 869.47, 847.71, 823.54, 799.98, 772.39. ESI-MS in MeCN (m/z): 544.032, ([M-OTf]⁺ calcd.: 544.034).

[Mn(OTf)₂(*o,p*-di-Me-bapbpy)] (2)

Complex **2** was synthesized following a similar procedure as described for **1**. Starting from [Mn(OTf)₂(MeCN)₂] (218 mg, 0.50 mmol) and *o,p*-di-Me-bapbpy (198 mg, 0.50 mmol), **2** was isolated as a yellow powder in 81% yield (305 mg, 0.41 mmol). Anal. Calcd for 2.0.5(H₂O).0.5(MeCN): C, 41.62, H, 3.43; N, 11.69; Found: C, 41.67; H, 3.71; N, 11.65. Yellow rod-like crystals, suitable for X-ray analysis were obtained by slow evaporation of a concentrated solution of **2** over a week. Electronic absorption in MeCN at RT (λ, ε ((mM×cm)⁻¹): 267, 19; 312, 25; 368, 10. Solid state Raman, 785 nm (cm⁻¹): 1648, 1622, 1598, 1584 (major), 1536, 1454 (major), 1394, 1384, 1370, 1338 (major), 1284, 1266, 1234, 1036, 1004, 762, 730, 638. FTIR (cm⁻¹): 3349.95, 3234.85, 3165.53, 1647.99, 1603.37, 1585.04, 1542.97, 1472.64, 1453.42, 1370.35, 1286.95, 1222.13, 1174.26, 1159.61, 1028.70, 1002.22, 880.45, 842.42, 798.25, 762.47, 739.99 and 695.70. ESI-MS in MeCN (m/z): 600.089, ([M-OTf]⁺ calcd.: 600.096).

X-ray crystal structure determinations

X-ray intensities were measured with Mo-Kα radiation (λ = 0.71073 Å) on a Nonius KappaCCD diffractometer with rotating anode and graphite monochromator (compound **1**) or on a Bruker Kappa ApexII diffractometer with sealed tube and Triumph monochromator (compound **2**). The intensities were integrated using HKL2000^[14] (compound **1**) or Eval15^[15] (compound **2**). Absorption correction and scaling was performed with SADABS^[16] (compound **2**). The structures were solved using the program SHELXS-97^[17] (compound **1**) or using the coordinates of the isostructural Fe compound (compound **2**). Least-squares refinement was performed with SHELXL-97^[17] against F² of all reflections. Non-hydrogen atoms were refined with anisotropic displacement parameters. All hydrogen atoms were located in difference Fourier maps. C-H hydrogen atoms were refined with a riding model; N-H hydrogen atoms were refined freely with isotropic displacement parameters. Geometry calculations and checking for higher symmetry was performed with the PLATON program.^[18] Compound **1**: C₂₂H₁₆F₆MnN₆O₆S₂, Fw = 693.47, yellow block, 0.18 × 0.15 × 0.06 mm³, T = 150(2) K, monoclinic, P2/c (no. 13), a = 14.8317(1), b = 9.6261(1), c = 19.2043(2) Å, β = 110.4330(4) °, V = 2569.31(4) Å³, Z = 4, D_x = 1.793 g/cm³, μ = 0.77 mm⁻¹. 45931 Reflections were measured up to a resolution of (sin θ/λ)_{max} = 0.65 Å⁻¹. 5895 Reflections were unique (R_{int} = 0.057), of which 4487 were observed [I > 2σ(I)]. 396 Parameters were refined with no

restraints. R1/wR2 [$I > 2\sigma(I)$]: 0.0340 / 0.0823. R1/wR2 [all refl.]: 0.0540 / 0.0893. S = 1.048. Residual electron density between -0.53 and $0.35 \text{ e}/\text{\AA}^3$.

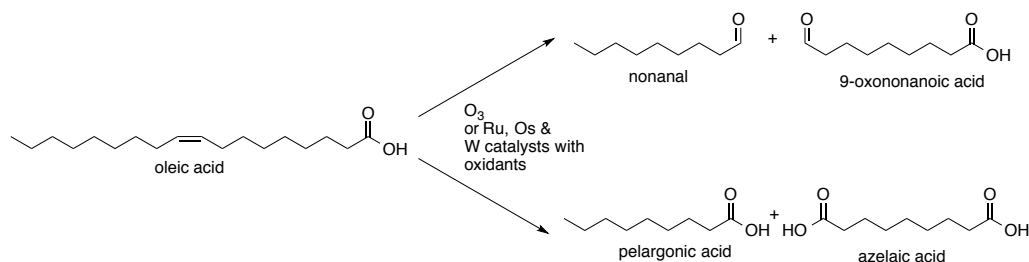
Compound 2: $\text{C}_{26}\text{H}_{24}\text{F}_6\text{MnN}_6\text{O}_6\text{S}_2$, Fw = 749.57, pale yellow needle, $0.28 \times 0.06 \times 0.05 \text{ mm}^3$, T = 110(2) K, monoclinic, P2₁/c (no. 14), a = 11.6499(5), b = 17.7555(6), c = 16.2800(5) Å, $\beta = 118.473(2)^\circ$, V = 2960.19(19) Å³, Z = 4, D_x = 1.682 g/cm³, $\mu = 0.68 \text{ mm}^{-1}$. 31854 Reflections were measured up to a resolution of $(\sin \theta/\lambda)_{\text{max}} = 0.65 \text{ \AA}^{-1}$. 6781 Reflections were unique ($R_{\text{int}} = 0.042$), of which 5040 were observed [$I > 2\sigma(I)$]. 436 Parameters were refined with no restraints. R1/wR2 [$I > 2\sigma(I)$]: 0.0341 / 0.0691. R1/wR2 [all refl.]: 0.0595 / 0.0768. S = 1.010. Residual electron density between -0.42 and $0.39 \text{ e}/\text{\AA}^3$.

References

- [1] I. Gamba, I. Mutikainen, E. Bouwman, J. Reedijk, S. Bonnet *Eur. J. Inorg. Chem.* **2013**, 2013, 115.
- [2] E. Molenbroek, N. Straathof, S. Duck, Z. Rashid, J. H. van Lenthe, M. Lutz, A. Gandubert, R. J. M. Klein Gebbink, L. De Cola, S. Bonnet *Dalton Trans.* **2013**, 42, 2973.
- [3] C. Bucher, E. Duval, J. Barbe, J. Verpeaux, C. Amatore, R. Guilard, P. Le Laurent, J. Latour, S. Dahaoui, C. Lecomte *Inorg. Chem.* **2001**, 40, 5722.
- [4] S. Bonnet, M. A. Siegler, J. S. Costa, G. Molnar, A. Bousseksou, A. L. Spek, P. Gamez, J. Reedijk *Chem. Commun.* **2008**, 5619.
- [5] S. Bonnet, G. Molnar, J. Sanchez Costa, A. L. Spek, A. Bousseksou, W. T. Fu, P. Gamez, J. Reedijk *Chem. Mater.* **2009**, 21, 1123.
- [6] Z. Arcis-Castillo, S. Zheng, M. A. Siegler, O. Roubeau, S. Bedoui, S. Bonnet *Chem. Eur. J.* **2011**, 17, 14826.
- [7] T. W. Chow, Y. Liu, C. Che *Chem. Commun.* **2011**, 47, 11204.
- [8] I. Garcia-Bosch, A. Company, X. Fontrodona, X. Ribas, M. Costas *Org. Lett.* **2008**, 10, 2095.
- [9] P. A. Daugherty, J. Glerup, P. A. Goodson, D. J. Hodgson, K. Michelsen *Acta Chem. Scand.* **1991**, 45, 244.
- [10] J. F. Kirner, W. Dow, W. R. Scheidt *Inorg. Chem.* **1976**, 15, 1685.
- [11] K. Robinson, G. V. Gibbs, P. H. Ribbe *Science* **1971**, 172, 567.
- [12] K. S. Hagen *Inorg. Chem.* **2000**, 39, 5867.
- [13] M. A. H. Moelands, S. Nijse, E. Folkertsma, B. de Bruin, M. Lutz, A. L. Spek, R. J. M. Klein Gebbink *Inorg. Chem.* **2013**, 52, 7394.
- [14] Z. Otwinowski, W. Minor, *Methods in Enzymology, Volume 276*, **1997**, 307-326.
- [15] A. M. M. Schreurs, X. Xian, L. M. J. Kroon-Batenburg *J. Appl. Cryst.* **2010**, 43, 70.
- [16] G. M. Sheldrick, **1999**, SADABS: Area-Detector Absorption Correction, Universität Göttingen, Germany.
- [17] G. M. Sheldrick *Acta Crystallograph. Sect. A* **2008**, 64, 112.
- [18] A. L. Spek *Acta Crystallograph. Sect. D* **2009**, 65, 148.

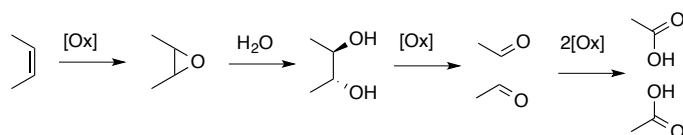
Summary

The oxidative cleavage of unsaturated fatty acids into either aliphatic aldehydes or carboxylic acids gives access to valuable products for the chemical industry. Currently, ozonolysis is applied industrially to cleave the fatty acid oleic acid into nonanal and 9-oxononanoic acid or into pelargonic and azelaic acid (Scheme 1). The use of ozone as oxidant comes with considerable disadvantages, however, as it is considered hazardous because of the associated severe explosion risks and, accordingly, needs to be made in-situ. Catalytic alternatives to the use of ozone for oxidative alkene cleavage are described in **Chapter 1** of this thesis and mostly concern methods based on the metals Ru, Os, or W. Such catalyst systems come with the disadvantage of being expensive and environmentally unfriendly due to scarcity and toxicity of the metals used. The development of new, more benign methods that make use of alternative, preferably first-row transition metals such as Fe are highly desired. Several reports describe the use of first-row transition metals in the oxidative cleavage of alkenes, but these are limited to the conversion of activated styrene derivatives. Indeed, examples of the oxidative cleavage of aliphatic substrates such as unsaturated fatty acids with first-row transition metal catalysts were not yet available at the start of the work described in this thesis.



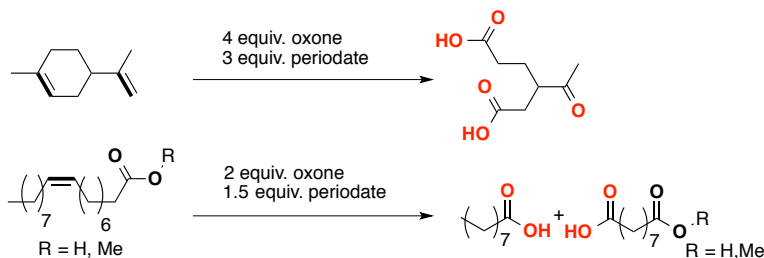
Scheme 1. Oxidative cleavage of oleic acid into either aldehydes or carboxylic acids. This process is currently commercially applied with the use of ozone as oxidant, with alternative catalytic methods being primarily based on the combination of Ru, Os or W-based catalysts and various oxidants.

The main oxidative cleavage strategy that has been developed over the subsequent chapters was envisaged to consist of a sequence of steps starting with alkene epoxidation, followed by hydrolysis towards the *trans*-diol and further oxidation to either the aldehyde or the carboxylic acid stage (Scheme 2).



Scheme 2. Main oxidative cleavage strategy for the transformation of alkenes into either aldehydes or the further oxidation to carboxylic acids

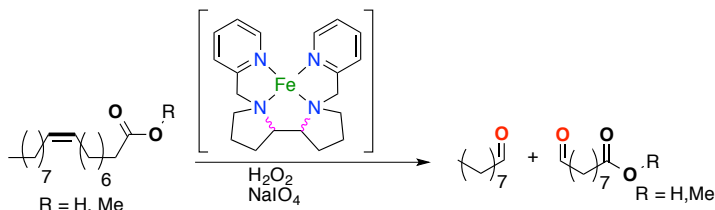
In search of a suitable set of oxidants for the catalytic cleavage of unsaturated fatty acids a combination of oxidants was found that allows for this reaction to proceed in a stoichiometric manner without the involvement of any transition metal. **Chapter 2** describes how a combination of oxone ($2\text{KHSO}_5 \cdot \text{KHSO}_4 \cdot \text{K}_2\text{SO}_4$) and sodium periodate (NaIO_4) can cleave a series of alkenes, including terpenes and unsaturated fatty acids, in aqueous MeCN in a clean and highly selective manner (Scheme 3). The mechanism involves oxone (containing the active oxidizing species KHSO_5 and acidic protons) performing the epoxidation, hydrolysis and aldehyde oxidation, and NaIO_4 oxidizing the diols into aldehydes. The choice of an appropriate solvent system to dissolve both the substrates and oxidants was found to be crucial for the successful outcome of these reactions. The synthetically straightforward, one-pot procedure for the cleavage of unsaturated fatty acids requires reflux temperatures in a solvent mixture that is initially composed of 3:1 (v/v) MeCN:H₂O and later diluted with water to 1:3 (v/v) MeCN:H₂O for the final periodate-mediated cleavage of the diol intermediate. In contrast, terpenes and simple alkenes can be cleaved at ambient temperatures and all steps in the catalytic sequence can be performed in 3:1 (v/v) MeCN:H₂O. The new methods allow for very high carboxylic acid yields (>95%) to be obtained within 18 to 72 h. The ease of the procedure make this method a convenient and readily applicable synthetic protocol for the lab-scale synthesis of carboxylic acids from alkenes. Indeed, the method's high yields and facile product isolation by simple solvent extraction compare well to methods that use stoichiometric oxidants such as KMnO_4 or catalytic systems using Ru, Os or W, which often require additional purification steps.



Scheme 3. Oxone/periodate-induced oxidative cleavage of the terpene limonene and unsaturated fatty acids into carboxylic acids.

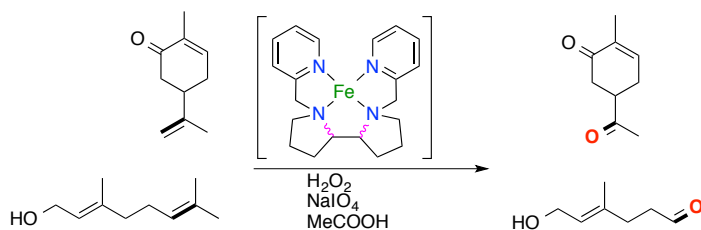
In **Chapter 3**, a method for the iron-catalyzed oxidative cleavage of unsaturated fatty acids is presented. Catalytic amounts of $[\text{Fe}(\text{OTf})_2(\text{mix-BPBP})]$ (0.5 mol%, mix-BPBP = mixture of *R,S*-, *R,R*- or *S,S*-isomers of *N,N'*-bis(2-picolyl)-2,2'-bipyrrrolidine) and an oxidant combination of H_2O_2 and NaIO_4 were found capable of converting unsaturated fatty acids to the corresponding aldehydes by oxidative cleavage. The catalyst is a considerably cheaper alternative for such processes than the optically active complex $[\text{Fe}(\text{OTf})_2(\text{R,R-BPBP})]$. The sequence of reactions in this one-pot procedure involves an Fe-catalyzed

olefin epoxidation step with H_2O_2 , H_2SO_4 -catalyzed epoxide hydrolysis, and finally neutralization of the pH of the reaction mixture and NaIO_4 -induced cleavage of the diol to yield the aldehyde cleavage products in over 90% yield. No acetic acid or other additives are required in this procedure, again allowing for simple product isolation by means of solvent extraction. In addition to providing an alternative to the 2nd or 3rd row transition metal catalysts, this catalytic procedure produces less waste than the stoichiometric oxone/periodate system presented in Chapter 2, because of the substitution of oxone by H_2O_2 and the use of the Fe-catalyst at loadings as low as 0.5 mol%.



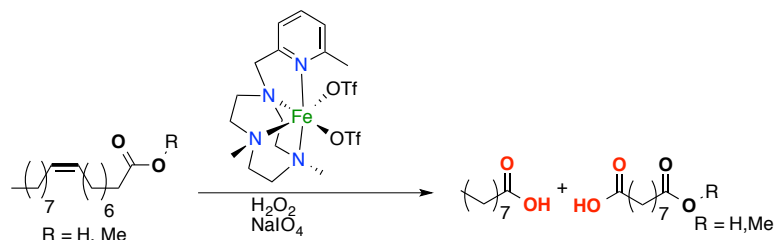
Scheme 4. Oxidative cleavage of unsaturated fatty acids and their esters into aldehydes catalyzed by $[\text{Fe}(\text{OTf})_2(\text{mix-BPBP})]$ in combination with H_2O_2 and NaIO_4 . The coordinating triflate atoms are omitted for clarity.

The substrate scope of the $[\text{Fe}(\text{OTf})_2(\text{mix-BPBP})]$ -based method is further investigated in **Chapter 4**, where it is shown that this system is able to carry out the regioselective oxidative cleavage of various dienes. Examples include the regioselective cleavage of a number of readily available, renewable terpenes. The addition of trace amounts of acetic acid (1.5 mol%) is shown to significantly increase the overall reaction rate and, more importantly, increases the selectivity towards the cleavage of the more electron-rich double bond in dienes with double bonds of different nature. In carvone, for instance, only the terminal double bond is quantitatively cleaved to yield the corresponding ketone, with the internal double bond being left untouched. Discrimination is also seen between the two double bonds in geraniol, for which 4-oxo-1-pentenone is obtained in high yield (77% selectivity at 70% conversion, Scheme 5). Likewise, the system also shows chemoselectivity, as alkenes are preferentially oxidized over alcohols. The ability to selectively cleave the more electron-rich double bonds in dienes constitutes a considerable advantage of this Fe-based catalytic system over the conventional 2nd and 3rd row transition metal-based catalysts that generally over-oxidize dienes.



Scheme 5. The electron-rich double bonds in the terpenes carvone and geraniol are cleaved regioselectively by $[\text{Fe}(\text{OTf})_2(\text{mix-BPBP})]$ with H_2O_2 and NaIO_4 as oxidants to give the corresponding aldehydes. The coordinating triflate atoms are omitted for clarity.

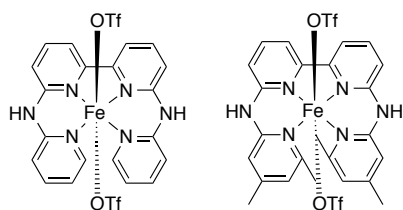
Complementary to the oxidative cleavage of alkenes to aldehydes by the combination of $[\text{Fe}(\text{OTf})_2(\text{mix-BPBP})]$ with $\text{H}_2\text{O}_2/\text{NaIO}_4$, the non-heme iron complex $[\text{Fe}(\text{OTf})_2(6\text{-Me-PyTACN})]$ described in **Chapter 5** is a suitable catalyst for the oxidative cleavage of unsaturated fatty acids into carboxylic acids (Scheme 6). While both methods comprise a one pot procedure, mechanistically the systems are different: $[\text{Fe}(\text{OTf})_2(\text{mix-BPBP})]$ catalyzes the initial epoxidation step, while the first $[\text{Fe}(\text{OTf})_2(6\text{-Me-PyTACN})]$ -catalyzed step consists of *cis*-dihydroxylation of the alkene. The combination of H_2O_2 and NaIO_4 results in reasonable to good yields of the carboxylic acids (50-55%) in this case, with some epoxides and aldehydes as byproducts. Further optimization of the procedure, i.e. by addition of H_2SO_4 at an intermediate reaction stage, followed by pH neutralization and addition of an extra amount of catalyst, resulted in an increase in the overall carboxylic acid yield to 80-85%. The method is rather versatile, as reaction conditions can be chosen such that either *cis*-diols, aldehydes or carboxylic acids can be obtained as products.



Scheme 6. Oxidative cleavage of unsaturated fatty acids into carboxylic acids catalyzed by $[\text{Fe}(\text{OTf})_2(6\text{-Me-PyTACN})]$ with H_2O_2 and NaIO_4 as oxidants.

In search of new iron catalysts capable of oxidative cleavage reactions, **Chapter 6** describes the development of mononuclear non-heme iron complexes derived from oligopyridine ligands that are expected to enable the formation of high valent iron-oxo intermediates. Such intermediates are not only involved in the oxidative cleavage reactions described in this thesis, but have also been invoked as the active oxidizing species in certain mononuclear non-heme iron enzymes. Accordingly, Chapter 6 describes the synthesis of the complexes $[\text{Fe}(\text{OTf})_2(\text{bapbpy})]$ and $[\text{Fe}(\text{OTf})_2(o,p\text{-diMe-bapbpy})]$ and

details their characterization by means of single crystal X-ray diffraction and a number of spectroscopic techniques (Scheme 7). These complexes are found in a high-spin $S = 2$ electronic configuration in solution and in the solid state and show spin crossover phenomena in MeCN solution. DFT calculations predict the high-valent species $[\text{Fe}(\text{O})(\text{bapbpy})(\text{MeCN})]^{2+}$ to be stable and to be able to epoxidize propene in a seemingly barrier-less manner. Oxidation of the Fe(II) complexes allows one to isolate the dinuclear oxo-bridged Fe(III) complexes $[\text{Fe}_2(\text{O})(\text{OTf})_2(\text{L})_2](\text{OTf})_2$, which was fully characterized. A detailed spectroscopic investigation of this reaction shows that the formation of the dimer is preceded by a putative mono-nuclear iron-oxo species. Interestingly, low temperature ESI-MS measurements at $-40\text{ }^\circ\text{C}$ have provided direct evidence for the formation of such a $[\text{Fe}(\text{O})(\text{bapbpy})]^{2+}$ species in this reaction. The Fe(II) complexes show some activity in the epoxidation of simple olefins, albeit that low products yields are observed (26%) and the reaction has to be carried out at temperatures above $50\text{ }^\circ\text{C}$. Nonetheless, higher turnover numbers are obtained with these complexes than with structurally related non-heme iron complexes.

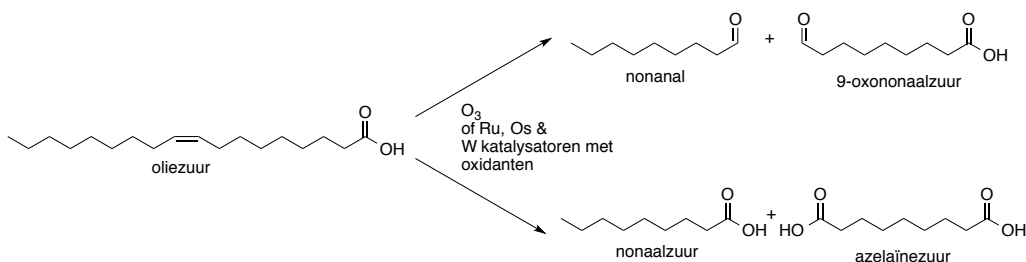


Scheme 7. Structures of $[\text{Fe}(\text{OTf})_2(\text{bapbpy})]$ (left) and $[\text{Fe}(\text{OTf})_2(o,p\text{-di-Me-bapbpy})]$ (right).

In conclusion, this thesis describes the development of a number of procedures for the oxidative cleavage of unsaturated fatty acids into aldehydes or acids. One of the procedures relies on the stoichiometric use of a combination of inorganic oxidants and does not require the involvement of a transition metal catalyst, while a complementary set of methods makes use of different non-heme iron catalysts in combination with hydrogen peroxide and sodium periodate to bring about these reactions. The development of these procedures may be regarded as a step forward towards the development of benign protocols for the oxidative valorization of biomass-derived olefins.

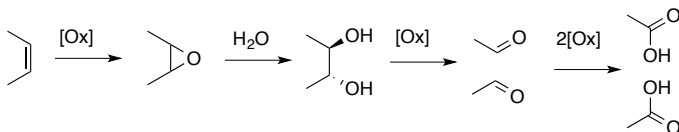
Samenvatting

De oxidatieve splitsing van onverzadigde vetzuren naar aldehydes of carbonzuren levert waardevolle bouwstenen op voor de chemische industrie. Hedendaags wordt het vetzuur oliezuur op industriële schaal via ozonolyse oxidatief gesplitst tot nonanal en 9-oxononaaizuur, of tot nonaaizuur en azelaïnezuur (Schema 1). Echter, het gebruik van ozon is gevaarlijk vanwege explosiegevaar, en dit oxidant moet derhalve ter plekke worden gegenereerd. **Hoofdstuk 1** van dit proefschrift beschrijft alternatieve katalytische reacties voor de oxidatieve splitsing. De katalysatoren die daarbij gebruikt worden zijn met name gebaseerd op de metalen Ru, Os of W. Het nadeel van het gebruik van dit soort metalen is dat ze algemeen worden gezien als duur, giftig of schaars. Het is daarom van belang dat duurzamere methoden worden ontwikkeld voor deze omzetting. Dergelijke methoden zijn bij voorkeur gebaseerd op overgangsmetalen uit de eerste rij van het periodiek systeem, zoals ijzer. De reeds gepubliceerde voorbeelden van katalysatoren gebaseerd op eerste rij overgangsmetalen voor de oxidatieve splitsing van alkenen beperken zich tot het gebruik van styreenderivaten als substraten. Katalytische systemen voor de oxidatieve splitsing van onverzadigde vetzuren op basis van eerste rij overgangsmetalen waren aan het begin van het promotietraject nog onbekend.



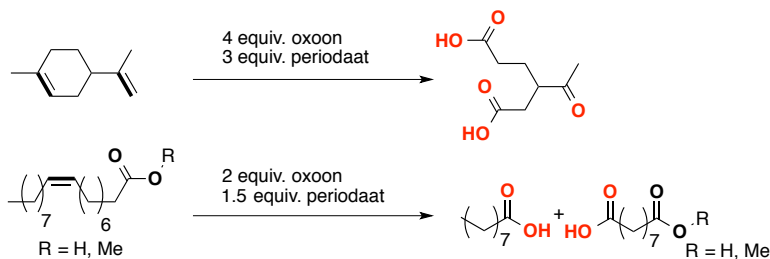
Schema 1. Oxidatieve splitsing van onverzadigde vetzuren tot aldehydes of carbonzuren. Tegenwoordig wordt deze reactie industrieel uitgevoerd met ozonolyse. Alternatieve katalytische methodes berusten op Ru, Os of W complexen met verschillende oxidanten.

Op basis van de in Hoofdstuk 1 beschreven systemen en bijbehorende mechanismes is voor een algemene strategie voor de oxidatie van een alkeen naar aldehydes of carbonzuren gekozen die de volgende stappen omvat: epoxidatie van het alkeen, gevolgd door hydrolyse naar het *trans*-diol en verdere splitsing naar óf het aldehyde óf het carbonzuur (Schema 2).



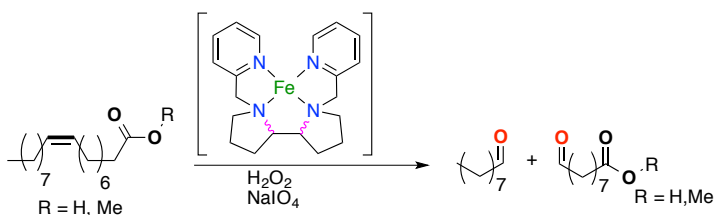
Schema 2. Algemene strategie voor de oxidatieve splitsing van alkenen naar aldehydes of verdere oxidatie naar carbonzuren.

Al zoekende naar een geschikte combinatie van oxidanten om deze reacties te katalyseren, werd ontdekt dat het gebruik van een combinatie van stoichiometrische oxidanten reeds resulteerde in alkeensplitsing. Het gebruik van een overgangsmetaal bleek niet nodig met dit systeem. **Hoofdstuk 2** beschrijft hoe de combinatie van oxoon ($2\text{KHSO}_5 \cdot \text{KHSO}_4 \cdot \text{K}_2\text{SO}_4$, met kaliumperoxosulfaat als het actieve oxidant) en natriumperiodaat (NaIO_4) in staat is om verschillende alkenen, waaronder terpenen en onverzadigde vetzuren, oxidatief te splitsen in water-acetonitrilmengsels, op een schone en selectieve manier (Schema 3). Het mechanisme veronderstelt dat oxoon (dat zure protonen bevat) zowel de epoxidatie, als ook de hydrolyse en aldehydeoxidatie naar het carbonzuur uitvoert, terwijl periodaat de oxidatie van het diol naar het aldehyde tot stand brengt. Optimalisatie van het oplosmiddelmengsel van water en acetonitril bleek cruciaal om de substraten en oxidanten voldoende op te lossen voor een goede opbrengst. Voor de splitsing van de onverzadigde vetzuren moet het reactiemengsel in een verhouding van 3:1 (v/v) MeCN:H₂O tot refluxtemperatuur worden verhit, en vervolgens worden verdund met water tot 1:3 (v/v) MeCN:H₂O om de laatste stap efficiënt te laten verlopen. Voor eenvoudige alkenen en de terpenen kan worden volstaan met 3:1 (v/v) MeCN:H₂O mengsel en kamertemperatuur voor de oxidatieve splitsing en is geen verdere toevoeging van water nodig. Op deze manier kunnen carbonzuuropbrengsten van >95% worden verkregen na reacties tussen de 18 en 72 uur. Door het relatief eenvoudig uit te voeren protocol, alsook de eenvoudige zuivering en isolatie van de producten door middel van extractie in een organisch oplosmiddel, is deze één-pot methode interessant voor de synthese van carbonzuren uit alkenen op labschaal. De eenvoudige productisolatie is een duidelijk voordeel vergeleken met procedures die gebruik maken van stoichiometrische oxidanten zoals KMnO_4 of katalytische systemen met Ru, Os of W, aangezien deze methodes vaak aanvullende zuiveringsstappen vereisen.



Schema 3. Oxoon/periodaat geïnduceerde oxidatieve splitsing van terpenen en overzadigde vetzuren naar carbonzuren.

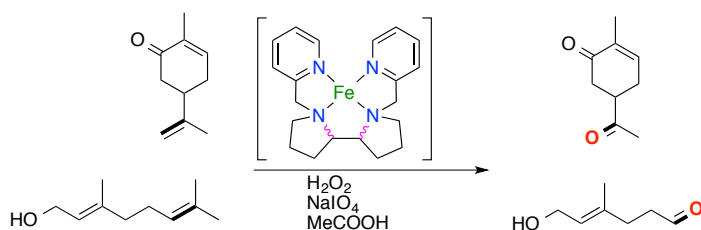
Hoofdstuk 3 omschrijft oxidatieve splitsingsreacties van onverzadigde vetzuren met ijzer door middel van katalytische hoeveelheden $[\text{Fe}(\text{OTf})_2(\text{mix-BPBP})]$ (mix-BPBP = mengsel van *R,S*-, *R,R*- of *S,S*-isomeren van *N,N'*-bis(2-picolyl)-2,2'-bipyrrolidine) en de oxidantcombinatie H_2O_2 en NaIO_4 . Met deze methode kunnen onverzadigde vetzuren omgezet worden tot aldehydes in een één-potsreactie (Schema 4). Het gebruik van het complex met het mengsel van isomeren is wezenlijk goedkoper dan het gebruik van het optisch actieve complex $[\text{Fe}(\text{OTf})_2(\text{R,R-BPBP})]$. De opeenvolgende reactiestappen in dit protocol omvatten een Fe-gekatalyseerde alkeenepoxidatie met H_2O_2 , gevolgd door H_2SO_4 -geïnduceerde hydrolyse, en tenslotte splitsing van het diol met NaIO_4 na neutralisering van de pH. Op deze manier kunnen aldehydeopbrengsten van meer dan 90% worden bereikt. De procedure vereist verder geen toevoeging van azijnzuur of andere additieven, waardoor het product weer eenvoudig kan worden gezuiverd en geïsoleerd middels extractie met ether. Niet alleen biedt dit systeem een alternatief voor de tweede en derde rij overgangsmetaalkatalysatoren, maar resulteert de toepassing ervan ook in aanzienlijk minder afvalstoffen dan het oxone/periodaat protocol uit Hoofdstuk 2. Oxone wordt namelijk vervangen door H_2O_2 en er is slechts 0.5 mol% ijzerkatalysator nodig voor de conversie.



Schema 4. Oxidatieve splitsing van onverzadigde vetzuren naar aldehydes, gekatalyseerd door middel van $[\text{Fe}(\text{OTf})_2(\text{mix-BPBP})]$ in combinatie met oxidanten H_2O_2 en NaIO_4 . De coördinerende triflaatatomen zijn voor de duidelijkheid weggelaten.

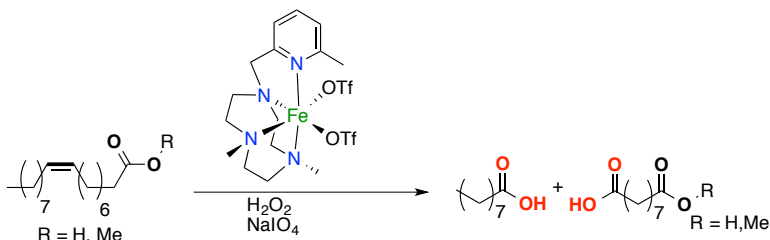
De substratscoop van het op $[\text{Fe}(\text{OTf})_2(\text{mix-BPBP})]$ -gebaseerde protocol is verder onderzocht in **Hoofdstuk 4**, waarin wordt aangetoond dat het systeem zelfs in staat is regioselectieve oxidatieve splitsingen uit te voeren in diënen. Voorbeelden hiervan zijn de

regioselectieve splitsing van een aantal terpeensubstraten, welke ruimschoots verkrijgbaar zijn uit biomassa. De toevoeging van minieme hoeveelheden azijnzuur (1.5 mol%) versnelt de reactie aanzienlijk en heeft bovendien een hogere selectiviteit voor de splitsing van de elektronrijkere dubbele bindingen in diënen als gevolg. Zodoende kan in het terpeen carvon uitsluitend de exocyclische C=C binding worden omgezet naar het keton. Het terpeen geraniol wordt ook regioselectief omgezet, waarbij voornamelijk 4-oxo-1-pentenon wordt gevormd in hoge opbrengst (77% selectiviteit bij 70% omzetting, Schema 5). Dit laatste voorbeeld laat ook de chemoselectiviteit van het systeem zien, aangezien alleen het alkeen en niet de alcohol functionele groep wordt geoxideerd. De mogelijkheid om elektronrijke dubbele bindingen in diënen te splitsen met de op ijzergebaseerde methode laat zien dat dit systeem niet alleen een alternatief is voor de tweede en derde rij overgangsmetalen, maar dat het deze katalytische systemen in dit opzicht ook overtreft.



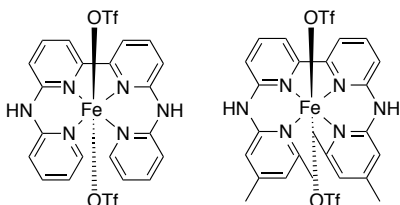
Schema 5. Regioselectieve splitsing van elektronrijke dubbele bindingen in terpeendiënen naar aldehydes, gekatalyseerd door $[\text{Fe}(\text{OTf})_2(\text{mix-BPBP})]$ met H_2O_2 en NaIO_4 als oxidanten. De coördinerende triflaatatomen zijn voor de duidelijkheid weggelaten.

Als aanvulling op de $[\text{Fe}(\text{OTf})_2(\text{mix-BPBP})]$ -gekatalyseerde splitsing van alkenen naar aldehydes, wordt in **Hoofdstuk 5** het niet-heem ijzercomplex $[\text{Fe}(\text{OTf})_2(6\text{-Me-PyTACN})]$ beschreven als geschikte katalysator voor de oxidatieve splitsing van onverzadigde vetzuren naar carbonzuren, wederom in een één-potsreactie (Schema 6). Hoewel beide methodes een splitsingsproces bewerkstelligen in één pot, zijn de mechanismes verschillend: waar $[\text{Fe}(\text{OTf})_2(\text{mix-BPBP})]$ epoxidatie van het alkeen katalyseert, voert $[\text{Fe}(\text{OTf})_2(6\text{-Me-PyTACN})]$ voornamelijk de *cis*-dihydroxylering van het alkeen uit. De combinatie van H_2O_2 en NaIO_4 laat met dit systeem goede opbrengsten van het carbonzuur toe (50-55%), met kleine hoeveelheden epoxides en aldehydes als nevenproducten. Verdere optimalisering van dit protocol laat zien dat de tussentijdse toevoeging van H_2SO_4 , gevolgd door pH neutralisering en het toevoegen van een extra hoeveelheid katalysator leidt tot verbetering van de algehele opbrengst van het carbonzuur naar 80-85%. Het systeem is verder breed toepasbaar, aangezien de reactieomstandigheden dusdanig kunnen worden aangepast dat de oxidatie eindigt bij ofwel het *cis*-diol, het aldehyde of het carbonzuurproduct.



Schema 6. Oxidatieve splitsing van onverzadigde vetzuren naar carbonzuren, gekatalyseerd door $[\text{Fe}(\text{OTf})_2(6\text{-Me-PyTACN})]$ met H_2O_2 en NaIO_4 als oxidanten.

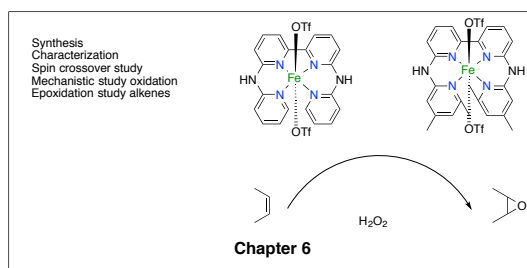
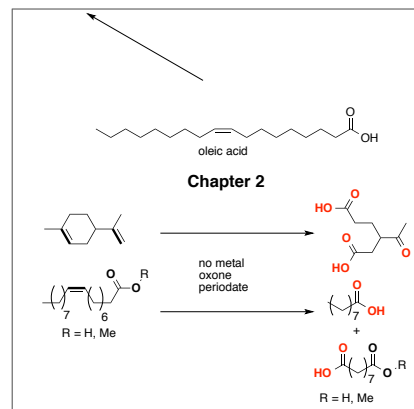
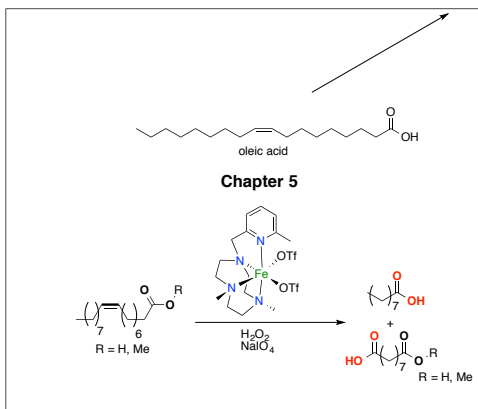
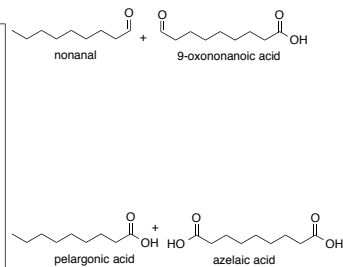
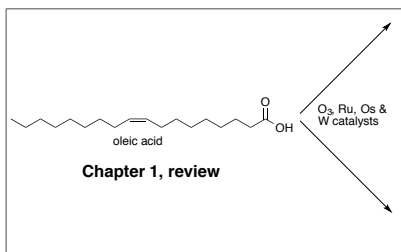
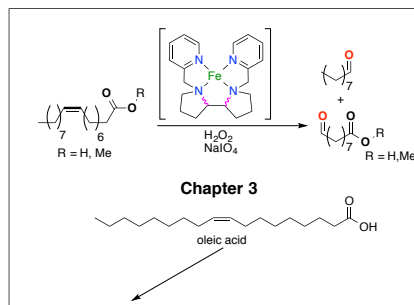
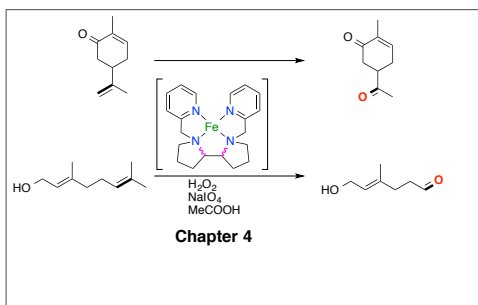
Als onderdeel van de zoektocht naar nieuwe ijzerkatalysatoren die toepasbaar zijn in oxidatieve splitsingsreacties, beschrijft **Hoofdstuk 6** de ontwikkeling van mononucleaire niet-heem ijzercomplexen met oligopyridine liganden die hoogvalente ijzer-oxo intermediären zouden moeten kunnen stabiliseren. Zulke intermediären komen niet alleen in oxidatieve splitsingsreacties voor, maar worden ook aangetroffen in de actieve centra van mononucleaire niet-heem ijzerenzymen. In dit hoofdstuk wordt de synthese beschreven van de complexen $[\text{Fe}(\text{OTf})_2(\text{bapbpy})]$ en $[\text{Fe}(\text{OTf})_2(o,p\text{-di-Me-bapbpy})]$ en wordt de karakterisering daarvan door middel van röntgendiffractie en spectroscopische technieken geschetst (Schema 7). De complexen hebben een hoge spin elektronenconfiguratie ($S = 2$) in oplossing en als vaste stof, en vertonen spin crossover verschijnselen in MeCN oplossing. Dichtsheidsfunctionaaltheorieberekeningen voorspellen dat het hoogvalente deeltje $[\text{Fe}(\text{O})(\text{bapbpy})(\text{MeCN})]^{2+}$ in staat moet zijn om propenen te epoxideren met een nagenoeg verwaarloosbare energiebarrière. De oxidatie-experimenten met de Fe(II) complexen laat zien dat oxo-gebrugde Fe(III) complexen worden gevormd, waarbij het product $[\text{Fe}_2(\text{O})(\text{OTf})_2(\text{bapbpy})_2](\text{OTf})_2$ werd geïsoleerd en volledig werd gekarakteriseerd. Een gedetailleerde spectroscopische studie van deze reactie laat zien dat de vorming van het dimeer via mononucleaire ijzer-oxo intermediären verloopt. ESI-MS metingen bij $-40\text{ }^\circ\text{C}$ vertonen een duidelijk bewijs dat $[\text{Fe}(\text{O})(\text{bapbpy})]^{2+}$ ook daadwerkelijk wordt gevormd in deze reactie. De Fe(II) complexen laten een redelijke activiteit zien in de epoxidatie van simpele alkenen, al worden de productopbrengsten (26%) pas bij temperaturen boven de $50\text{ }^\circ\text{C}$ gerealiseerd. Desalniettemin worden hogere omzettingstalmen waargenomen dan met andere, structureel-gerelateerde niet-heem ijzercomplexen.



Schema 7. Structuren van $[\text{Fe}(\text{OTf})_2(\text{bapbpy})]$ (links) and $[\text{Fe}(\text{OTf})_2(o,p\text{-di-Me-bapbpy})]$ (rechts).

Samenvattend laat dit proefschrift zien dat een aantal procedures zijn ontwikkeld voor de oxidatieve splitsing van onverzadigde vetzuren naar aldehydes, danwel naar carbonzuren. Eén van deze procedures berust op het stoichiometrisch gebruik van anorganische oxidanten en vereist verder geen overgangsmetaal, terwijl andere methodes hiervoor juist gebruik maken van niet-heem ijzerkatalysatoren in combinatie met waterstofperoxide en natriumperiodaat. De ontwikkeling van deze procedures kan worden gezien als een significante stap in de ontwikkeling van duurzame protocollen voor de oxidatieve valorisatie van biomassa-gerelateerde alkenen.

Graphical Abstract



List of publications

'A metal-free, one-pot method for the oxidative cleavage of internal aliphatic alkenes into carboxylic acids', P. Spannring, P. C. A. Bruijninx, B. M. Weckhuysen and R. J. M. Klein Gebbink, *RSC Adv.* **2013**, *3*, 6606.

'Fe-catalyzed one-pot oxidative cleavage of unsaturated fatty acids into aldehydes with hydrogen peroxide and sodium periodate', P. Spannring, V. A. Yazerski, P. C. A. Bruijninx, B. M. Weckhuysen and R. J. M. Klein Gebbink, *Chem. Eur. J.* **2013**, *19*, 15012.

'Fe(6-Me-PyTACN)-catalyzed one-pot oxidative cleavage of methyl oleate and oleic acid into carboxylic acids with H₂O₂ and NaIO₄', P. Spannring, I. Prat, M. Costas, P. C. A. Bruijninx, B. M. Weckhuysen and R. J. M. Klein Gebbink, *Catal. Sci. Technol.* revision in progress.

'Regioselective cleavage of electron-rich double bonds in dienes with [Fe(OTf)₂(mix-BPBP)] and a combination of H₂O₂ and NaIO₄', P. Spannring, V. A. Yazerski, P. C. A. Bruijninx, B. M. Weckhuysen and R. J. M. Klein Gebbink, manuscript in preparation.

'Synthesis, characterization and catalytic properties of non-heme [Fe(OTf)₂(bapbpy)] and [Fe(OTf)₂(o,p-di-Me-bapbpy)]', P. Spannring, E. Hernando Martinez, L. Gómez Martin, M. Costas, A. Draksharapu, W. R. Browne, S. Zheng, S. Bonnet, M. Lutz, M. Q. Quesne, S. P. De Visser, P. C. A. Bruijninx, B. M. Weckhuysen and R. J. M. Klein Gebbink, manuscript in preparation.

'Transition metal-catalyzed oxidative double bond cleavage of simple and bio-derived alkenes and unsaturated fatty acids', P. Spannring, P. C. A. Bruijninx, B. M. Weckhuysen and R. J. M. Klein Gebbink, manuscript in preparation.

'Synthesis and structure of [Mn(OTf)₂(bapbpy)] and [Mn(OTf)₂(o,p-di-Me-bapbpy)]', P. Spannring, M. Lutz, P. C. A. Bruijninx, B. M. Weckhuysen and R. J. M. Klein Gebbink, manuscript in preparation.

'Making Fe(BPBP)-catalyzed C-H/C=C oxidations more affordable', V. Yazerski, P. Spannring, D. Gatineau, C. H. M. Woerde, S. M. Wieclawska, M. Lutz, H. Kleijn and R. J. M. Klein Gebbink, manuscript in preparation.

Dankwoord

Allereerst wil ik mijn paranimfen bedanken. **Manuel**, after one month of knowing you I already knew that you were eventually going to be my paranymp. I actually learned half of the Spanish I will be speaking in this section from you, thank you for being such a fun and cheap teacher. Both of us liked to organize things for our group and we certainly enjoyed it. Thanks for letting me stay over when necessary, keeping my confidence high during my PhD research, and for the good times at conferences and in hotel rooms.

Svetia, je spreekt inmiddels al aardig Nederlands, of niet? Pero voy a tratar de hablar en español. Tú no eres mi paranimfa porque tú eres la chica di Manuelo, sino porque tú eres mi amiga. Svetia y Manuelo, cuando tenga dinero me voy a visitar en México. Me gusta le gente mexicana.

Verder wil ik mijn directe begeleider **Bert** Klein Gebbink ervoor bedanken dat ik voldoende ruimte voor creativiteit en zelfontplooiing heb gekregen. Ook was er voldoende tijd om te overleggen, aangezien ik weet dat niet elke professor dusdanig veel tijd met zijn medewerkers doorbrengt. Bovendien gaat er dank uit voor de medewerkingen aan de projecten in Groningen en in Girona. **Pieter** Bruijninx wil ik bedanken voor zijn ontspannen houding in gesprekken en dat ik altijd het gevoel had dat ik een vraag kon stellen. Ik wil beide begeleiders bedanken voor de zorgvuldige en snelle reacties op verschillende delen van mijn proefschrift, vooral in mijn laatste jaar als promovendus. **Bert** Weckhuysen, ook mijn promotor, wil ik bedanken om een strenge inspiratiebron aan het begin van mijn traject te zijn en om vertrouwen uit te stralen aan het einde van het traject.

Ik ga verder met mijn lofuitingen naar mijn (andere) directe collega's, om te beginnen met **Vital**. Hij is medeauteur van twee hoofdstukken en ik heb meegewerkt aan één van zijn hoofdstukken, wat onze goede samenwerking illustreert. Thank you for your great help with Chapters 3 and 5, and for our many good scientific discussions. **David**, thank you for your help with the iron chemistry throughout my thesis and for some practical skills you taught me. Also, I want to thank you for the pleasant time in Utrecht and when I visited you in Marseille. **Eric**, my former roommate, thanks for paying half of my rent for three months, for your help at the glove box and for some good times when I dropped by in Heidelberg. **Stefan**, je kwam mij ineens achterna en werd op het allerlaatst van mijn PhD traject toch nog collega van mij. De groep had nog wel een tweede 'Amsterdammer' nodig. Nog bedankt voor jouw inbreng omtrent Hoofdstuk 5. **Suresh**, my other former roommate, thank you for all the Chicken Curry, for the pleasant time when working after office hours and for trying to keep the lab clean. I also want to acknowledge **Yuxing** for almost the same reasons (you are welcome for helping you move so many times) and I enjoyed speaking about iron chemistry with you. **Dide**, buiten het feit dat we allebei

littkens hebben na operaties aan ons lichaam, delen we ook soortgelijke humor en het feit dat we een ontspannen werksfeer willen hebben. **Bas**, dankjewel dat je mijn taak hebt overgenomen om onze borrels te organiseren. Uiteraard wil ik ook mijn andere collega's **Emma, Charl, Leon, Morgane, Yves, Marc-Etienne, Dennis, Johann, Sylvestre, Marcel, Mozaffar, Niels, Jord** en **Leo** bedanken voor de koffiepauzes, borrels, sociale activiteiten en uiteraard voor de wetenschappelijke discussies.

I also would like to acknowledge some foreign (PhD) students that joined our group for internships. Primero, **Edu**, la fin de semana en 'Euskal Herria' fue muy bueno. The 1500 km driving in one weekend all alone was totally worth it. I will never forget our discussions about baseball. Segundo, **Jorge**, muchas gracias por ver la Copa del Rey, tienes que nadar en nuestro canal, recuerdas? In terzo luogo, **Giacomo**, my office in the Kruyt building was never as fun as when you joined it. **Cristina**, thank you for the pleasant time during your stay in Utrecht and also for your help in Girona. Finally **David FG**, thank you for the good time in Utrecht, for letting me keep your bike and for your help with organic chemistry in Girona.

Van al deze Spanjaarden is het maar een kleine stap naar mijn collega's tijdens mijn verblijf in Girona, waarin ik de resultaten voor Hoofdstuk 5 heb behaald en een deel van de resultaten uit Hoofdstuk 6. Tengo tambien muchas amigos en Girona, lo siento catalanes, per sólo puedo hablar castellano. Primero, **Irene**, muchas gracias por tu ayuda en mi proyecto y por todo el café en la oficina. **Laura**, 'gracies' por tu ayuda con mi otro proyecto, me gustó mucho tu cama, tu casa y tu bici. **Zoelo**, gracias por tu bici, el tupperware, por crear la palabra 'fiesta extrema', por las copitas de café y por ser un buen estudiante en inglés. **Olafo**, creo que tu tienes un poco de 'Pere' en tu cuerpo también, pero come más pan! **Arnau**, viva Catalunya. Finalmente, gracias también a **Marc, Joan, Gerard, Anna, Julio, Alicia, Miquel, Imma Xavi, Ming, Mireia, Carlota, Carla, Oriol, Raquel** y **Carmen**.

Een aparte paragraaf uit dit proefschrift moet ook worden besteed aan de studenten van onze groep. Ten eerste mijn eigen studenten. **Tanja** en **Karst**, ik heb jullie inmiddels vergeven dat jullie direct na mijn begeleiding met het Bachelorproject zijn overgestapt naar 'Anorganische Chemie en Katalyse'. Ik wil jullie allebei bedanken voor jullie werk aan Hoofdstuk 6 en ervoor dat jullie me nog steeds komen opzoeken op mijn verjaardag. Verder was het eigenlijk elke dag wel lachen met jullie. **Christiaan B**, eerst was je mijn relaxte Bachelorstudent en tenslotte een relaxte collega, want daar schaalde ik Masterstudenten ook onder in. Helaas komt jouw werk niet terug in dit proefschrift, maar misschien wel in het werk van Emma. Samen hebben wij wel veel geleerd over de IR en UV-Vis machines, en veel lol beleefd in mijn Suzuki Alto op weg naar het zweefvliegen. Bij dezen ook een bedankje aan **Joost** en **Lon**, die met hun resultaten hebben bijgedragen om Hoofdstukken 2 en 3 te bewerkstelligen. Tenslotte moet ik mijn dank uitbrengen aan

Pauline, Elier, Nitesh en **Duco** voor hun werk aan Hoofdstuk 6. Al mijn studenten hebben mij resultaten opgeleverd en hebben bijgedragen aan veel wetenschappelijke discussies, wat we zeker niet mogen onderschatten.

Ten tweede richt ik mij op de studenten uit onze groep welke ik niet begeleid heb, maar waarmee ik wel een goede tijd heb doorgebracht. Ik wil de vrolijke **Annet**, mijn (daadwerkelijke) buurvrouw **Laura**, mijn buurvrouw op het lab **Sara**, my former neighbor in the Kruyt building **Aurore**, mijn maatje uit het Kruytgebouw **Kimberley**, my fitness- and lab-mate **Hun-Kun** (or mister H.), **Richt, Minke, Gerda, Paul, Bart S, Bart L, Sander, Tim, Christian, Esther, Jurriaan, Naiara, Thomas** en **Martin** bedanken voor de gezelligheid en de atmosfeer op het lab.

Aangezien ik ook officieel was aangesteld aan de 'Anorganische Chemie en Katalyse' groep, wil ik ook daarvan een paar mensen bedanken. **Fouad**, bedankt voor jouw expertise omtrent onze gezamenlijk IR en Raman metingen. **Peter H**, je blijft helaas toch de Peter van Anorganisch in mijn ogen, maar ook bedankt voor de samenwerking op ons lab. **Annelie**, jij was vroeger mijn jaargenoot, toen een medebestuurslid, toen een medewerker bij 'Anorganische Chemie en Katalyse' en tenslotte zelfs een directe collega van mij. Nog bedankt voor alle tips om mijn proefschrift af te ronden. Verder wil ik vooral **Rob, Carlo, Joe, Robin, Frank, Matti, Zoran, Thomas, Thomas, Wouter, Gonzalo, Roy, Wenhao, Jesper, Charlotte, Lars, Jovana** en **Qinyun** uit jullie groep bedanken voor de gesprekken bij de koffiemachine, een inspirerende 'training school' op Schiermonnikoog, jullie talrijke borrels en voor onze leuke voetbalavonden.

I would also like to acknowledge **Wesley** and **Appu** for their help with some experiments I performed at the University of Groningen for Chapter 6, and for keeping up the good spirit at days when we had to work even far beyond office hours.

Mijn vrienden uit Amsterdam mogen hier natuurlijk ook niet tekort schieten. Sommigen zeggen dat de beste vriendschappen tijdens je studententijd ontstaan, dit zou zomaar ook toepasbaar kunnen zijn bij mij. **Bartje, Vlien, Ruben, Niels, Guido, Annemarie, Rutger, Pieter, Ilona, Jan-Hein, Linda, Soraya**, bedankt voor de muziekkfestivals, de voetbalpartijtjes en de wintersporten. Dan zijn er uiteraard nog een flink aantal mensen uit mijn studentenstad met wie ik ook een goede tijd heb doorgebracht en hier niet kunnen ontbreken, zoals **Krizz, Paddy, Robin, Janneke, Arthur, Esther, Jannie, Dayintha, Zea, Susanne, Tibert, Ruben P, Sandra, Lianne, Carien, Sara A, Rebecca, Peter, Juanma, Laura, Paulien, Merel, Amber, Sofia, Julien, Marta, Sjoerd, Anouk, Feline, Vincent, Kasper, Chu Chu** en vergeeft het mij als ik hier nog iemand ben vergeten. Tenslotte wil ik **Lin** bedanken voor het jarenlang gezellig samenleven, voor de stiekeme rijlessen, voor de leuke vakanties en uiteraard ook voor de handige commentaren op mijn werk tijdens mijn promotietraject.

De mensen van atletiek wil ik hier eveneens niet vergeten, dus bedankt, **Teun, Patrick, Patricia, Pijke, Kirsten, Dennis, Jeroen (allemaal), Bas, Jurre, Tieme, Lars, Iris, Pascale, Aniek, Matthijs, Peter-Paul, Eelco, Wim, Alice, Marloes, Janine, Mara, Rob, Koen, Nader, Joost, Annique, Monique, Maartje, Nicole, Vivian, Anne (allemaal), Martijn, Arjen, Ineke, Marijke, Marieke, Karin, Lorraine, Menno, Anton, Gerrieke, Steven, Lisa (allemaal), Leon, Siem, Niels, Rick, Maarten, Renée** en de rest, die ik vergeten ben, voor alle uren liggen, zweten en sporten met elkaar. Ook wil ik al mijn fysiotherapeuten ervoor bedanken dat ik snel beter ben geworden na mijn talloze blessures en dat ik mijn energie weer in het labwerk kon steken.

De mensen uit Alkmaar (of omstreken daarvan) verdienen ook een complimentje omdat we elkaar na al die jaren nog steeds zien, dus: dank jullie wel, **Jasper, Jacco** en **Tim**. Ook een bedankje aan mijn schoonouders, en aan mijn schoonzus en zwager **Sandra & Alex**.

Bovendien voel ik mij ook verplicht om mijn lofuitingen naar de groep van 'Biochemie van Membranen' te sturen, of heten jullie inmiddels alweer anders? **Remko**, wat waren wij toch een goed team om interdisciplinaire borrels te organiseren en om onze groepen wat dichter bij elkaar te brengen. **Jacques**, thanks a lot for always joining our borrels in the Kruyt, for being my financial advisor at times and for spreading so much joy with your luminescent clothing. I want to thank **Jessica** for spending so much more time with our group (and the social activities) than with her own. The same goes for **Lorena** (para ti de mi, venga para Día del Rey un otra vez) and **Ivan**. Ook een bedankje aan **Eefjan, Martijn, Joost, Nick, Stefan, Lisette, Sabine, Yao, Diana, Marloes, Paulien, Yvonne, Jonas** en **Sam**.

Ik ben verder blij dat mijn broertje **Philip** steeds meer op mij begint te lijken. Alleen moeten we nog iets aan dat kapsel van je doen. Tenslotte moet ik nog mijn ouders bedanken voor het opvoeden van deze rebelse jong, voor genoeg avonturen tijdens mijn jeugd en ook nog lang daarna.

Dit gedeelte moet ik natuurlijk afsluiten door **Inge** te bedanken. Gezien de hoeveelheid tekst die ik voor andere mensen heb gebruikt, is een simpel 'ik hou van je' hier niet voldoende natuurlijk. Sinds ik elke dag met je samen ben, heb ik het idee dat ik oprecht rustiger, volwassener en uiteraard gelukkig ben geworden. Wat heb ik met jou, onder anderen, veel gelachen, veel gesport, veel voetbal gekeken, veel Turks brood met knakworst gegeten, veel gereden en daardoor toch wel veel gezien van de wereld. Opdat we nog heel veel jaren samen kunnen genieten.

Curriculum Vitae

Peter Spannring is a Dutch citizen and was born on the 29th of October in 1985. He was raised in Alkmaar, Noord-Holland, and went to primary and secondary school in Bergen, Noord-Holland. After graduating from secondary school in 2003, he started his undergraduate studies in Chemistry at the University of Amsterdam in that same year. He obtained his Bachelor's degree in 2006 with a thesis performed in the 'Molecular Simulations' group of prof. dr. E. J. Meijer entitled 'Ab Initio Study of Asymmetric Oxidations with Ru and Ir Complexes'. In that same year, he started the 'Amsterdam Physical Master of Science' Master's program, from which he switched in 2007 to the 'Molecular Design, Synthesis & Catalysis' Master's program. He obtained his Master's degree in 2008 with a thesis in the 'Coordination & Organometallic Chemistry' group under the supervision of prof. dr. C. J. Elsevier, which was entitled 'Amphiphilic Ruthenium Catalysts: Synthesis & Characterization of [Ru(bpy-R)₂L₂]₂X Complexes'. In 2009, he started his PhD research at Utrecht University, funded by the 'Focus en Massa' program. The research was performed in the 'Organic Chemistry & Catalysis' and 'Inorganic Chemistry & Catalysis' groups under the supervision of prof. dr. R. J. M. Klein Gebbink, prof. dr. ir. B. M. Weckhuysen and dr. P. C. A. Bruijninx. The topic and results are described in this thesis. From the 1st of December 2013, he is employed as a postdoctoral researcher at the Radboud Universiteit Nijmegen in the 'Synthetic Organic Chemistry' group under the supervision of prof. dr. F. P. J. T. Rutjes.